

Investigation of the Mobility and Extraction Potential of Vanadium and
Coupled Metals (Nickel and Lead) in Oily Sludge Matrix under
Electrokinetic Conditions

Ammar Badawieh

A Thesis
In the Department
of
Building, Civil, and Environmental Engineering

Presented in Partial Fulfillment of the Requirements
For the Degree of
Doctor of Philosophy (Civil Engineering) at
Concordia University
Montreal, Quebec, Canada

January 2016

© Ammar Badawieh, 2016

**CONCORDIA UNIVERSITY
SCHOOL OF GRADUATE STUDIES**

This is to certify that the thesis prepared

By: **Ammar Badawieh**

Entitled: **Investigation of the Mobility and Extraction Potential of Vanadium and Coupled Metals (Nickel and Lead) in Oily Sludge Matrix under Electrokinetic Conditions**

and submitted in partial fulfillment of the requirements for the degree of

Doctor of Philosophy (Civil Engineering)

complies with the regulations of the University and meets the accepted standards with respect to originality and quality.

Signed by the final examining committee:

_____	Chair
Dr. R. Bhat	
_____	External Examiner
Dr. Shiv. O. Prasher	
_____	External to Program
Dr. G. Vatisas	
_____	Examiner
Dr. A. M. Hanna	
_____	Examiner
Dr. Z. Chen	
_____	Thesis Co-Supervisor
Dr. M. Elektorowicz	
_____	Thesis Co-Supervisor
Dr. H. El-Sadi	

Approved by _____
Dr. F. Haghighat, Graduate Program Director

2016

Dr. A. Asif, Dean, Faculty of Engineering and Computer Science

Investigation of the Mobility and Extraction Potential of Vanadium and Coupled Metals (Nickel and Lead) in Oily Sludge Matrix under Electrokinetic Conditions

Ammar Badawieh, Ph.D.

Concordia University, 2016

Abstract

Oily sludge is a viscous complex mix of hydrocarbons, water, metals, and suspended fine solids. This by-product's persistent toxic composition poses serious environmental concerns, making its containment one of the biggest challenges facing petroleum industries. The main objective of this research was to monitor and trace target heavy metals (with particular focus on vanadium) mobilized in a petroleum sludge matrix under electrokinetic conditions. This exploratory study would facilitate furthering reclamation procedures, and presents the prospect of converting oily sludge into high quality added-value products. The research was carried out in three experimental and analytical phases. Phase 1 consisted of the formulation of adequate Upstream/Downstream petroleum waste, where three target metals, namely vanadium, lead and nickel were considered. In Phase 2, electrokinetic (EK) technology was used to separate valuable oily sludge components, and mobilize metals. A series of EK cells containing sole and mixed metals permitted investigating the synergistic and antagonistic effects of the three target metals (V, Ni, and Pb). Phase 3 focused on behaviour and mobility of metals in the separated matrices. In this phase, a combination of procedures including, Fourier Transform Infrared (FTIR) analysis, and X-Ray diffraction (XRD) were applied simultaneously. Rheological tests confirmed

electro-demulsification and phase separation in oily sludge matrices. Furthermore, Ethylenediamine-Tetraacetate acid (EDTA), and Diisooctylidithiophosphini acid (Cyanex 301) were compared in the metal supercritical fluid extraction (SFE) process in order to enhance metals' extraction from the oily sludge matrix. The results obtained in this research provide insight into the mobility of target heavy metals (V, Ni, and Pb) in an oily sludge matrix under EK treatment. Furthermore, vanadium was found to be an accelerator for the separation of oily sludge components under EK conditions. The results demonstrated an excellent vertical and horizontal electro-separation of phases in the upstream cells. In the downstream oily sludge, the presence of non-polar solvents affected the separation process. However, in both upstream and downstream cells, metal mobility created interesting scenarios, such that metals accumulated in the specific areas of the matrix. This mapping of metals would permit on their further removal. This research leads to development of a new oily sludge management system (EK-SEF-Cyanex 301), which would not only help in the reclamation of sludge, but may also create a stream of revenue from the recovery of metals (particularly vanadium).

Acknowledgments

I would like to express my deepest gratitude and appreciation to my thesis advisor Prof. Maria Elektorowicz for her guidance, constant encouragement, and patience during course of dissertation.

My sincere thanks are addressed to my Co-supervisor Dr. Haifa Al-Sadi for her comments, suggestions, and valuable advice.

I wish to acknowledge the assistance of Dr. Rosalia Chifrina for her comments and suggestions, Dr. Yacine Boumghar and his research team from CEPROCQ (College de Maisonneuve) in Montreal for allowing generously the use of their laboratories, and my colleague Dr. Shadi Hasan for providing the raw material for this research.

I would like to acknowledge a financial support for this research from the Discovery Grant awarded to Dr. Elektorowicz, by the Natural Science and Engineering Research Council (NSERC) of Canada.

Special thanks to my dear friends Zaid Ghouleh, and Charles Desjardin for them being of great help whenever I needed them.

Dedication

I would like to express my heartfelt thanks for the unconditional love and limitless support from my wonderful parents, my amazing wife, Hanin, beautiful kids, Hashem and Zena, great brothers, Emad and Husam, and my lovely sister Sara.

Table of Contents

Glossary	xvii
Chapter 1 Introduction	1
Chapter 2 Literature Review	5
2.1 Petroleum oily sludge	5
2.1.1 Components and characteristics	6
2.1.2 Quantities	7
2.1.3 Hazardous effect	7
2.1.4 Oily sludge as a controlled Haz-Mat	8
2.1.5 Canadian federal and provincial petroleum wastes disposal regulations	9
2.2 Heavy metals	12
2.2.1 Vanadium	13
2.2.1.1 Physical and chemical properties	13
2.2.1.2 Sources and behavior in soil	14
2.2.1.3 Vanadium applications and effects	14
2.2.2 Nickel	15
2.2.2.1 Physical and chemical properties	15
2.2.2.2 Sources and behavior in soil	16
2.2.2.3 Nickel applications and effects	16
2.2.3 Lead	18
2.2.3.1 Physical and chemical properties	18
2.2.3.2 Sources and behavior in soil	18
2.2.3.3 Lead applications and effects	19
2.3 Heavy metals in petroleum sludge	21
2.4 Emulsions	23
2.5 Oily sludge management	25
2.5.1 Recycling	25
2.5.2 Filtration	26
2.5.3 Treatment with fly ash	26

2.5.4 Incineration	27
2.5.5 Coking	28
2.5.6 Biological treatment.....	29
2.5.6.1 Biodegradation of Oily Sludge	29
2.5.6.2 Composting	30
2.5.7 Landfarming	31
2.5.8 Centrifugation.....	33
2.5.9 Phytoremediation	34
2.5.10 Unconventional methods/studies	36
2.6 Oily sludge management with respect to metals	37
2.6.1 Electrokinetics (EK)	38
2.6.1.1 Electromigration	39
2.6.1.2 Electroosmosis	40
2.6.1.3 Electrophoresis.....	41
2.6.1.4 Applications of electrokinetic phenomena.....	42
2.6.2 Supercritical fluid extraction (SFE).....	44
2.6.2.1 Applications of SFE	46
Chapter 3 Research Hypothesis and Objectives	49
Chapter 4 Methodology	52
4.1 Matrix preparation	52
4.1.1 Upstream scenario.....	54
4.1.2 Downstream scenario.....	58
4.2 Experimental Phase-2	60
4.2.1 Objectives of Phase 2.....	60
4.2.2 EK cells setup-stage 1	61
4.2.3 EK experiments-Stage 2	63
4.3 Apparatus, reagents, and equipment.....	64
4.4 Characterisation of the sludge.....	66
4.4.1 Oily sludge components.....	66
4.4.1.1 Liquid content.....	67
4.4.1.2 Solid content	67

4.4.1.3	Non-volatile organic content (NVOC)	67
4.4.2	Measurement procedure of pH.....	67
4.4.3	Electrical parameters.....	68
4.4.4	Sampling procedure	68
4.5	FTIR analysis (Phase-3).....	69
4.6	XRD analysis (Phase-3).....	70
4.7	Rheological properties (Phase-3).....	71
4.8	Metal analysis	72
4.8.1	Digestion procedure	72
4.8.2	Atomic Adsorption Spectroscopy (AAS)	73
4.8.3	Supercritical fluid extraction (SFE)	74
Chapter 5	Discussion and Results.....	76
5.1	Separation of components.....	76
5.1.1	Vanadium Cells (V Cells).....	80
5.1.2	Nickel Cells (Ni Cells).....	81
5.1.3	Lead Cells (Pb Cells)	83
5.1.4	Mixed metals Cells (Mix Cell)	85
5.2	Electrical parameters.....	88
5.2.1	Resistance changes in Vanadium Cells.....	88
5.2.1.1	Upstream oily sludge	88
5.2.1.2	Downstream oily sludge	90
5.2.2	Resistance changes in Nickel Cells.....	92
5.2.2.1	Upstream oily sludge	92
5.2.2.2	Downstream oily sludge	94
5.2.3	Resistance changes in Lead Cells	96
5.2.3.1	Upstream oily sludge	96
5.2.3.2	Downstream oily sludge	98
5.2.4	Resistance changes in Mix Cells.....	100
5.2.4.1	Upstream oily sludge	100
5.2.4.2	Downstream oily sludge	103
5.2.5	Average power and energy consumption.....	105

5.3	Measurements of pH.....	106
5.3.1	pH changes in upstream/downstream - Vanadium Cells	107
5.3.2	pH changes in upstream/downstream - Nickel Cells	109
5.3.3	pH changes in upstream/downstream - Lead Cells.....	111
5.3.4	pH changes in upstream/downstream - Mix Cells	113
5.4	Rheological analyses.....	116
5.4.1	Upstream oily sludge matrix.....	116
5.4.2	Rheological properties of the upstream/downstream Vanadium Cell	117
5.5	Metals mobility and distribution.....	123
5.5.1	Vanadium distribution	123
5.5.1.1	Upstream oily sludge matrix.....	123
5.5.1.2	Downstream oily sludge matrix.....	126
5.5.2	Nickel distribution	128
5.5.2.1	Upstream oily sludge matrix.....	128
5.5.2.2	Downstream oily sludge matrix.....	131
5.5.3	Lead distribution	134
5.5.3.1	Upstream oily sludge matrix.....	134
5.5.3.2	Downstream oily sludge matrix.....	137
5.6	Supercritical fluid extraction (SFE).....	140
5.6.1	SFE efficiency with Cyanex 301 as chelating agent.....	140
5.6.2	SFE efficiency with EDTA as chelating agent	142
5.6.3	Efficiency of SFE techniques in enhancing extraction potential	145
5.7	FTIR analysis.....	147
5.7.1	Upstream Cells.....	148
5.7.2	Downstream cells.....	151
5.8	X-Ray diffraction (XRD).....	154
Chapter 6	Metals mobility under electrokinetic phenomena in oily sludge matrix	159
6.1	Behaviour of vanadium in EK modified oily sludge matrix.....	159
6.1.1	Upstream oily sludge matrix	160
6.1.2	Downstream oily sludge matrix	164
6.2	Nickel mobility	168

6.2.1	Upstream oily sludge matrix	168
6.2.2	Downstream oily sludge matrix	172
6.3	Lead mobility	174
6.3.1	Upstream oily sludge matrix	174
6.3.2	Downstream oily sludge matrix	176
6.4	Metals distribution in the mixed metals oily sludge matrix.....	178
6.4.1	Upstream oily sludge matrix	179
6.4.2	Downstream oily sludge matrix	184
Chapter 7	188
Conclusions	188
7.1	Conclusion	188
7.2	Contributions	191
7.3	Potential applications and benefits	192
7.4	Future work.....	193
References	195
Appendices	209
Appendix A: FTIR spectra for all upstream/downstream cells	209
Appendix B: Photographs comprising key cells	233
Appendix C: Solubility diagrams of target metals.....	236

List of Tables

Table 2.1: Sources of oily sludge.....	5
Table 2.2: Average content of oil, water, and solids in sludge wastes	6
Table 2.3: Contaminant standard limit.....	12
Table 2.4: Comparison between vanadium, nickel and lead general properties.....	21
Table 2.5: Metal content of petroleum oily sludge from different sources.....	23
Table 4.1: Crude oil characteristics	55
Table 4.2: Raw material created in Phase-1	60
Table 4.3: Summary of experimental cells conditions in Phase-2.....	64
Table 4.4: Sampling procedure	69
Table 4.5: SFE operating parameters.....	75
Table 5.1: Concentration of target metals in samples after acid digestion and SFE.....	145
Table 5.2: XRD results, downstream samples in Vanadium Cell after EK....	157
Table 6.1: Summary of the results: upstream Vanadium Cell after EK	161
Table 6.2: Summary of the results: downstream Vanadium Cell after EK.....	164
Table 6.3: Summary of the results: upstream Nickel Cell after EK	169
Table 6.4: Summary of the results: downstream Nickel Cell after EK.....	173
Table 6.5: Summary of the results: upstream Lead Cell after EK	175
Table 6.6: Summary of the results: downstream Lead Cell after EK	177
Table 6.7: Summary of the results: upstream Mix Cell after EK	180
Table 6.8: Summary of the results: downstream Mix Cell after EK.....	184

List of Figures

Figure 2.1 Phase diagram of a pure component revealing location of supercritical conditions in the presented binary system (Patterson, 2005).....	45
Figure 2.2 Illustration of a simplified SFE system (Alonso et al., 2002)	46
Figure 4.1 Detailed Experimental Methodology.....	52
Figure 4.2 Methodological approach for sludge preparation.....	53
Figure 4.3 Components used to prepare a synthetic sludge for upstream scenario	57
Figure 4.4 Synthetic oily sludge prepared for downstream scenario.....	59
Figure 4.5 Electrokinetic system for experimentation in Phase-2	62
Figure 4.6 Configuration of the electrokinetic cell.....	63
Figure 5.1 Movement of the liquid components toward the cathode and solid components to the anode in an upstream cell.....	77
Figure 5.2 Vertical and horizontal directions in the EK cells.....	78
Figure 5.3 Original upstream oily sludge (before applying EK)	79
Figure 5.4 Original downstream oily sludge (before applying EK)	79
Figure 5.5 Percentages of fractions of oily sludge in upstream Vanadium Cell (after EK)	80
Figure 5.6 Fractions of oily sludge in downstream Vanadium cell (after EK).....	81
Figure 5.7 Fractions of oily sludge in an upstream Nickel Cell (after EK)	82
Figure 5.8 Fractions of oily sludge in a downstream Nickel Cell (after EK)	83
Figure 5.9 Fractions of oily sludge in upstream Lead Cell (after EK).....	84
Figure 5.10 Fractions of oily sludge in downstream Lead Cell (after EK).....	85
Figure 5.11 Fractions of oily sludge in upstream Mix Cell (after EK).....	86
Figure 5.12 Fractions of oily sludge in a downstream Mix Cell (after EK)	87
Figure 5.13 Resistance changes in upstream Vanadium Cell (anode area)	89
Figure 5.14 Resistance changes in upstream Vanadium Cell (cathode area)	90
Figure 5.15 Resistance changes in downstream Vanadium Cell (anode area)	91
Figure 5.16 Resistance changes in downstream Vanadium Cell (cathode area)	92
Figure 5.17 Resistance changes in upstream Nickel Cell (anode area)	93
Figure 5.18 Resistance changes in upstream Nickel Cell (cathode area)	94

Figure 5.19 Resistance changes in downstream Nickel Cell (anode area)	95
Figure 5.20 Resistance changes in downstream Nickel Cell (cathode area)	96
Figure 5.21 Resistance changes in upstream Lead Cell (anode area).....	97
Figure 5.22 Resistance changes in upstream Lead Cell (cathode area)	98
Figure 5.23 Resistance changes in downstream Lead Cell (anode area)	99
Figure 5.24 Resistance changes in downstream Lead Cell (cathode area)	100
Figure 5.25 Resistance changes in upstream Mix Cell (anode area)	101
Figure 5.26 Resistance changes in upstream Mix Cell (cathode area)	102
Figure 5.27 Resistance changes in downstream Mix Cell (anode area)	103
Figure 5.28 Resistance changes in downstream Mix Cell (cathode area)	105
Figure 5.29 Average electrical power consumption in upstream and downstream cells	106
Figure 5.30 pH changes in upstream Vanadium Cell	108
Figure 5.31 pH changes in downstream Vanadium Cell	109
Figure 5.32 pH changes in upstream Nickel Cell	110
Figure 5.33 pH changes in downstream Nickel Cell	111
Figure 5.34 pH changes in upstream Lead Cell	112
Figure 5.35 pH changes in downstream Lead Cell	113
Figure 5.36 pH changes in upstream Mix Cell	114
Figure 5.37 pH changes in downstream Mix Cell	115
Figure 5.38 Viscosity of the upstream Control Cell (initial oily sludge matrix)	117
Figure 5.39 Viscosity of the bottom anode sludge as a function of the strain rate	118
Figure 5.40 Viscosity of the bottom cathode sludge as a function of the strain rate	118
Figure 5.41 Viscosity of the bottom central area sludge as a function of the strain rate	119
Figure 5.42 Elastic modulus as a function of frequency for bottom anode, cathode.....	119
Figure 5.43 Elastic modulus as a function of frequency for bottom anode, cathode.....	120
Figure 5.44 Viscosity as a function of strain for top anode, cathode and center samples	121
Figure 5.45 Vanadium horizontal distribution in upstream a) Vanadium, and b) Mix metal Cells	124
Figure 5.46 Vanadium vertical distribution in a) Vanadium and b) Mix metals Cells...	125

Figure 5.47 Vanadium horizontal distribution in downstream a) Vanadium and b) Mix metals Cells.....	126
Figure 5.48 Vanadium vertical distribution in downstream a) Vanadium and b) Mix metals Cells.....	127
Figure 5.49 Nickel horizontal distribution in upstream a) Nickel and b) Mix metals Cells	129
Figure 5.50 Nickel vertical distribution in upstream a) Nickel and b) Mix metals Cells	130
Figure 5.51 Nickel horizontal distribution in downstream a) Nickel and b) Mix metals Cells	132
Figure 5.52 Nickel vertical distribution in downstream a) Nickel and b) Mix metals Cells	133
Figure 5.53 Lead horizontal distribution in upstream a) Lead and b) Mix metals Cells	134
Figure 5.54 Lead vertical distribution in upstream a) Lead and b) Mix metals Cells	136
Figure 5.55 Lead horizontal distribution in downstream a) Lead and b) Mix metals Cells	137
Figure 5.56 Lead distribution in downstream a) Lead and b) Mix metals Cells	139
Figure 5.57 Extraction efficiency change in upstream Mix Cell after applying.....	141
Figure 5.58 Extraction efficiency change in downstream Mix Cell after applying.....	142
Figure 5.59 Extraction efficiency change in upstream Mix Cell after applying SFE.....	143
Figure 5.60 Extraction efficiency change in downstream Mix Cell after applying.....	144
Figure 5.61 FTIR absorbance spectra of the original upstream cell before EK treatment	148
Figure 5.62 Distribution of water and hydrocarbons in upstream cells based on OH/SiO and CH/SiO ratios at the top sections of the cells.....	149
Figure 5.63 Distribution of water and hydrocarbons in upstream cells based on OH/SiO and CH/SiO ratios at the bottom sections of the cells.....	150
Figure 5.64 FTIR Absorbance spectra of the initial downstream oily sludge before EK treatment	151
Figure 5.65 Distribution of water and hydrocarbons in downstream cells based on OH/SiO and CH/SiO ratios at the top sections of the cells.....	153

Figure 5.66 Distribution of water and hydrocarbons in downstream cells based on OH/SiO and CH/SiO ratios at the bottom sections of the cells	154
Figure 5.67 XRD spectra of the downstream samples in Vanadium Cell before and after EK treatment	156
Figure 6.1 Upstream Vanadium Cell post EK	167
Figure 6.2 Downstream Vanadium Cell post EK (formation of thin layer of dense hydrocarbons on the surface)	168
Figure 6.3 Vanadium distribution variation in upstream Vanadium Cell and Mix Cell.	181
Figure 6.4 Nickel distribution variation in upstream Nickel Cell and Mix Cell.....	182
Figure 6.5 lead distribution variation in upstream Lead Cell and Mix Cell	183
Figure 6.6 Vanadium distribution variation in the downstream Vanadium Cell and Mix Cell	185
Figure 6.7 Nickel distribution variation in the downstream Nickel Cell and Mix Cell..	186
Figure 6.8 Lead distribution variation in the downstream Lead Cell and Mix Cell	186

Glossary

API: American Petroleum Institute.

Electrophoresis: The motion of colloidal species caused by an imposed electric field.

Electroosmosis: The motion of liquid through a porous medium caused by an imposed electric field.

EPA: American Environmental Protection Agency.

EQA: Environmental Quality Act (Quebec standards).

Lead Cell: Electrokinetic cell that contains oily sludge matrix enriched with lead only.

Mix Cell: Electrokinetic cell that contains oily sludge matrix enriched with a mix of vanadium, nickel, and lead in equal proportions.

Nickel Cell: Electrokinetic cell that contains oily sludge matrix enriched with nickel only.

NVOC: Non-volatile organic content.

Original Cell: Cell that contains oily sludge matrix enriched with vanadium, nickel and lead, and not connected to DC source.

Ostwald-de Waele-power model: Model that describes the behaviour of a real non-Newtonian fluid by showing effective viscosity as a function of the shear rate.

O/W: When oil is the dispersed phase (oil-in-water).

PACE: Petroleum Association for Conservation of the Canadian Environment.

RCRA: Resource Conservation and Recovery Act.

SCF: Supercritical fluid.

SFE: Supercritical fluid extraction.

Upstream sludge: Sludge generated as by-product from extracting and producing crude oil.

Vanadium Cell: Electrokinetic cell that contains oily sludge matrix enriched with vanadium only.

W/O: When water is the dispersed phase (water-in-oil).

Chapter 1

Introduction

Oil is the major source of energy of this century, and with the increase of energy consumption, crude oil extraction and processing have significantly increased.

One out of major challenges facing the petroleum industry today is finding an acceptable and cost-effective solution, to manage the growing amounts of oily sludge, generated through the upstream, midstream, and downstream sectors of this industry. The latter sectors refer respectively to the extraction and production, storing, and transporting petroleum crude oil, and finally refining and treating of oil.

Oily sludge belongs to a multi-component system, mainly characterized as an oil-in-water, or water- in-oil systems, mixed with suspended solids. This homogeneous viscous mix is usually in full emulsification. The components of oily sludge form a stable dispersion state due to hydration and electronegativity, and are extremely stable suspended illiquid (Guolin et al., 2009). Therefore, the first step of treatment should include the demulsification of the system, by targeting the stabilized state of the sludge, and separating the components into recyclable, degradable organic and non-organic compounds, which includes heavy metals. Most of these metals are considered harmful but valuable at the same time, which demonstrates possibility to find a new feasible methods for extracting metals from sludge, preventing the toxicity, moreover preserving the value of these metals.

According to the American Environmental Protection Agency (EPA), Oil production processes generate an estimated 230,000 MT sludge each year (EPA, 2000). Saudi Arabia having the largest petroleum reserves in the world, produces about 10.45 million barrels of

crude oil every day (Saefong, 2015). A study conducted by Japan External Trade Organization (JETRO) (2010) on oily sludge produced by Saudi Aramco, estimated an annual production of oily sludge by Saudi refineries, bulk plants, and tank farms for more than 30,000 m³ per year. In Russia, more than 3 MT of sludge is formed annually, mainly from the following sources: a) around 1 MT of sludge and contaminated soils generated by oil production companies (upstream), b) 0.7 MT of sludge produced by refineries (downstream), and c) oil terminals, railroads, sea port, and other sources (US Reporter, 2010).

Oily sludge, under the resource conservation and recovery act (RCRA), is classified as hazardous waste (EPA code No. F037, F038 and a series of K) (EPA, 1998). Oily sludge hazardous classification comes from the fact that many constituents of the oily sludge are carcinogenic and are potential immunotoxicants. These constituents contain a mixture of heavy metals, hydrocarbonic compounds (e.g. benzene, benzo(α)pyrene, toluene, etc), PCBs (polychlorinated biphenyls), and other hazardous substances depending on the origin of the sludge (Mishra et al., 2001; Propst et al., 1999). Such components can bring a potential hazard to the environment (soil, water, plants and animals), and eventually humans.

In the past, landfilling was the common disposal method for oily sludge. However, land disposal of oily sludge was banned in 1990, after it was listed by the EPA as a hazardous waste under the code of K (Abrishamain et al., 1992). This ban was related to the contamination caused by the leaching of heavy metals, and hydrocarbons from disposal sites to the surrounding environment.

Oily sludge can't be recycled, utilized as fuel oil, or in roads pavement, as studies confirmed the presence of various heavy metals, at high concentrations in some cases, such as vanadium (1500 mg/kg), and iron (2200 mg/kg) (Badawieh, 2006).

Despite the fact that some technologies proved to be effective in oily sludge handling, they were not entirely adequate. For example, applying incineration procedure to oily sludge, would result in the conversion of most hydrocarbon-based wastes into carbon dioxide and water (50% to 100%) (Shleck, 1990). However, combusting large amounts of toxic organic compounds results in large amounts of hazardous gas effluents, in addition to high costs associated with this technology, and more important, the presence of heavy metals in the final ash and fumes. Other technologies that are currently available are: recycling, filtration, treatment with fly ash, coking, biological treatment, and others that are still under investigation.

Recently, centrifugation technology is being used in a wide range of refineries worldwide. Centrifugal processing of oily sludge includes the removal of the solids, and the dropping off the liquid into a fine mesh shaker to dewater the remnant liquid. The main disadvantage of this process is that the centrifugation process (even after double and triple centrifuging) cannot recover the heavier oil contents of the sludge, and 5 to 10 wt % oil content remains in the solid residue of the sludge after treatment (JETRO, 2010).

None of these technologies proved to be entirely successful yet. Some of them have operational problems, others carry a lot of environmental risks, and most of them are expensive. Furthermore, none of them focuses on the metal removal. Therefore, it was necessary to investigate a new approach (at acceptable costs, and environmentally friendly) for oily sludge management, particularly considering recovery of value added products

from wasted oily sludge. In such case, an application of electrokinetic (EK) phenomena into oily sludge might be beneficial. Electrokinetic remediation is an emerging green technology that aims to mobilize contaminants inside diverse matrices under the influence of an applied direct current (DC). Electrokinetics proved to be an effective technology to separate and extract heavy metals, and organic matter from contaminated soil and sludge (Elektorowicz, 2009; Elektorowicz et al., 1996). EK phenomena was also used for an effective separation of oily sludge into phases including water, hydrocarbons, and solid phase (Habibi and Elektorowicz, 2005). Thus, an extended investigation is required to properly apply EK phenomena in a complicated oily sludge matrix, for the sole purpose of mobilizing heavy metals, and increase their extractability potential, to guarantee a recyclable sludge and recovery of value added products.

Chapter 2

Literature Review

2.1 Petroleum oily sludge

Sludge itself is referred to as an oxidized product resulting from the oxidation of the hydrocarbons in the oil, forming insoluble materials, mostly organic in nature, such as dirt, grit, tank rust-scale... etc. Combining this product with other inorganic sediments and water yields what is known in general as petroleum oily sludge (E-Oil, 2002). Petroleum oily sludge is a viscous oily residue produced in almost every process in the oil industry, starting from digging for the oil, transporting it, refining, and finally storing it in the storage tanks. The Resource Conservation and Recovery Act (RCRA), which is issued by the Environmental Protection Agency (EPA), identified the main sources of oily sludge and residues under code of K and F037 and F038. Table 2.1 shows the main sources of petroleum oily sludge (Abrishamian et al., 1992).

Table 2.1: Sources of oily sludge

RCRA Code	Sludge Source
F037	Petroleum refinery separation sludge
F038	Petroleum refinery secondary separation sludge
K048	Dissolved air flotation (DAF) float
K049	Slop oil emulsion solids
K050	Heat exchange bundle cleaning sludge
K051	API sUSEPArator residue
K052	Leaded tank bottoms
K169	Crude oil storage tanks from refining processes
K170	Clarified slurry oil tank sediments

(EPA, 1998; Abrishamain et al., 1992)

2.1.1 Components and characteristics

The composition of oily sludge is complex, and it contains a large number of aging crude oil components, wax, colloidal, suspended solids, bacteria, salts, acid gases, corrosion products, and includes a large number of flocculants, corrosion inhibitors, scale inhibitors, fungicides and other water treatment agents in the production process of petroleum (Kriipsalu et al., 2007). The composition of the petroleum oily sludge varies depending on the origin of the crude oil, and the material used through the refining processes. Oil component consists of a mixture of hydrocarbon and non-hydrocarbon organic compounds, with some traces of inorganic compounds, which includes significant amounts of heavy metals (Ni, Cu, Cd, V, Pb, and others) (Badawieh., 2006). According to a survey conducted by the Petroleum Association for Conservation of the Canadian Environment (PACE), a typical composition of oily sludge produced from about thirty-eight refineries is as shown in Table 2.2.

Table 2.2: Average content of oil, water, and solids in sludge wastes

Sludge Source	Oil %	Water %	Solids %
Desalter bottoms	25.5	53	21.5
Neutralization pit sludge	0.5	66.5	33
Lub& grease production wastes	85 to 100	4 to 50	0 to 15
API sludge	7.5	62	30.5
Biological sludge	0.5	94.5	5
Basin settling	3	75	22
Unleaded sludge	43	12	45

(Geadah, 1987)

Oily sludge belongs to multiphase systems; oil-in-water (O/W), water-in-oil (W/O), and suspended solids. The full emulsification, and large viscosity, makes it hard to settle. The

composition of suspended components have layers of water attached to the particle surface, while the sludge particles are generally negatively charged, so the majority of particles of oily sludge are mutual exclusiveness which obstruct the combination of particles. Because of hydration and electronegativity, the particles of oily sludge form a stable dispersion state, and are extremely stable suspended illiquid (Guolin et al., 2009).

2.1.2 Quantities

One of the problems concerning the quantities of waste, and sludge produced, is that most of the oil companies do not give exact numbers of the wastes they are generating. But according to the American Environmental Protection Agency (EPA), it is estimated that each major refinery in the United States alone, produces not less than 30,000 tons of different types of sludge annually (Habibi, 2004). In Saudi Arabia, a major oil company (Saudi Aramco) facilities generate 20,000 to 30,000 cubic meters of tank oily sludge annually according to its website. However, according to a study by JETRO these amounts does not include drill cuttings generated in oil fields, and tank oil sludge generated by joint ventures between Saudi Aramco and foreign oil companies, which indicates much higher numbers throughout the country (JETRO, 2010).

2.1.3 Hazardous effect

Oily sludge affects nature in the following aspects:

1. Occupies large stretches of land. Since there is not yet a fully successful method for disposing oily sludge, it piles up in an area, and uses more and more land. This will produce large amounts of toxic gases in addition to methane gas, which could cause combustion and explosions.

2. Soil contamination. Storing oily sludge with its harmful components severely contaminates soil, and consequently groundwater.
3. Pollution of water bodies. Oily sludge with natural precipitation flows into the rivers, lakes, plus the smaller particles can be carried with the wind, and land into surface water.
4. Atmospheric pollution. Being easily biodegradable, exposed oily sludge with the appropriate temperature and humidity is easily decomposed by microorganisms, releasing many harmful gases.
5. With its toxic components, such as organic pollutants, heavy metals and other harmful substances, storing oily sludge in oil tanks for long times, increases the chances of runoffs due to leakage or any type of accidents that could cause big releases into the surrounding environment (Guolin et al., 2009).

2.1.4 Oily sludge as a controlled Haz-Mat

Oily sludge is rapidly becoming one of the big environmental problems in the world; managing it is an expensive, time consuming, and not fully guaranteed process. The toxic varied constituent this oily sludge is made of control the disposal process. Therefore, when the sludge wastes are inconsistent, thick and viscous, this complicates their treatment, and further influences equipment performance.

In 1990, the Pollution Prevention Act, Congress established a new policy of “pollution prevention” that aims to reduce hazardous wastes or limit its discharge. EPA responded in 1992 with a plan “statement of definition” that contains a group of approaches that should be followed while dealing with hazardous wastes, including refinery wastes and especially

oily sludge (EPA, 2000). These approaches in general are; a) pollution prevention; b) recycling; c) treatment prior to disposal; and d) disposal.

In the past, landfilling was the common disposal method for oily sludge, but US EPA through its Resource Conservation and Recovery Act (RCRA), listed oily sludge from different sources under code K and F as a hazardous waste, that are prohibited from land disposal (Abrishamian et al., 1992).

2.1.5 Canadian federal and provincial petroleum wastes disposal regulations

The Canadian Environmental Protection Act (CEPA) was established in 1999. This act deals with the identification, control and/or prevention of toxic substances in the environment. CEPA also acknowledged the need to eliminate essentially all persistent and bioaccumulative substances from the environment. CEPA also fulfills Canada's international and national commitments with respect to regulating air pollution and ocean dumping (CEPA, 1999). To deal with various amounts of environmental issues, CEPA issued subsystem acts that help the country in every environmental aspect.

Petroleum sludge disposal falls under the Waste Management Act. This act authorizes the provincial Environment Ministers to make guidelines and regulations pertaining to every person, commercial, industrial or public organization that produces, stores, transports, handles, treats, destroys, discharges, or disposes of wastes and special wastes. The Acts deal with licensing of disposal facilities as well as the transportation of wastes (CEPA, 1999).

In Quebec, hazardous waste disposal falls under the Environmental Quality Act regulations, where sludge containing hydrocarbons is classified under code B or J (if

contains PCBs), It states that oil wastes are prohibited from land disposal. This ban comes from section 4 in chapter 1 of (EQA) where the following is considered a toxic material:

1. Any mineral or synthetic oil;
2. Any grease that is mineral oil or synthetic oil to which thickeners have been added;
3. Any empty vessel other than an aerosol container or gas cylinder that is contaminated by:
 - a. a toxic material;
 - b. a deposit of more than 2.5 cm of oil, grease or other hazardous materials;or,
 - c. oil, grease or other hazardous materials whose quantity is greater than 3% of the volume of the vessel when its volume is less than 440 litres, or when the quantity is greater than 0.3% of the volume of the vessel when its volume is 440 litres or more;
4. Any gas cylinder or aerosol container holding oil, grease or other hazardous materials and whose internal pressure is greater than the normal atmospheric pressure (20 °C);
5. Any material or object containing only 3% or more of hazardous materials in oil or grease mass;
6. Any material and object that, when tested in accordance with the methods prescribed in the Liste des méthodes d'analyses relatives à l'application des règlements découlant de la Loi sur la qualité de l'environnement (published by the Ministère du développement durable, de l'environnement et des parcs), contains more than 1,500 ppm of total organic halogen;

7. Any material and object containing PCBs or contaminated by PCBs — polychlorinated biphenyls whose molecular formula is $C_{12}H_{10-n}Cl_n$, “n” being a whole number is greater or equal to 2 but less than or equal to 10 — that is listed below:
 - a. any liquid containing more than 50 mg of PCBs per kg of liquid; or
 - b. any solid containing more than 50 mg of PCBs per kg of solid; or
 - c. any substance containing more than 50 mg of PCBs per kg of substance;
 - d. any object — equipment, machinery, capacitor, transformer, manufactured object — containing a liquid, solid or substance mentioned above or that is contaminated by such a material;
 - e. any object or exposed metal part whose surface is contaminated by more than 1 mg of PCBs per m^2 ; and
8. Any other material or object whose surface is contaminated by oil, grease or other hazardous material (Quebec Environmental Quality Act [EQA], 2010).

Also according to the Quebec Environmental Quality Act, leachable material that produces a leachate containing a contaminant in a concentration higher than the standard set forth in Table 2.3 is considered toxic and banned from land disposal:

Table 2.3: Contaminant standard limit

Metal	Concentration (mg/L)
Arsenic	5.0
Barium	100.0
Boron	500.0
Cadmium	0.5
Chromium	5.0
Mercury	0.1
Lead	5.0
Selenium	1.0
Uranium	2.0

Maximum Concentration of a contaminant in liquids or leachates from solid materials (EQA, 2010)

2.2 Heavy metals

Heavy metals are natural components of the earth's crust; they cannot be degraded or destroyed. To a small extent they enter our bodies through food, water resources, and air. Some heavy metals are essential to maintain the metabolism of the human bodies (e.g. copper, zinc, iron), and others, such as vanadium, nickel and lead are of high industrial values (Bockris, 1977). However, at higher concentrations, they can lead to poisoning (in case of humans and living organisms) and to major industrial problems.

Heavy metals have great ecological importance, because of their toxicity and bioaccumulation. Contrary to most pollutants (e.g. petroleum hydrocarbons) they are not biodegradable, and they cannot be removed from the soil in a natural way. Since they are often immobilized within different soil components, they have long-lasting effects in soil due to relatively strong adsorption of many metals on humic and clay colloids in soils. The duration of contamination may be for hundreds and thousands of years in many cases, depending on the soil types and physicochemical properties (Alloway and Arye, 1994).

Metal mobility in the rhizosphere could be influenced by many factors, which some of them are not well documented. Basic factors include pH, temperature, redox potential, and cation exchange capacity. Researchers also included the competition between metal ions, which affect the uptake of metals by plant roots (Merian, 1991). Sorption could also affect metal mobility in the soil, given that heavy metals can be sorbed into the soil organic matter limiting the mobility of metals (Camobreco et al., 1996).

Metals in soil can be found in various forms: (a) free ions in the soil solution; (b) soluble metal complexes; (c) bound to carbonates, (this fraction is sensitive to changes of pH); (d) bound to soil organic matter (result in the release of soluble trace metals during the oxidizing or degrading processes of organic matter); and (e) precipitated residuals such as oxides and hydroxides (Tessier et al., 1979).

2.2.1 Vanadium

2.2.1.1 Physical and chemical properties

Vanadium is a white to gray metal, which is often found as crystalline form. Metallic vanadium has a density of 6.11 g/cm³, atomic mass of 50.94, melting temperature of 1890 °C, and it reaches boiling state at 3000 °C. Vanadium exists in multiple oxidation states (II, III, IV, and V) (Merian, 1991). Naturally occurring vanadium consists of around 99% ⁵¹V and the rest as ⁵⁰V. It has no particular odor. It is usually combined with other elements in the environment such as, oxygen, sodium, sulfur, or chloride. The surface of vanadium metal is protected by an oxide layer and does not react with water under normal conditions (Merian, 1991). Vanadium has a relatively low electrical resistivity of (20 x 10⁻⁸ Ω m), however, vanadium oxides regularly change structural forms under certain electrical conditions, and such changes would affect resistivity simultaneously (Corr et al., 2008).

2.2.1.2 Sources and behavior in soil

Vanadium is widely distributed in the earth's crust at an average concentration of 100 ppm (approximately 100 ppm), similar to that of zinc and nickel (Merian 1991). Vanadium is the 22nd most abundant element in the earth's crust (Baroch 2006). There are about 65 different vanadium-containing minerals; carnotite, roscoelite, vanadinite, and patronite are important sources of this metal along with bravoite and davidite (Baroch 2006; Lide 2008). It is also found in phosphate rock and certain ores and is present in crude oils as organic complexes (Lide 2008). These organic complexes are divided into three basic groups: 1) mixed-ligand tetradendates, 2) humate complexes (i.e. vanadyl-organic complexes), and 3) tetrapyrrole complexes (Lewan and Maynard, 1981). Rock weathering, soil erosion, and any process that involves conversion of the less-soluble vanadium form to a more soluble one; all contribute in releasing vanadium to water and soils (Agency for Toxic Substances and Disease Registry [ASTDR], 1992).

One of vanadium characteristics; it has high retention time in the air, water, and soil, it forms complexes with other elements and particles, and it adsorb to soil sediments. The transport of vanadium in water and soil is largely influenced by pH, redox potential, and particulate presence (ASTDR, 1992).

2.2.1.3 Vanadium applications and effects

Vanadium oxides has been recently linked to improving the performance of the high-voltage lithium ion batteries, by using V_2O_5 in surface coating of electrodes , which enhances the electrochemical performance of these electrodes, and increase their life expectancy (Wang et al., 2015). Vanadium structural strength promoted vanadium compounds to be utilized in strengthen steel and as a rust proof additives (Moskalyk and

Alfantazi, 2003). Also vanadium neutron cross section properties makes it useful in nuclear applications, where the short half-life of the isotopes produced by neutron capture, makes vanadium a suitable material for the inner structure of a fusion reactor (Matsui et al., 1996). Human exposure to vanadium could happen through food chain (olive oil, sunflower oil, apple and eggs) or it might happen through other exposure path such as air, which could cause bronchitis, irritation of lungs, throat, eyes and nasal cavities. Vanadium uptake has many known toxic effects, such as sickness and headaches, weakening, severe trembling and paralyses, skin rashes, damage to the nervous system, and inflammation of stomach and intestines (International Program on Chemical Safety [IPCS], 1988).

It was found that small amounts of vanadium in the environment might tend to stimulate plants but large amounts are toxic. Vanadium can be found in the environment in algae, plants, invertebrates, fishes and many other species. In mussels and crabs, vanadium strongly bio accumulates, which can lead to concentrations of about 10^5 to 10^6 times greater than the concentrations that are found in seawater. Vanadium toxicity is attributed to its ability to inhibit enzyme systems in animals, which have several harmful effects. It could also cause breathing disorders, paralyses and negative effects on the liver and kidneys for the animal (Merian, 1991).

2.2.2 Nickel

2.2.2.1 Physical and chemical properties

Nickel is a silver-white, hard, ductile, ferromagnetic metal, with an atomic mass of 58.78, melting point of metallic nickel is 1453°C and it reaches the boiling state 2732°C . Nickel has multiple oxidation states that include: -1, 0, +1, +2, +3, and +4 but the prevalent valences are 0, as in nickel metal, and +2 in common water-soluble nickel compounds,

such as bromide, chloride, nitrate, and sulfate salts. While nickel exists in aqueous solutions mostly as $[\text{Ni}(\text{H}_2\text{O})_6]^{+2}$, which is poorly absorbed by most living organisms, and it could be also be found in water insoluble forms, such as, NiO , Ni_2O_3 , $\text{Ni}(\text{OH})_2$, NiAs , and NiCrO_4 .

2.2.2.2 Sources and behavior in soil

Nickel makes up for almost 0.008% of the earth's crust. It is obtained primarily from sulfides ores, and to a fewer extent, from oxides ores by hydro-metallurgical refining processes.

Agricultural soil originally contains up to 1000 mg/kg of nickel. The primary sources of nickel emissions into the atmosphere are the combustion of coal and oil for heat or power generation, incineration sewage sludge, and steel manufacture. Nickel compounds, generated from these processes usually include nickel sulfate, oxides, and sulfides, and to a lesser extent, metallic nickel (Badawieh, 2006).

In various soil types, nickel show high mobility within the soil layers finally reaching ground water and, consequently rivers and lakes. Nickel could be mobilized in soil by acid rain, and by special plants, which have the ability of up-taking and accumulating metals in roots or shoots. This movement depends on a group of parameters that include: (a) type of soil, (b) soil pH and humidity, (c) the organic matter content of the soil, and (d) the concentration of extractable nickel (Hertel et al., 1991).

2.2.2.3 Nickel applications and effects

Nickel tends to create organo-metallic compounds such as $\text{Ni}(\text{CO})_4$, which could be used for nickel refining processes, and it is used as a catalyst in the chemical and petroleum industries. Nickel alloys are used in vehicles, processing machinery, tools, electrical

equipment, and household appliances, Nickel compounds are also used in batteries (Merian, 1991).

Inhalation of the nickel compounds seems to be the most dangerous method of absorption. It is confirmed that an acute inhalation of nickel to humans may produce headache, nausea, respiratory disorders, diarrhea, shortness of breath, and in some cases death (ATSDR, 2005). Other ways of exposure includes: drinking water, eating food or smoking cigarettes, even skin contact with nickel-contaminated soil or water may also result in nickel exposure. Exposure to large amounts of nickel could result in, birth defects, lung embolism, allergic reactions, heart disorder, and in the case of up-taking less soluble forms of nickel compounds such as (Nickel carbonyl - $\text{Ni}(\text{CO})_4$); higher chances of developing lung cancer, nose cancer, and prostate cancer will rise (CEPA, 1999).

Nickel is not a very mobile element in soil; since the larger part of all nickel compounds released to the environment will be adsorbed to soil particles and become immobile as a result. However, in acidic groundwater, nickel becomes more mobile and it will often rinse out to the groundwater in runoff, either from natural weathering or from disturbed soil. It could also enter bodies of water through atmospheric deposition (Young, 1953).

There is lack of research regarding the effects of nickel upon organisms other than humans. Never the less some studies confirmed high nickel concentrations on sandy soils can clearly damage plants, but some plants react to these high concentrations in a way that reduces toxicity effects, such plants could be either excluders or hyperaccumulators. Nickel is considered an essential food substance for animals, but in small amounts. However, it could also be dangerous when the maximum tolerable amounts are exceeded, which, could cause various kinds of cancer on different sites within the bodies of animals (Young, 1953).

2.2.3 Lead

2.2.3.1 Physical and chemical properties

Lead is a bluish-white, soft metal with a density of 11.34 g/cm³, melting point of 327.5°C, and a boiling point of 1740 °C. It has an atomic number of 82, and an atomic mass of 207.19 g/mol. Lead has an oxidation state of +2 in most organic compounds. The salts of Pb (II), lead oxides and lead sulfide are not readily soluble in water, with the exception of lead acetate, lead chlorate and to a lower degree lead chloride. On the other hand, inorganic lead compounds Pb (IV) are unstable and strong oxidizing agents (Merian 1991).

2.2.3.2 Sources and behavior in soil

Native lead is rare in nature; currently lead is usually found in ore with zinc, silver, copper and vanadium, and it is extracted together with these metals. The main lead mineral is Galena (PbS), but there are also deposits of cerrussite and anglesite which are mined. Galena is mined in Australia, which produces 19% of the world's new lead, followed by the USA, China, Peru' and Canada. Some is also mined in Mexico and West Germany. World production of new lead is 6 million tonnes a year, and workable reserves total are estimated 85 million tonnes, which is less than 15 year's supply (ATSDR 2005).

Lead occurs naturally in the environment; however, most lead concentrations that are found in the environment are a result of human activities. Due to the application of lead in gasoline an unnatural lead-cycle has consisted. In car engines lead is burned, so that lead salts (chlorines, bromines, oxides) will originate (Merian, 1991).

These lead salts used to enter the environment through the exhausts of cars. Now using lead in gasoline is forbidden. The larger particles used to drop to the ground immediately and pollute soils or surface waters, and the smaller particles travelled long distances

through air and remained in the atmosphere. Part of this lead falls back on earth when it rains. This lead-cycle caused by human production is much more extended than the natural lead-cycle.

Due to the low water solubility of lead compounds, lead is easily adsorbed to all clayey soils. Harter (1983) showed the adsorption tendencies of lead ions and the variance for different types of soils. Results showed that the adsorption of lead ions strongly depends on pH, with higher pH values promoting the adsorption of lead onto soil surfaces.

The soil organic content is also considered a major contributor to the retention of lead. Lead tends to form organometallic complexes, where retention of lead is more likely to happen through complexation rather than metal-organic precipitation (Yong, et al., 1992; Harter, 1983)

2.2.3.3 Lead applications and effects

Lead is used in applications where its low melting point, ductility and high density are advantageous, e.g. casting small arms and ammunitions, roofing material, cladding, and to reduce wearing of machine tools. Lead is largely used in lead car batteries, mostly as electrodes (Merian, 1991).

Lead is one out of four metals that have the most damaging effects on human health. It can enter the human body through uptake of food (65%), water (20%) and air (15%). Foods such as fruit, vegetables, meats, grains, seafood, soft drinks and wine may contain significant amounts of lead (ATSDR, 2007). Cigarette smoke also contains small amounts of lead.

Lead can enter into drinking water through pipes corrosion. This is more likely to happen when the water is slightly acidic. That is why public water treatment systems are now required to carry out pH-adjustments in water that will serve drinking purposes.

Lead can cause several unwanted effects, such as (ATSDR, 2007); Disruption of the biosynthesis of haemoglobin and anaemia, rise in blood pressure, kidney damage ,disruption of nervous systems, brain damage, declined fertility of men through sperm damage, diminished learning abilities of children, and behavioural disruptions of children, such as aggression, impulsive behavior and hyperactivity.

Lead accumulates in the bodies of water organisms and soil organisms. These will experience health effects from lead poisoning. Health effects on shellfish can take place even when only very small concentrations of lead are present. Body functions of phytoplankton can be disturbed when lead interferes. Phytoplankton is an important source of oxygen production in seas and many larger sea-animals eat it. That is why we now begin to wonder whether lead pollution can influence global balances (ASTDR, 2007).

Table 2.4 gives a brief comparison of the basic properties of the three metals (vanadium, nickel, and lead).

Table 2.4: Comparison between vanadium, nickel and lead general properties

Property	Vanadium	Nickel	Lead
Melting point	1890	1453°C	327.5
Boiling point	3000	2732 °C	1740
Density (@20°C)	6.00 g/cm ³	8.91 g/cm ³	11.34 g/cm ³
Colour	Greyish	Silver-White	Bluish-White
Atomic number	23	28	82
Atomic mass	50.94	58.71	207.19
Electrochemical potential	-1.20 V	-0.24 V	-0.126 V
Oxidation states (bold most stable)	-1,+2,+3, +4 ,+5	-1,0,+1, +2 ,+3,+4	+1, +2 ,+3,+4
pH effect on mobility of the most stable oxidation state of the metal.	pH<8 mobile pH>8 less mobile	pH<6.5 mobile pH>6.5 immobile	pH<4.2 mobile pH>4.2 mobile slowly to immobile

(Merian 1991; ATSDR 2012; Choudhury 1998)

2.3 Heavy metals in petroleum sludge

The crude oil fraction of the oily sludge contains three different fractions: paraffinic, naphthenic, and aromatic which also contains sulfur and nitrogen. The second part of the crude oil is the resins coating, and asphaltenes. The resins are a brown sticky hydrocarbon which contain nitrogen, oxygen, and sulfur, are soluble in n- pentane but insoluble in propane, and have molecular weights greater than 3000. The asphaltenes contain the chelated metals, vanadium, nickel, and possibly some calcium along with sulfur, oxygen,

and nitrogen (Muslat 2005). During crude oil distillation, the asphaltenes are not volatilized, and remain in the vacuum reduced crude oil, along with most of resin fraction, which would eventually settle as a dense oily sludge fraction (Muslat 2005). Crude oils, typically contains traces of heavy metals, where vanadium, nickel, and iron being the most common. Usually they are in an oil-soluble form, not removable by water-washing or filtration, and in conventional refining processes they become concentrated in the residual fuel oil fractions. In some cases the concentration of vanadium in petroleum sludge samples reached up to 1500 ppm (Amorim et al., 2007) which is higher than any other trace metal. The presence of metals in petroleum sludge is highly undesirable; it complicates the treatment processes by being neither degradable nor destroyable, which eliminates common procedures such as landfills and incineration. The presence of heavy metals in oily sludge can influence the biodegradation of organic materials, where it proved to have harmful effect on the hydrocarbon oxidizers in decomposing petroleum hydrocarbons (Muslat 2005). In addition, a study by Jensen (1977) illustrated the effect of lead on the biodegradation of oily waste in soil, where a change in the population of soil microbiota was noticed in the soil because of the presence of lead in particular. Measurements of oxygen consumption revealed increased microbial activity after the waste was added to soil. Adversely, the presence of lead noticeably reduced this activity with prolonged lag phase in the biodegradation of oily sludge. It affects the yield of fuels in the recycling processes of the sludge by producing impure fuels, when burned, metal rich fuels produce toxic oxides and cause corrodibility and produce ashes that can damage engines. Metals in sludge could be found in different ratios according to the sources and handling processes of the sludge, such as refining, chemicals added, storage and even transportation.

Table 2.5 shows different concentrations of heavy metals in a bottom tank oily sludge samples collected from different sources.

Table 2.5: Metal content of petroleum oily sludge from different sources

Metal (ppm)	Canadian refinery (1)	Omani refinery (2)	Greek refinery (3)
Fe	2200	NA	NA
Pb	8	206	422
Cd	63	NA	17
Ni	40	18.8	1249
Cu	12	33.4	438
Zn	80	759	NA
V	30	NA	NA

(1)Badawieh, (2006), (2) Al-Futaiasi et al., (2007), (3) Karamalidis and Voudrias (2008)

Moreover, Iwegbue et al., (2009) investigated the characteristic levels of heavy metals in soils that have received significant impact of crude oil spillage in the Niger Delta. The results showed a significant presence of metals (Cu, Zn, Pb, Ni, Cr, Cd, Mn) in the soil, which affected the properties of the soil negatively.

2.4 Emulsions

Emulsion is a mixture of two immiscible liquids in which fine droplets of one liquid is dispersed in another, as droplets of colloidal sizes(0.1-10 μ m) (Gillies et al., 2000). There are thermodynamically stable and unstable emulsions. For stable emulsions, certain energy is required through shaking, stirring, homogenizers, or spray processes to form unstable stable system (demulsification) (Mackay, 1987).

Emulsions are undesirable in petroleum industry because of their influences on pipeline transportation difficulties (Piondexter and Lindemuth, 2004).

Demulsification (leading to separation of phases) can be achieved through the following processes: flocculation, sedimentation (creaming) and coalescence (Piondexter and Lindemuth 2004). The first two result from variation of density between two phases, and promoted by large droplet sizes, high differences in density and low viscosity of the continuous phase (dispersion medium) (Morrison and Ross, 2002). Flocculation is a reversible formation of droplet clusters where two or more droplets clump together, touching only at certain points, and with virtually no change in total surface area. Oil-in-water (O/W), and water-in-oil (W/O) emulsions undergo special flocculation mechanism, where the individual droplets retain their size and shape, but lose their kinetic independence, because of the sedimentation-creaming rate. All three processes are reversible, where applying agitation will promote the recovery of original dispersion state. However, coalescence is considered more aggressive, where the complete merging of two full droplets into one is facilitated by film drainage and film rupture between two aqueous drops (Ahmed et al., 1999).

The properties of the interface between water and oil are important in determining the stability of an emulsion system. The formation of an interface between the dispersed phase and the continuous phase increases the system free energy, therefore the emulsions are thermodynamically stable, and tend to minimize the surface area by break-up of emulsions. If the interfacial film is weak, the emulsions stability will be poor. The dispersed droplets will collide and the collisions will lead to droplet fusion, i.e. coalescences (Karbaschi et al., 2014; Piondexter, and Lindemuth 2004). Indigenous amphiphilic substances in the crude oil, i.e., asphaltenes and resins, are traditionally considered as natural emulsifiers responsible for the stabilization of W/O emulsions. Formation of three-dimensional films

of asphaltene aggregates at the oil-water interface is believed to protect water droplets from coalescence. In addition, waxes, fine solids (e.g. scale, sand and clay) and naphthenates may contribute to the film strength at the oil-water interface (Ahmed et al., .1999).

2.5 Oily sludge management

Oily sludge large volumes and toxic components require feasible disposal method that guarantees both; economic and environmental benefits. Unfortunately, the variant composition of petroleum sludge, resulting from different sources of extraction and refining processes, rendered most conventional methods obsolete. However the following procedures were able to provide a partial solution of the problem.

2.5.1 Recycling

New legislations demand that, oily sludge shouldn't be disposed, unless its oil content is reduced to a certain limit (Jean and Lee, 1999). Different methods could be used to achieve this purpose, including on-site treatment and oil reclaimers. These processes will result in minimizing the waste generated, and the recovery of the valuable oil that could be used or sold. RCRA defined recycled oil as “any used oil which is reused following its original use, for any purpose, including the purpose for which the oil was originally used; thus, recycled oil includes oil which is re-refined, reclaimed, burned, or reprocessed” (Atlas, 1984).

Refineries could use on-site oil reclaimers, which follow different methods for oil, water and solids separation. Jean and Lee (1999) described the mechanical separation of oil and water from oily sludge by the deliquoring process of oily sludge, which still needs a lot of research. Habibi and Elektorowicz (2004) used the electrokinetic phenomena for an

effective separation of oily sludge into phases including water, hydrocarbons, and solid phase. They suggested that this method allows for recycling of hydrocarbon residue from a waste product to a usable refinery product, by reducing the water content by 63%.

2.5.2 Filtration

It could be considered a method of dewatering oily sludge; usually this process yields a reduced amount of oily cake, and little oil in the liquid phase. Applying filtration before sending the sludge into a disposal or incineration site will reduce the cost of these processes considerably, depending on the sludge volume, and oil or water content. It is preferable that the oily sludge introduced to the filters would contain low oil concentrations, since it was found that sometimes this oil blocks the filter cloth, but adding calcium carbonate to the sludge could prevent it (Dando, 2003).

2.5.3 Treatment with fly ash

Dewatering is a very important process to reduce sludge volume; however the presence of oil in the sludge causes operational problems. It was found that adding fly ash to the oily sludge, decreases the specific resistance to filtration, and capillary suction time C.S.T (dewaterability) of the sludge (Hwa and Jeyaseelan, 1997).

Hwa and Jeyaseelan (1997) added in their experiment different dosages of fly ash to multiple samples of oily sludge. After each dosage, the sludge characteristics (capillary suction time (CST), filtration resistance, solid content in the sludge cake, and the particle size distribution in the sludge after conditioning) were measured. The optimum dosage that yielded in the least CST, and the lowest specific resistance to filtration was 3%. However, this value would vary depending on the original characteristics of the sludge. As a result,

solid content increased in the sludge cake, and there were less suspended solids with filtrates. But the volume of toxic waste increased. On the other hand, fly ash might contain heavy metals, which means more toxicity in the final mixture.

2.5.4 Incineration

One of the most common methods for oily sludge disposal is incineration. Rotary kiln and fluidized bed incinerators are the most known incinerators; they are either integrated with the refinery or placed off-site, where the process could be carried out by a contractor.

A rotary kiln usually 8-12 m long, 1-5 m in diameter, and the average combustion temperature inside is between 800 to 1400°C, for a duration of 60 minutes. The fluidized bed incinerator consists of a vertically cylindrical brick-lined combusting chamber. Sludge or wastes in general are introduced into the chamber from the sides into the fluidized bed where it is incinerated at a relatively low temperature (800-950°C) (UNIDO, 1993).

In the process, the contaminated oily sludge is fed into the incinerator that contains gas or oil burners that provide an operating temperature of (800 to 1400 °C). Waste material is combusted in the presence of a relatively large excess of oxygen (air), which will result in the conversion of most of the hydrocarbon-based wastes to carbon dioxide and water vapor (50% to 100%) (Shleck,1990). Despite the fact that incineration is a very effective method, it is considered not environmentally friendly. The following shows some concerns associated with incineration (Szente et al., 2003):

1. The combusting of toxic organic compounds results in a large amount of hazardous gas effluents that need to be treated before being released into the atmosphere;

2. In the case of off-site incinerators (which is the case in most refineries), transportation costs are high due to environmental risks;
3. Incineration processes are usually very expensive, and it is more expensive in case of oily sludge incineration, because a typical oily sludge from most refineries could contain up to 60% water, which implies a high amount of energy to burn;
4. Fly ash, resulting from the incineration process, contains heavy metals, and since this ash is usually sent to landfills, the heavy metal leaching becomes another problem to be solved.

2.5.5 Coking

EPA explained that the main purpose of cokers, is to thermally convert longer-chain hydrocarbons to recover light hydrocarbons that are used to produce fuels. The typical coker yield about 30% petroleum coke and 70% light hydrocarbons that will be refined to high-grade fuels (Orr and Maxwell, 2000).

Coking operations are used to dispose of undesirable residues by converting them into valuable products. Coker plants produces coke from oily sludge that is collected from different sources in the refinery. In the operation, while most of the oily sludge fed into the coker vaporizes in the hot coking process, the lighter fractions are returned through the upper lines back to the refinery fractionation process. The final coke product will combine solids and non-volatiles from the original oily sludge which include heavy metals (Shah, 2004).

2.5.6 Biological treatment

Organic content defined by Biological Oxygen Demand (BOD) can be reduced in the refineries' effluent by a biological oxidation of the organic matter into inorganic matter and microbial cells. The goal of biological treatment is to reduce organic wastes and its toxic effects to very low levels. In biological treatment, factors such as; pH, sulfides, nutrients, and temperature should be controlled. Also the availability of nutrients is essential for microorganisms (Davis, 1967).

Oxidation ponds, activated sludge treatment, and biological contactors are considered the major units of the biological treatment facility (Atlas, 1984). However, organic forms and their concentrations have to be at the level, which do not inhibit the microbial growth.

2.5.6.1 Biodegradation of Oily Sludge

Biodegradation is carried out by soil bacteria and fungi as a natural process. Recently and after an extended research, many microbial communities demonstrated their ability of breaking down certain hydrocarbons, or transforming some chemical substances present in petroleum wastes into nonhazardous products (Korda et al., 1997).

Bioremediation in comparison to other technologies (e.g. incineration), is considered a cost-effective technology that rarely yields undesirable side compounds in specific biodegradable compounds treatment. In this technique, organic sludge is mixed with active microbial seeds and appropriate nutrients in an engineered reactor. This treatment increases the speed of biodegradation of the organics, by providing optimal conditions (pH, temperature, nutrients, and dissolved oxygen) for these microorganisms (Korda et al., 1997).

Some microbial strains are available commercially for bioremediation. Each of them is responsible for degrading specific compounds. Soriano and Pereira (2002) grew microorganisms in a medium that contains only oily sludge as a source of carbon and energy. The two parameters that were investigated were the microbial adaptation to the environmental variables around it, and the aeration process. The consumption rate was 89%, 99%, and 93% for oil and grease, n-paraffins, and total polyaromatics, respectively. Usually hydrocarbons in oily sludge are found as a mixture; thus, and because none of the organisms could degrade all the different kinds of hydrocarbons, the larger the diversity cultures, the better remediation achieved. Said et al. (2004) applied a fungal strain (*Paecilomyces variotii*) and a bacterial strain (*Bacillus cereus*) as a co-culture to an oily sludge that was taken from a crude oil storage tanks. About 35% of the non-volatile total petroleum hydrocarbons and 81% of the aliphatic hydrocarbons were degraded. It is obvious that the biological treatment is only concerned with the organic hydrocarbon part of the oily sludge. The other major toxicant, such as heavy metals are ignored, which indicate, that these methods are solving part of the problem only.

2.5.6.2 Composting

EPA defined composting as “the use of a biological system of micro-organisms in a mature, cured compost to sequester or break down contaminants in water or soil” (EPA, 1997). Oily sludge composting techniques, are very similar to the open and closed composting systems, already used in treating organic wastes such as municipal sewage solids, agricultural crops, manure and others. On the other hand, some adaptation is necessary, due to the fact that the behavior of soil is different from that of organic wastes. Aeration of the soil is required in the composting process which allows microorganisms to use

contaminants in the soil transforming them into carbon dioxide, water, and salts (Dando, 2003).

In the case of having oily sludge as the contaminant, the ultimate goal will be to reduce the hazardous organic compounds concentrations in the sludge, in order to stabilize it. Giles et al., (2001) examined the feasibility of using composting as an effective bioremediation method. They found that nine out of the twenty strains that were isolated from the sludge used the sludge as the carbon and energy source. These strains were used in their experiments which resulted in the following: the total petroleum hydrocarbons (TPH's) at 46 µg/g were reduced in the sludge by 97.4% in 10 weeks.

2.5.7 Landfarming

Landfarming (called also land treatment) is a technique that depends on the soil microbial communities to degrade and stabilize hydrocarbon wastes. Landfarming involves spreading excavated contaminated soils or sludge in a thin layer on the ground surface and stimulating aerobic microbial activity within the soils through aeration and the addition of minerals, nutrients, and moisture. The enhanced microbial activity results in degradation of adsorbed petroleum product constituents through microbial respiration (EPA, 1994). Unlike landfilling, land treatment was an accepted land-disposal technique under RCRA (with some conditions applied), and it does not use any physical barriers to isolate hazardous waste and prevent leaching or migrating. Instead, soil processes (precipitation, cation exchange reactions, and complexations) ensure, to some extent the immobility of these constituents. EPA defined landfarming as “an open system that relies on dynamic physical, chemical, and biological processes to degrade, transform, or immobilize hazardous organics in the soil” (Atlas, 1984).

A general report evaluating land treatment was conducted by the Environmental Research and Technology association (ERT) in 1984 and handed in to API. In the report ERT indicated that land treatment, could successfully result in degrading the organic matter, immobilizing multiple heavy metals and any other inorganic matter, if the appropriate environmental and operational conditions exist (EPA, 2000). Such operational conditions according to EPA and under RCRA directions include that:

- a. Landfarming location should be outside of a 10-year flood zone;
- b. The depth of the waste should not exceed 1.5 m;
- c. Continued monitoring of the groundwater must be repeated for 90 days from the last waste application.

Despite the fact that land farming is unexpansive, and effective technique for oily sludge treatment, there are still operational and environmental concerns associated with it. For example, complete degradation period is very long, and carries some environmental risks that involve all media: surface and ground water, soil, and atmosphere.

Hejazi et al., (2003) indicated that, the highly volatile organic compounds associated with the degradation processes, impose high environmental health risks to workers on the site.

Other disadvantage is associated with the heavy metals permanent presence in land used for landfarming. These metals might migrate into groundwater if the appropriate membrane liners are not provided to protect soil from erosion or any extreme weather conditions.

Despite the metals are immobilized, their presence implies the problem is not solved yet.

In 1992, EPA published a final rule for various hazardous wastes disposal that include hydrocarbons. This law prohibited the land disposal of untreated hazardous waste. As a

result, most of the traditional landfarming areas in North America were closed (Hejazi et al., 2003).

2.5.8 Centrifugation

Centrifugation is a mechanical separation process where solids and liquid are separated by centrifugal force. This technique is being used in a wide range in the gulf oil rich countries ECO (Emirates Environmental Protection Company, 2009). Centrifugal processing of oily sludge includes the removal of the solids and the dropping of the liquid into a fine mesh shaker to dewater the remaining liquid. The sludge will be pumped to a set of desilter hydrocyclones, to separate fine particles from the liquid, the oily water. Oily water from the centrifuge will be sent to a dropout tank for gravity separation in the tank. It will be then pumped to the interceptor tank for oil-water separation. Through a dissolved air flotation unit, the water is treated with a coagulant and flocculent to separate oil from water. The oil will float on water and transfer to an oil collecting unit (JETRO, 2010).

The main disadvantage of the this process is that centrifugal process (even after double and triple centrifuging) cannot recover the heavier oil contents of the sludge and 5 to 10 wt % oil content remains in the solid residue of the sludge after treatment. Also centrifuge dewatering requires a high-energy input to increase the centrifugal speed, or to flocculate sludge at optimal dosage (Chu et al., 2005), and the addition of polymer or flocculants demands operational input. Meanwhile, the produced cake needs further treatment for disinfection, and more importantly removal of heavy metals, regularly available in upstream or downstream petroleum oily sludge.

2.5.9 Phytoremediation

Using plants for environmental remediation is a very old idea. However recent studies and field applications yielded very interesting results, which in many cases, confirm the feasibility of phytoremediation as a trusted remediation option.

Phytoremediation is the use of green plants to remove pollutants from the environment, or contain their toxic effect to render them harmless. These pollutants could be heavy metals, hydrocarbons, organic chemicals, and other contaminants that could be found in soil, and water bodies (Lasat, 2002).

Badawieh (2006) applied this technique successfully on oily sludge samples contaminated with high amounts of heavy metals. In the study, scented geraniums were planted in a series of pots containing oily sludge, where heavy metal concentrations were artificially increased up to 2000 ppm. Scented geraniums were able to survive the harsh conditions for 50 days, accumulating up to 1600 mg, 1000 mg, and 1200 mg, of Cd, Ni, and V respectively per kg dry weight of the plant.

Phytoremediation varies depending on the type of contaminant to be treated into the following techniques: phytoextraction, phytodegradation, phytovolatilization, and phytostabilization.

- a. Phytoextraction is the uptake of pollutants from the contaminated zones by plants that accumulate these contaminants in their tissues. In some cases, the contaminant could be restored and reused again, like the case of some heavy metals. This process requires specific plants that have the ability to accumulate high concentrations of a particular contaminant (e.g. heavy metals). These species are known as hyperaccumulators (Prasad and Freitas, 2003). For example *Brassica*

juncea (Indian Mustard) is a high-biomass plant that could transport lead to the shoots, accumulating >1.8% lead in the shoots (dry weight) (Kumar et al., 1995).

b. Phytodegradation (or phytotransformation) is the process of up-taking organic contaminants from soil, and transforming it to non-hazardous forms, by any plant-associated microflora (Schnoor, 1997). Similar to phytoextraction, phytodegradation requires organic contaminants to be biologically available for absorption or uptake by plants. Bioavailability of organic matter depends on the soil characteristics (organic matter content, pH, clay or sand type and content), age of the contaminant, and the characteristics of the compound (Cunningham et al., 1995). For example, growing Willow stand (*Salix viminalis*) in oil contaminated sediment, resulted in 79% oil degradation in the root zone of the stand (Vervaeke et al., 2003).

c. Phytovolatilization is another form of phytoremediation, whereby volatile compounds are absorbed in the plants and released into the atmosphere through transpiration processes. Phytovolatilization is observed when plants take up water, organic and inorganic contaminants. Some of these contaminants could go directly through the plants to the leaves and volatilize into the atmosphere at rather low concentrations (Interstate Technology and Regulatory Cooperation [ITRC], 1999). One problem associated with phytovolatilization, is that by transferring contaminants from soil or groundwater into the atmosphere, toxic gases are being released into the air. As a result, phytovolatilization must be monitored to avoid pollution translocation. According to Burken et al., (2001) introducing live hybrid

poplar plants into benzene contaminated soil, enhanced the volatilization process of the benzene without observing any toxicity effect on the plant itself.

d. Phytostabilization is an opposite process to phytoextraction. In this case, the goal is to make the contaminant (metals and organics) less bioavailable for plant uptake, which will protect plants from the toxic effect of these elements, and consequently prevent entering the food chain. Therefore, since metals will be insoluble and stable, lower leaching of metals into near groundwater aquifers is expected (Matso, 1995).

Time is the downfall of this technique, but applying this technique on large field for a long period of time could be feasible.

2.5.10 Unconventional methods/studies

Using non-ionic and anionic surfactant in the treatment of oily sludge were also investigated to improve oil sludge management. For example, Guolin et al., (2009) washed and mixed sludge with ethoxylation alkyl sodium sulfate (Na-AES) in order to achieve maximum recovery of crude oil. According to Guolin et al., (2009) applying this technique on bottom tanks oily sludge resulted in the recovery of 99.24% of crude oil at optimal conditions.

Different kind of studies aim to utilize the sludge commercially rather than treating, or storing it. Sengupta et al., (2002) tried to form bricks from petroleum effluent treatment plant sludge. In an attempt to utilize all the components of oily sludge, a laboratory-scale investigation was carried out on the partial replacement of raw materials used in making masonry bricks from the sludge. Bricks prepared by replacing about 30% of the raw materials (clay, sand, and water) with the sludge, were found to conform to the Indian

standard specification for common burnt clay building bricks. In the process, the water in the sludge served as the process water, the hydrocarbons burn provided about 5% of the fuel requirement for brick, and the inorganic materials are fixed as constituents of the bricks.

2.6 Oily sludge management with respect to metals

The majority of previously mentioned in situ and off-site techniques proved to be one dimensional treatment methods, with many disadvantages in most cases.

Some of the better newly developed methods such as soil/washing, bioremediation, and solidification/stabilization techniques are commonly used these days. However these techniques fail when low permeability soils are encountered. Flushing is very difficult with low permeability and stabilization agents are vulnerable in clayey colloids (Elektorowicz 2009; Elektorowicz et al., 2008b), and bioavailability of organic xenobiotics is limited (Elektorowicz, 2009).

The big challenge comes when a mixture of contaminants or contaminant with mixed content is present. For example petroleum oily sludge contains both organic waste and heavy metals, the following summarizes these challenges:

1. Both organic and inorganic contaminants influence their properties in soil;
2. Soil components behave in different ways upon the presence of these groups;
3. The method of treatment used to treat one waste product might have a large impact on the other contaminant and the environment eventually;
4. Treatment method might fail with the presence of the other waste group in soil.

The movement of heavy metals is greatly influenced by the quantity of organic matter in the matrix. For example humic and fulvic acids can form complexes with the metals and precipitate, which affect the fixation of metals (Serpaud et al., 1994; Kaschl et al., 2002; Elektorowicz, 2009). Furthermore the mixed metals compete for adsorption places in soil, depending on the type of soil, type of metals, and their concentrations. And since the fraction of soil might be occupied by residual organic contaminants, the adsorption capacity of heavy metals will decrease affecting their mobility in the process (Kaoser et al., 2004a; Kaoser et al., 2004b; Elektorowicz 2009). In addition, it is believed that the mobility of some metals is affected by synergistic and antagonistic factors especially with the presence of mixed contaminant in the matrix (Reddy et al., 1999).

Technologies that deal with mixed contaminants, both inorganic (e.g. heavy metals, radionuclides) and organic (e.g. PAHs), need to be developed. And the need of new complete sustainable technology for oily sludge treatment is a must.

2.6.1 Electrokinetics (EK)

Electrokinetic remediation is an emerging green technology that has attracted scientists, governments, and investors. This method aims to mobilize contaminants inside diverse matrices under the influence of an applied direct current (DC) (Virikutyte et al., 2002; Hatem, 1999; Cabrera-Guzman et al., 1990). When the DC electric fields are applied to the contaminated soils or colloidal matrix via special electrodes, positive ions travel towards the negatively charged cathode, while negative ions move towards the positively charged anode. Uncharged species would be carried through electroosmotic flow (initiated by the redox reactions), and other electrokinetic mechanisms (Ch. 2.6.1.1, 2.6.1.2, and 2.6.1.3) (Reddy and Cameselle, 2009; Acar et al., 1995).

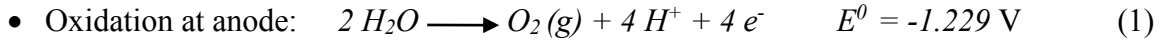
This innovative technique is used to separate and extract heavy metals, radionuclides and organic components from soils (Elektorowicz and Hakimipour, 2002; Reddy and Saichek 2004; Zhang et al., 2012), sludge (Ibeid et al., 2015; Elektorowicz and Habibi 2005), and ground water (Chu and Lee, 2009; Chew and Zhang 1999).

The two primary motions in soil and sludge are electromigration and electroosmosis. In sludge, the electrophoretic phenomenon also appears. In electromigration, charged particles are transported through the matrix. In contrast, electroosmosis is the movement of a liquid (e.g. water) relative to a stationary charged surface (e.g. fine clay particles).

2.6.1.1 Electromigration

Electromigration is defined as the migration of the dissolved ionic species in the pore fluid towards the electrodes, in the presence of an electrical field (Reddy et al., 2003). Anions such as chloride and fluoride ions move towards the anode while metal ions and ammonium ions move towards the cathode (Giannis et al., 2005). The degree of electromigration depends on the mobility of the ionic species which depends on the conductivity and porosity of the matrix, pH gradient, applied electric potential, initial concentration of the specific ions, and the presence of competitive ions (Reddy and Cameselle, 2009).

The pH gradient has an effect of the mobility of the components. In moist soil/colloidal systems electrochemical reactions are induced by applying an electrical current, which causes the decomposition of water (electrolyte) at the electrodes (electrolysis reactions). The electrolysis reactions generate oxygen gas and hydrogen ions (H^+) at the anode (oxidation), hydrogen gas and hydroxyl ions (OH^-) at the cathode (reduction), (Reddy and Cameselle, 2009). The endothermic reactions are shown in the following equations:



As a result, the hydrogen and hydroxyl ions migrating into each electrode generate the acidic conditions at the anode area, and alkaline conditions at the cathode area. The migration of H^+ and OH^- from the anode and cathode into the matrix leads to influential changes in the matrix pH, when initially introducing the electrical field (Reddy and Cameselle, 2009; Acar and Alshwabkeh, 1993). These electrolysis reactions are crucial in the transport, transformation, and degradation processes that affect the contaminant remediation when electrokinetics is applied.

2.6.1.2 Electroosmosis

Electroosmosis is the pore fluid movement, which contains dissolved ionic and nonionic species in soil under an electric field. Based on diffuse double layer theory, a relatively immobile layer of cations will be held in the Stern layer, surrounding the negatively charged particle core, while in the diffuse layer. Cations and some anions will be found as well as water molecules. Under an electric field, the excess ions the diffused layer migrate toward the oppositely charged electrodes. As they migrate, they create a momentum in the surrounding fluid, via viscous forces causing an electro-osmotic flow (Reddy and Cameselle, 2009). Electroosmosis is considered the major transport process for any organic and inorganic contaminant that is dissolved, suspended, or emulsified.

Electroosmotic flow velocity (v_{eo}) according to Helmholtz-Smoluchowski H-S theory is directly proportional to the applied voltage gradient (E_z), zeta potential (ζ), and dielectric constant (D) of the fluid, and inversely proportional to the fluid viscosity (η) :

$$v_{eo} = - (D\zeta/\eta) E_z \quad (3)$$

Where: v_{eo} in (m/s), ζ in (V), η in (Pa. s), E_z in (V)

Electroosmotic flow could be expressed by the volumetric flow rate (q_{eo}), depending on the electroosmotic permeability coefficient (K_{eo}) which is the volume flow rate of water flowing through a unit cross – sectional area due to unit electric gradient under constant conditions within a short duration (Habibi, 2004). The electroosmotic flow rate was estimated by Casagrande (1948) and expressed in the following equation:

$$q_{eo} = k_{eo} i_e A = k_i I \quad (4)$$

Where: q_{eo} = electroosmotic flow rate [cm^3/s]

k_{eo} = coefficient of EO permeability [$\text{cm}^2/\text{V.s}$]

i_e = gradient potential [V/cm]

A = cross-sectional area [cm^2]

k_i = coefficient of water transport efficiency [$\text{cm}^3/\text{A.s}$]

I = applied current [A]

2.6.1.3 Electrophoresis

Electrophoresis is the transport of charged particles of colloidal size upon the application of an electrical field (Virkytyte et al., 2002). Ideally, the highest charged particles can reach the farthest distance. Inside an electrical field matrix, molecules with the same size and charge, all move the same distance, whereas different size molecules move different distances. This concept should apply to all electrically charged particles such as clay particles, organic particles, droplets, surfactant micelles, complexes of chelation agents,

etc. These particles transfer the electrical charges, and affect the electrical conductivity and the electroosmotic movement (State Water Laboratory of Victoria, 1993). Electrophoresis is an important mechanism in electrokinetic soil remediation, when surfactant is added into the fluid to form micelles (charged particles) (Pamukcu and Wittle, 1992). This movement widely contributes to the transport of contaminants in the form of colloidal species. Ionic micelles often carry a high charge, and exhibit a high conductance in dilution. Therefore, by increasing the concentration of surfactants, a build-up of charge occurs due to further aggregation, and, as a result, the conductance increases (Pamukcu et al., 1995).

Mass transport by electrophoresis is considered negligible in low-permeability soil systems in comparison with ionic migration and electroosmotic transport. However, in sludge, electrophoresis might exhibit a more important role in the transport of constituents.

2.6.1.4 Applications of electrokinetic phenomena

Electrokinetics proved to be an effective technology to separate and extract heavy metals and organic matter from contaminated soil and sludge (Yuan and Weng, 2003; Elektorowicz et al., 1996). EK system applied on soil has demonstrated 85-95% efficiency in removing heavy metals such as arsenic, cadmium, chromium, lead, mercury, zinc, and nickel (Virkiute et al., 2002). Wang et al., (2005) achieved a high efficiency removal of heavy metals such as: 95% for Zn, 96% for Cu, 90% for Ni, 68% for Cr, 31% for As and 19% for Pb from a sewage sludge matrix. Amrate and Akretche (2005) used successfully EDTA enhanced EK remediation system for lead removal from contaminated soil.

In the field of organic remediation Li et al., (2011) applied electrokinetics-enhanced biodegradation technique to remediate soil contaminated with heavy polycyclic aromatic hydrocarbons, around iron and steel industrial areas. They achieved an increase of the

degradation extents of the three PAH samples by 7.9 to 8.6%, and 11.0–18.4% and 17.2–25.6% when the biodegradation technique was enhanced by electrokinetics. Elektorowicz and Boeva (1996), used electrokinetic system to supply of nutrients in soil for bioremediation purpose.

Maini et al., (2000) were able to remove 90% PAHs of a historically contaminated site in East London, using EK, and depending on electroosmosis phenomena. Furthermore, electrokinetic systems have been applied into sludge dewatering and thickening (Yuan and Weng, 2003; Banerjee and Law, 1998). The application of an electric current into waste sludge released the bound water in the sludge and increased solids content up to 65% (Eckenfelder et al., 1981).

Through the last two decades, the research group at Concordia University studied the possibility of applying electrokinetic technology for extraction and separation of phases in soil, municipal sludge, and oily sludge. One major study was conducted by Habibi and Elektorowicz (2004), where electrokinetic phenomena was used for an effective separation of oily sludge into phases including water, hydrocarbons, and solid phase. They suggested that this method allows recycling of hydrocarbon residue, from a waste product to a usable refinery product, by reducing water content by 63%. Chifrina and Elektorowicz (1998) applied this technology on a mixed system of soil-water-diesel fuel (which represented hydrophobic organic compounds). They aimed to optimize the organic contaminant removal from sludge by adding small amounts of surfactants. They were successful in the remediation of HOCs by inducing the flocculation rate in the system. Esmaily (2002) applied EK into a municipal and industrial wastewater sludge that contains around 5% of

solids, for the purposes of dewatering, metals and organic matter reduction as well as pathogen destruction to reduce the hazard associated with disposal or reuse in the future.

Habel (2010) demonstrated that enhanced EK treatment of pathogen contaminated biosolids, is capable of delivering a product virtually free of viable *Ascaris suum ova*, when introduced to the conditioned sludge.

2.6.2 Supercritical fluid extraction (SFE)

Supercritical fluid is a gas or liquid at conditions above its critical temperature and pressure (above its critical point). The critical point in Figure 2.1 is the point located at the end of the vapor pressure curve (Krukonis et al., 1994). The highlighted region in Figure 2.1 denotes supercritical fluid space, where many fluids exhibit the ability to dissolve materials because of their in-between properties of those of liquid and gases. These properties induce the solubility of many contaminants, and make it easily transferable from their original medium (LaGrega et al., 2001).

Because of its low viscosity and high diffusivity, transport rate of solutes in supercritical fluid may be significantly higher than that in conventional solvents (Abd El-Fatah et al., 2004). The most common supercritical fluid used is carbon dioxide. CO₂ in comparison to other supercritical fluids is considered inexpensive, and the waste while using CO₂ is nontoxic (Elektorowicz and Ju, 1997; Abd El-Fatah et al., 2004; Erkey, 2000). CO₂ reaches its' critical point at relatively low temperature (31.1 °C) and pressure (7.38 MPa). (Hansen et al., 1992).

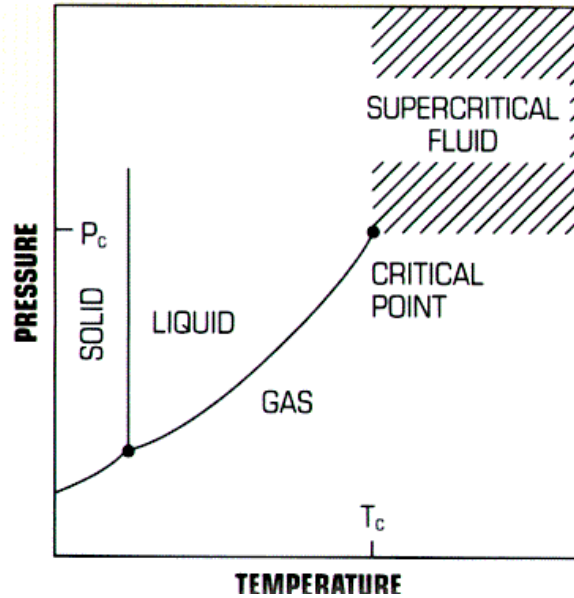


Figure 2.1 Phase diagram of a pure component revealing location of supercritical conditions in the presented binary system (Patterson, 2005)

Supercritical fluid extraction process is a technique that uses solvents at their critical states, to extract low-soluble species from different mediums such as wastes, soils, and sediments (Elektorowicz and Ju, 1997).

The mechanism of the process goes as follows: for typical batch extraction. Raw material is charged into the extraction vessel as a stream of contaminant. The vessel is equipped with temperature controllers and pressure valves at both ends to bring the fluid to its critical extraction point. As soon as the components (organic or inorganic) come in contact in with the supercritical fluid, it dissolves in it (El-Sadi, 1999). Then the fluid and the solubilized components are transferred into the separator, where the SCF is recompressed and recycled to the extraction vessel. The temperature can be reduced by passing the SCF through a heat exchanger (Sihvonen et al., 1999). A simplified SFE system is shown in Figure 2.2.

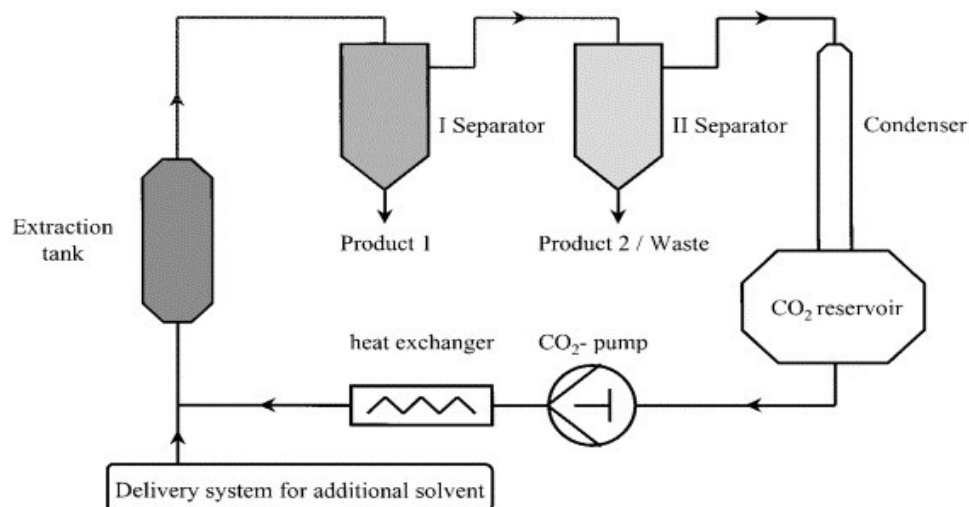


Figure 2.2 Illustration of a simplified SFE system (Alonso et al., 2002)

2.6.2.1 Applications of SFE

Although SFE has been used since the late 1970s, it only started to attract real interest of industries in the 1990s. Nowadays, SFE can be used commercially, and as a remediation technique. The most common commercial application is in the decaffeination of coffee and tea, extraction of hop components for beer, flavoring, and extraction of essential oils high value flavors and aromas from spices and botanicals (Mukhaopahyay, 2000).

In the remediation aspect, many publications and studies were conducted regarding the feasibility of applying SFE on organic and inorganic waste. Recently, SFE has been widely applied in extracting organic waste from multiple mediums such as soil, sludge and slurries. Elektorowicz and Ju (1999) used SFE to extract naphthalene and phenanthrene from dry and wet clayey soils. They achieved PAHs recovery from 16% to 99% depending on clay sample and parameters employed. El-Sadi (1999); Elektorowicz et al., (2007); and Elektorowicz et al., (2008) assessed the removal of PAHs from different clayey soils using SFE.

Ramsey (2007) aimed to determine the amount of oil in water using automated direct aqueous SFE extraction, interfaced to infrared spectroscopy. Using a rapid calibration method, the accuracy of SFE infrared method for determining Brent Delta crude oil in water samples was 94–98.9%.

Naeeni et al., (2011) suggested the use of SFE coupled with dispersive liquid–liquid microextraction (DLLME) for the extraction and determination of ultra-trace amounts of seven organophosphorus pesticides (OPPs) (o,o,o-triethylphosphorothioate, thionazin, sulfotepp, disulfoton, methyl parathion, parathion, and famphur) in soil and marine sediment samples. They reported extraction recoveries from 44.4% to 95.4% and relative standard deviation for four-replicate measurements was below 7.5%.

Metal extraction is considered the new hot topic in SFE. Literature reviews suggests that only a few studies has been conducted regarding supercritical fluid extraction (SFE) of metal species. Direct extraction of metal ions is considered a challenge because of charge neutralization requirements and the weak solute–solvent interactions (Ghoreishi et al., 2012; Abd El-Fatah et al., 2004).

Abd El-Fatah et al., (2004) studied the feasibility of applying SFE to extract Cu, Cr, and As from CCA wood using supercritical CO₂ modified with chelating agents. At 24 MPa pressure, and temperature of 333 °K, the extraction efficiencies for Cu, Cr and As were 63.5, 28.6, and 31.3%, respectively.

Yazdi and Beckman (1997) used CO₂-soluble chelating agents for the extraction of Cu, Li, and Pb from metal enriched water. They attached CO₂-philic fluoroethers to picolyi amines, dithiol, bis-picolyi amine and dithiocarbonate. The results showed high solubility of the three metals complexes in super critical CO₂. Tai et al., (2000) used an *in situ* chelation-

SFE method to extract zinc (II) from water and waste water. CO₂ was used as the SC fluid with Cyanex 302 as the chelating agent. The optimum extraction (60%) was at a temperature of 313 °K.

Ghoreishi et al., (2012) achieved an extraction yield of 98.1 %, 28.9 %, and 65.2% for three toxic metals (Uranium (U), Hafnium (Hf), and Zirconium (Zr) respectively) from a wastewater sample. This research group used a very similar approach to the one used above but with Cyanex 301 as a chelating agent.

Chapter 3

Research Hypothesis and Objectives

The main objective of this research is to monitor mobility of target heavy metals (with particular focus on vanadium) in petroleum oily sludge system, while subjected to electrokinetic (EK) conditions. This objective is formulated in order to prepare the sludge for further remediation procedures, e.g. metal extraction, which would eventually turn hazardous and wasted oily sludge into high quality added-value products.

The following hypothesis were defined for this study

1. Electrokinetic phenomena can be initiated in oily sludge matrices produced in both, upstream and downstream petroleum industry;
2. Electrokinetic phenomena can provoke demulsification of oily sludge, and induce separation of its phases;
3. Metals can be mobilized in DC electrical field, and accumulated in specific areas for further management;
4. Extraction of metals from oily sludge can be improved by applying supercritical fluid;
5. Metal removal from oily sludge is not a one step process, but requires a combination of methods provided in an appropriate order.

Detailed objectives of this work are:

1. Formulation of oil in water (upstream), and water in oil (downstream) thermodynamically stable oil sludge;
2. Exposing vanadium, lead and nickel mobility in oily sludge matrix, when applied separately in EK cells;

3. Demonstrating mobility of vanadium and accompanying metals, such as lead and nickel in EK Mix cells (downstream and upstream Mix Cells);
4. Exploring changes of oily sludge properties under electrokinetic phenomena;
5. Conducting comparative study of extraction methods targeting electrokinetically mobilized metals in oily sludge.

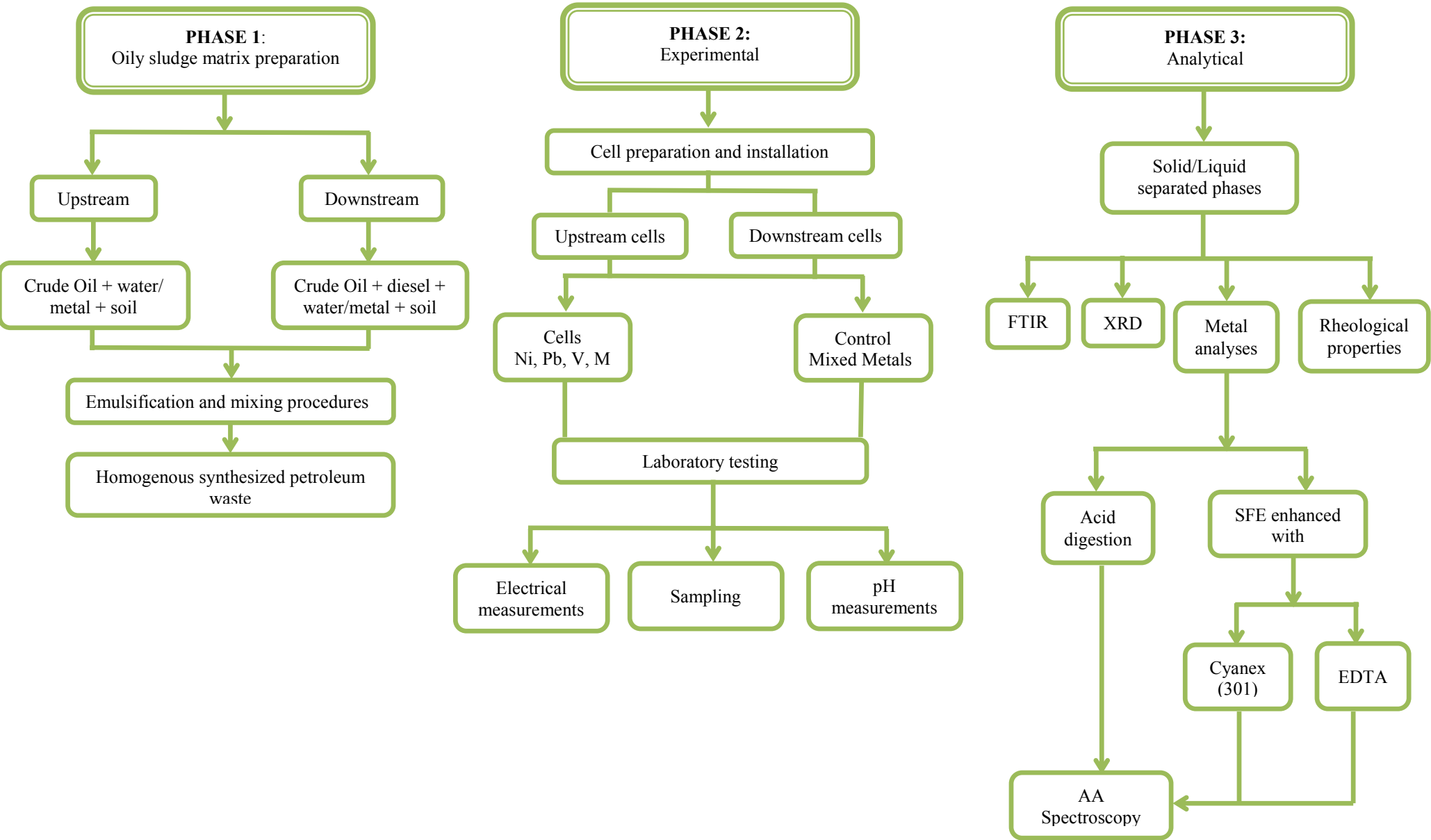


Figure 4.1 Detailed experimental methodology

Chapter 4

Methodology

To achieve the proposed objectives and verify the hypothesis, the research was carried out in three phases. Figure 4.1 provides a detailed schematic that illustrates the order of these phases, and the tests performed in each step.

The research is characterized by three basic phases that represent the stages and links between each tests, and the analysis to follow. First phase consists of creating metal rich stable emulsions of water-in-oil (upstream) and oil-in-water (downstream) sludge like matrix. These matrices would represent the oily sludge produced in the exploration and refining stages of petroleum processing. The second stage (Phase-2) is characterized by applying the electrokinetic phenomena (Ch. 4.2) to initiate the separation of components, thus moving the metals in the matrix. During this stage, laboratory testing were applied during and after the disconnection of the electrical DC current. These tests permitted to identify the physicochemical properties of the treated sludge. In Phase-3, advanced analytical methods were applied to identify behaviour of matrix and metals related to metal mobility with respect to electrokinetically modified oil sludge components.

4.1 Matrix preparation

The main objective of Phase-1 is to create systems that mimic different upstream and downstream petroleum waste scenarios. These scenarios, as described in Chapter 2.1.2, consist of multiphase systems of oil-in-water, and water-in-oil emulsions, which also contain solid fraction (e.g. sand and clay). In these studies three target metals (V, Ni, and

Pb) were added to each system to observe and track their mobility. Previous work by (Badawieh and Elektorowicz, 2006) showed that relatively big amounts of these metals were traced in samples of oily sludge. Furthermore, each of these metals demonstrated distinctive behaviour in contaminated soil (Choudhury and Elektorowicz 1997; Elektorowicz 2009) and municipal sludge (Esmaeily et al., 2005) where DC field was applied. Figure 4.2 summarizes the methodological approach for Phase 1.

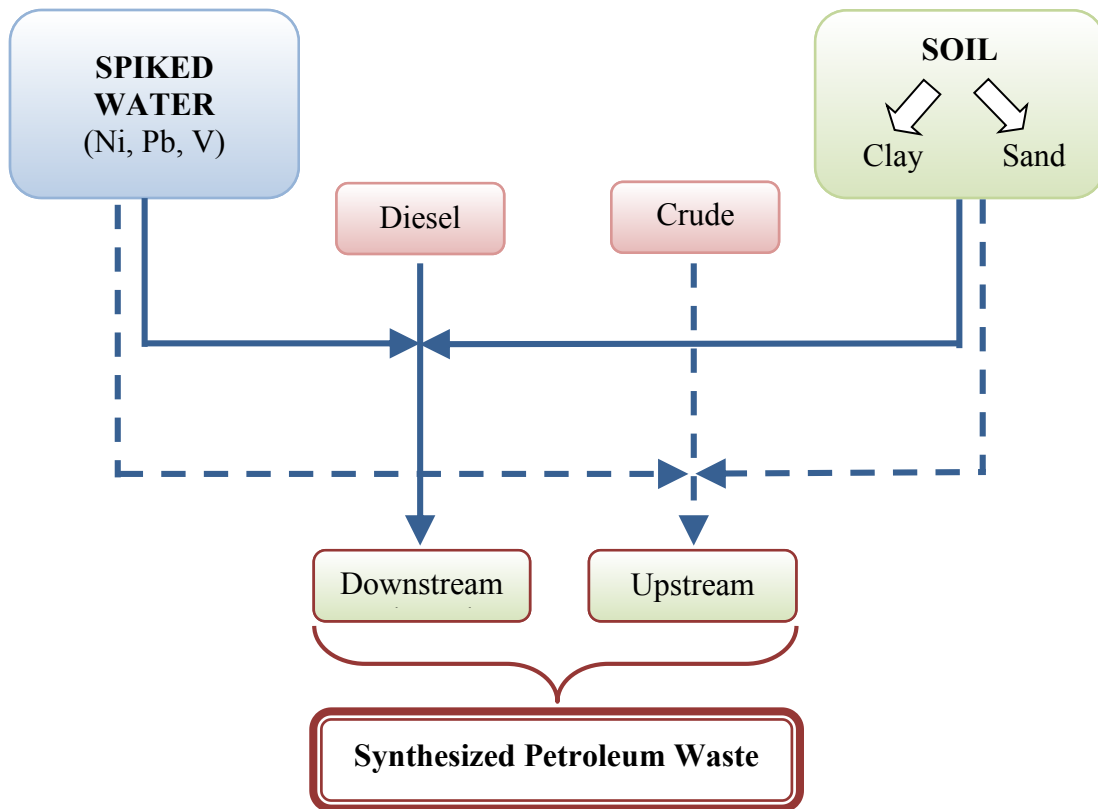


Figure 4.2 Methodological approach for sludge preparation

4.1.1 Upstream scenario

Sludge generated in upstream petroleum industry is considered an oil-in-water phase. Ideally the ratio of sludge components (oil, water, solids) at the petroleum excavation and extraction processes might be as follows (30% oil, 60% water, and 10% solids) (Guolin et al., 2009) .

In comparison with refining processes (downstream), up stream consumes relatively large amounts of fresh water. Water here is used for well construction processes such as drilling and completion in oil and gas resource development. Primary oil and natural gas production, which uses natural reservoir pressure to flow fluids to the wellbore, requires considerable amounts of water.

To create an oil-in-water emulsion, Yan et al. (2001) added known amount of clay particles to a given volume of crude oil, and sheared using a homogenizer for 30 minutes. Water was added to the resulting clay in oil suspension and sheared using the same homogenizer at predetermined speed for 10 minutes. The resulting emulsion demonstrated stability of components. In this research, a modified procedure has been followed to create a similar emulsion that would represent an upstream oily sludge waste.

Lab prepared systems in this scenario contained the following components:

- 1460 ml of water enriched with the target heavy metals (V, Ni, Pb), in three separate cells, and a mixture of the three metals in one cell.
- 150 ml of crude oil (containing already traces of heavy metals) which properties are shown in Tab 4.1.
- 400 g of sand and 200 g clay (Bentonite).

Table 4.1: Crude oil characteristics

Property	Value
Density	995 kg/m ³
Viscosity	127 cSt
API ⁰ Gravity	10.71

(Hasan, 2007)

Upstream cells contained around 1400 ml of sludge for every cell, which is equivalent to 2040 g of sludge. Each metal contaminated system was prepared as follows:

- i. Contamination with target metals:
 - Single metal cell: contains 1260ml of water spiked with 900 mg of each target metal. The cell was divided into three 420 ml water cells, where 300 mg chloride of each target metal (NiCl₂, PbCl₂, VCl₃) were added separately to each sub-cell, to produce 715 ppm of each metal in the mix. Subsequent vigorous shaking was applied for 15 min.
 - Mixed metal cell: water was enriched directly by the three target metals, where 300 mg of all the three metal chlorides were combined in one 420 ml water solution. This mixture was repeated 3 times as before. Also shaking was applied for 15 minutes, and the separated sections were ready for further mixing.
- ii. Mixing the crude oil with the solid content: each cell contained total of 150 ml crude oil, 400 g sand, and 200 g clay. Each component (crude oil, sand, and clay) was divided into three parts and mixed together manually until the soil is combined with crude oil completely. Like the case of water, the three sections were left apart for further mixing with the spiked water sections.

- iii. Final mixture (full upstream cell): Preparing this mix was a challenge, since water and oil are considered immiscible liquids and create emulsions, which might be stable or unstable. Polar water molecules and oil molecules, which are mostly considered non-polar, are not attracted to each other, as oil molecules does (Sanchez, and Zakin, 1994). To create an emulsion, a combination of fluid properties are involved, including temperature, electrolyte, surface tension, relative viscosity, density difference, phase and volume ratio, and surfactants or stabilizers (Habibi, 2004). Usually an intense mixing is usually required to form a stable emulsion. The relative amounts of mixing intensity and stabilizing agents must be balanced to make a practical emulsion. In a lot of cases, greater mixing intensity will create smaller dispersed phase droplets, which should help create a more stable emulsion. In many cases, mixing intensity alone is sufficient to form an emulsion (Ahmed et al., 1999). In other cases, a stabilizing agent (surface active agent) is necessary to form small droplets and prevent coalescence.

In this research, emulsification of oil and water was based on great mixing intensity. Each cell preparation required around 6 to 7 days to ensure the stability of the emulsion produced. This system of mixing was carried out throughout the whole cell preparations procedure. Figure 4.3 shows the sub-cells used to create one full 1400 ml upstream sludge cell:

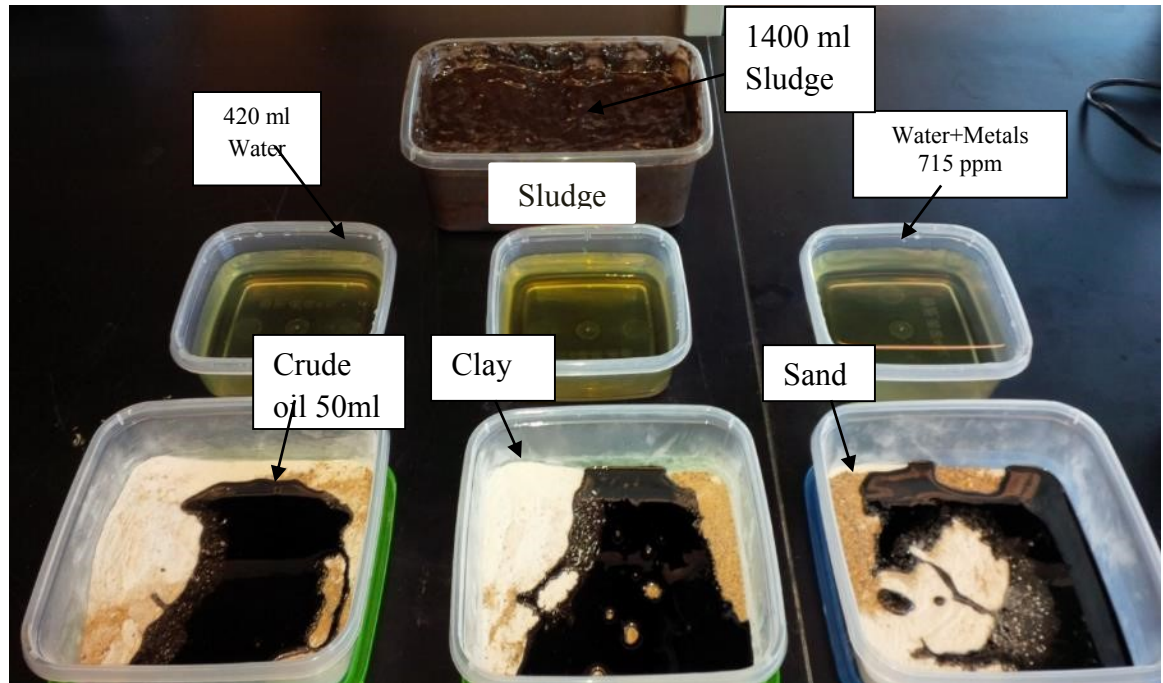


Figure 4.3 Components used to prepare a synthetic sludge for upstream scenario

Each 420 ml water-metal contaminated portion was combined with the portion containing 50 ml oil, and 200 g soil. Manual mixing was applied for 15 minutes to distribute the water over the dense oil-soil mix. The mix was left for 6 hours on the shaker (model AROS 160) to ensure a good distribution of components. To provide great mixing intensity and thus stable emulsion, the components of each portion were fed slowly into a six speed blender that provides up to 400 Watts of power. The content of each portion was introduced in three smaller portions, since the crude oil was sticking to the blades and slowing down the process. Each portion was mixed for 15 minutes at a constant level-two speed, total 45 minutes for each smaller portion and 2 hours 15 minutes for the whole portion. The resulted emulsion of each portion was poured into the target main cell until the 1400 ml mark was reached. The mixed material was left for 24 hours to allow diffusion to take place afterward. To ensure the stability of the produced emulsion, the final portion was left on an adjusted

reciprocal shaker (model AROS160) for the following 5 days. At the end, ASTM D 6922 standard procedure was applied to ensure the homogeneity and stability of the emulsion.

4.1.2 Downstream scenario

Sludge generated in downstream petroleum industry is considered a water-in-oil system. Crude oil refining consumes fresh water for cooling, boiler feed water, crude desalting, and many other processes. This requires refineries to secure large amounts of water (OGPS, 2010). In the case of cooling and boiling the water consumed does not mix with the oil content in pipes or tanks, and the sludge will contain large amounts of refined oil by-products such as diesel and other fuels. Thus, the sludge produced will contain less amounts of water in oil than in the case of upstream industry, which makes it water-in-oil system.

In previous studies for oily sludge treatment using electrokinetics, Chifrina and Elektorowicz, (1998) used an emulsion of diesel fuel and water, with fine soil in order to create a downstream petroleum refining sludge. Also Yan et al., (2001) created a water-in-oil emulsion by directly dispersing colloidal particle suspension into an organic solvent, then dispersing known amounts of water in the suspension with a blender.

In the presented study, a similar system was introduced; however, crude oil and heavy metals were added to the mix. The systems created in this scenario contained the following components: 500 ml of water (enriched with heavy metals (V, Ni, Pb)), 700 ml diesel fuel, 200 ml crude oil, 400 g sand, and 200 g clay.

- i. Metal enrichment: this step proceeded with the metal spiking process as it showed in the upstream case. However, to achieve a concentration of 715 mg/l of each metal, the amounts added of each metal to the water solution were decreased to 357 mg metal chloride for each 500 ml of water.

- ii. Adding 700 ml of diesel fuel to the mix. To create such emulsion, the components were subjected to 6 hours of shaking time at higher intensity. As in the upstream scenario the 1200 ml water-diesel cell is divided into three 400 ml portions.
- iii. Final mixture (full downstream cell): Combining the crude oil – soil with the water-diesel emulsion for the final mix. The same amounts of soil were introduced in this step, while crude oil was increased by 50 ml per portion. The same divide and mix procedures that were illustrated in the final paragraph of upstream sludge (Ch 4.1.1) were applied here. The final 1400 ml downstream cell is shown in Figure 4.4.



Figure 4.4 Synthetic oily sludge prepared for downstream scenario

The following observations were noted through the preparation of the cells;

- The matrix used in each cell was the final product of many attempts to create a stable emulsion.
- Producing each cell took around 7 day's period of preparation and observation.

- Emulsion stability tests were applied on all the cells.

Table 4.2 reveals the final products of Phase-1. These products showed stable emulsification behaviour throughout the whole mixing and storing procedures, where very small mechanical settling was noticed.

Table 4.2: Raw material created in Phase-1

Name\Component	Crude oil	Sand	Clay	Diesel	Spiked water
Upstream V Cell	150 ml	400 g	200 g	-----	1260 ml
Downstream V Cell	200 ml	400g	200g	700 ml	500 ml
Upstream Ni Cell	150 ml	400g	200 g	-----	1260 ml
Downstream Ni Cell	200 ml	400 g	200g	700 ml	500 ml
Upstream Pb Cell	150 ml	400g	200 g	-----	1260 ml
Downstream Pb Cell	200 ml	400g	200g	700 ml	500 ml
Upstream Mix Cell	150 ml	400 g	200 g	-----	1260 ml
Downstream Mix Cell	200 ml	400g	200g	700 ml	500 ml
Upstream Control Cell	150 ml	400g	200 g	-----	1260 ml
Downstream Control Cell	200 ml	400g	200g	700 ml	500 ml

4.2 Experimental Phase-2

Phase-2 is characterized by the application of electrokinetic (EK) phenomena on the upstream and downstream metal rich sludge produced in Phase-1 .

4.2.1 Objectives of Phase 2

- To separate electrokinetically the homogeneous upstream and downstream oily sludge into their basic components;

- b. To investigate movement of metals initiated by the application of electrokinetics within the upstream and downstream systems;
- c. To compare the extent of separation in both systems (upstream, and downstream), with regard of the applied parameters.

Horizontal and vertical movements of oily sludge fractions in the system were investigated, in order to find out the optimum technique for metal extraction. In addition, factors controlling the mobility of metals were identified.

Previous studies demonstrated feasibility of application of EK to oil sludge remediation (Elektorowicz et al., 2006; Elektorowicz and Habibi, 2005). They also showed that metals are transported very well within DC field in sewage sludge (Wang et al., 2005). However, no study was carried out with regards to metals behaviour in oily sludge matrix under EK conditions.

4.2.2 EK cells setup-stage 1

In Phase-2, EK cells were designed in a way to facilitate the measurement of EK parameters and simplify sampling for analyses. Ten uniform cells were used in this research: 4 upstream cells, 4 downstream cells and 2 control units.

Cell material was made of rigid non-conductive or expensive polyethylene; to ensure proper resistance to sludge components, and to facilitate sampling and handling. Figure 4.5 demonstrates the installed electrokinetic system used in this research.

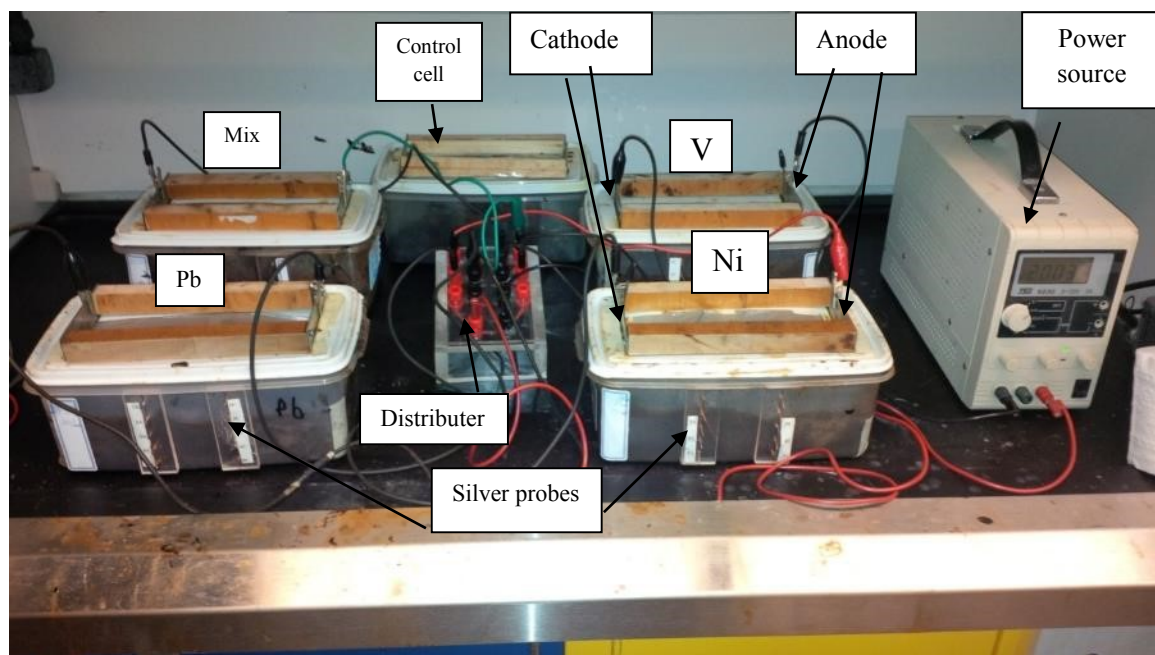


Figure 4.5 Electrokinetic system for experimentation in Phase-2

Electrokinetic cells had the following dimensions of: $L=25\text{cm}$, $W=14.5\text{ cm}$, and $H= 10.5\text{ cm}$ where two stainless steel (304)-plate electrodes of $12 \times 10 \times .2\text{ cm}$, were placed 19.5 cm apart in each cell (Fig 4.6). To measure the resistance changes inside the cell, one side of each cell was equipped with silver probe-electrodes positioned in two vertical lines. Each line contained 4 probes placed 1.5 cm over one another. The probes were inserted 2.75 cm inside the cell. Top of the cells had 5 holes to facilitate pH reading and sampling, throughout the sludge.

Eight cells were connected to a power supply (BK Precision® 1902, 1-60 VDC, 15 A) simultaneously through control panel. Two control cells were not connected to DC. Depending on previous work (Habibi 2004; Chifrina and Elektorowicz 1998) a range of voltage gradient of 0.5 V/cm to 1 V/cm was proved to create an optimal condition for EK separation, while 1 V/cm and higher were recommend for metals recovery (Esmaily, 2002).

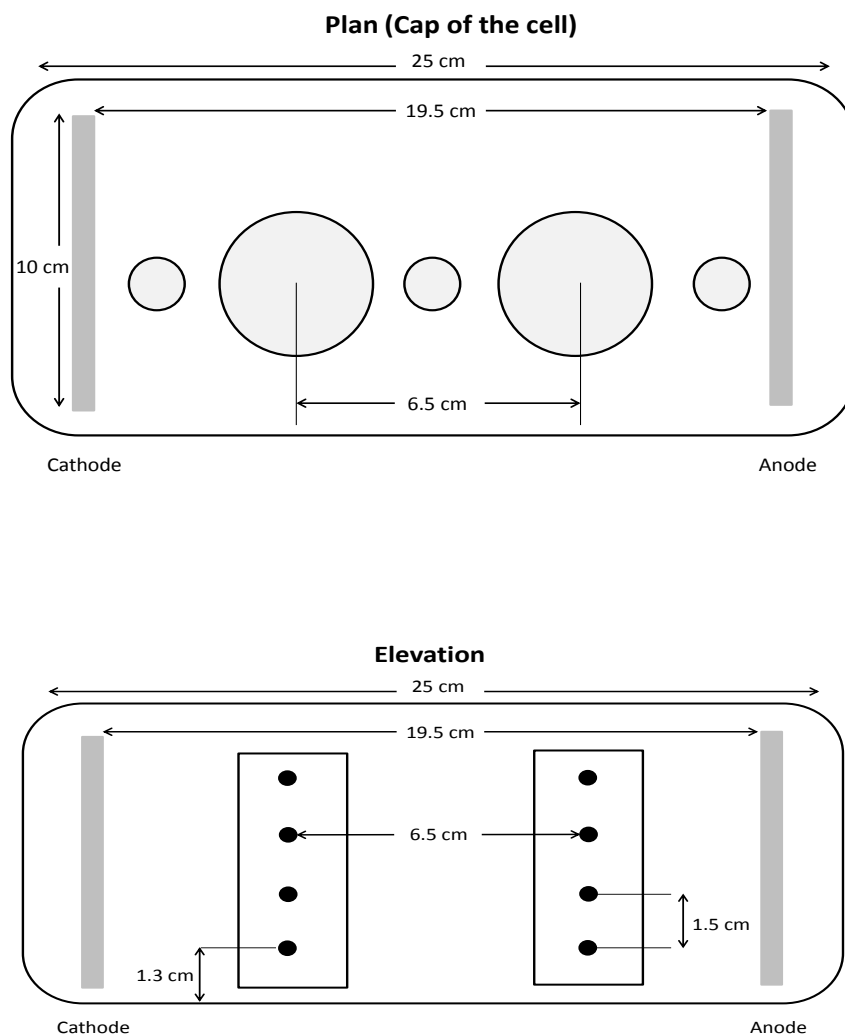


Figure 4.6 Configuration of the electrokinetic cell

4.2.3 EK experiments-Stage 2

The experiment was carried out in the fume hood, since gases and hydrocarbons were produced continuously. And because of space limitations, only four cells were connected

to the electrical power supply at a time (excluding the control cells) for 14 days. These cells represented 4 upstream, and 4 downstream.

According to previous work (Chifrina and Elektorowicz, 1998; Choudhury 1998; Elektorowicz and Hakimpour, 2001; Elektorowicz and Habibi 2005); further movements, diffusion, and separation are anticipated even after disconnecting the current. Thus, the cells were left for another 2 days before moving into the analysis stage, and finally metal extraction applications. Table 4.3 identify cells' characteristics and test conditions:

Table 4.3: Summary of experimental cells conditions in Phase-2

Cell#	Label	Cell composition
1	Control (U)	Control cell upstream sludge mixed metals
2	Control (D)	Control cell downstream sludge mixed metals
3	V Cell (U)	Upstream sludge(V spiked)
4	V Cell (D)	Downstream sludge(V spiked)
5	Ni Cell (U)	Upstream sludge(Ni spiked)
6	Ni Cell (D)	Downstream sludge(Ni spiked)
7	Pb Cell (U)	Upstream sludge(Pb spiked)
8	Pb Cell (D)	Downstream sludge(Pb spiked)
9	Mix (U)	Upstream sludge(Mix metals)
10	Mix (D)	Downstream sludge(Mix metals)

Note: D – Downstream sludge, U- Upstream sludge; Applied voltage gradient = 1V/cm; Control (U) Control upstream cell without EK; Control (D) Control downstream cell without EK,

4.3 Apparatus, reagents, and equipment

This section provides a summary of the instruments, reagents and equipment used in this study.

➤ Apparatus and consumables for Phases 1 and 2

- DC power supply (BK Precision® 1902, 1-60 VDC, 15 A)
- 16 stainless steel plate electrodes (12 x 10 x .2 cm)
- 64 silver probe electrodes
- Heater /Stirrer (Corning PC-420D)
- Digital multimeter (TES Scientific)
- Electrical distribution system
- Reciprocal shaker (model AROS160)
- Around 1000 Fisherbrand™ Poxygrid™ centrifuge plastic tubes
- 30 ml glass vials for AA analysis
- Filter paper - Whatman No. 41, No. 42

➤ **Reagents**

- Standard solutions of (Ni, Pb, and V) for AAS, 1000 ppm in 2% HNO₃
- NiCl₂ Powder, PbCl₂ Powder, VCl₃ Powder
- Petroleum Diesel H₁₂O₂₃
- Methanol CH₄O
- Diisooctyldithiophosphini Acid (Cyanex 301)
- Ethylenediamine-Tetraacetate Acid (EDTA) 0.5 M
- Hydrochloric Acid HCl
- Nitric Acid HNO₃
- Sulfuric Acid H₂SO₄
- Potassium Permanganate Solution N/10 , KMnO₄

- Distilled Water
- Buffer Solutions (pH= 7, pH=10, pH=4)

- **Equipment for measurements and analysis (Phases 2 and 3)**
- pH meter (Fisher scientific, AR25)
- Atomic absorption spectroscopy (AAS) PerkinElmer, models (PinAAcle 900F, and AAnalyst 100)
- Modular Compact Rheometer, Physica(Antoon Paar) model (MCR 500)
- FTIR (Nagna, Nicolet), and Omnic FT-IR Spectra software for analysis
- 5000 psi SFE system operated at CÉPROCQ (Collège de Maisonneuve), Montreal, QC
- Philips PW-1050/65 powder diffractometer , McGill University

4.4 Characterisation of the sludge

In the literature review, it has been illustrated that upstream and downstream oily sludge are basically made of water, soil, light and heavy hydrocarbons, crude oil, petroleum by-products, and suspended materials such as minerals and heavy metals (Kriipsalu et al., 2007). In this study; lab prepared sludge (Ch 4.1) was exposed to several experiments that caused shifting of the components in the homogeneous mix.

4.4.1 Oily sludge components

The following components were calculated throughout the different stages of the research, because of its' direct relationship with the metals behavior and mobility.

4.4.1.1 Liquid content

A standard test was used to calculate the liquid content in the sludge. This test determined the water, and light hydrocarbons amounts in the sample. A weighed sample was heated at 105 °C for 12 hours. The loss of weight indicated the moisture content of the sludge. With relation to the original weight, the moisture content was calculated as follows:

$$\text{Liquid content \% w} = ((\text{Sample original weight, g} - \text{Sample weight, g at } 105 \text{ } ^\circ\text{C}) / \text{Sample Original weight, g}) \times 100\% \quad (5)$$

4.4.1.2 Solid content

Standard method ASTM D2974 was used to calculate the solid content ratio in the sludge. After the liquid content was calculated, the (105 °C) dried samples were placed in the furnace at 550 °C for 8 hours. The solid content ratio was calculated as follows:

$$\text{Solid content \% w} = (\text{Weight of sample, g at } (550 \text{ } ^\circ\text{C}) / \text{Sample original weight, g}) \times 100\% \quad (6)$$

4.4.1.3 Non-volatile organic content (NVOC)

After calculating the solid and moisture content, the remaining fraction would represent the non-volatile organic content. This fraction was calculated as follows:

$$\text{NVOC} = 100\% - (\text{Solid content \%} + \text{Liquid content \%}) \quad (7)$$

4.4.2 Measurement procedure of pH

As it has been discussed earlier (Ch.2.6.1), pH gradient has great influence on the EK system. It can indicate the characteristics of different components in the system, and with other factors it controls the movements of ions in the matrix. The pH of each cell was initially measured at fixed selected points at the top, and in the bottom of each cell.

However, pH was measured at extra locations depending on other factors such as: visual observations, metal distributions, and any change of contents detected through FTIR and XRD tests. During the experiment, while the current was on, pH readings were taken at the starting point and on days 4, 9, and 14 at the top and bottom in three different locations, hence the opening in the cell cover (Fig 4.6). Furthermore, after the EK separation of fractions, pH was recorded for each sample used in each stage.

4.4.3 Electrical parameters

Resistance is a good indication of the sludge properties, including vertical and horizontal movements of components, fractioning, water movement, and metal movement. The electrical current (I) in each cell and the electrical potential (V) between cathode and each probe electrode were measured daily using a digital multimeter, and the resistance was calculated from Ohm's formula:

$$R=V/I \quad (8)$$

Where R = resistance (Ohm), V =electrical potential (V), and I = electrical current (A).

4.4.4 Sampling procedure

In order to prevent any interference in the electrical field inside the cells, samples were collected through specially designed holes in the cap. These samples were collected on days 4, 9, and 14. While Table 4.4 illustrates the general sampling patterns followed throughout the research, extra samples were collected at certain points according to visual observations, electrical parameters, and other analyses.

Table 4.4: Sampling procedure

Cell Name	Sampling points	Days	Connection (DC)	No of samples*
V Cells	3x3	4 th , 9 th , 14 th	on	54
Ni Cells	3x3	4 th , 9 th , 14 th	on	54
Pb Cells	3x3	4 th , 9 th , 14 th	on	54
Mix Cells	3x3	4 th , 9 th , 14 th	on	54
Control Cells	3x3	4 th , 9 th , 14 th	off	54
V Cells	3x3	16 th	off	18
Ni Cells	3x3	16 th	off	18
Pb Cells	3x3	16 th	off	18
Mix Cells	3x3	16 th	off	18
Total number of samples				342

4.5 FTIR analysis (Phase-3)

FTIR (Fourier Transform Infrared) analysis was applied to the oily sludge matrix before EK, as well as to each cell after the completion of EK application in Phase-2. This analysis was carried out using Nicolet Magna 860 Fourier transform instrument. The main reason for applying these analyses was to trace any formation of organometallic complexes in the various EK cell sections, which can be defined by observation of the shifting of CH bands. Furthermore, such analysis would define changes in distribution of sludge fractions (water and hydrocarbons) in the main sampling points; vertically (top, middle, and bottom), and horizontally (anode, cell center, and cathode).

After the background noise was collected, 64 scans were performed for each sample, and absorbance of radiation was considered as a final format of measurement (See Appendix A). Depending on initial scan and noise reduction, the spectral range for observations was taken between 600 cm^{-1} and 4000 cm^{-1} .

The band 1040 cm^{-1} which belongs to Si-O stretching vibration in bentonite and sand was used as an internal standard. However, to compare the distribution of water and hydrocarbons in the cells, two ratios; OH/SiO ($3370\text{cm}^{-1}/1040\text{cm}^{-1}$), and CH/SiO ($2920\text{cm}^{-1}/1040\text{cm}^{-1}$) were taken into consideration, where 2920cm^{-1} , and 3370cm^{-1} were attributed to the deformation vibrations of CH and OH bonds, respectively.

4.6 XRD analysis (Phase-3)

In this study, X-ray diffraction (XRD) has been used to find out the fingerprint characterization of crystalline materials, and the determination of their structure. Each crystalline solid has its unique characteristic X-ray powder pattern, which may be used as a "fingerprint" for its identification.

In principle, it employs X-rays to irradiate and scan a specimen throughout a predetermined angle range. A diffraction spectrum originates when the X-rays interact with the crystalline material. The built-in detector collects this spectrum and projects it as a series of peaks with distinctive intensities and angle positions. For the identification of the crystalline phase(s) present in the sample, position and intensity matching of the spectrum was performed with reference to the established ICDD (International Centre for Diffraction Data) database. This latter task was carried out with the aid of the accompanied software. XRD analysis was used to identify the crystalline phase(s) that forms in the produced solid material, particularly metallic forms. The analyses were carried out using a Philips PW-

1050/65 powder diffractometer. Twenty scans range between 10° and 100° were used at a step size of 0.02° , and an angle residence time of 2 seconds. Before applying the test, the samples were crushed and dried for 24 hours at 105°C . Around 0.5 g powder of each sample was introduced to the chamber where each test would take around 60 minutes of running time.

4.7 Rheological properties (Phase-3)

It was noted from the FTIR analysis on samples post EK that the movement and separation of water and hydrocarbons (HC) were more obvious in cells where vanadium was present. As a result, some rheological properties were investigated in these cells, in order to better understand the deformation and flow of sludge components in upstream and downstream vanadium enriched cells. These tests were done by MCR500 rheometer (Omnicon) using a plate/plate measuring system.

A frequency sweep was performed on samples taken from different locations in the Vanadium Cells, as well as two samples from initial (before application of EK) upstream and downstream matrices. For each test; two angular frequency intervals were taken: i) 100 rad/s to 10 rad/s, and ii) 10 rad/s to 1 rad/s. Each interval was divided into 16 points. In order to identify and compare several sludge properties (viscosity vs. shear rate) and (elastic modulus vs. frequency), such parameters as viscosity (Pa.s), complex viscosity (Pa.s), elastic modulus (Pa), strain (%), and torque (μNm) were measured.

While the viscosity, elastic modulus, and frequency were measured by the rheometer software, the shear rate was calculated based on the shear stress and viscosity using the following equation:

$$\tau = \dot{\gamma}\eta \quad (9)$$

Where:

$\dot{\gamma}$ = strain rate (1/s), η = dynamic viscosity (Pa.s)

4.8 Metal analysis

After verifying the distribution of components of the sludge post EK, the following sections describe the experiments and analysis applied to track the target heavy metals (V, Ni, Pb) in the multi-phase matrix. To insure the availability of metals for analysis, acid digestion was applied to all samples collected from each cell. Then, metal content was detected using atomic absorption analysis (AAS), via Pin AAcle 900F, and AAnalyst 100 models.

4.8.1 Digestion procedure

Acid digestion was used to extract target metals from the sludge samples. This process consisted of applying strong acid to each sludge fraction after EK separation, for further analysis by AAS. Standard acid digestion method of sediments, sludge, and soil developed by EPA (1996) was slightly modified to fit the matrix in this research as follows (El-Sadi et al., 2015):

1. A homogenized representative sample of 2 g (\pm 0.1 g) was placed in a beaker.
2. 2 g of potassium permanganate powder was added to the sample so that the ratio of sludge to potassium permanganate was 1:1. Then, sample and permanganate powder were mixed thoroughly until obtaining a homogeneous matrix.
3. 4 ml of concentrated H₂SO₄, was added to the mix matrix and stirred with stirring device model Corning PC-420D for 15 minutes. The addition of acid was gradual

and slow, since the reaction between sulfuric acid and such rich hydrocarbon matrix was very quick, vigorous, and exothermic.

4. 4 ml of concentrated HNO_3 was added to the mix and stirred for 5 minutes using Corning PC-420D, then placed on the shaker for 15 min. This reaction was slightly exothermic. When the digest was no longer giving off brown fumes, the process moved to the next step.
5. 10 ml of concentrated HCl was added to the mix and was stirred for 5 minutes followed by 15 minutes on the shaker. This reaction was slightly exothermic; also gas formation and foaming frequently occurred. This step worked as an indicator also to differentiate between light and heavy oils, since light oils usually would produce more foam than heavier oils.
6. The beaker was heated up to $120\text{ }^\circ\text{C}$ until there was no further gas evolution.
7. The final product took the form of yellow or green liquid with black or dark reddish-brown particulates.
8. In order to operate the AAS, the extract should be clear, thus, the mix was filtered through Whatman 41 filter papers and collected in a beaker. To insure the recovery of all metals, the digestion beaker and filter paper was washed (while still in the funnel), with 5 ml of hot HCl .

4.8.2 Atomic Adsorption Spectroscopy (AAS)

AAS was performed after each extraction procedure to evaluate the content of each metal. While default parameters were followed for each metal, nitrous oxide was used instead of air acetylene as an oxidant gas for vanadium detection, because vanadium has high melting point, and vanadium oxides dissociate at high temperatures. Nitrous oxide can be used as

an oxidant gas when hotter flames are required. Two Machines (PinAAcle 900F, and AAnalyst 100) were used for this experiment. Each test was repeated three times for each sample, average concentration was recorded and standard deviation was taken into consideration while constructing the error bars as shown in the results (Ch. 5.5).

4.8.3 Supercritical fluid extraction (SFE)

The acid digestion method might not always extract full amounts of metals from some matrices, given that elements strong bound to matrix structures makes them less mobile in the environment. However, for some compounds associated with colloidal matrices, supercritical fluid extraction method has already demonstrated higher extraction rates than normal acid digestion methods (Elektorowicz and Ju, 1997, Elektorowicz et al., 2007).

SFE is not commonly used method for metal extraction. Literature reviews suggested that only a few studies has been conducted regarding supercritical fluid extraction (SFE) of metal species (Ghoreishi et al., 2012; Abd El-Fatah et al., 2004), especially in such a complicated matrix.

As it has been explained in the literature review (Ch. 2.6.2), in order to extract heavy metals from any matrix, utilization of chelating agent is recommended (Ghoreishi et al., 2012, Choudhury, 1998). Without conditioners, metal ions are not easily removed by supercritical fluids (SCF) (Iwao et al., 2007). When metal ions are chelated by suitable organic ligands, their solubility in SC-CO₂ will significantly increase (Abd El-Fatah et al., 2004).

Based on literature review, two complexation agents were used in this research, Cyanex 301 (Ghoreishi et al., 2012; Smart et al., 1997) and EDTA (Elektorowicz and Muslat, 2008; Lin et al., 2003; Choudhury, 1998) in order to provide better extraction efficiency for nickel

and lead. However, no extensive research on vanadium extraction by SFE was carried out to my knowledge. Subsequently, 36 samples containing mix metals were subjected to SFE extraction process in this study. Samples were collected from different locations in EK cells. Subsequently, wet and dry types of samples had undergone extraction using different operational parameters for SFE, as they are defined in Table 4.5. SFE unit operated in CÉPROCQ (Collège de Maisonneuve), Montreal, QC.

After collecting the extract, the quantities of heavy metals in the original and extracted samples were determined by AAS analysis. The extraction yield (E.Y.) of each metal was calculated using the following formula:

$$E.Y. = (\text{Initial amount of metal-residue of metal}) / \text{Initial amount of metal} \times 100\% \quad (10)$$

Table 4.5: SFE operating parameters

Operating Parameters	Wet	Dry
Temperature	90 °C	80 °C
Pressure	15 MPa	20 MPa
Dynamic Extraction	30 min	50 min
Static Extraction	75 min	50 min
CO ₂ Flow	5 ml/min	5 ml/min
Modifier (MeOH)%	15% of CO ₂	15% of CO ₂

The results of SFE extraction would be compared to those of acid extraction in the following chapter (Ch. 5.6.3).

Chapter 5

Discussion and Results

This chapter describes the results of the conducted experimental work of Phase-2 and Phase-3. The results were divided into sections to help understanding interactive influence of physicochemical processes, and electrokinetic phenomena on metals mobility in upstream and downstream oily sludge.

5.1 Separation of components

Applying the DC electrical field into oily sludge resulted in its phase separation, and was subjected to electrokinetic phenomena at different extend, depending on the EK cell matrix. A series of tests demonstrated the presence of vertical and horizontal movements in the cells. These movements were characterized by a visually clear shift of components in the system, and were detected by physical, chemical, electrical, and pH measurements during and after the tests.

Electrical field generated by applying a direct current of 1 V/cm, caused breakdown of the colloidal aggregates, and created an electro-demulsification process (Ch. 2.4). By the end of the first week most cells demonstrated movements of colloidal particles and separated solids toward the anode, due to electrophoresis. These movements were clearer in the upstream cells (oil-in-water emulsion). On the other hand, liquid phase which consists of water and light hydrocarbons moved toward the cathode area, where they were accumulated. This happened as a result of electroosmotic forces in the horizontal direction.

Figure 5.1 demonstrates the movement of liquids towards the cathode area, and the accumulation of solids closer to the anode area.

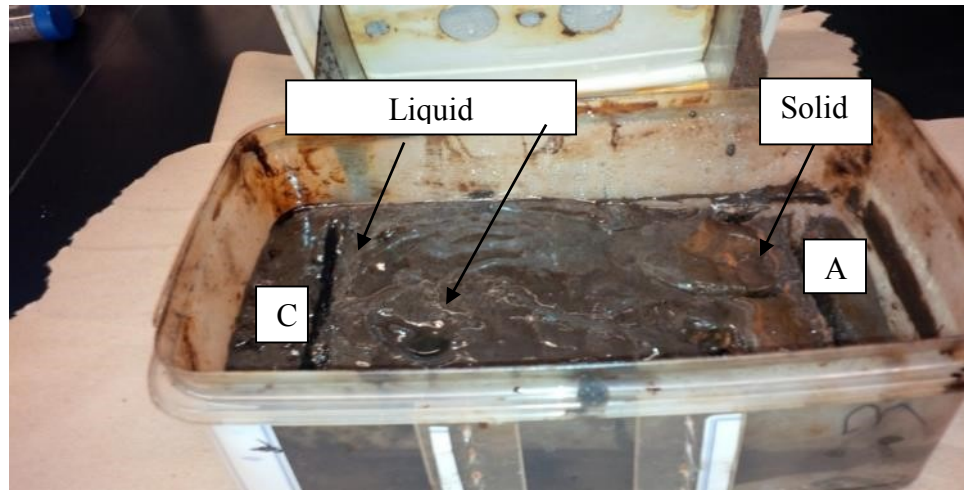


Figure 5.1 Movement of the liquid components toward the cathode and solid components to the anode in an upstream cell

During the separation process, the solid part of the sludge started to accumulate near the anode as a result of electro-coagulation process. Total solids reached up to 80% around the anode area in some cells (Fig. 5.10) after 14 days of the application of EK. However, the separation process has been already observed after 48 hours of the sludge being subjected to the DC field.

While electrical parameters (Ch. 5.2) and pH readings (Ch. 5.3) gave a proof of the demulsification process, it also gave an indication of the rate this process is happening at. The characterization of the shifted components through various experiments (Ch.5.4, 5.5, and 5.6) clarified the mobility, thus the distribution of the target heavy metals in the treated sludge.

After disconnecting the electrical current, cells were divided into segments depending on the following parameters:

- a- Visual observations;
- b- Electrical results obtained during the experiment;
- c- General; vertical (top, middle, bottom) and horizontal (anode area, middle area, cathode area) divisions.

The first two parameters were used to illustrate the obvious differences in the separation processes between the upstream and downstream cells. On the other hand, all the segments resulted from the general division underwent extensive analyses to eventually define the mobility, and distribution of metals in oily sludge under EK conditions.

Figure 5.2 describes the distribution patterns followed in the cells, where the horizontal direction refers to the samples (accumulation of the metals) at the anode, center, or cathode areas, and the vertical direction refers to the samples (phase separation, metal accumulation) at the bottom, middle, and top areas of each horizontal section.

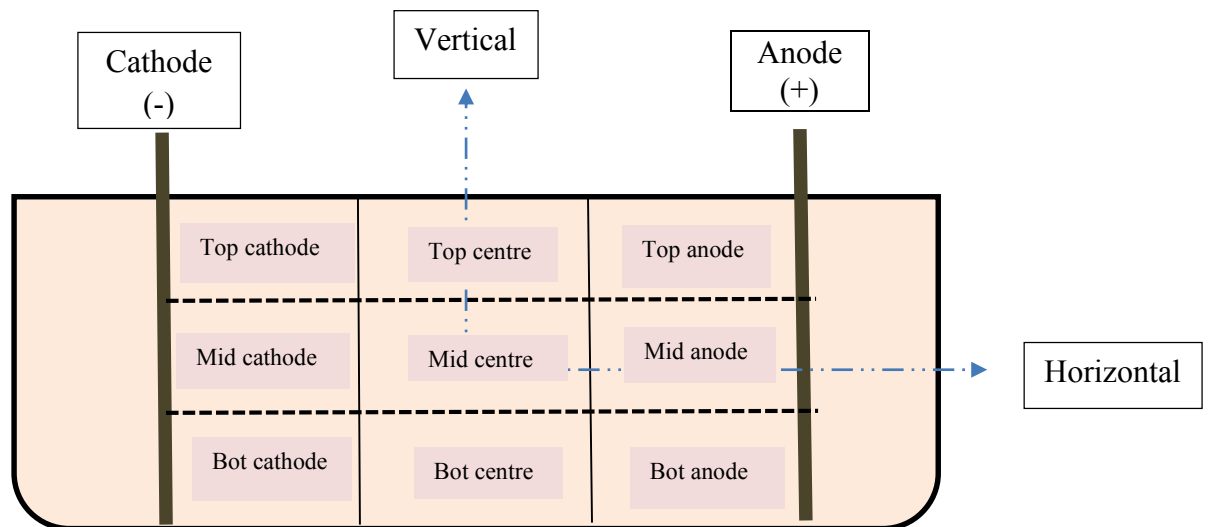


Figure 5.2 Vertical and horizontal directions in the EK cells

Physical characterization of the separated segments, which include moisture, solid, and non-volatile organic contents are introduced in Figures (5.3 to 5.9). These percentages are results of the tests conducted in Chapter 4.4.

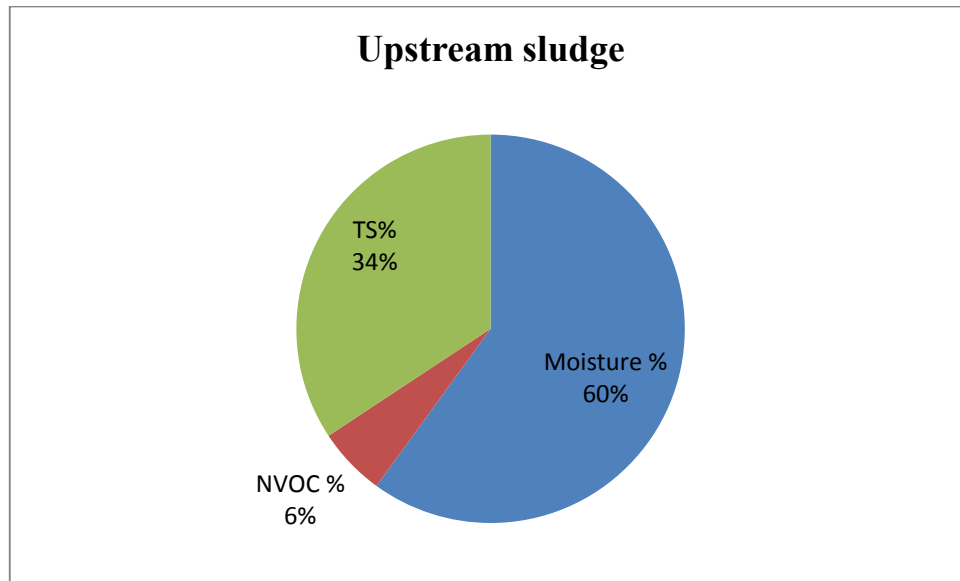


Figure 5.3 Original upstream oily sludge (before applying EK)
Note: TS= Total solid content, NVOC = Non-volatile organic content

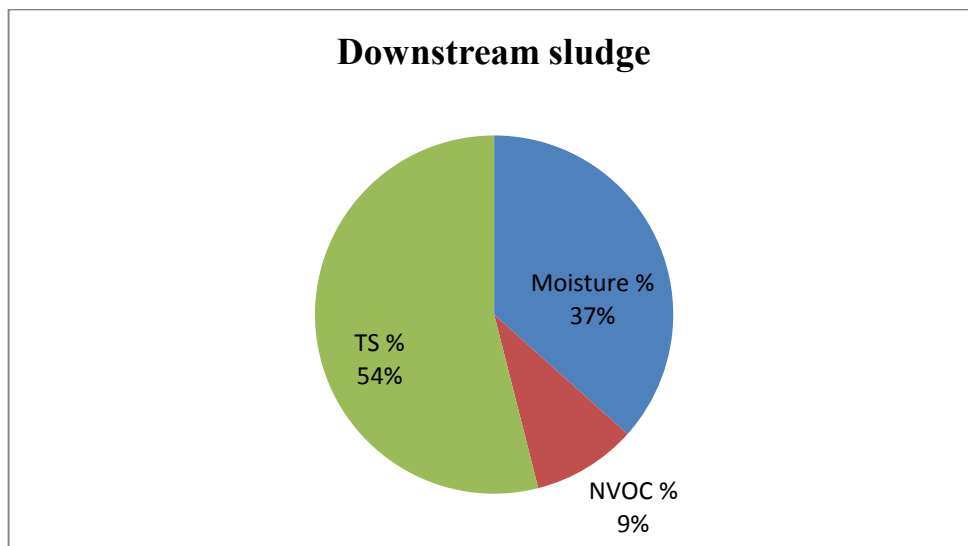


Figure 5.4 Original downstream oily sludge (before applying EK)
Note: TS= Total solid content, NVOC = Non-volatile organic content

5.1.1 Vanadium Cells (V Cells)

In the upstream Vanadium Cell (Fig 5.5), the maximum accumulation of solid particles after EK was at the bottom of the anode area (71%). That same section seemed to accumulate highest NVOC (22%). Consequently, the remaining 7 % of weight represented the moisture and volatile hydrocarbons. This moisture content was the lowest between all the Nickel, Lead, and Mix cells. Alternatively, the lowest solid content (29 %), lowest NVOC (5.6 %), and highest moisture content (65%) were observed at the top of the cathode area, which demonstrated a good vertical separation following various fraction densities.

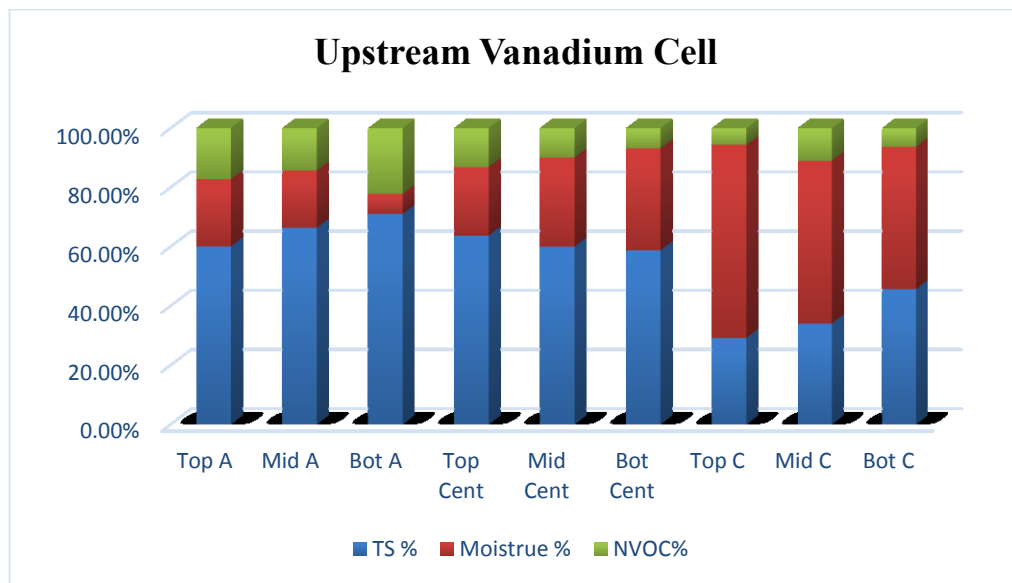


Figure 5.5 Percentages of fractions of oily sludge in upstream Vanadium Cell (after EK)

Note: TS= Total solid content, NVOC = Non-volatile organic content, Top A= Top anode area, Mid A= Middle anode area, Bot A= Bottom anode area, Top Cent = Top of center area, Mid Cent = Middle of center area, Bot Cent = Bottom of center area, Top C= Top cathode area, Mid C = Middle cathode area, Bot C = Bottom cathode area

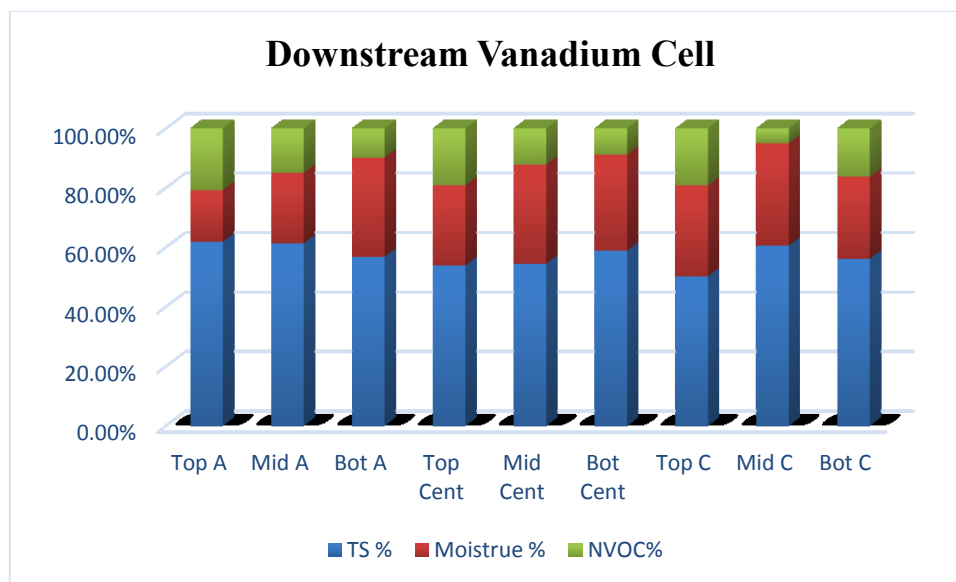


Figure 5.6 Fractions of oily sludge in downstream Vanadium cell (after EK)

Note: TS= Total solid content, NVOC = Non-volatile organic content, Top A= Top anode area, Mid A= Middle anode area, Bot A= Bottom anode area, Top Cent = Top of center area, Mid Cent = Middle of center area, Bot Cent = Bottom of center area, Top C= Top cathode area, Mid C = Middle cathode area, Bot C = Bottom cathode area

Figure 5.6 shows a significant reduction of the moisture content from 37% to 17 %, at the top of the anode area. Such reduction was not noticed in the downstream Nickel and Lead Cell. Total solid content ranged between a maximum of 61 % at the top of anode area to a minimum of 50% at the top of the cathode area. Those two areas contained high NVOC (20%), countered with a minimum of 5%, at the middle of the cathode area.

5.1.2 Nickel Cells (Ni Cells)

Figures 5.7 and 5.8 show the distribution of components at various areas in upstream and downstream Nickel Cells. In the original upstream sludge (Fig 5.3), the distribution of moisture, total solids (TS) and non-volatile organics (NVOC) were 60%, 34%, and 6% respectively. However, the original downstream oil sludge (Fig 5.4) contained 37% moisture, 54% solids, and 9% non-volatile organics.

After 14 days of applying EK conditions, those values changed because of the occurrence of many physical and chemical processes. These processes caused the electro-demulsification of the oily sludge, simultaneously disturbing the homogeneous distributions of the sludge fractions.

In the upstream Nickel Cell (Fig 5.7), there was an obvious increase of the solid fraction close to the anode area, where it reached around 78% at the top of this area. At that same area, the moisture content dropped to a minimum of 19%. Simultaneously, the solid content decreased to a minimum value of 30% at the cathode area, and an increase of the moisture content to a maximum value of 65% at the bottom of the cathode. The non-volatile organic content increased to almost 14 % at the top of the anode area, and decreased to a minimum value of 3% at the middle part of the cathode area.

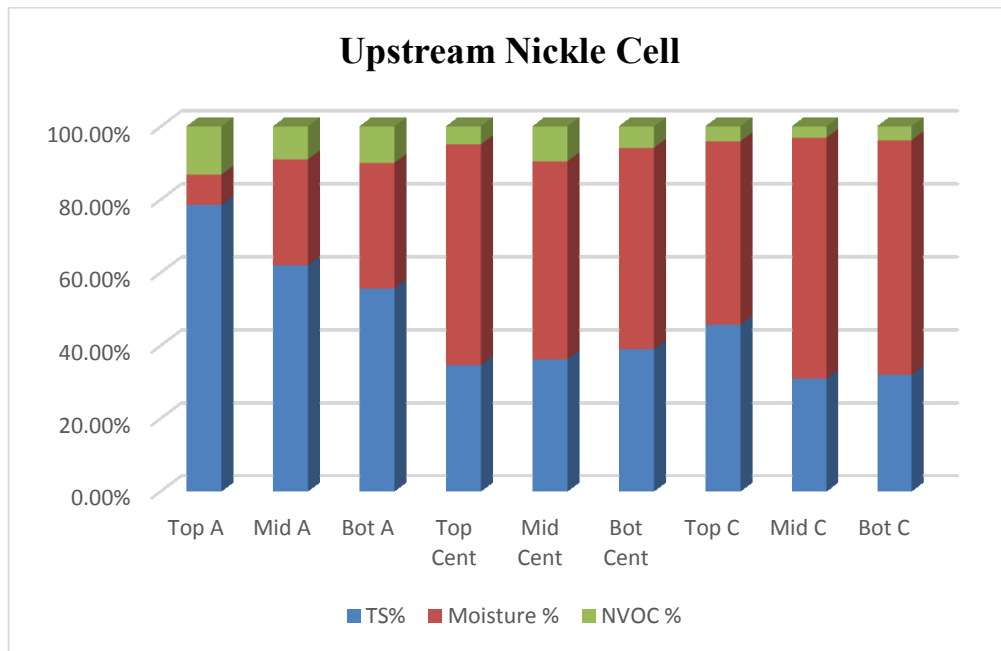


Figure 5.7 Fractions of oily sludge in an upstream Nickel Cell (after EK)

Note: TS= Total solid content, NVOC = Non-volatile organic content, Top A= Top anode area, Mid A= Middle anode area, Bot A= Bottom anode area, Top Cent = Top of center area, Mid Cent = Middle of center area, Bot Cent = Bottom of center area, Top C= Top cathode area, Mid C = Middle cathode area, Bot C = Bottom cathode area

In the downstream Nickel Cell the separation of components was not as clear as in the upstream cell. Figure 5.8 shows that the maximum increase of solid content was from 53% in the original cell to a maximum 60% after EK at the top of the center and anode areas. But unlike the upstream cell, where maximum moisture content was noticed at the cathode area, the maximum moisture content in the downstream cell was observed at the bottom of the center area, where it has risen from 37% to 51%. Also the NVOC increased to a maximum value of 19% at top of the anode area, and decreased to a minimum value of 4% at the center of the Nickel Cell.

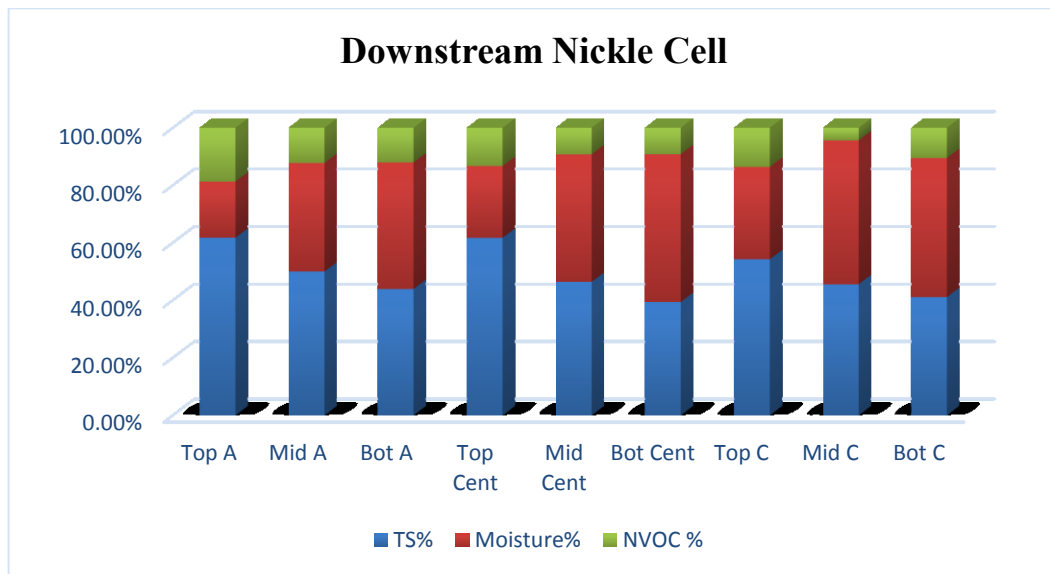


Figure 5.8 Fractions of oily sludge in a downstream Nickel Cell (after EK)

Note: TS= Total solid content, NVOC = Non-volatile organic content, Top A= Top anode area, Mid A= Middle anode area, Bot A= Bottom anode area, Top Cent = Top of center area, Mid Cent = Middle of center area, Bot Cent = Bottom of center area, Top C= Top cathode area, Mid C = Middle cathode area, Bot C = Bottom cathode area

5.1.3 Lead Cells (Pb Cells)

Figure 5.9 demonstrates the distribution of components in the upstream Lead Cell after EK treatment, where the most accumulation of solids was observed at the top of the anode area

(71%). It seems that the distribution of sludge components in this cell followed Nickel Cell patterns. That area (top anode) contained the lowest moisture content (14.8 %). On the other hand, the bottom of the cathode area contained the highest moisture content (69%) and lowest solid content (36%). The non-volatile organic content had a maximum value of 17.2 % at the middle of the anode area and a minimum value of 3.4 % at the middle of the cathode area.

Visual observations demonstrated obvious vertical and horizontal separation of fractions, in all upstream cells (Appendix B; Figs B.1-B.6).

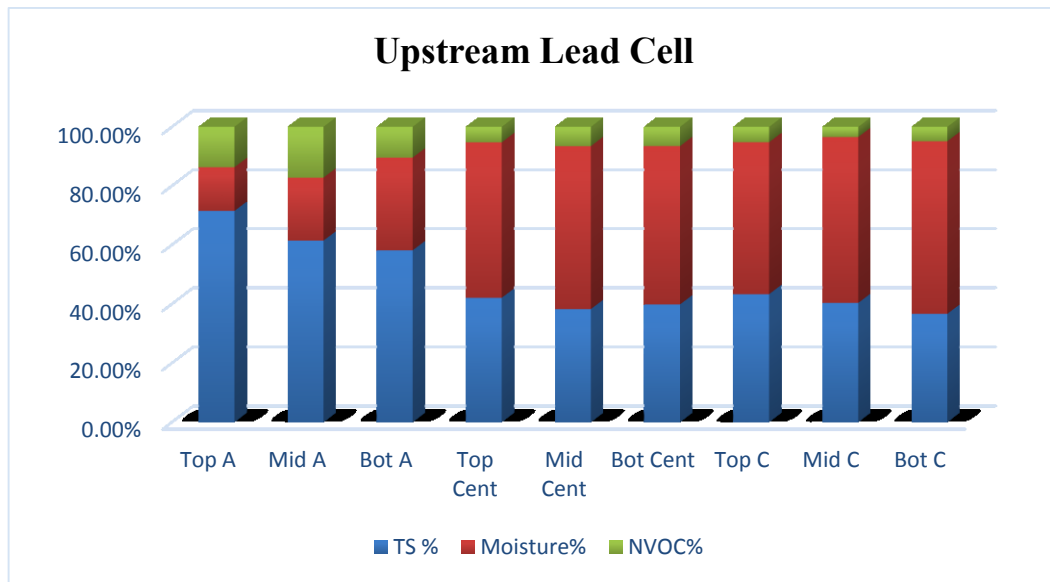


Figure 5.9 Fractions of oily sludge in upstream Lead Cell (after EK)

Note: Top A= Top anode area, Mid A= Middle anode area, Bot A= Bottom anode area, Top Cent = Top of center area, Mid Cent = Middle of center area, Bot Cent = Bottom of center area, Top C= Top cathode area, Mid C = Middle cathode area, Bot C = Bottom cathode area

In the downstream Lead Cell (Figure 5.10) results had a slightly different nature than those in the downstream Nickel and Vanadium Cells. While the shift between moisture and solid

content was small throughout the cell, NVOC showed higher values all over the cell, where it ranged between 15% and 11% at the middle segment of the anode, and bottom segment of the cathode respectively. Minimum and maximum moisture contents were registered at the middle of the anode (32%) and bottom of the cathode (51%) respectively. Minimum and maximum moisture contents were registered at the middle of the anode (32%) and bottom of the cathode (51%) respectively.

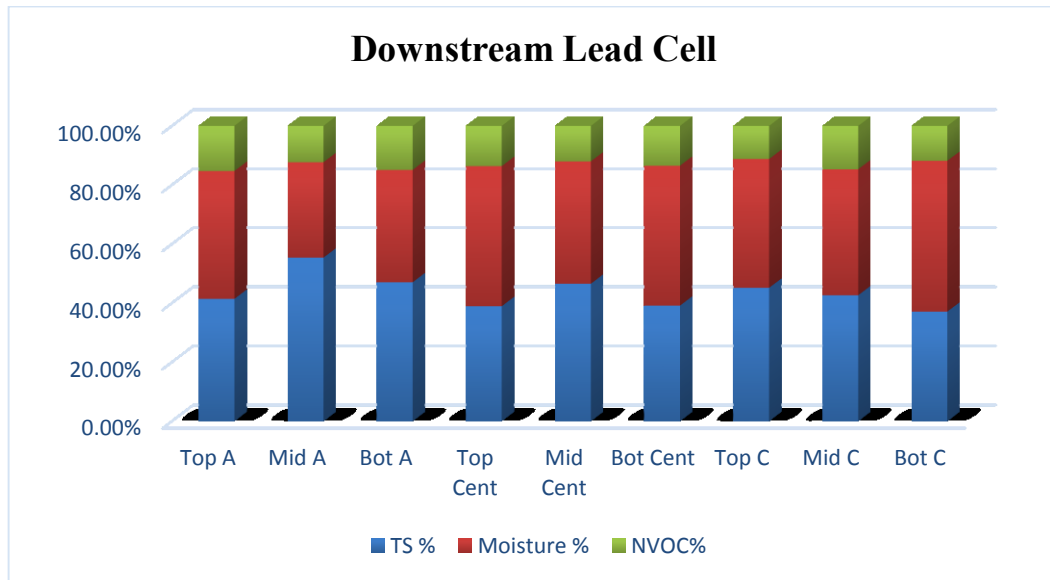


Figure 5.10 Fractions of oily sludge in downstream Lead Cell (after EK)

Note: TS= Total solid content, NVOC = Non-volatile organic content, Top A= Top anode area, Mid A= Middle anode area, Bot A= Bottom anode area, Top Cent = Top of center area, Mid Cent = Middle of center area, Bot Cent = Bottom of center area, Top C= Top cathode area, Mid C = Middle cathode area, Bot C = Bottom cathode area

5.1.4 Mixed metals Cells (Mix Cell)

Figure 5.11 illustrates the distribution of components in the upstream Mix Cell. After applying EK, the distribution of fractions took a similar pattern to the distribution of the oily sludge fractions of the previous three upstream (V, Ni, and Pb) Cells. This can be seen from the accumulation of solids (78 %) at the top of the anode area, which was similar to

the Nickel and Lead Cells, and the bottom of the anode area (79%) similar to the Vanadium Cell. Bottom of the anode area had the minimum amount of moisture (9.8 %) which is similar to the Vanadium upstream Cell. The amount of moisture increased at the center and cathode areas, where it reached a maximum of 48% at the bottom of cathode area. This pattern of moisture distribution was similar to the upstream Lead Cell, where moisture content had similar values between the center and cathode area. NVOC was high at the bottom of the anode area (10 %) and low at bottom of the cathode area (4 %).

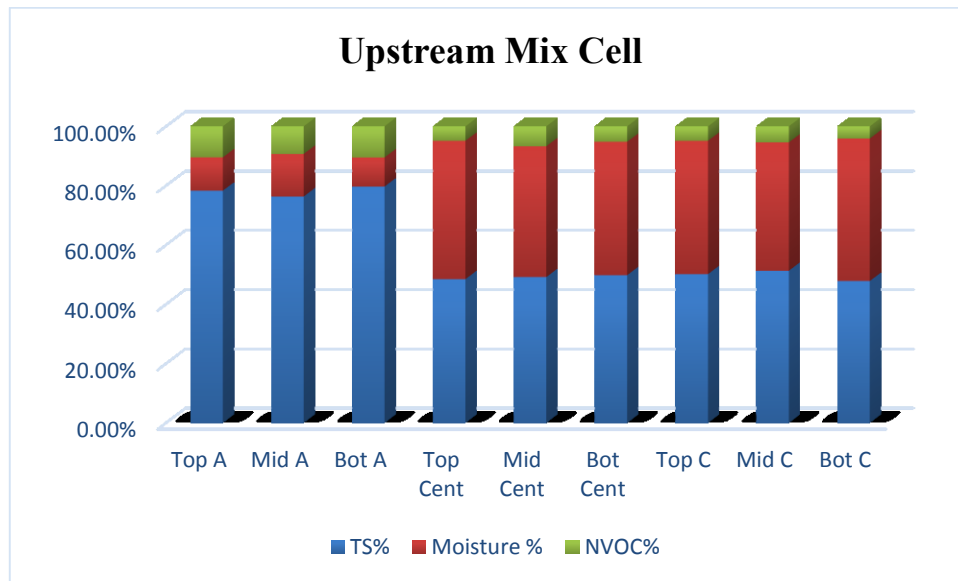


Figure 5.11 Fractions of oily sludge in upstream Mix Cell (after EK)

Note : TS= Total solid content, NVOC = Non-volatile organic content, Top A= Top anode area, Mid A= Middle anode area, Bot A= Bottom anode area, Top Cent = Top of center area, Mid Cent = Middle of center area, Bot Cent = Bottom of center area, Top C= Top cathode area, Mid C = Middle cathode area, Bot C = Bottom cathode area

The downstream Mix Cell showed different patterns in comparison to those of sole metal downstream cells. The percentage of the solid content was high throughout the cell, with a maximum of 68% at the bottom of the cathode area, and a minimum of 54% at the top of the cathode area. Conversely, the moisture content was lower than other downstream cells

throughout the matrix, where the maximum accumulation (32%) was detected at the bottom of the center area, and the lowest moisture was at the bottom of the cathode area (17%). The center area contained the maximum (17%) and minimum (11%) NVOC located at the top and bottom of cell, respectively (Figure 5.12).

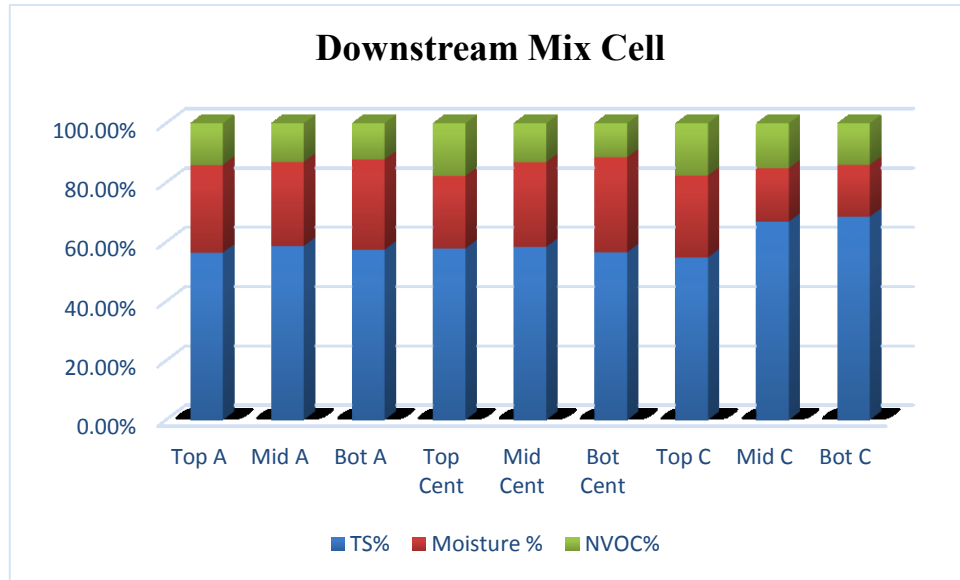


Figure 5.12 Fractions of oily sludge in a downstream Mix Cell (after EK)

Note: TS= Total solid content, NVOC = Non-volatile organic content, Top A= Top anode area, Mid A= Middle anode area, Bot A= Bottom anode area, Top Cent = Top of center area, Mid Cent = Middle of center area, Bot Cent = Bottom of center area, Top C= Top cathode area, Mid C = Middle cathode area, Bot C = Bottom cathode area

The characterisation of the sludge fractions in the upstream and downstream cells gave a physical confirmation of the vertical and horizontal separation of the oily sludge matrix, which produced new phases.

All upstream cells showed significant horizontal and vertical separation of sludge fractions. However, upstream Vanadium Cell showed better movement of liquids towards the cathode, and very high accumulation of solids at the bottom of the anode area (Fig 5.5). On the other hand, downstream cells showed random patterns in the distribution of components

after EK. For example, while downstream Nickel Cell showed higher accumulation of solids at the anode area, downstream Lead Cell showed higher moisture content at the cathode area. Such results affected the distribution of metals in these sections (Ch. 5.5).

5.2 Electrical parameters

Using the silver probes installed in each cell (Fig 4.6), electrical gradient was measured between the electrodes and the probes daily. The voltage between the electrodes was set at 20 Volt (1 Volt per cm distance between the cathode and anode), and the variation of current was detected daily. The resistance was calculated for each probe (Eq. 8) versus time in every cell. The variation of resistance along with pH readings would be a good indicator of separation of phases in different cells. Figures 5.13 through 5.28 display these results inside eight EK cells.

5.2.1 Resistance changes in Vanadium Cells

5.2.1.1 Upstream oily sludge

Figures 5.13 and 5.14 illustrate the changes in resistance versus time in the upstream Vanadium Cell anode and cathode areas respectively. The first 3 days in the anode/cathode areas, the resistance changes were relatively small, most probably because of the high stability of the mixture. From day 3 to day 8 resistances started to increase more rapidly but without any indication of vertical separation at the anode and cathode areas. This could be noticed from the matching resistance values at the vertical probes in each section. After day 8 especially in the cathode area, there was an obvious variation of readings between the top and bottom; which gave an indication of the occurrence of electro-separation processes.

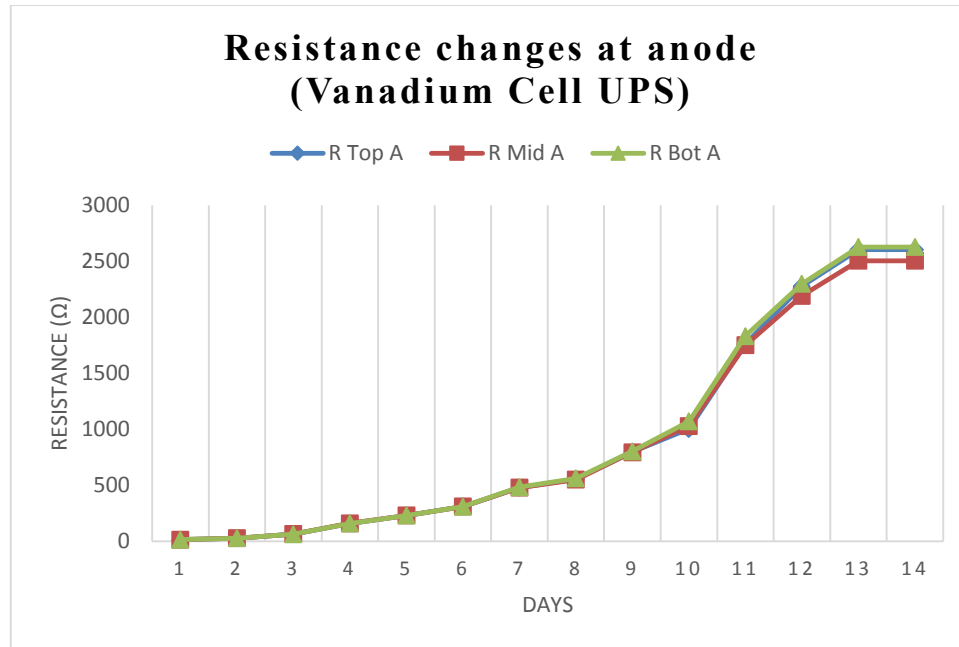


Figure 5.13 Resistance changes in upstream Vanadium Cell (anode area)

Note: UPS= Upstream, R Top A= Resistance top anode, R Mid A= Resistance middle anode, R Bot A= Resistance bottom anode

The resistance variation was less obvious at the anode area, this could be explained by the characterization of the sludge component in Chapter 5.1.1, where less moisture content was detected at the anode area, hence the low variation of resistance. From visual observations; accumulation of water and hydrocarbons was noticed at the cathode area. The maximum difference was noticed at day 13 where the resistance on the top of the cathode area was lower by around 700 Ω than the bottom cathode area. While the variation of resistance in each section indicated the vertical separation, the gradual increase in the resistance indicated the horizontal separation. In both (anode and cathode) areas, the horizontal separation was more obvious between day 8 and 13, where the increase in resistance was bigger versus time.

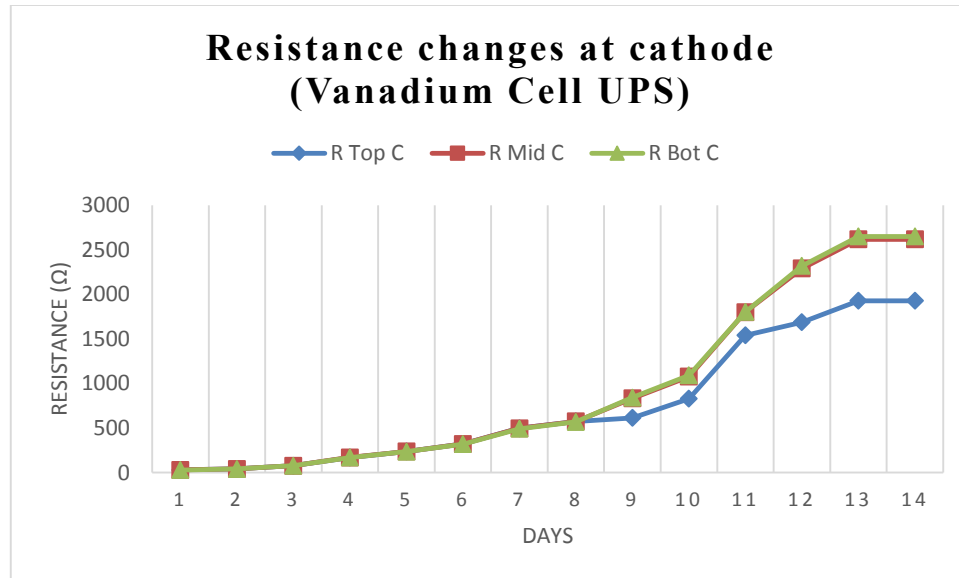


Figure 5.14 Resistance changes in upstream Vanadium Cell (cathode area)

Note: UPS= Upstream, R Top C= Resistance top cathode, R Mid C= Resistance middle cathode, R Bot C= Resistance bottom cathode

5.2.1.2 Downstream oily sludge

Figures 5.15 and 5.16 represent the changes in resistance in the downstream Vanadium Cell. In the anode area (Fig 5.15) for the three sections (top, middle, and bottom) the increment of resistance was very small the first three days, which suggested that the horizontal movements were very small. From day 3 to day 6 the resistance increased from (55 Ω to 250 Ω) this increment almost doubled from day 6 to day 9. From day 9 to day 13 the increase of resistance was very high, which is an indication of bigger horizontal movement of the components. From day 13 onward the current was very low and the resistance was high but stable. The vertical separation started to take place around day 6, where the resistance readings started to vary between top and bottom area probes, but the most notable variation was noticed at the last three days of the experiment where the gap between top and bottom reached 300 Ω.

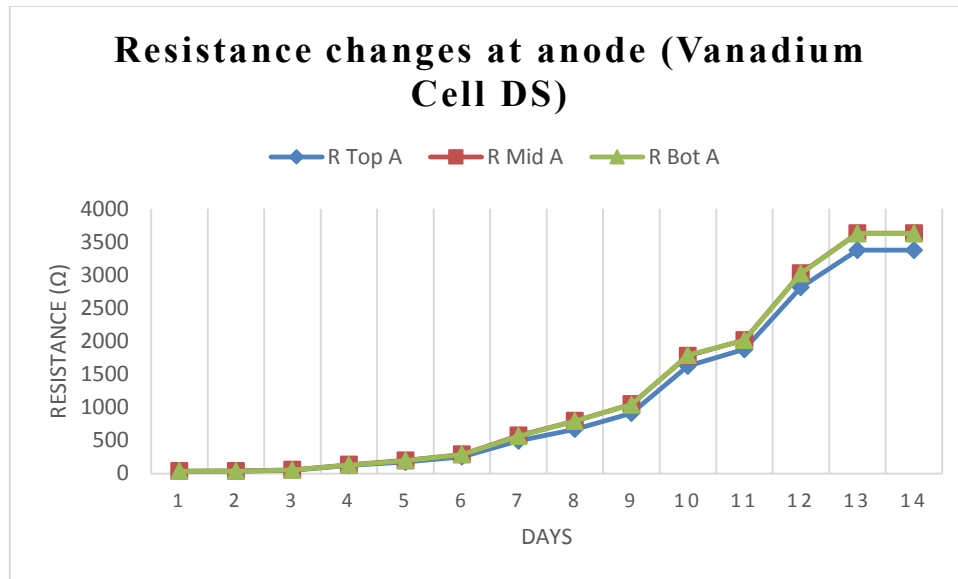


Figure 5.15 Resistance changes in downstream Vanadium Cell (anode area)

Note: DS= Downstream, R Top A= Resistance top anode, R Mid A= Resistance middle anode, R Bot A= Resistance bottom anode

The cathode area in the downstream Vanadium Cell (Fig 5.16) showed a similar pattern to that in the anode area, where the gradual increase of resistance started at day 3, then increased more rapidly from day 6 until day 13. On the other hand, the vertical separation started to take place earlier (day 4) than the anode area (day 6). Also from day 6 to day 11 the drop of resistance values between top and bottom areas was bigger in the cathode area than in the anode area. For example at day 10 in the cathode area the difference between the resistance at the top and bottom was around 275 Ω. While in the anode area for that same day the difference was around 160 Ω.

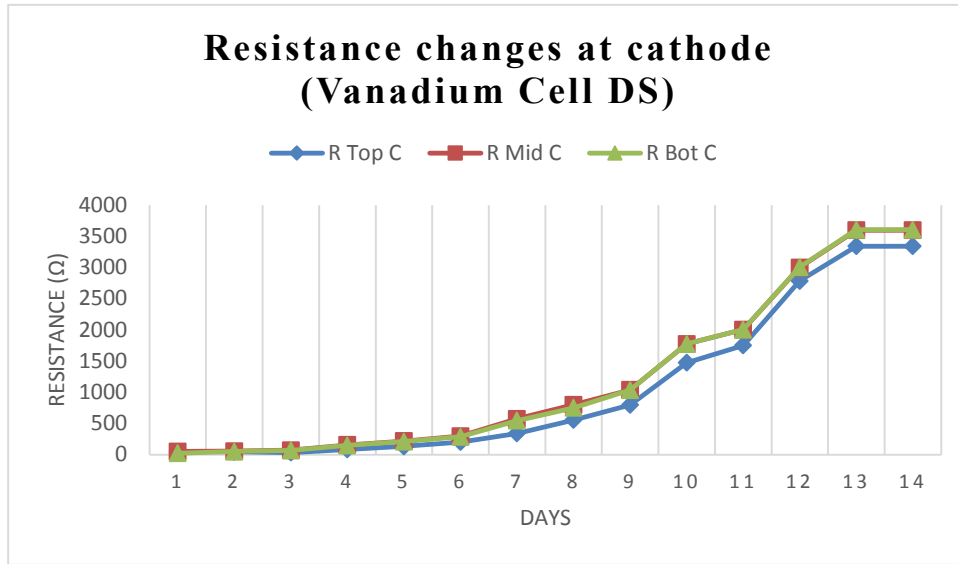


Figure 5.16 Resistance changes in downstream Vanadium Cell (cathode area)

Note: DS= Downstream, R Top C= Resistance top cathode, R Mid C= Resistance middle cathode, R Bot C= Resistance bottom cathode

It was concluded that seven days period is required to observe phase separation in Vanadium containing matrix for the voltage gradient and electrode distance, as defined in this investigations.

5.2.2 Resistance changes in Nickel Cells

5.2.2.1 Upstream oily sludge

Figure 5.17 illustrate the resistance changes in the upstream Nickel Cell at the anode section. As it had been the case in the upstream Vanadium Cell, due to the stability of the mix, and the relatively low voltage (1 V/cm) the first three days showed very little increase in the resistance values. But from day 3 to day 10 there was a gradual increase in the resistance, where it reached around 1000 Ω at day 10. This gradual increase gave an indication of the horizontal movement of components inside the cell. Between day 9 and 10, an indication of vertical separation was noticed in the anode section. This can be shown

by the lower value of resistance at day 10 for the mid anode section, where moisture could have been transported from the bottom of the cell in the vertical direction because of the electro-osmotic flow. This variation of resistance was obvious around day 12, where top, mid, and bottom of the anode area had different readings. The highest value was recorded at the bottom of the anode area and reached around 2800 Ω . That area included the most solid content with respect to the previous sludge characterization section 5.2.1.

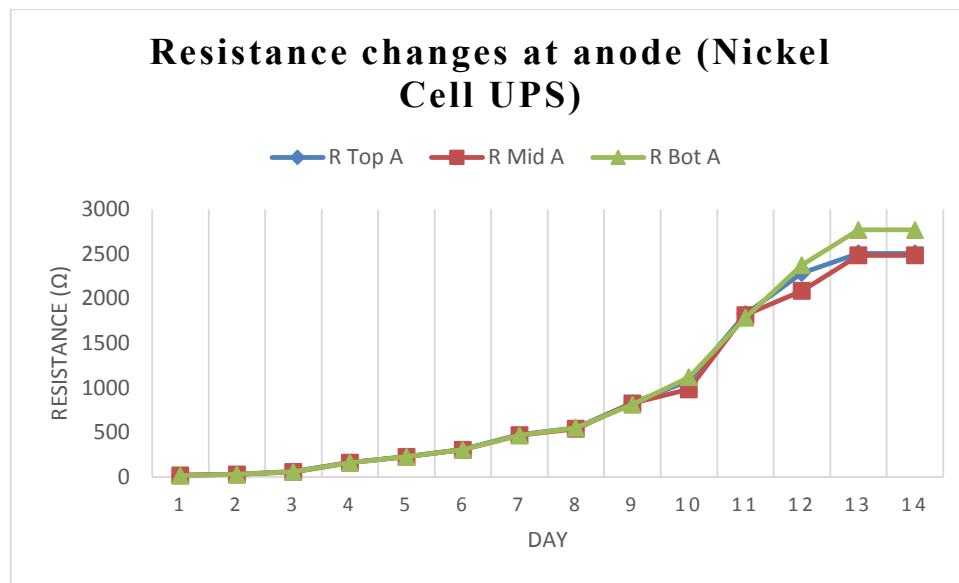


Figure 5.17 Resistance changes in upstream Nickel Cell (anode area)

Note: UPS= Upstream, R Top A= Resistance top anode, R Mid A= Resistance middle anode, R Bot A= Resistance bottom anode

Figure 5.18 shows the resistance changes in the cathode area in the upstream Nickel Cell. Unlike the anode area, horizontal separation in the cathode area started around day 2, where it increased gradually until day 8. After day 8, the increase of resistance was more obvious until day 13, where it became constant at around 2600 Ω . Despite the fact that visual observations and sludge characterization after EK showed accumulation of big amounts of liquid hydrocarbons at the top of the cathode area, resistance values didn't fluctuate

between the three sections (top, mid, and bot) until day 12, where top of the cathode area resistance dropped 100 Ω below the resistance reading of the mid and bottom cathode area.

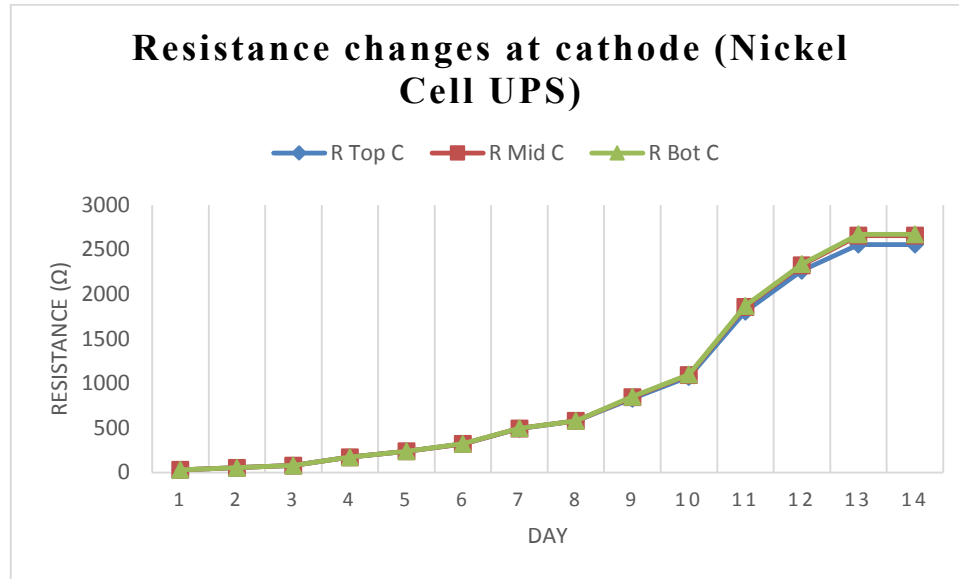


Figure 5.18 Resistance changes in upstream Nickel Cell (cathode area)

Note: UPS= Upstream, R Top C= Resistance top cathode, R Mid C= Resistance middle cathode, R Bot C= Resistance bottom cathode

5.2.2.2 Downstream oily sludge

Figure 5.19 shows slight increase of the resistance since day one, suggesting early horizontal movement of the oily sludge components in the anode area in the downstream Nickel Cell. During the 14 days, the increase of resistance took the shape of intervals; day 1 to 6, 6 to 9, 9 to 10, 10 to 11, 11 to 13, and 13 to 14. The biggest slope was from day 9 to day 10 (from 1040 Ω to 1821 Ω) which indicate a larger horizontal movements of the components after day 9. In the vertical direction, the separation was very slow. After day 10 some variation of the resistance values started to appear between the middle and bottom areas, though these variations were very small. At the end of the experiment, the top and middle anode areas had a maximum resistance of around 3760 Ω , while the bottom area

had a maximum resistance of 3640 Ω . This difference was relatively small to indicate that the vertical separation actually took place in this section.

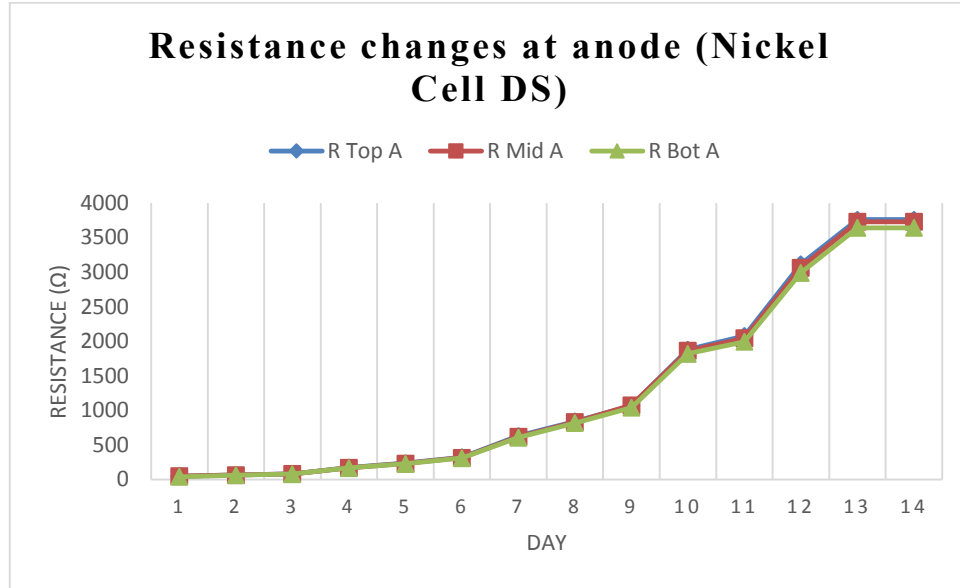


Figure 5.19 Resistance changes in downstream Nickel Cell (anode area)

Note: DS= Downstream, R Top A= Resistance top anode, R Mid A= Resistance middle anode, R Bot A= Resistance bottom anode

From Figure 5.20, the resistance changes appeared to take almost an identical pattern as the anode area. These identical patterns indicated that despite the increase of resistance during the 14 days experiment, the horizontal and vertical separations were not spotted using electrical parameters. Additional tests would give more accurate conclusions regarding the separation in the downstream Nickel Cells. These tests include (pH, FTIR analysis, XRD analysis, and rheological characteristics), which would be introduced in Sections 5.3, 5.4, 5.7, and 5.8.

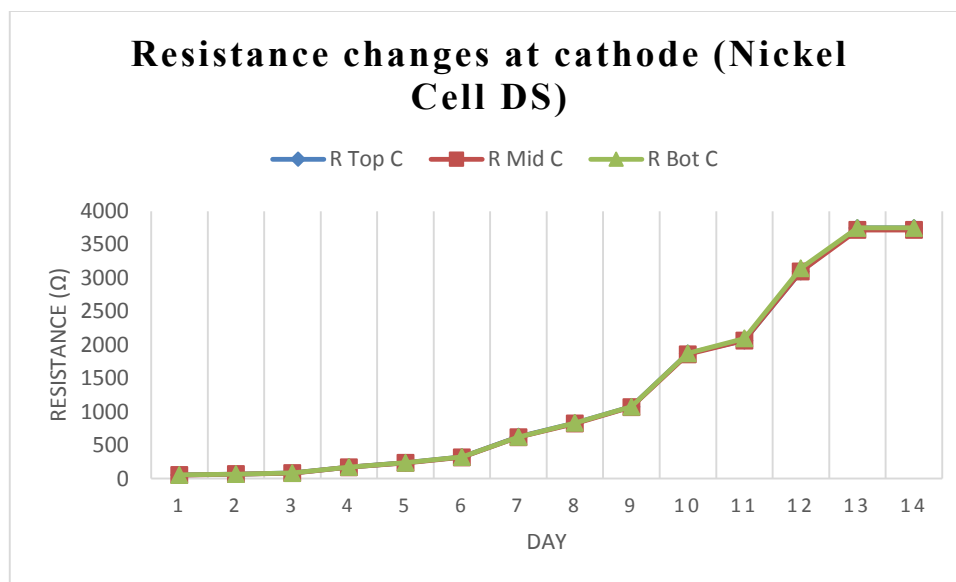


Figure 5.20 Resistance changes in downstream Nickel Cell (cathode area)

Note: DS= Downstream, R Top C= Resistance top cathode, R Mid C= Resistance middle cathode, R Bot C= Resistance bottom cathode

The phase separation under DC field was observed in oily sludge (containing nickel) from the beginning of EK the experiment but it was rather slow and insignificant in the downstream cells.

5.2.3 Resistance changes in Lead Cells

5.2.3.1 Upstream oily sludge

Figure 5.21 represents resistance changes in the upstream Lead Cell at the anode area. Similar to Nickel and Vanadium upstream Cells, first week showed gradual and slow increase in the resistance. This pattern started to change from day 8 to day 9, where the resistance increase was more significant in shorter time, which indicated a sudden movement of components horizontally. Consequently, the resistance started to increase more rapidly from day 8 onward, where it reached a maximum value of 2700 at the bottom of the anode area, where anode area showed high accumulation of solid particles. Vertical

separation started to take place around day 11, taking into consideration that changes in resistance started to be more visible in the three sections (top, mid, and bot) in the anode area. While the middle and top areas behaved the same, the bottom showed a higher resistance for the current, which suggests a higher accumulation of dry solid particles at the bottom area.

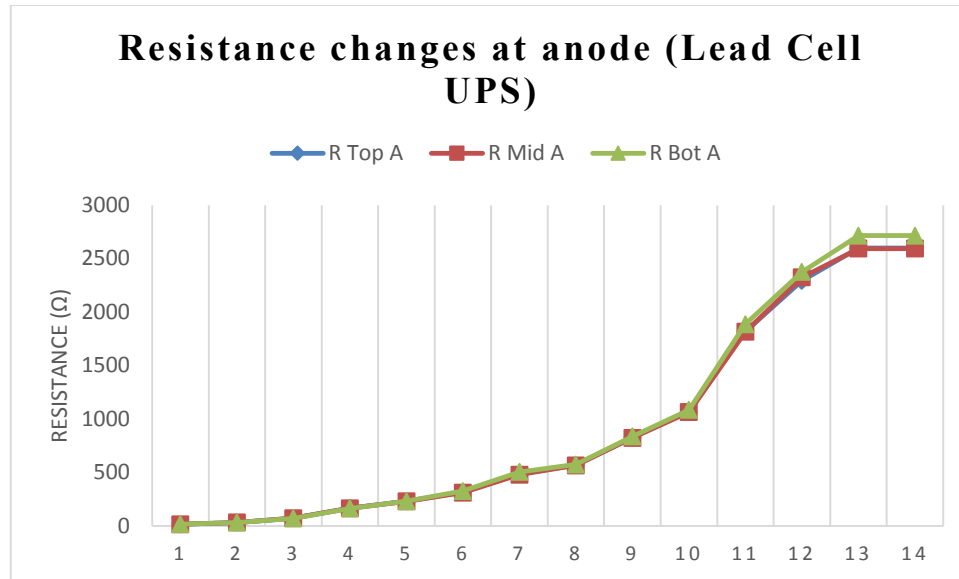


Figure 5.21 Resistance changes in upstream Lead Cell (anode area)

Note: UPS= Upstream, R Top A= Resistance top anode, R Mid A= Resistance middle anode, R Bot A= Resistance bottom anode

Figure 5.22 shows the changes in resistance in the cathode area in the upstream Lead Cell. Similar to the anode area, there has been a gradual increase of resistance from day 2 to day 8, followed by a higher increase versus time, from day 8 to day 10. Subsequently, from day 10 onward the increase in resistance was much bigger, which can be related to the same horizontal movements explained previously in upstream cells. On the other hand, the vertical separation started to take place around days 10, when resistance values of the top cathode area started to drop below the values of the middle and bottom areas. This gave an indication of the breakdown of the oil-in-water emulsion at the cathode, where the liquid

components were detected through visual observations and characterization of the resulted sludge fractions.

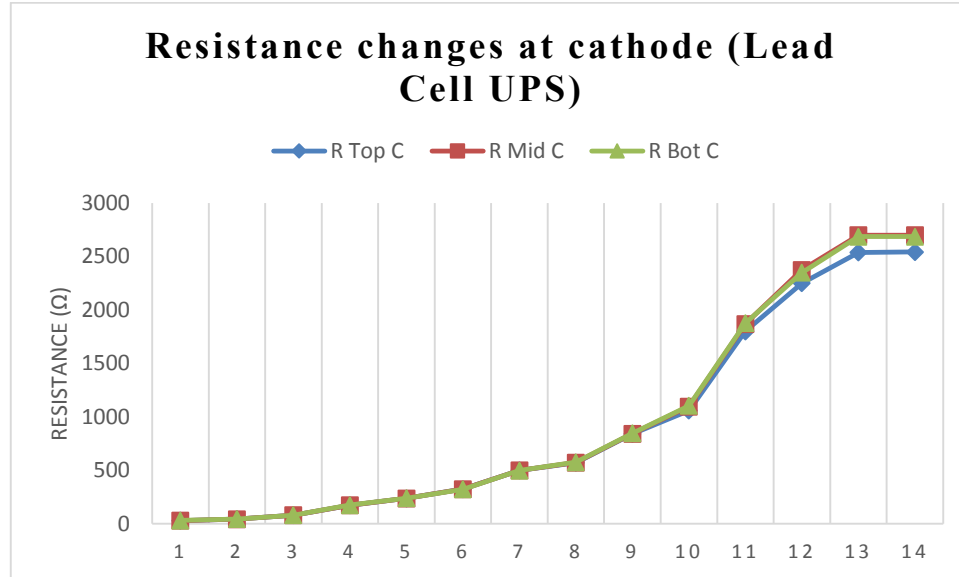


Figure 5.22 Resistance changes in upstream Lead Cell (cathode area)

Note: UPS= Upstream, R Top C= Resistance top cathode, R Mid C= Resistance middle cathode, R Bot C= Resistance bottom cathode

A significant separation was observed in the Lead Cell after one week of exposure to EK conditions as defined in methodology.

5.2.3.2 Downstream oily sludge

Figure 5.23 shows the changes in resistance at the anode area in the downstream lead Cell. Vertical separation was not clearly spotted in the cell. Although the Figure does not show unusual patterns if compared to the Nickel and Vanadium downstream Cells, some results were taken into consideration; first, the gradual increase of the resistance started from day one, which means the EK effect started to take place very early. However, this effect was more in the horizontal direction through the whole experiment. Day 7 showed a slight variation of the resistance between top and bottom area. This deviation was noticed again at the end of the experiment, but in between, the resistance readings were similar. These

results could be related to the limited movement of liquids between the top and bottom, which could have happened on these intervals.

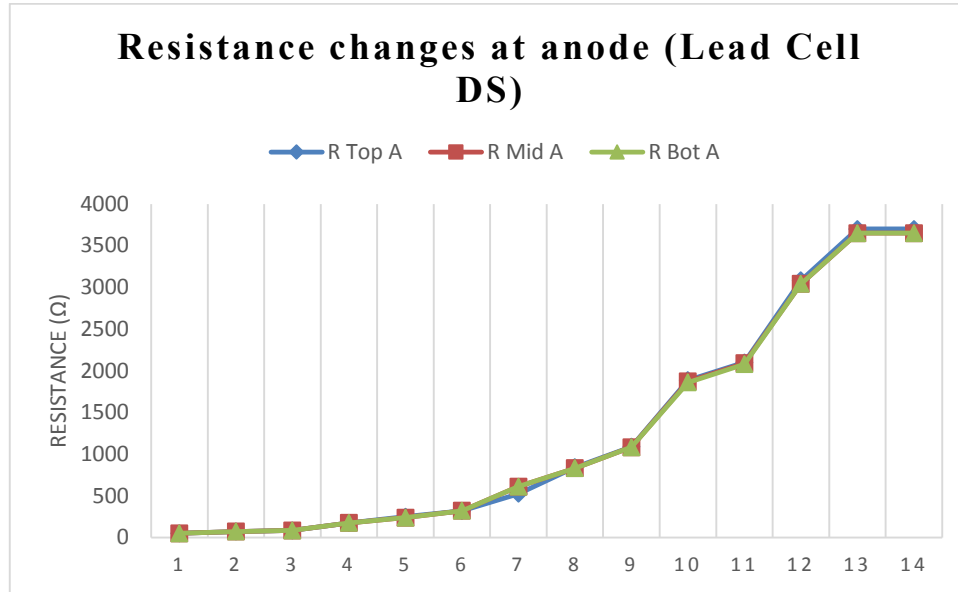


Figure 5.23 Resistance changes in downstream Lead Cell (anode area)

Note: DS= Downstream, R Top A= Resistance top anode, R Mid A= Resistance middle anode, R Bot A= Resistance bottom anode

As it can be seen from Figure 5.24, that horizontal movements and vertical separation was largely spotted in this section of the cell mainly depending on the electrical parameters (resistance changes). From day 1 to day 8 results were similar to those in previous downstream cells. But from day 8 to day 10 there was an increase in the resistance for the bottom and middle areas, countered by a decrease of resistance at the top of cathode area. The gap between these two sections reached 1310 Ω at day 10, which clearly indicated a big vertical separation in the cathode area. The drop in resistance in the top of the cathode area could have happened because of the demulsification process of the water-in-oil based sludge. It clearly took place at day ten, and resulted in the migration of moisture rapidly

through electro-osmotic transport to the top, where horizontal movements were very slow on the top. This gap started to decrease on day 12 (200 Ω), then from day 12 to day 14 the gap increased again (600 Ω). This could indicate that vertical separation happened on intervals depending on the rate of the demulsification process.

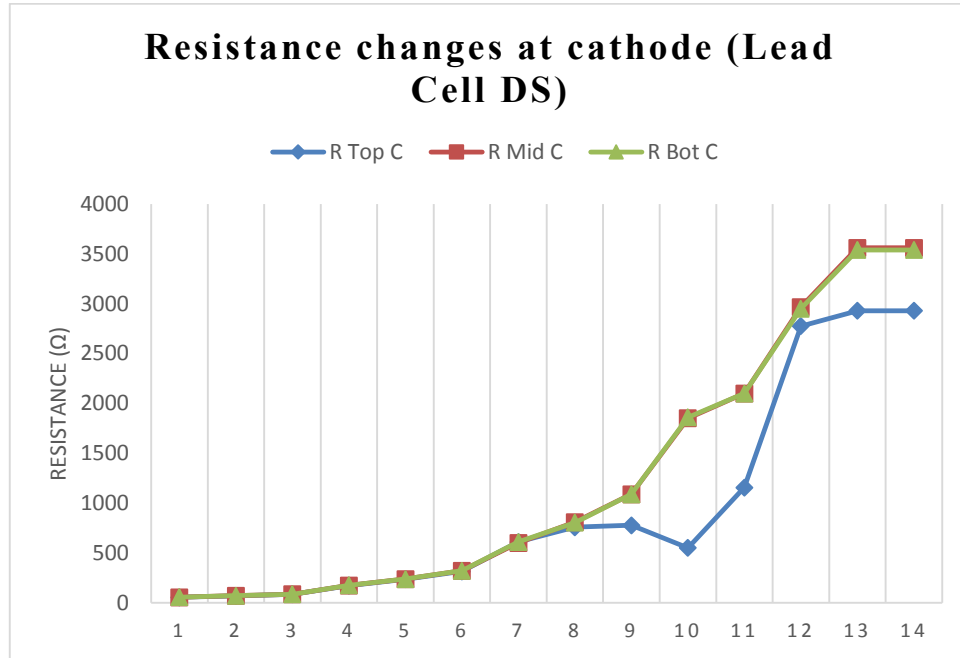


Figure 5.24 Resistance changes in downstream Lead Cell (cathode area)

Note: DS= Downstream, R Top C= Resistance top cathode, R Mid C= Resistance middle cathode, R Bot C= Resistance bottom cathode

5.2.4 Resistance changes in Mix Cells

5.2.4.1 Upstream oily sludge

Figure 5.25 shows the resistance changes in the anode area in the upstream Mix metal Cell. This cell initially contained equal amounts of chlorides of the three metals (V, Ni, and Pb). In the literature review it was explained that chloride compounds can conduct electricity when fused or dissolved in water (Ch. 2.2). Chloride materials can be decomposed by

electrolysis to chlorine gas and metal. Accordingly the solubility of each metal chloride in the emulsion would affect the resistance reading in the Mix Cell. Until day 3, no noticeable change in the resistance was detected, which means no visible horizontal or vertical separation yet to take place. From day 3 to day 8 gradual increase of resistance started to happen accompanied by small variation of resistance between the top, middle and bottom sections. These changes indicated the initiation of the horizontal and vertical separation at the anode. But between day 8 and day 11 the resistance increase was rapid but equal for all the three sections, until day 13 where resistance reached a maximum value of 2707 Ω at the bottom of the anode area. At that same point, the middle area had a maximum resistance of 2594 Ω which is lower than the top and bottom areas, which could be related to the presence of trapped moisture pockets in that area.

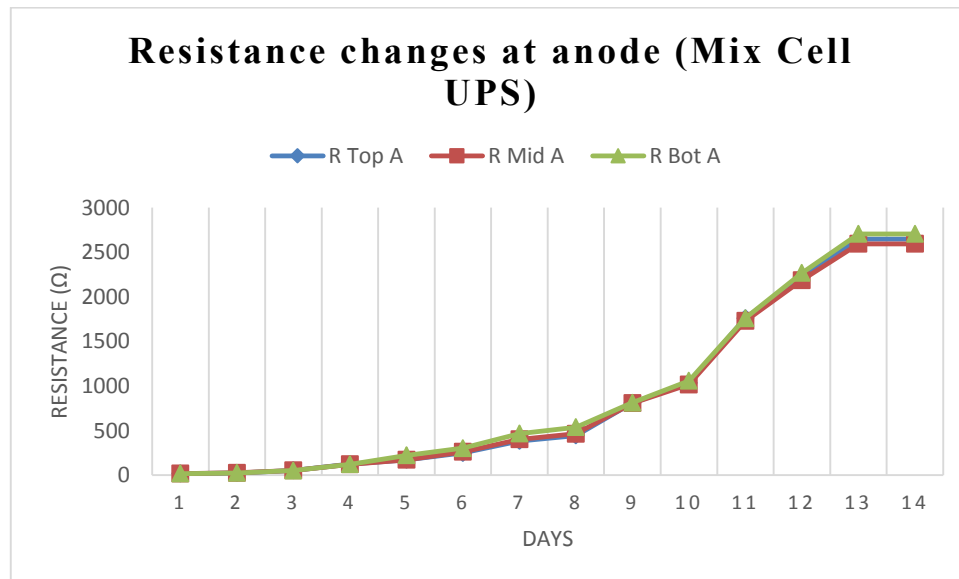


Figure 5.25 Resistance changes in upstream Mix Cell (anode area)

Note: UPS= Upstream, R Top A= Resistance top anode, R Mid A= Resistance middle anode, R Bot A= Resistance bottom anode

The resistance changes in the cathode area are shown in Figure 5.26. In the cathode area horizontal and vertical separation of components were more visible, which means the electro-demulsification rate was higher in this part of the cell. From visual observations it was clear that liquid components migrated to the cathode area (Appendix B, Fig B.6) and accumulated on the top of the cathode area. This caused the resistance to drop in that area. From day 1 until day 5 there was a gradual yet equal increase in the resistance for all the sections of the cathode. But from day 5 onward there was an obvious fluctuation in the resistance between the top, middle, and bottom. These variations of resistance values indicate vertical and horizontal separation of components in the cell. The top of the cathode area had lower resistance values after day 5 until day 13, where the value were almost equal because of the drop of the current to a very small values. This phenomenon was followed until the disconnection of the system at day 14.

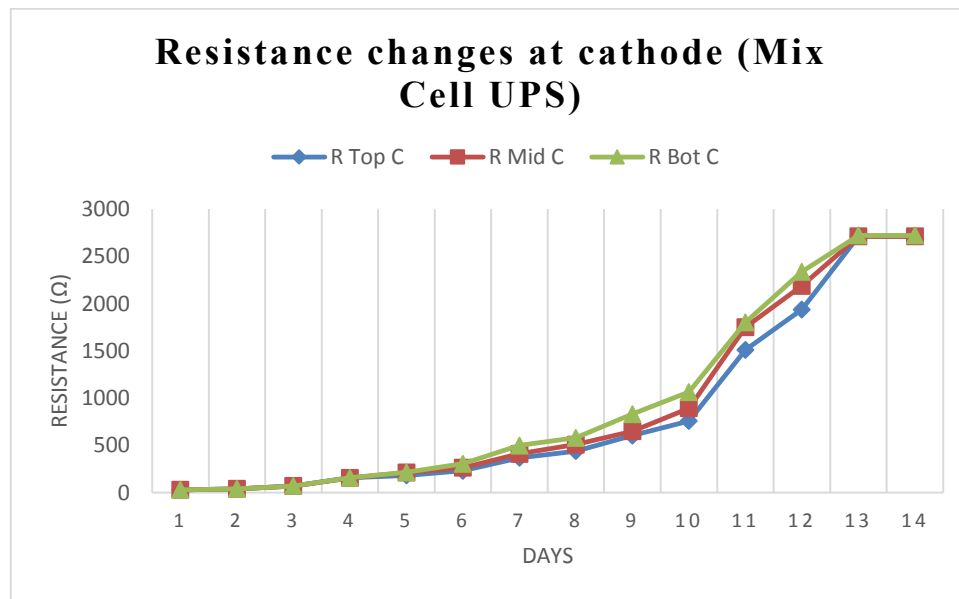


Figure 5.26 Resistance changes in upstream Mix Cell (cathode area)

Note: UPS= Upstream, R Top C= Resistance top cathode, R Mid C= Resistance middle cathode, R Bot C= Resistance bottom cathode

5.2.4.2 Downstream oily sludge

The addition of diesel in the downstream cells decreased the conductivity of the sludge. This was noticed in all the four downstream cells, where the resistance increased to higher values than the upstream cells. Figure 5.27 shows the resistance changes in the downstream Mix Cell. The first three days showed a slight drop in resistance (from 45 Ω to 25 Ω), which was an indication that horizontal movement of the oily sludge components started to take place since day one, hence the slight fluctuation of the resistance. Through the 14 days, the increase of resistance took the shape of intervals; day 1 to 3, 3 to 6, 6 to 9, 9 to 10, 10 to 11, 11 to 13, and 13 to 14. This pattern was similar to the one in the Nickel downstream Cell.

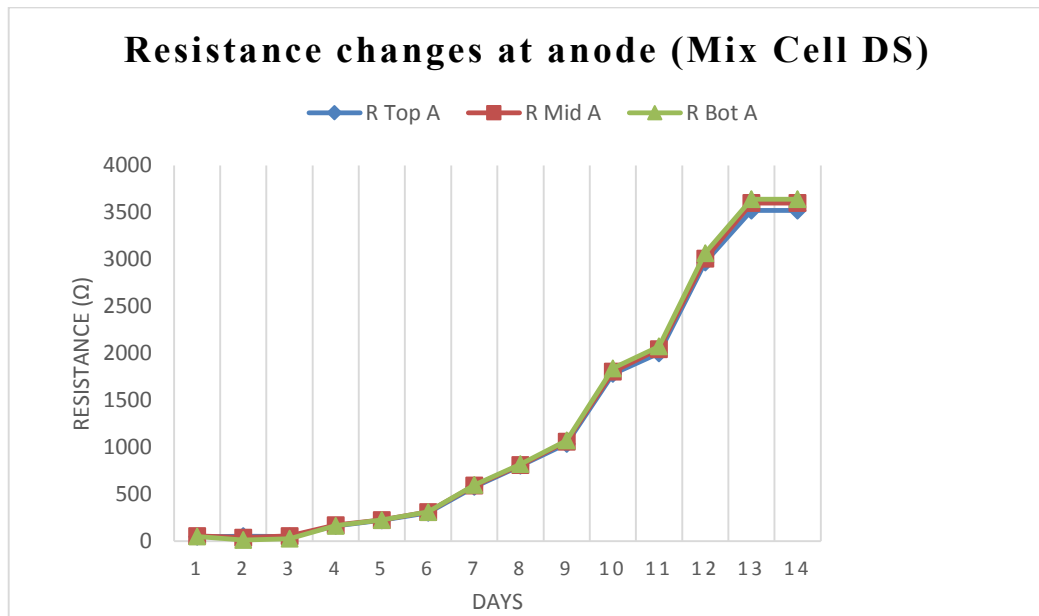


Figure 5.27 Resistance changes in downstream Mix Cell (anode area)

Note: UPS= Upstream, R Top A= Resistance top anode, R Mid A= Resistance middle anode, R Bot A= Resistance bottom anode

The biggest slope was from day 11 to day 12 (from 2070 Ω to 3000 Ω) which indicate larger horizontal movements of the components after day 11. In the vertical direction, the separation was not spotted using electrical parameters, but after day 12 some variation of the resistance values started to appear between the middle top and bottom areas, though these variations were very small. At the end of the experiment, the top, middle, and bottom anode areas had maximum resistances of around 3540 Ω , 3600 Ω , and 3660 Ω respectively. These differences were relatively small to indicate that the vertical separation actually took place in this section. So other parameters should be taken into consideration.

Figure 5.28 illustrates the changes in resistance in the downstream Mix Cell at the cathode area. The mix showed more variation in the electrical parameters than the anode area, when after day 7, the top of the cathode area had a slight drop of the resistance reading. At day 10 slight variations were detected between the top, middle and bottom, which later developed into a bigger gap between the bottom and middle on one side, and the resistance at the top on the other. This gap between top and bottom resistance reached 500 Ω at day 13. This difference gave an indication of possible vertical separation, which was already certified by visual observations, where pockets of oil found on the top of the cathode area. Some resistance values were not fully detected there, due to location of probe electrodes above the sludge surface.

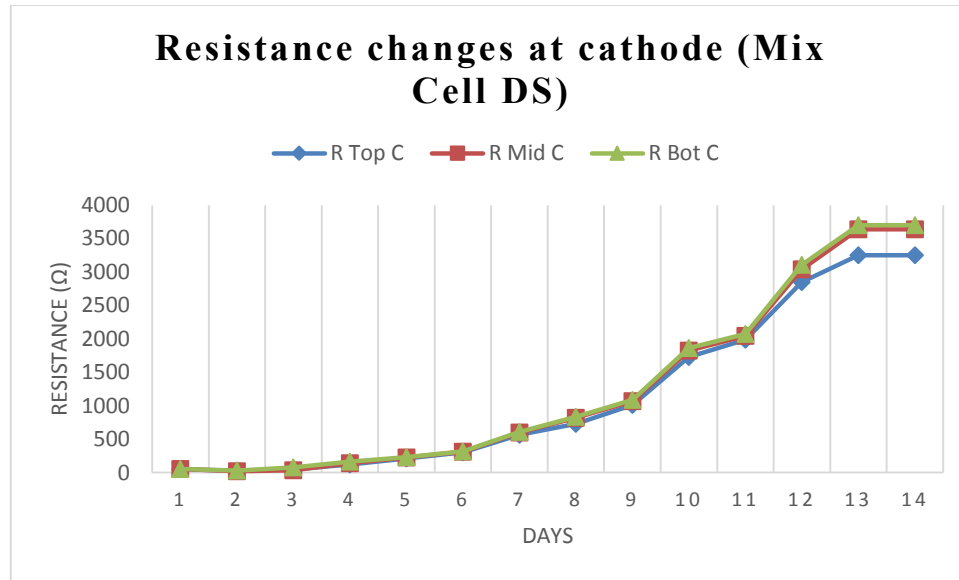


Figure 5.28 Resistance changes in downstream Mix Cell (cathode area)

Note: DS= Downstream, R Top C= Resistance top cathode, R Mid C= Resistance middle cathode, R Bot C= Resistance bottom cathode

5.2.5 Average power and energy consumption

Figure 5.29 shows the average power consumption in the upstream and downstream cells. In both scenarios it was obvious the decrease of power consumption versus time. The power consumption was assessed according to the following equation:

$$P= VI \tag{11}$$

Where

P: is the electric power (W) V: constant DC potential (V), I: current intensity (A)

Calculations were based on Figures 5.13 through 5.28, where daily resistance (R), current intensity (I) and electric gradient (V) (Eq. 8, Ch. 4.4.3) were deployed in Eq. 11 to calculate the daily average power consumption of all upstream and downstream cells (Fig 5.29).

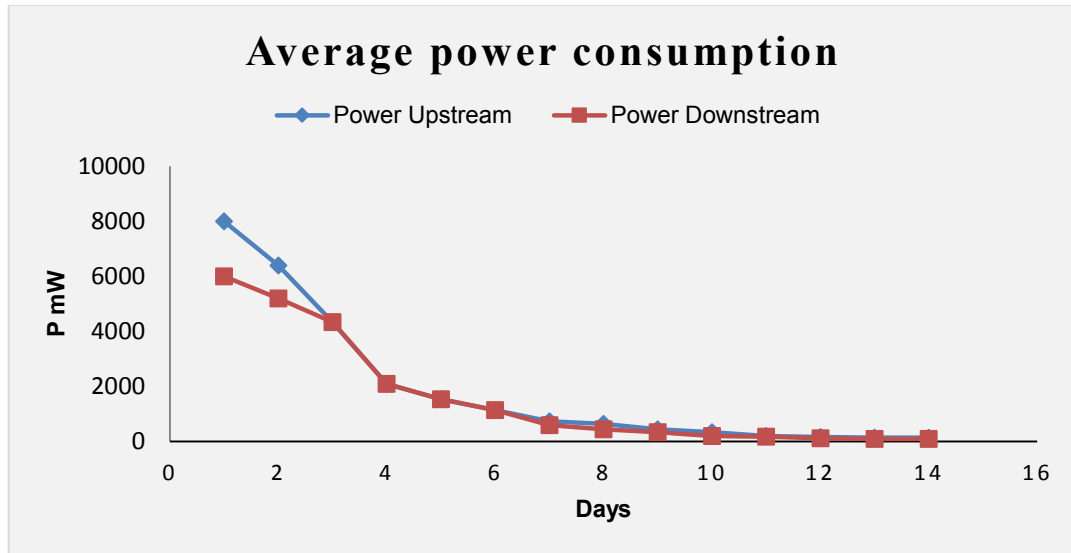


Figure 5.29 Average electrical power consumption in upstream and downstream cells

The total energy consumption over the 14 days period was based on the hourly power consumption (W.h). Accordingly, the upstream cells consumed higher energy (631.68 W.h) than the downstream cells (537.6 W.h). This could be a result of the higher water content in the upstream cells, which increased the conductivity and lowered the resistivity of the system, thus increasing the current in the EK cell. It was noticed that the consumption of energy in the final stages was similar in both upstream and downstream cells. Moreover, it is anticipated that energy consumption and costs would decrease with scaling up the process.

5.3 Measurements of pH

As it has been explained in the methodology (Ch. 4.4.2), pH measurements were initially taken 4 times during the experiment (days 1, 4, 9, and 14). Readings on days 4 and 9 were taken through the special holes in the cover (Fig 4.6) while the electrical current is on. On

the other hand, readings on days 1 and 14 were taken while the cover was open, and the current was on and off respectively.

The pH gradient has great influence on EK systems (Ch. 2.6.1). Alkalinity indicates the characteristics of different components in the system, and with other factors it controls the movements of ions in the matrix. The pH of each cell was initially measured at fixed selected points at the top, and in the bottom of each cell. However, pH was measured at extra locations depending on other factors such as: visual observations, metal distributions, and any change of contents detected through FTIR and XRD tests.

Figures 5.30 through 5.38 show the pH deviation in all the upstream and downstream cells. Most of the cells showed an increase of pH values close to the cathode area countered by a decrease of pH close to the anode area in the first few days of the experiment. However, each cell showed different readings and random patterns with the pH increase and decrease while the experiment went on. Generally, the increase of pH at the cathode area was because of the constant release of the OH^- ions in the reduction process near the cathode. While the oxidation process near the anode caused the drop of pH since the formation of the H^+ ions in that area (Ch. 2.6.1).

5.3.1 pH changes in upstream/downstream - Vanadium Cells

Figure 5.30 shows the changes of pH in the upstream Vanadium Cell. Readings were taken at six fixed points initially, and three sampling intervals were taken into consideration. Readings at the end of the first interval showed an increase of pH in all the sections except for the bottom anode area, where there was a drop from 8 to 6. The decrease of pH usually is related to the formation of H^+ ions because of the oxidation of the anode or the hydrolysis of water. Second interval (from day 4 to 9) showed variation of patterns, where the top

(12) and bottom (12) cathode areas, and bottom anode area (6) pH readings stayed constant. On the other hand, there was a slight drop in pH at the top and bottom central areas from 11 to 10, and a big drop in pH at the top anode area from 11 to 6.5. These changes between the readings at the different sections confirms the beginning of the separation process, consequently, the transportation and transformation of vanadium inside the matrix. The last interval from day 9 to 14 showed a decrease of pH for all the sections by 1 or 2 points.

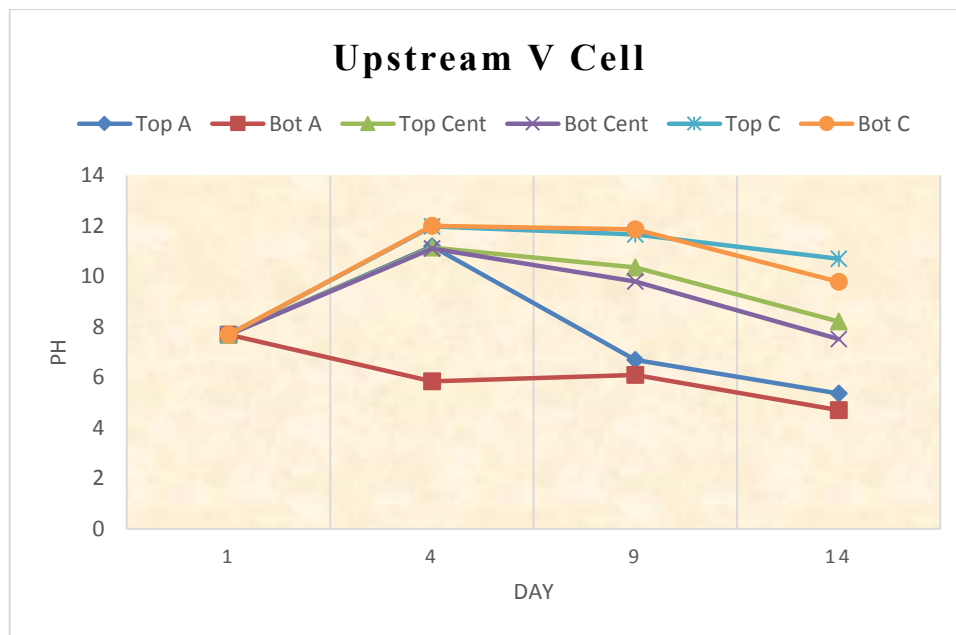


Figure 5.30 pH changes in upstream Vanadium Cell
 Note: Cent: central area, A: anode, C: cathode, Bot: bottom

Figure 5.31 displays the values of pH in the downstream Vanadium Cell. First four days showed a slight increase of the pH values at the top (9 to 10) , and bottom (9 to 11) of the cathode area. Also the central part showed an increase at the top (9 to 11) and bottom (9 to 10). However, pH at the top and bottom of the anode area didn't change by more than 0.2 points, which suggests that, rate of prudction of H^+ and OH^+ for this period were relatively constant. For the second interval, pH values started to drop slowly for all the sections

except for the bottom anode area, where there was a 0.3 increase of pH . The last interval showed a stability for the bottom cathode and anode areas . The top of the center area stayed around 10, which was the highest in the matrix. While top of the anode and bottom of the center areas slightly increased, top of the cathode area dropped from 10 to 9. By looking at the figure and relating these values to the electrical parameters in the same cell, it can be seen that separation was not confirmed using these two parameters. The presence of diesel in the downstream cells obviously affected the separation process. Nevertheless, further tests in the following sections demonstrated the movements of the minerals and metals inside the cell.

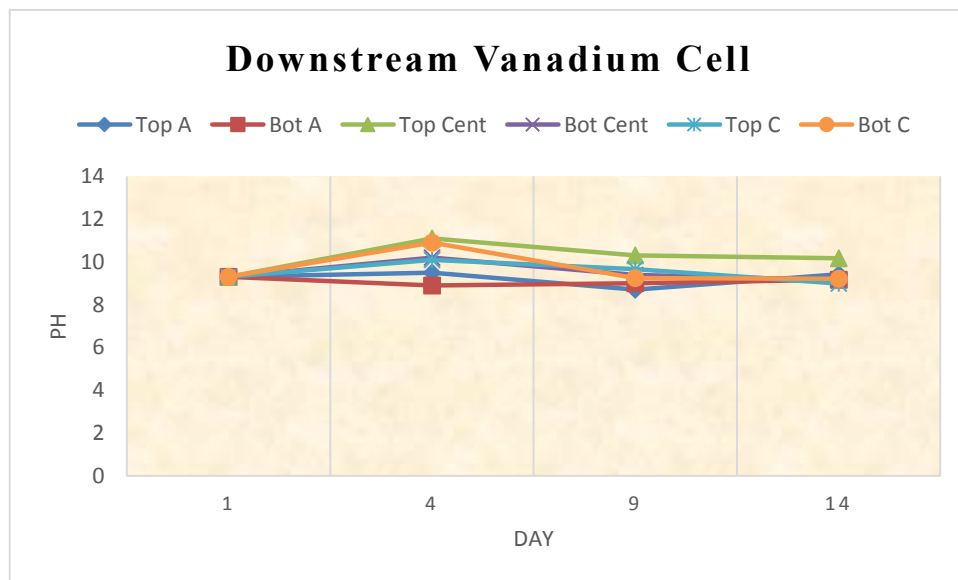


Figure 5.31 pH changes in downstream Vanadium Cell
 Note: Cent: central area, A: anode, C: cathode, Bot: bottom

5.3.2 pH changes in upstream/downstream - Nickel Cells

Figure 5.32 shows the changes of pH in the upstream Nickel Cell. Readings at the end of the first interval showed an increase of pH in all sections, except for the bottom anode area,

where there was a slight drop from 8 to 7.3. Top and bottom of the cathode showed the highest increase of pH (8 to 11.77) and (8 to 11.31) respectively, followed by the top central (8 to 11), top anode (8 to 10.8), and bottom central area (8 to 10) respectively. The bottom anode area was the only place where the pH slightly dropped from 8 to 7.3. Second and third intervals showed similar patterns, where pH slightly dropped at the top and bottom cathode, top central areas, and sharply dropped at the top (from 10.8 to 6) and bottom (7.3 to 4) anode areas. Bottom central area was the only section where an increase of pH was noticed (from 10 to 11.3).

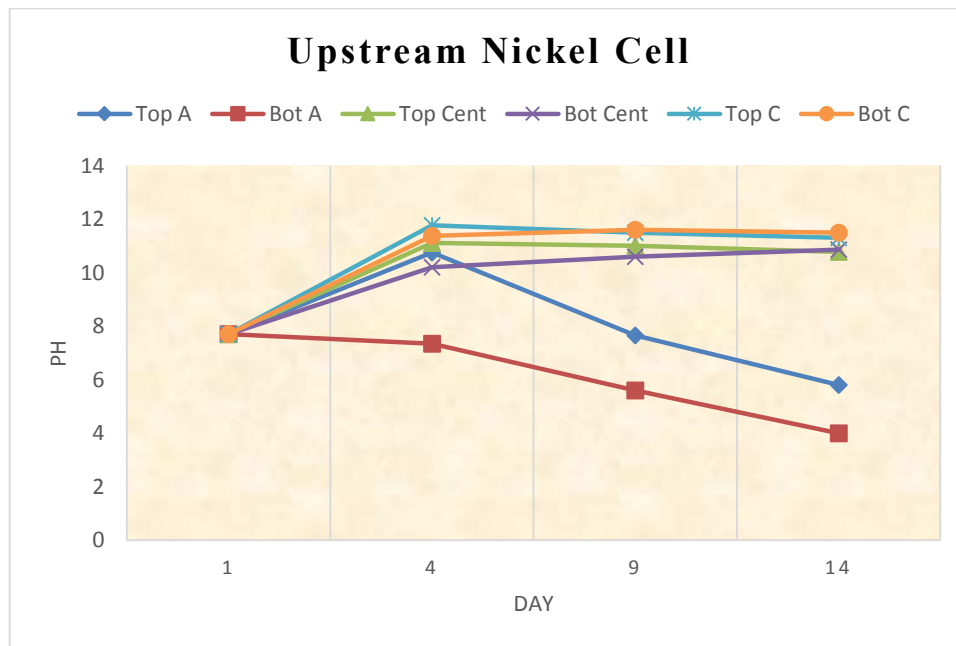


Figure 5.32 pH changes in upstream Nickel Cell
 Note: Cent: central area, A: anode, C: cathode, Bot: bottom

Figure 5.33 shows the pH variations in the downstream Nickel Cell. Although the final pH reading was around 8 for all the sections in this cell, the first (1 to 4) and second (4 to 9) intervals showed a variation in the pH values. For example, for the first 4 days there was an increase of pH at the cathode area, opposed by a slight decrease at the center, and bigger

drop at the bottom anode area. Second interval showed a drop in pH at the cathode area and all the other top sections. However, the bottom anode and central area showed an increase in pH. These randomness in pH results suggests that components in the cell were constantly shifting when the electric current was on.

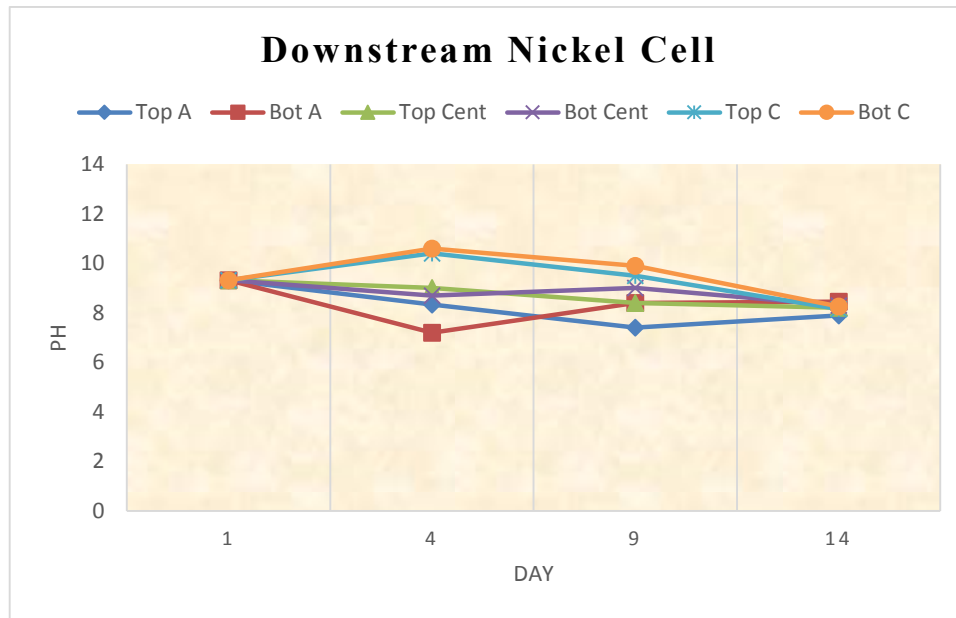


Figure 5.33 pH changes in downstream Nickel Cell
 Note: Cent: central area, A: anode, C: cathode, Bot: bottom

5.3.3 pH changes in upstream/downstream - Lead Cells

Figure 5.34 shows the changes in pH for the upstream Lead Cell. In the first interval, pH values showed similar patterns of those of upstream Nickel and Vanadium Cells, the only difference could be noted as the increase of pH at the anode area for the first few days, which suggests less formation of the hydrogen ions at that area. In the second interval, there was a drop in pH in the whole cell, especially at the anode area where the drop was from 11 to 9 at the top, and from 9.5 to 8 at the bottom. This decrease in pH is associated with the increase of formation of hydrogen ions, especially at the anode area where oxidation

was set to take place. In the last interval of the experiment, liquids had already shifted to the cathode through electroosmotic flow, and solids to the anode through electrophoresis, which justify the constant pH in the last few days, except for the bottom anode area where the oxidation of the anode contributed to the formation of hydrogen ions at high rate, which caused a big drop of pH to around 5.

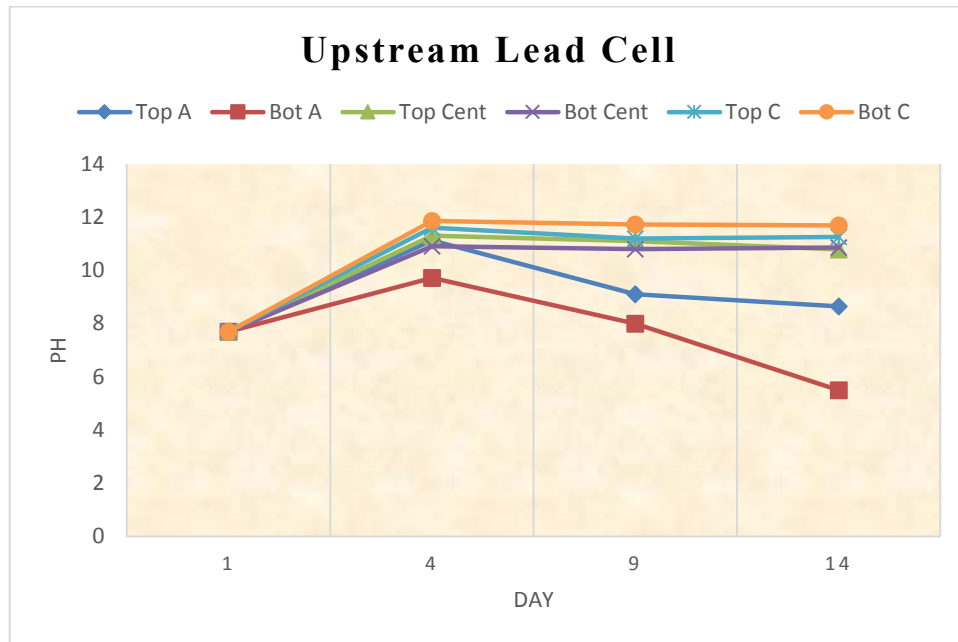


Figure 5.34 pH changes in upstream Lead Cell
 Note: Cent: central area, A: anode, C: cathode, Bot: bottom

Figure 5.35 demonstrates the pH changes in the downstream Lead Cell. From visual observations in this cell, separation was not clearly visible after the 14 days experiment. pH changes varied between 9 and 10 for most of the cell sections, except for the top anode section, where pH dropped to around 7.9 at the end of the experiment. This drop probably was related to the oxidation at the anode area. The presence of diesel in the downstream cells prevented the sudden increase of pH values in the first interval like the upstream cells scenarios. Especially, the diesel fuel has an average pH of 5.6, and by the end of the

experiment diesel was still spread in the whole cell, as it would be explained later by the FTIR analyses (Ch. 5.7).

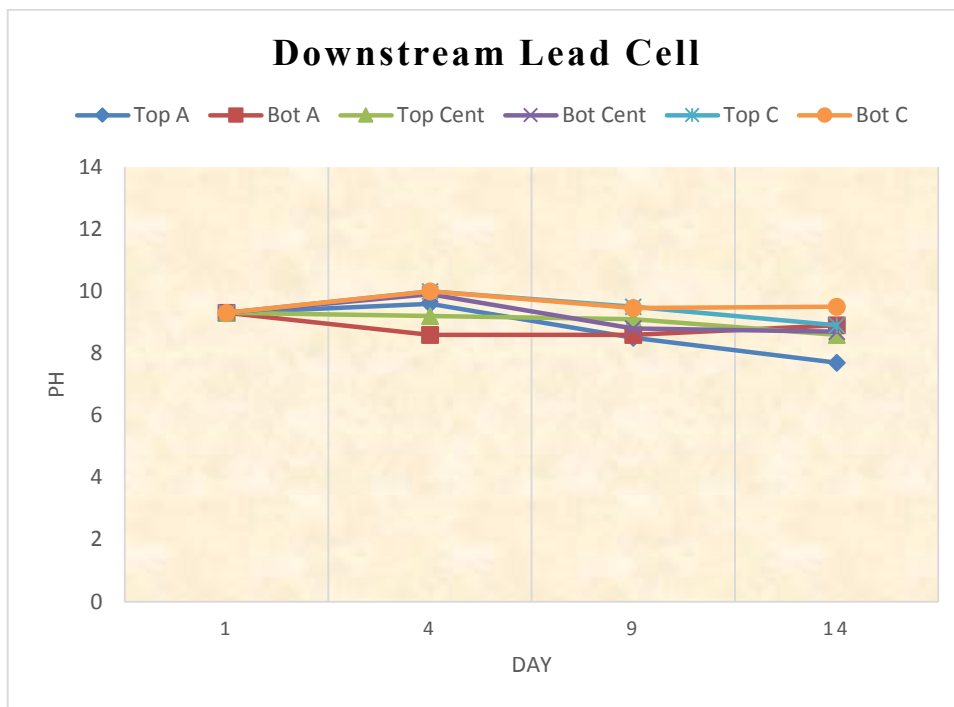


Figure 5.35 pH changes in downstream Lead Cell
 Note: Cent: central area, A: anode, C: cathode, Bot: bottom

5.3.4 pH changes in upstream/downstream - Mix Cells

Figure 5.36 displays the changes in pH in the upstream Mix Cell (V, Ni and Pb). In the first interval there has been an increase of pH in the whole cell. Except for the bottom anode area, where the pH dropped from 7.8 to 6.2, which suggests, the formation of the hydrogen ions at a higher rate next to the bottom anode area. In the second interval, the hydrolysis of water and metals chlorides, and possible oxidation process of the upper part of the anode, caused the pH to drop from 9 to around 7 at the that area. In the center parts, pH kept increasing because of the horizontal separation of the liquid phase and the movement

towards the cathode. The cathode area maintained stable but high pH values (around 12) through this period, which suggests a high constant rate of hydroxide ions production at the cathode. The third and final interval of the experiment showed a significant decrease in the cell pH. At the cathode and center areas, pH dropped to around 8.5, and at the anode area pH reached a minimum of 4.2 around the bottom section of the anode. From the pH patterns in this cell, it can be noticed that vertical separation was more obvious at the anode area where pH values were different at the top and bottom throughout the experiment. On the other hand, pH values were similar at the top and bottom of the center area and almost identical at the top and bottom of the cathode area. This suggests a stronger horizontal separation than vertical separation at these sections.

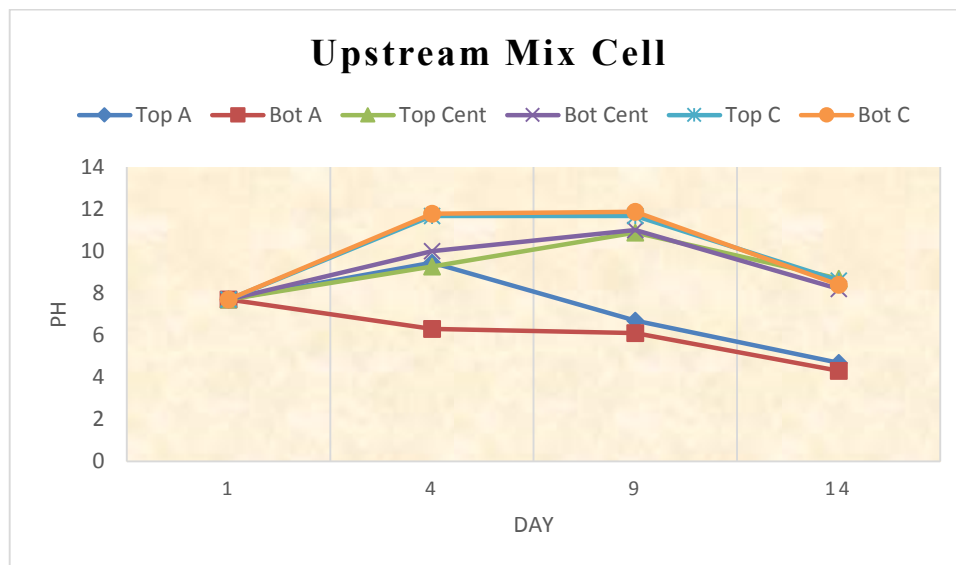


Figure 5.36 pH changes in upstream Mix Cell
 Note: Cent: central area, A: anode, C: cathode, Bot: bottom

Figure 5.37 shows the pH variations in the downstream Mix Cell. The first few days showed an increase of the pH values at the cathode area, countered by a decrease at the center and anode areas. On the 4th day pH reached a maximum of 11 at the bottom cathode

area, and a minimum of 7 around the bottom anode area. The center area had identical pH values at the top and bottom, which suggests very little vertical separation throughout the experiment. The cathode area showed higher pH values at the top than the bottom, but the general pattern was the same throughout the experiment, where there was an increase in pH in the first interval followed by a decrease in pH until the end. In the anode area first two intervals showed a decrease of pH especially at the bottom, followed by an increase of pH in the last interval. By the end of the experiment, pH ranged between (8.2 and 8.7) for the whole cell, which suggests that the separation process was stronger at the beginning. At the end when the resistance was very high and the current was low, the component seemed to be evenly distributed throughout the cell.

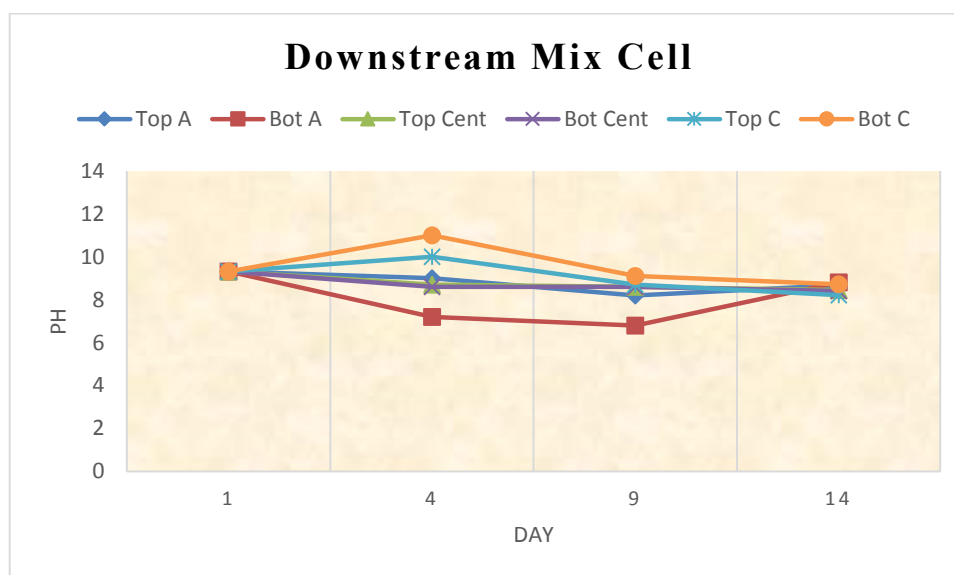


Figure 5.37 pH changes in downstream Mix Cell
 Note: Cent: central area, A: anode, C: cathode, Bot: bottom

5.4 Rheological analyses

From Visual observations, pH readings, electrical parameters, and characterization of the cells after applying EK, it was clear that vanadium enriched cells showed a better separation throughout the experiment.

Petroleum sludge is considered a non-Newtonian fluid, which means that the viscosity usually decreases with the applied shear rate (Chang et al., 1999). However, after the application of EK phenomena, demulsification of the matrix took place, and separated phases started expressing different behaviours. The diffuse double layer of the sludge components, particularly those known as emulsifiers (e.g. asphaltenes, and resins), were affected by DC field. Since they were affected in different ways, the separation of phases was facilitated, where each component expressed different physicochemical properties (including viscosity, and shear rate). Accordingly, the measurement of rheological properties permitted to follow adequately the changes observed in the oil matrix. Then, viscosity was measured as a function of strain at the top, middle, and bottom areas of the anode, cathode and central areas. However, the elastic modulus, which is a measure of the stiffness of the sludge, was presented as a function of frequency for the same areas.

5.4.1 Upstream oily sludge matrix

Figure 5.38 shows the viscosity changes with respect to the strain rate in the upstream control cell. Viscosity was decreasing while increasing the strain rate. When the strain rate reached 6 1/s the viscosity had insignificant changes afterward.

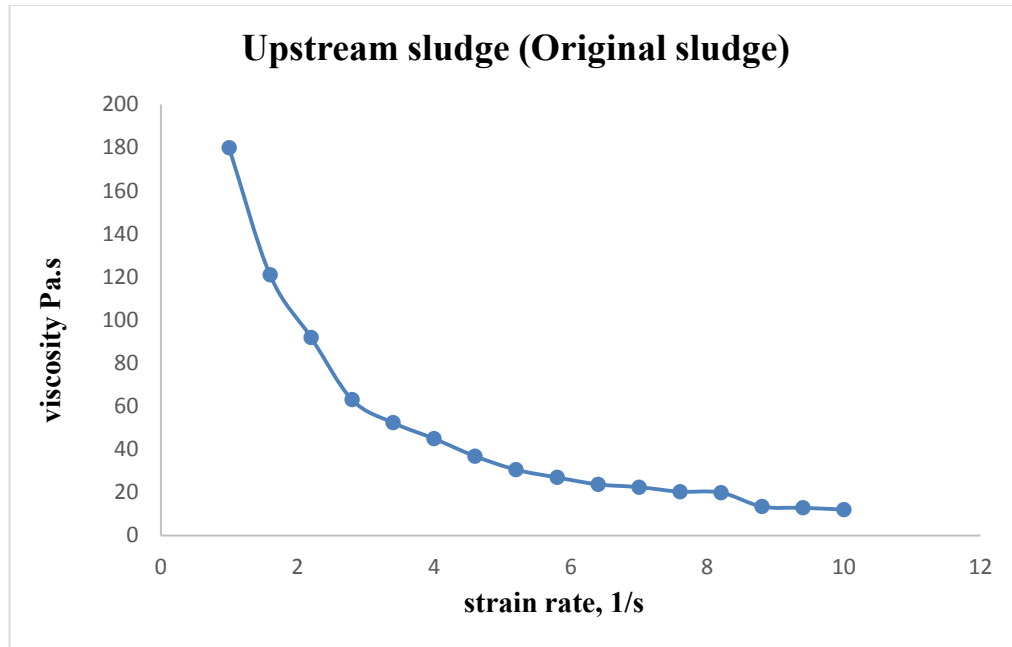


Figure 5.38 Viscosity of the upstream Control Cell (initial oily sludge matrix) as a function of the strain

Note: Original Cell: oily sludge matrix not exposed to DC field

5.4.2 Rheological properties of the upstream/downstream Vanadium Cell

Figures 5.39 to 5.43 describe the changes in viscosity at the bottom areas of the cell. These areas are considered more important when it comes to rheological properties, since bottom areas accumulated higher amounts of the solid sludge than the top parts, where the liquids had accumulated (Ch. 5.1). The precipitated fractions of oily sludge usually contain emulsifiers, such as asphaltene, where the polar fraction of this compound has been found to contain relatively high amounts of vanadium and nickel (Vaibhav et al., 1999).

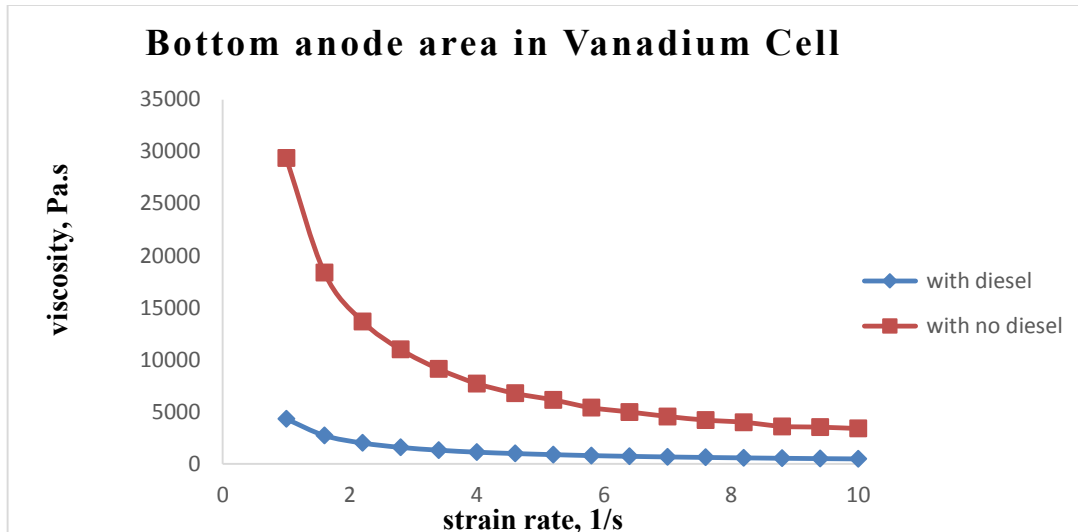


Figure 5.39 Viscosity of the bottom anode sludge as a function of the strain rate

Figures (5.40, 5.41, and 5.41) show that the viscosity was constant while increasing the strain rate, for the cathode and center samples, either with diesel or without diesel. It also reveals that diesel did not affect the samples rheological properties. On the other hand, in the bottom anode area (Fig 5.39) of the upstream sludge matrix (without diesel), the viscosity decreased while increasing the strain rate, but downstream, a slight changes with increasing the strain rate were to be seen due to the microstructure changes.

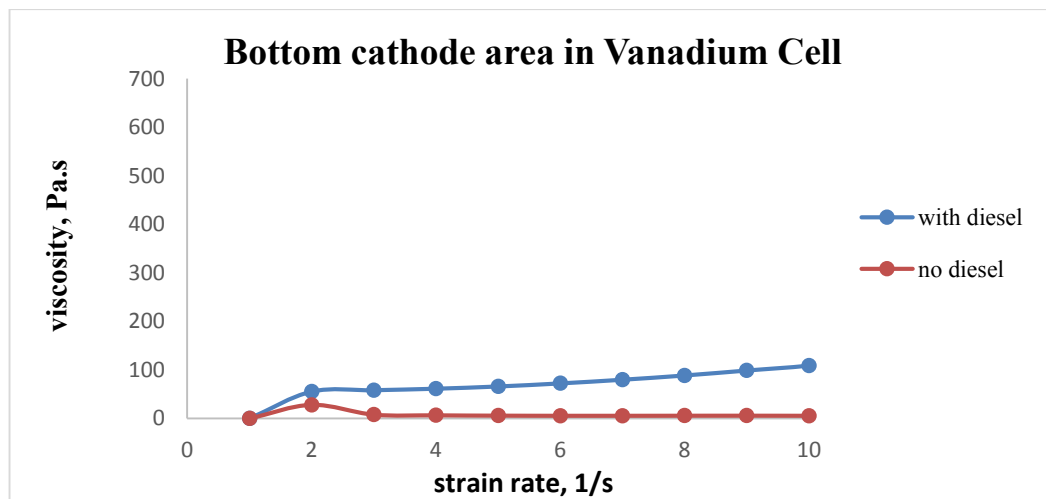


Figure 5.40 Viscosity of the bottom cathode sludge as a function of the strain rate

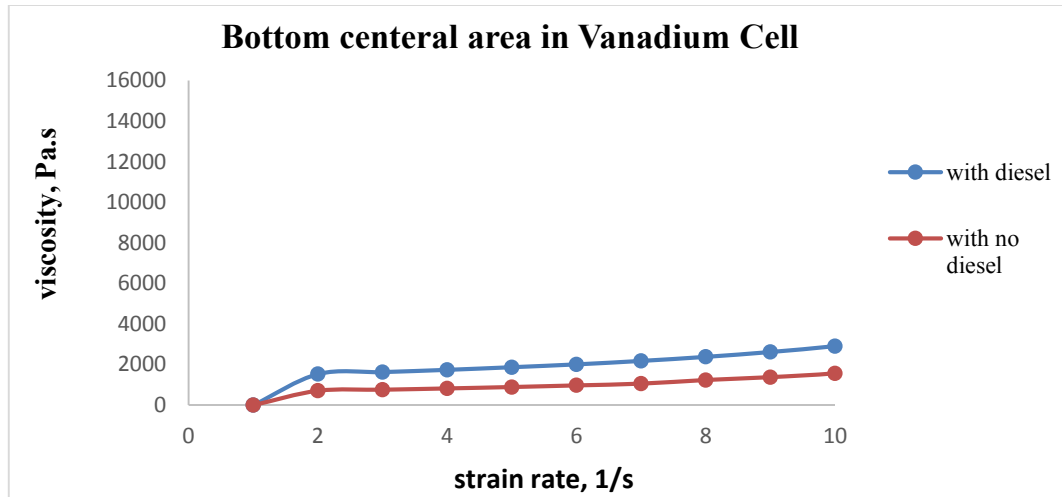


Figure 5.41 Viscosity of the bottom central area sludge as a function of the strain rate

Figure 5.42 shows that the bottom anode has a higher storage modulus than the cathode and center areas. The storage modulus for bottom center sample was high when compared to the bottom cathode. However samples from the anode had the highest storage modulus. Due to a possible experimental error, bottom cathode curve was not a straight line. Also we can observe that elastic modulus is independent of frequency.

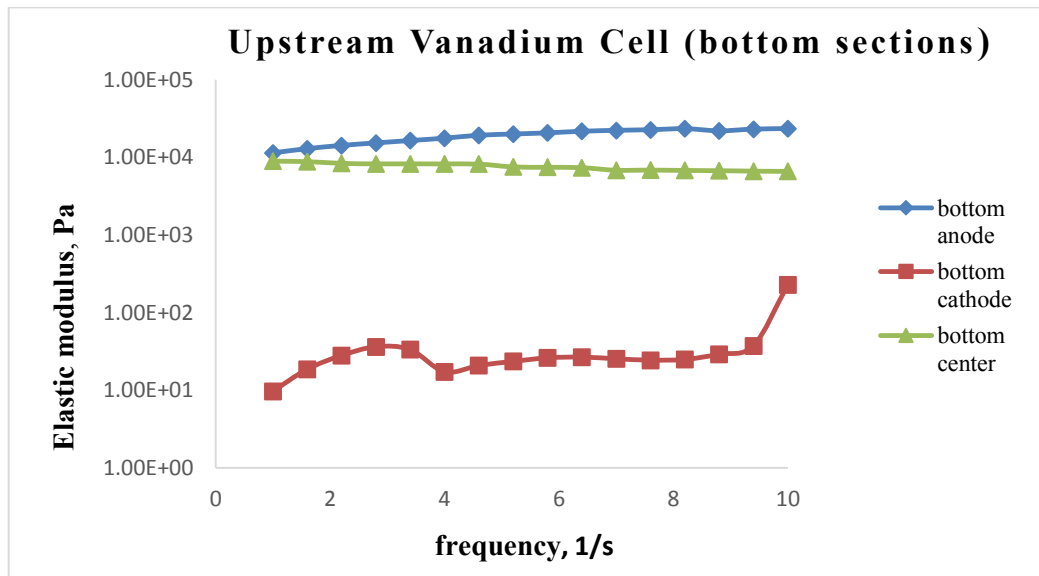


Figure 5.42 Elastic modulus as a function of frequency for bottom anode, cathode and center upstream Vanadium Cell

Figure 5.43 illustrate the storage or elastic modulus as a function of frequency for bottom anode, cathode and center samples in the downstream cell (with diesel). It was obvious that the bottom center samples had very high elastic modulus. The bottom cathode had lower elastic modulus than the anode. In all samples the elastic modulus is constant with the frequency.

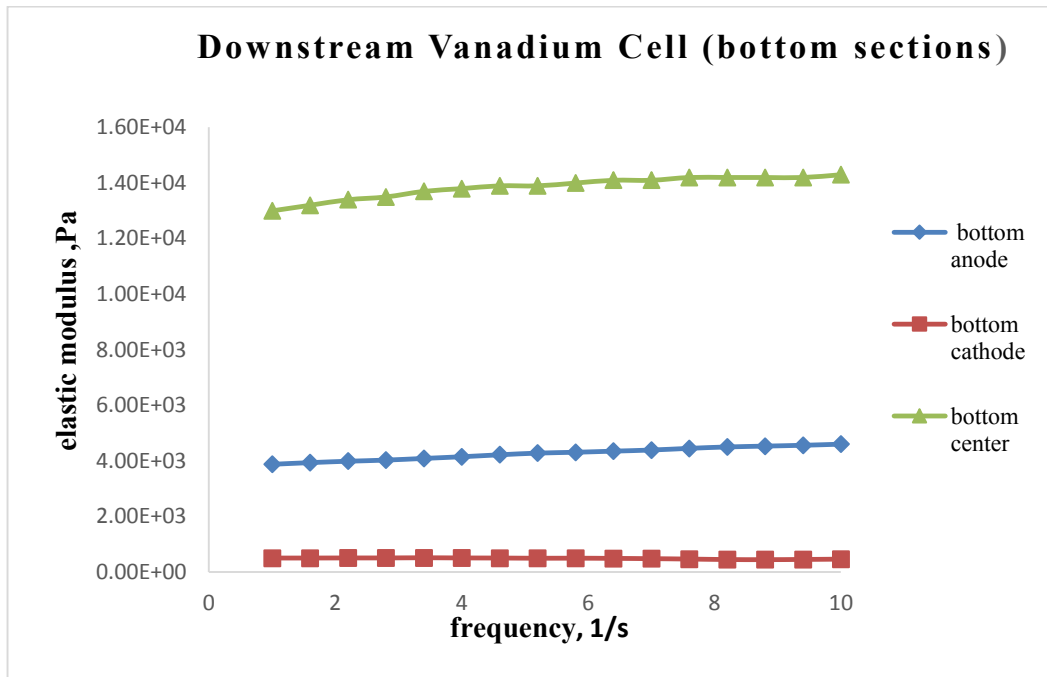


Figure 5.43 Elastic modulus as a function of frequency for bottom anode, cathode and center downstream Vanadium Cell

Figure 5.44 describes the changes in viscosity of the top anode, cathode and center upstream samples with respect to strain rate. The figure shows that the viscosity is constant with increase of strain rate at the top cathode area. However, top of the anode sample has much higher viscosity than top of the cathode and center. When the strain rate reached 10 1/s the viscosity reached 15000 Pa.s

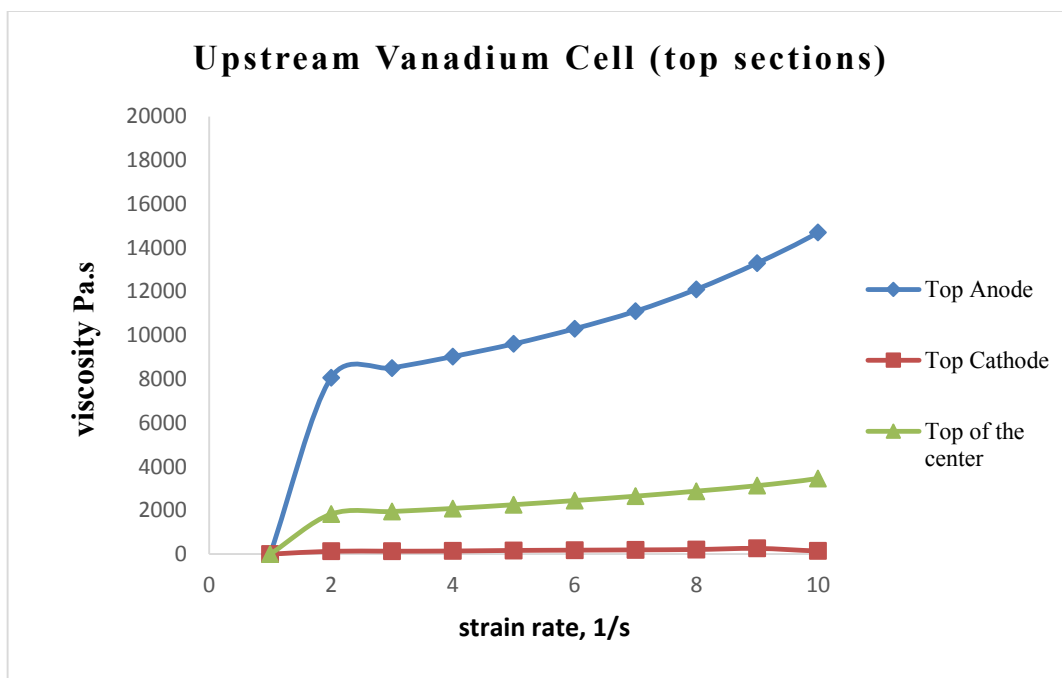


Figure 5.44 Viscosity as a function of strain for top anode, cathode and center samples

It can be concluded, that the EK remediation directly affects the rheological properties of the sludge, by targeting the microstructure of the sludge. Disturbing the thermodynamically stable system, and affect the energy barrier (resultant of the attractive and repulsive forces), which prevents particles from coalescence. It seems that DC field affected the zeta potential of the system, by changing the balance of ions in the diffuse double layer. It is visible particularly in the presence of high conductive metals. Thus, the highest and fastest demulsification was observed in presence of vanadium (Ch.5.5.1). In fact, the term “electro-rheology” phenomena could be used, which lead to change of matrix properties and appearance of distinctive phases, in various parts of the cells. For example Figures 5.39, and 5.44 illustrate higher viscosity with respect to strain rate at the anode in Vanadium Cell, comparing to the center and cathode areas. Such viscosity increase is directly related to the increase of zeta potential, and the drop of pH.

By the end of the experiment, stable separated fractions demonstrated characteristics such as, low pH values at the anode (Ch. 5.3.1), high pH values at the cathode (Ch. 5.3.1), high viscosity at the anode, and low viscosity at the cathode, indicating an excellent separation of phases that took place after the electro-demulsification of the oily sludge matrix.

From visual observations, pH values and characterization of the sludge, Nickel and Lead Cells showed generally similar characteristics of that in Vanadium Cell. Therefore a simple rheological model was implemented depending on Figures 5.38 and 5.39, where the viscosity “ μ ” (as a function of rate of strain “ $\dot{\gamma}$ ”) is decreasing in what is referred to as shear is thinning. The best rheological model that could fit such behavior was found to be Ostwald –de Waele-power model:

$$\mu = K (\dot{\gamma})^{n-1} \quad (12)$$

Where:

K : is the sludge flow consistency index (Pa.s), $\dot{\gamma}$: is the strain rate (1/s), and n : is the dimensionless flow behavior index (in these results it is negative because the flow is shear thinning, $n = -0.944$).

However, Figures 5.40 to 5.44 viscosity seemed to be mostly independent of the rate of strain, therefore the best rheological model fit these figures is the Newton model:

$$\tau = \mu \dot{\gamma} \quad (13)$$

Where:

τ : is the shear stress (Pa), μ : is the dynamic viscosity (Pa.s), and $\dot{\gamma}$: is the strain rate (1/s)

5.5 Metals mobility and distribution

The following sections describe the distribution of the three target metals (V, Ni, and Pb) in all the upstream and downstream cells after applying the EK system. Furthermore, the feasibility of using supercritical fluid extraction (SFE) followed by acid digestion will be illustrated in Ch. 5.6.3. Distribution of the metals in the EK cells has been traced in the horizontal and vertical directions.

5.5.1 Vanadium distribution

5.5.1.1 Upstream oily sludge matrix

Figure 5.45 shows the horizontal distribution of vanadium in the upstream cells after applying the electrokinetic procedure. The area between the two electrodes has been divided into three main sections (anode, center, and cathode). In the Vanadium Cell, 44% of the metal accumulated at the anode area, while the center and cathode areas had 37% and 19% of the available vanadium respectively (Fig 5.45 a). On the other hand, in the cell rich with mixed metals (V, Ni, and Pb), the highest accumulation of vanadium was at the cathode area (36%), but only by a small fraction over the center area (Fig 5.45 b). The anode area contained 29% of vanadium in the Mix Cell. Lower by 15% of the accumulation at the anode in the Vanadium Cell. This suggests that in the cells with mixed metals, the presence of other metals accelerated the transportation of the vanadium towards the cathode area.

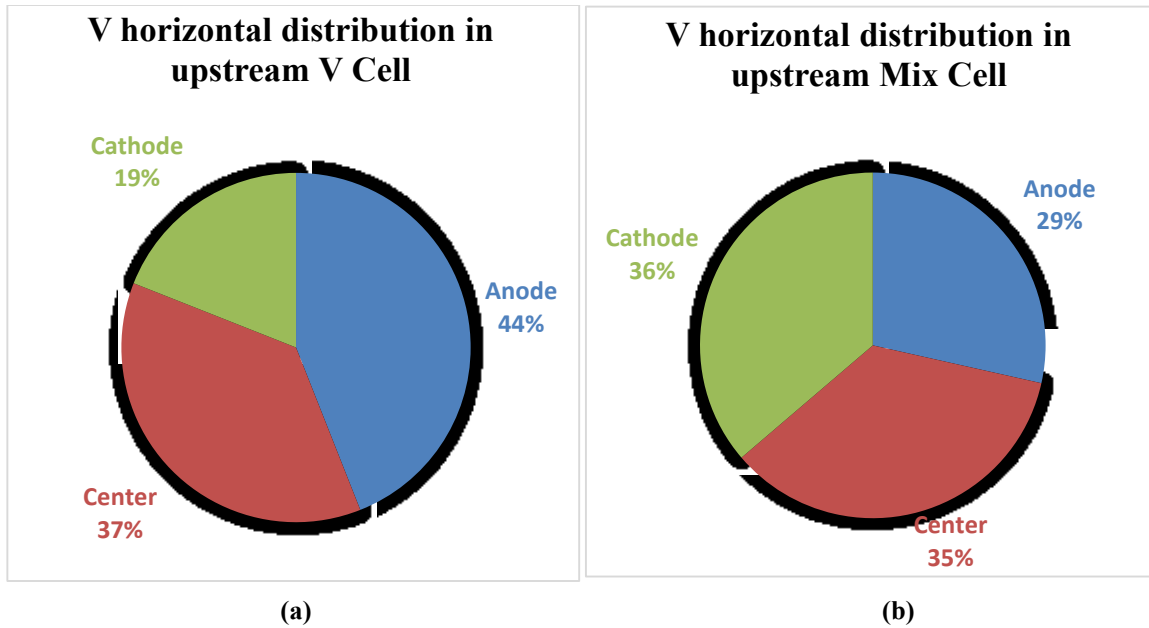


Figure 5.45 Vanadium horizontal distribution in upstream a) Vanadium, and b) Mix metal Cells

Figure 5.46 describes the vertical distribution of vanadium in the upstream Vanadium, and Mix Cells. The anode, cathode, and center areas were divided into layers to define the effect of vertical separation on the metals mobility, and to associate mobility with the separation of phases. Figure 5.46 (a) shows that the highest concentration of vanadium was recorded at the bottom of the anode area (around 70 ppm) followed by the top of the center area (60 ppm), which are the areas with the most solid mass with reference to section 5.1.1. The cathode area contained the least concentrations of vanadium, where it reached a minimum of 15 ppm at the top and bottom sections. Also from section 5.1.1, and visual observations (Appendix B. Fig B.1), it was clear that the cathode area contained the highest liquid content. As a result, vanadium was mostly available in the solid fraction of the cell.

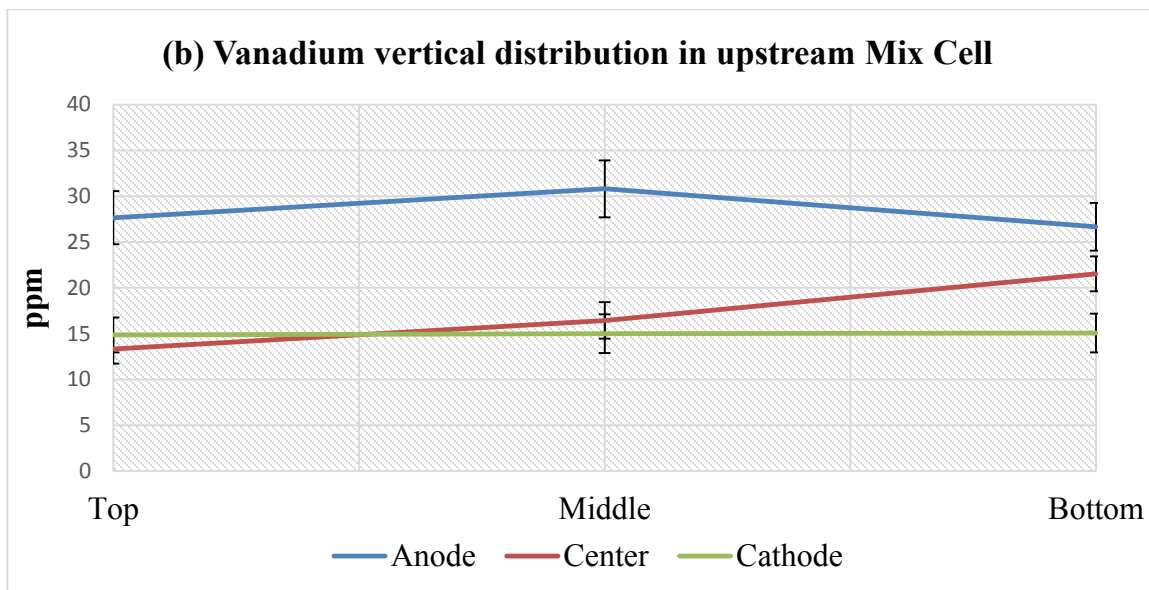
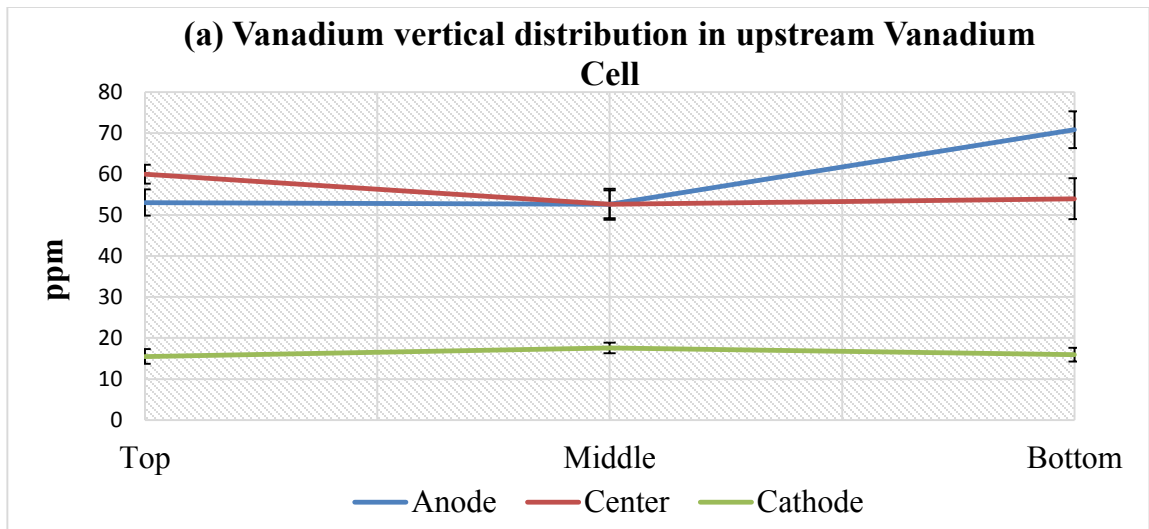


Figure 5.46 Vanadium vertical distribution in a) Vanadium and b) Mix metals Cells

The cathode area in the Mix Cell contained similar amounts of vanadium as the Vanadium Cell (Fig 5.46 b). However, the anode and center areas contained higher amounts of vanadium than the cathode area. Furthermore, they contained less amounts of vanadium when compared to the cell with vanadium alone. In the Mix Cell, the maximum vanadium concentration was around 31 ppm at the middle anode area.

5.5.1.2 Downstream oily sludge matrix

Figures 5.47 (a) and (b) demonstrate the distribution of vanadium in the cells containing downstream matrix with diesel.

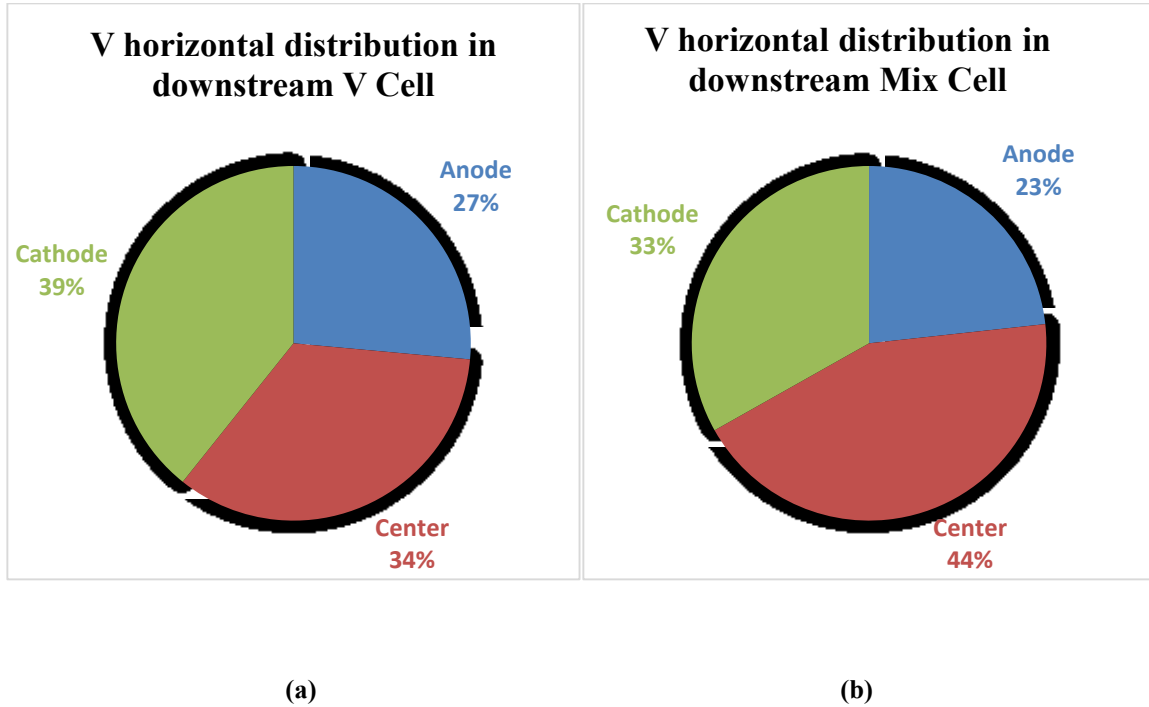


Figure 5.47 Vanadium horizontal distribution in downstream a) Vanadium and b) Mix metals Cells

In the cell with sole vanadium (V Cell), cathode area contained the highest portion of vanadium (39%) followed by the center area (34%), and finally the anode area contained the least amount of available vanadium (27%). In the Mix cell, the amount of vanadium was higher at the center area (44%), and lower at the anode (23%) and cathode (33%) areas. Since downstream matrix demonstrated lower separation of phases, the mobility of vanadium could be affected by factors other than distribution of phases in the cell; for example, the electromigratin of the ionic species in the liquid medium.

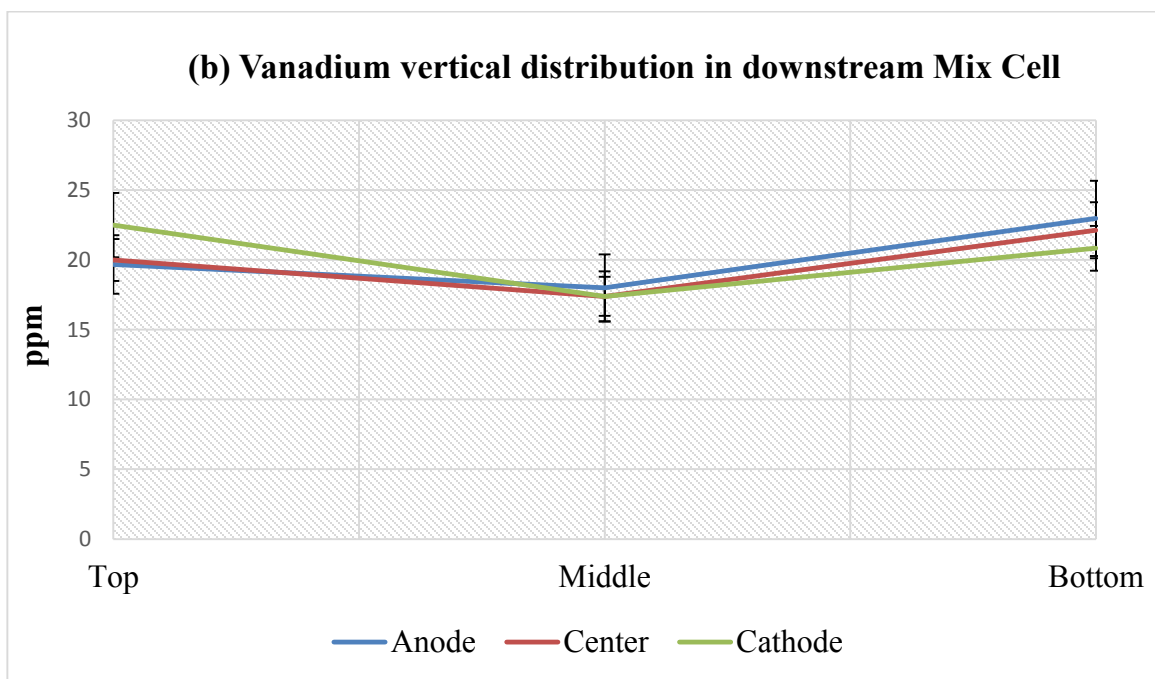
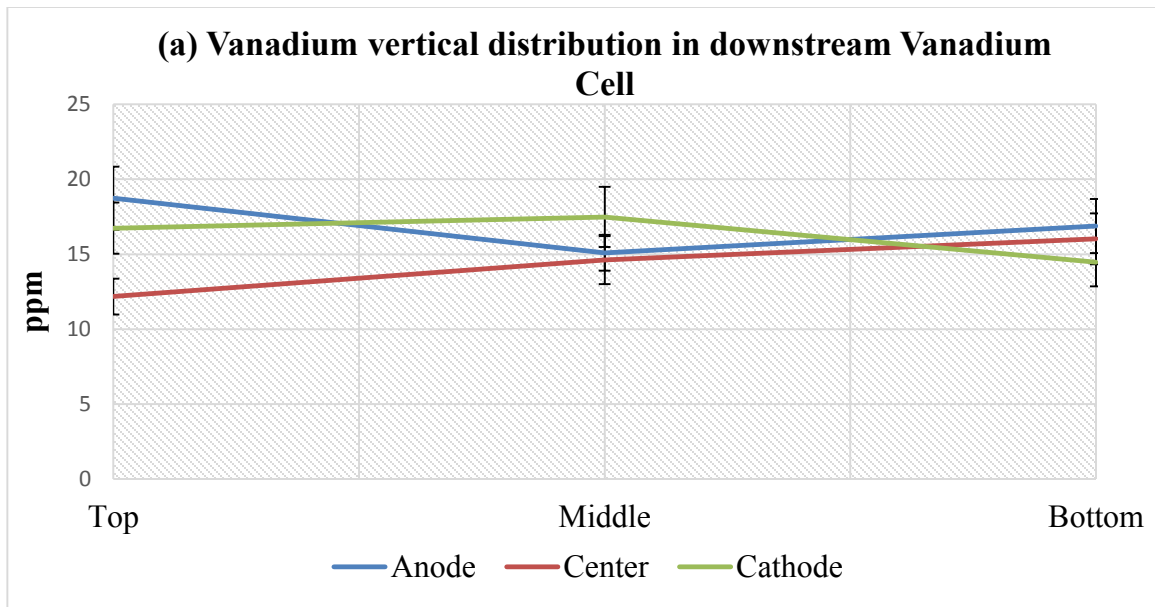


Figure 5.48 Vanadium vertical distribution in downstream a) Vanadium and b) Mix metals Cells

Unlike the upstream cell, the cell containing diesel showed smaller variations in vanadium concentrations in every layer of each section. For example, the concentration of vanadium at the center had a maximum value of 16 ppm at the bottom, and a minimum of 12 ppm at

the top. Highest concentration of vanadium was 19 ppm at the top of the anode area. The cathode had its highest concentration of vanadium at the middle section (17 ppm), and the lowest (15 ppm) at the bottom section (Fig 5.48 a). As for the vanadium distribution in the cell with mixed metals (Fig 5.48 b), all areas (anode, center, and cathode) showed similar distribution of vanadium in their vertical sections, where the middle layer contained the least concentration of vanadium in each section (around 18 ppm). This could be related to the less significant separation of phases in this cell, where the presence of diesel in the matrix affected the separation of components and reduced the accumulation of solids around the anode, where vanadium seemed to accumulate in the upstream cell. Nevertheless, in the cell with mixed metals the maximum concentration of the vanadium was around 23 ppm around the bottom of the anode area, which is higher than the value at the vanadium cell (19 ppm).

5.5.2 Nickel distribution

5.5.2.1 Upstream oily sludge matrix

Figures 5.49 (a) and (b) describe the distribution of nickel in the cells with upstream matrix containing nickel as a sole metal and cell with mixed metals, respectively. Both cases showed a relatively high accumulation of nickel at the anode area, where it reached around 54% and 52% in the sole and Mix metals, respectively. The cathode area in both cells contained a minimum content of 19% at Nickel Cell, and 13% at Mix Cell. The anode area contained the highest amounts of solids (Ch. 5.1.2), and the lowest pH values (Ch. 5.3.2), which brings the assumption that electrophoresis contributed to large extent in the translocation of nickel species (Ch. 6.2).

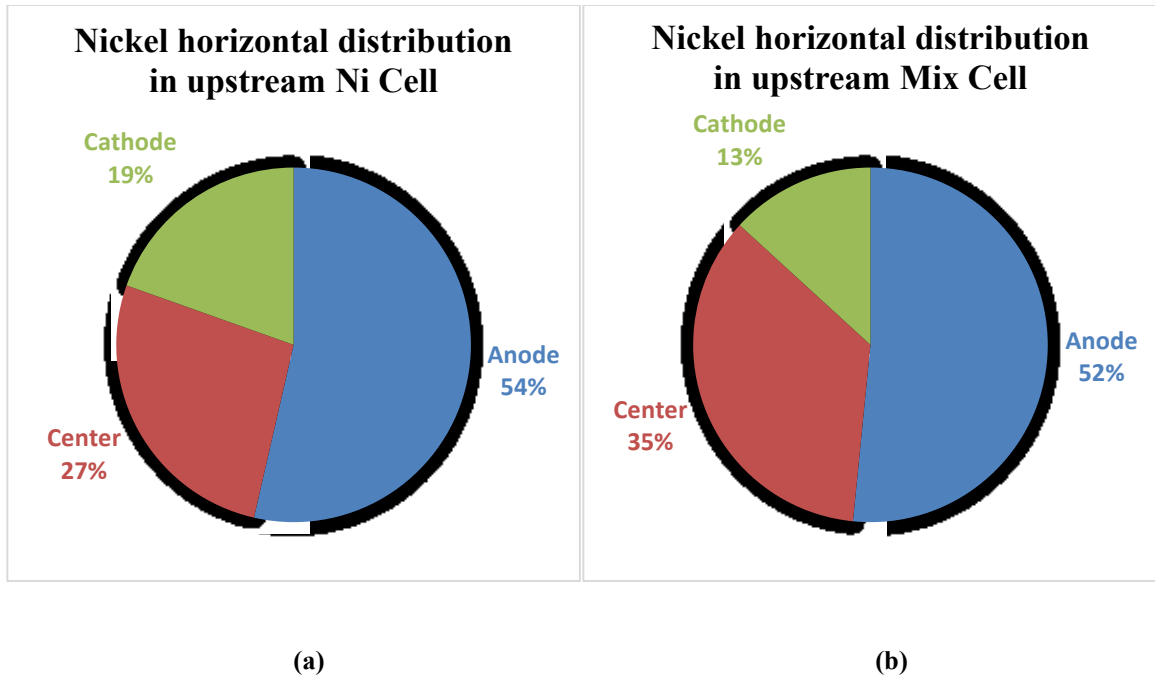


Figure 5.49 Nickel horizontal distribution in upstream a) Nickel and b) Mix metals Cells

The distribution of nickel in the vertical direction of the cell with sole nickel is illustrated in Figure 5.50 (a). These results confirm the ratios showed in the horizontal direction in Figure 5.49 (a), where the anode area showed the highest accumulation of nickel, and the cathode area contained the lowest amounts of nickel. Dividing the cell into layers showed that the bottom anode area contained the maximum concentration of nickel (50 ppm), and the bottom cathode area contained the minimum concentration (7 ppm). Also the variations of nickel concentration at the top, bottom, and middle of each area (anode, cathode, and center) demonstrated the occurrence of vertical separation in the cell.

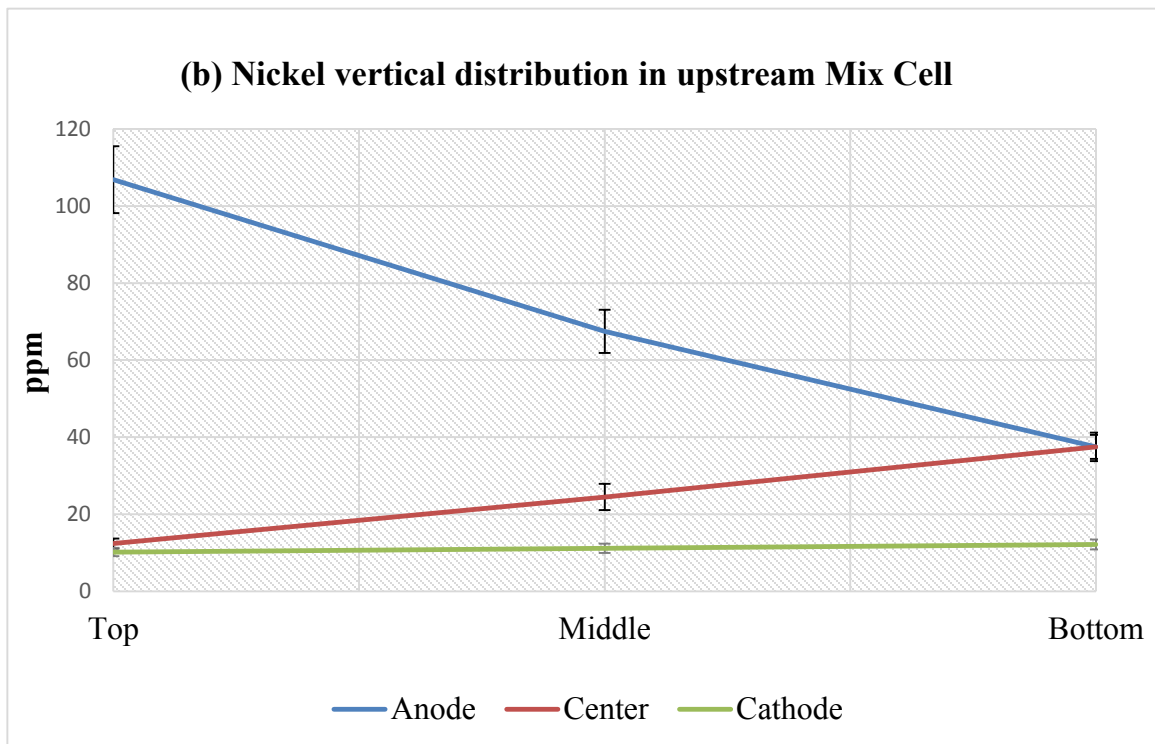
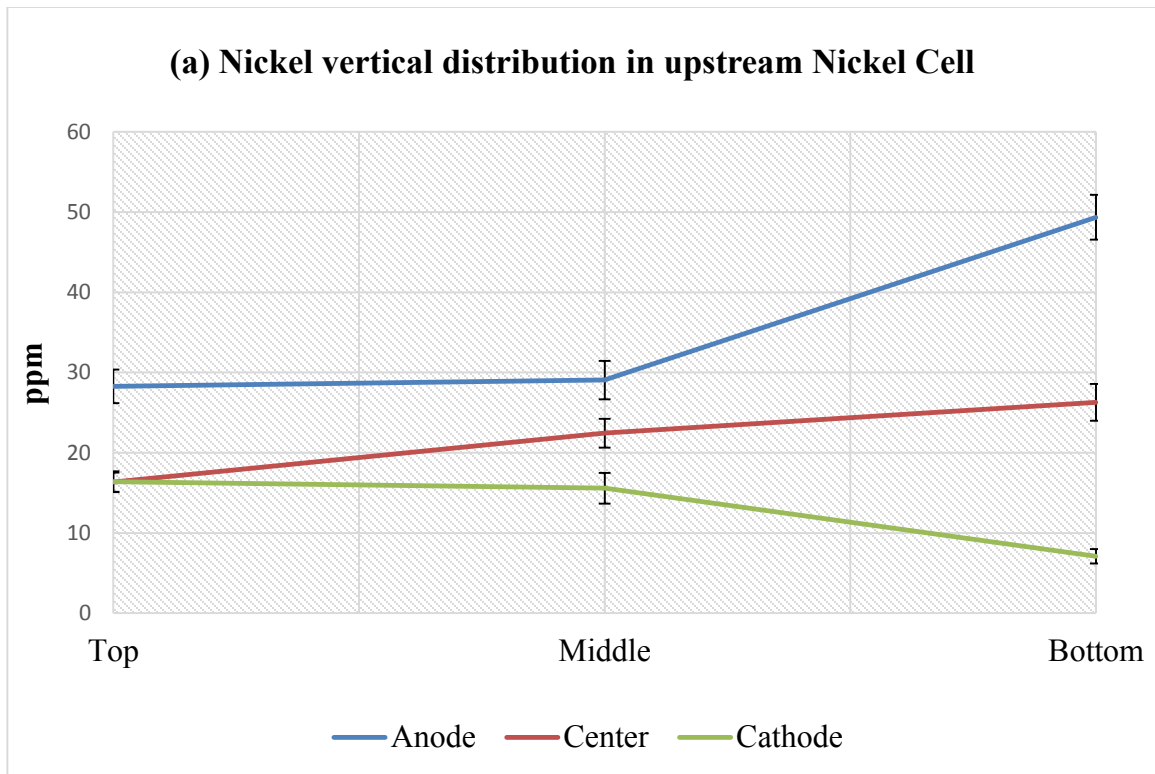


Figure 5.50 Nickel vertical distribution in upstream a) Nickel and b) Mix metals Cells

Figure 5.50 (b) illustrates the distribution of nickel in the upstream Mix Cell. Similar to the Nickel Cell, the concentration of nickel was at maximum levels at the anode area, where it reached around 105 ppm near the top of the anode area. The minimum concentration of nickel was recorded at cathode (around 10 ppm), where it was constant throughout the layers of that area. The center area behaved as transition area for the movement of the nickel ions towards the anode area. This can be spotted by the concentration values at that area, which is higher than the cathode values and lower than the anode area values.

5.5.2.2 Downstream oily sludge matrix

Figure 5.51 (a) shows the nickel distribution in the downstream Nickel Cell. As it has been explained earlier, the presence of diesel in the downstream cells affected the electro-demulsification process in the cell, and showed slower rate of phase separation than in the case of upstream matrix. This effect can be liable to lower variation of nickel accumulation in the cell; for example, the anode (34%) and cathode (37%) areas contained similar amounts of nickel.

Figure 5.51 (b) demonstrates the nickel distribution in the downstream Mix Cell. While the cathode area contained similar amounts of nickel as in the Nickel Cell (37%), the anode area contained around 24% of the nickel available in the cell. The center area held the most nickel 39%, which again suggests that distribution of nickel was affected with downstream conditions.

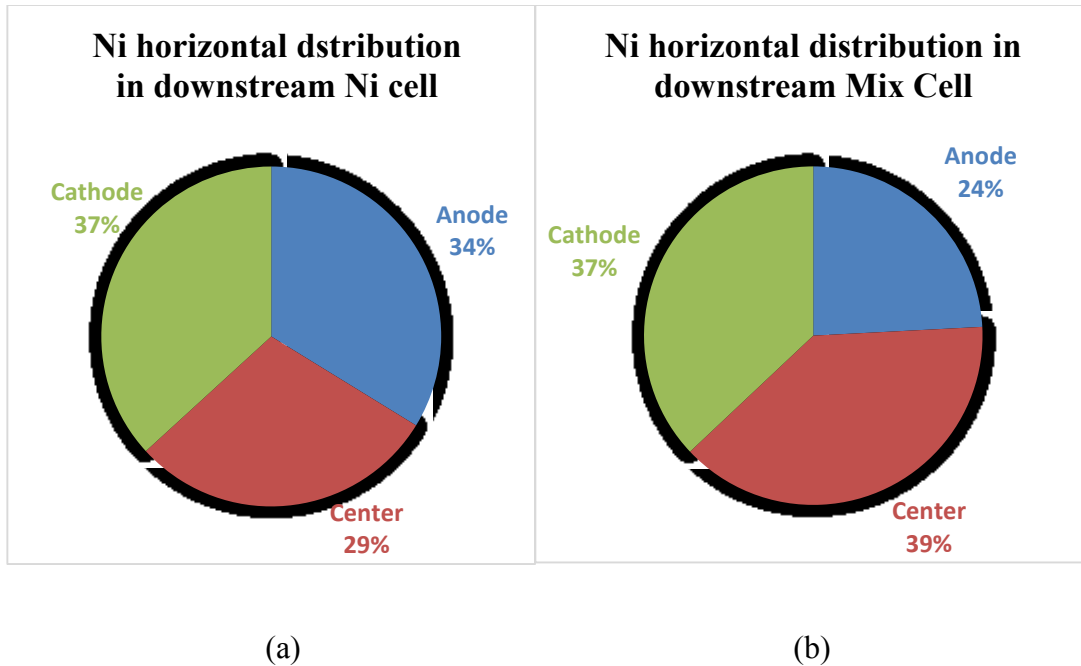


Figure 5.51 Nickel horizontal distribution in downstream a) Nickel and b) Mix metals Cells

Figure 5.52 illustrates the distribution of nickel in the vertical direction inside the Nickel, and Mix metal Cells. Figure 5.52 (a) showed similar patterns of those in the upstream Nickel Cell, where the bottom of the anode area contained the maximum concentration of nickel (23 ppm), and the bottom of the center area contained the second highest concentration (16.6 ppm). Alternatively, the top of the anode area contained the lowest concentration of nickel (12 ppm). The cathode area had a concentration of 16 ppm of nickel at both top, and bottom areas.

Figure 5.52 (b) represents the cell with mixed metal enriched matrix (Mix Cell). The maximum concentration of nickel was recorded at the bottom of the cathode area (16 ppm), and the minimum concentration was recorded at the top of the cathode area (6.5 ppm). By comparing these results to the Nickel Cell in Figure 5.52 (a), where the bottom anode contained the highest concentration of nickel in the cell, it is clear that the presence of other

metals (V and Pb) created synergistic-antagonistic factor that affected the transportation and behavior of nickel.

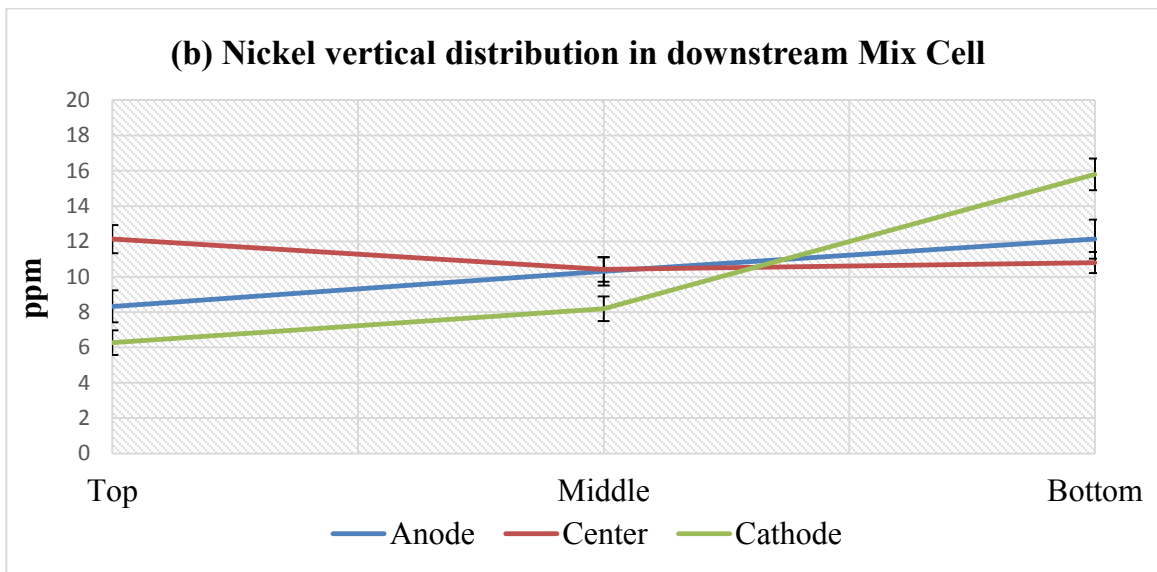
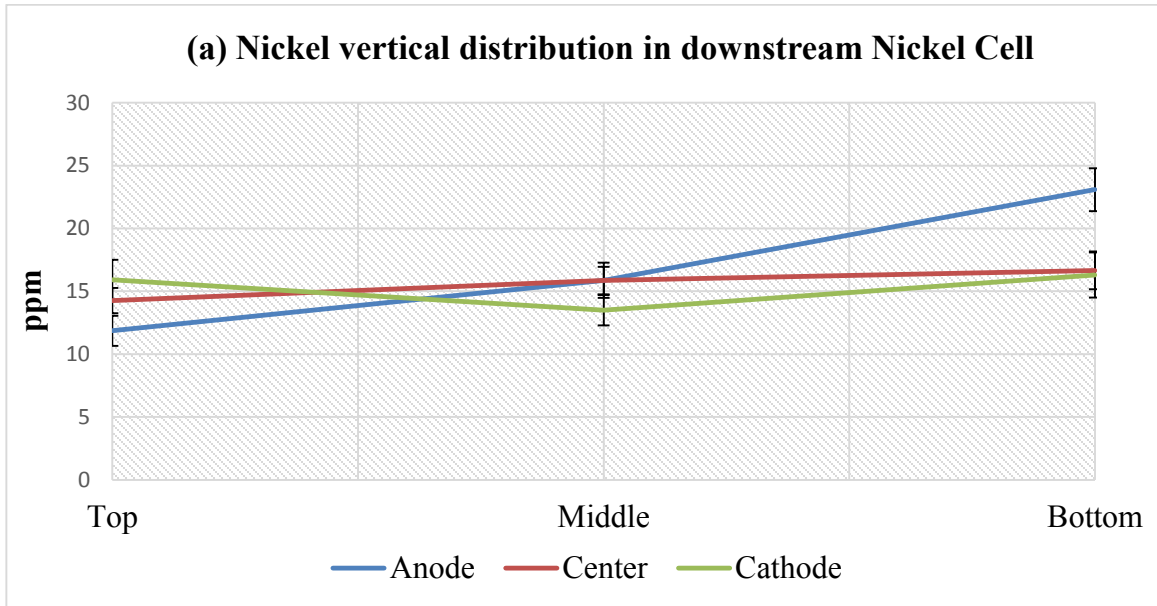


Figure 5.52 Nickel vertical distribution in downstream a) Nickel and b) Mix metals Cells

5.5.3 Lead distribution

5.5.3.1 Upstream oily sludge matrix

Figures 5.53 (a) and (b) describe lead horizontal distribution in the upstream cells. In the Nickel and Vanadium upstream Cells, the highest accumulation of the metal was at the dry anode area. Alternatively, lead in the Lead and Mix Cells was mostly accumulated at the wet cathode area with the following ratios: 44% in the Lead Cell, and 47% in the Mix Cell. The anode area had the least amounts of lead, where the accumulation was as follows: 16% at the Lead Cell, and 23% at the Mix Cell. After characterizing the cell components post EK, it was noted that water and liquid hydrocarbons accumulated at the cathode. Which means lead was transported through electromigration and electroosmotic flow toward the cathode area.

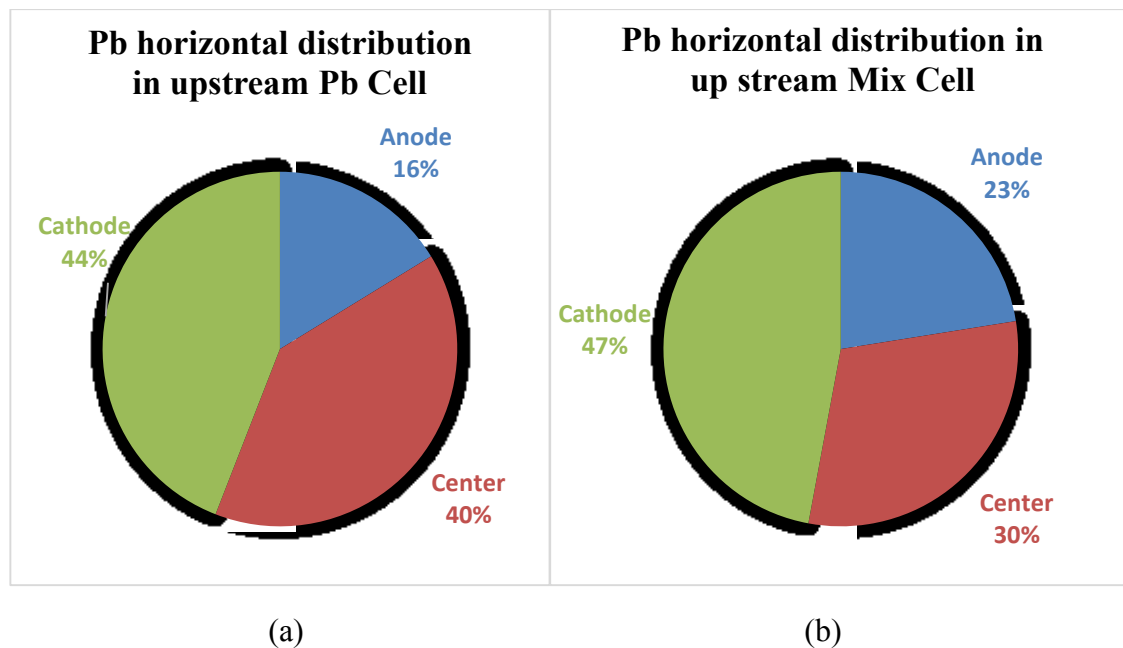


Figure 5.53 Lead horizontal distribution in upstream a) Lead and b) Mix metals Cells

Figure 5.54 (a) demonstrates the distribution of lead in the vertical direction in the upstream Lead Cell. Top of the cathode area (which contained the highest moisture content) had the smallest lead concentration (12.5 ppm). However the concentration at the middle and bottom areas was around 29 ppm each. On the other hand, the top of the center area contained the highest concentration of lead (45 ppm). The anode area lead concentration ranged between 25 ppm at the top, and 20 ppm at the bottom. The cathode area contained higher concentrations than the anode at the middle (28 ppm) and bottom (29 ppm) sections.

While Figure 5.54 (a) shows that the vertical distribution of lead did not oppose the horizontal distribution in the same cell, in the Mix Cell, Figure 5.54 (b) shows that concentration of lead at the top (12 ppm) and bottom (14 ppm) anode areas were higher than their counterparts at the cathode area (10 ppm at the top, and 11 ppm at the bottom). This to some extent is different than the horizontal distribution for the same cell where the cathode area contained over 45% of the lead available. Multiple factors affected the AAS readings, including the efficiency of acid digestion procedure in case of lead extraction, and the homogeneity of the samples used for analysis, however, no more than 8% of error was detected for such analysis.

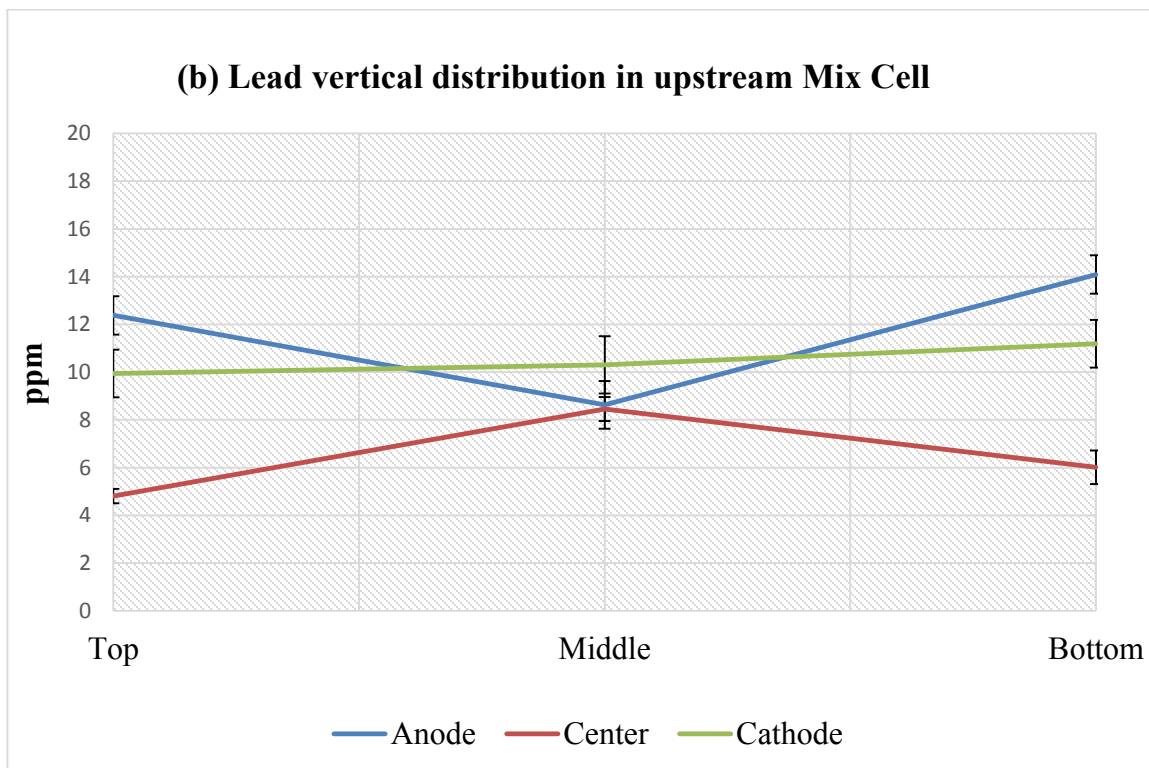
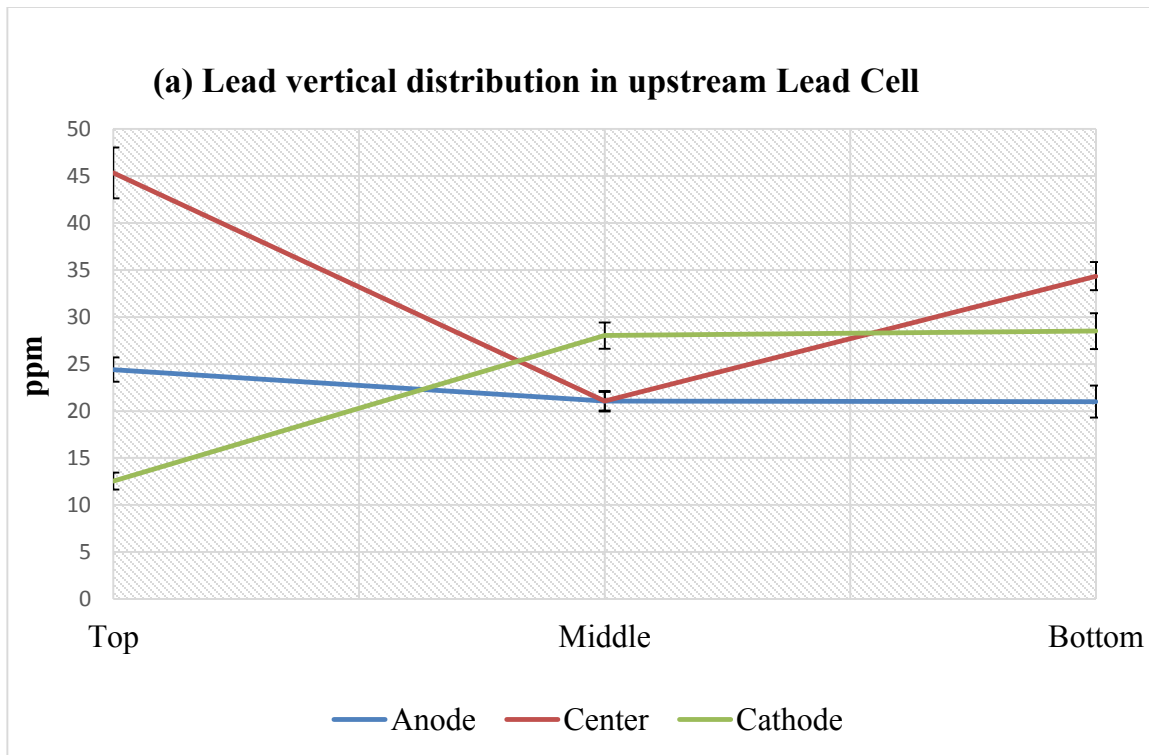


Figure 5.54 Lead vertical distribution in upstream a) Lead and b) Mix metals Cells

5.5.3.2 Downstream oily sludge matrix

Figure 5.55 illustrates the horizontal distribution of lead in the downstream Lead and Mix Cells. It can be seen from both Figures (a) and (b) that the distribution of lead in both cells was similar, and it took the following forms: cathode and center areas in both Lead and Mix downstream Cells contained around 40% of the available lead, the anode contained around 20%. Two facts could be concluded from these analyses; (1) both upstream and downstream cells showed that majority of the available lead was transported toward the cathode area; (2) the presence of other metals in the Mixed cell did not affect the distribution or behaviour of the lead.

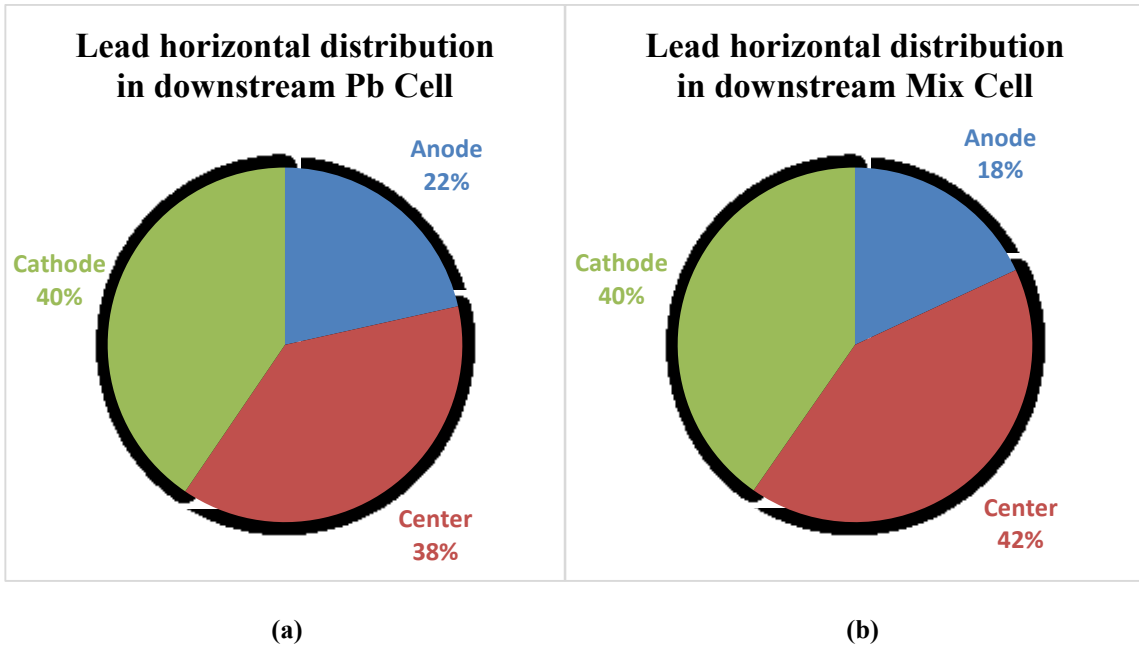


Figure 5.55 Lead horizontal distribution in downstream a) Lead and b) Mix metals Cells

Figure 5.56 (a) shows that lead concentration was similar in the three layers (top, middle, and bottom) at the three sections (anode, center and cathode) in the downstream Lead Cell. The highest concentration was found at the top of the center and anode areas (19 ppm), and the lowest concentration was registered at the bottom of the anode area (13 ppm). The small variation in concentrations in the three sections suggested that maybe the separation of phases was not stable or was less significant in the first place. On the other hand, Figure 5.56 (b) shows bigger variations in the results in the vertical direction in the downstream Mix Cell. For example, the concentration of lead at the bottom of the cathode reached a maximum value of 14 ppm, countered by a minimum of 3.5 ppm at the top area. The anode area had a concentration of 5 ppm at the top and middle areas, and 8.5 ppm around the bottom area. These results were similar to the horizontal distribution results for the same cell which confirms the movement of lead towards the cathode even in presence of diesel.

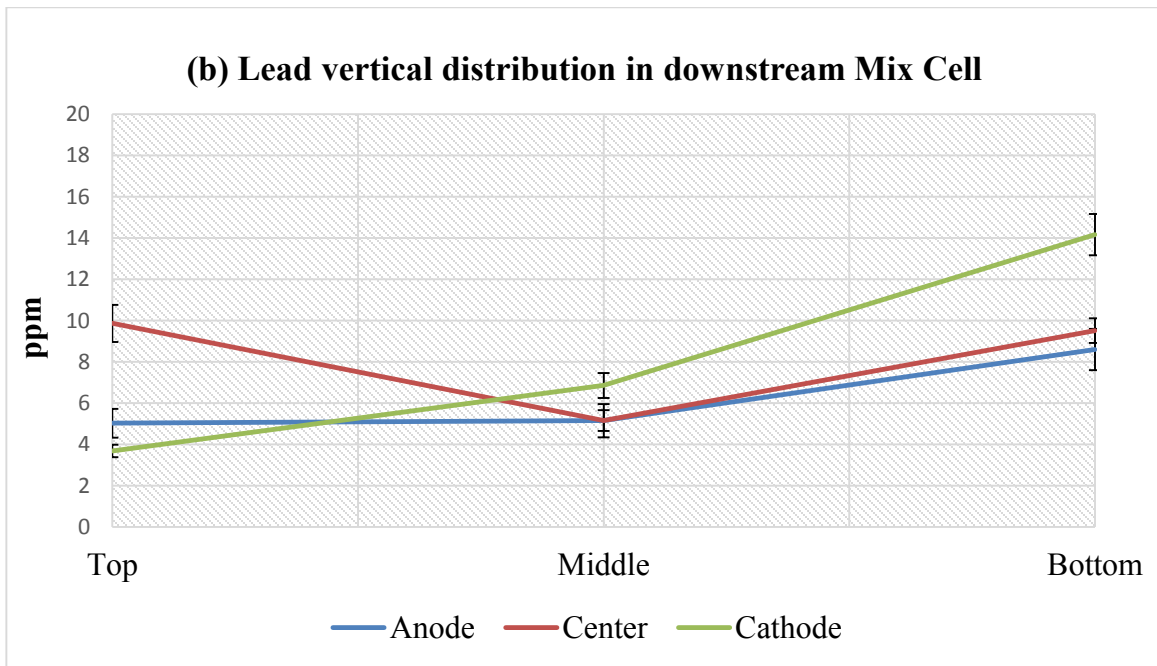
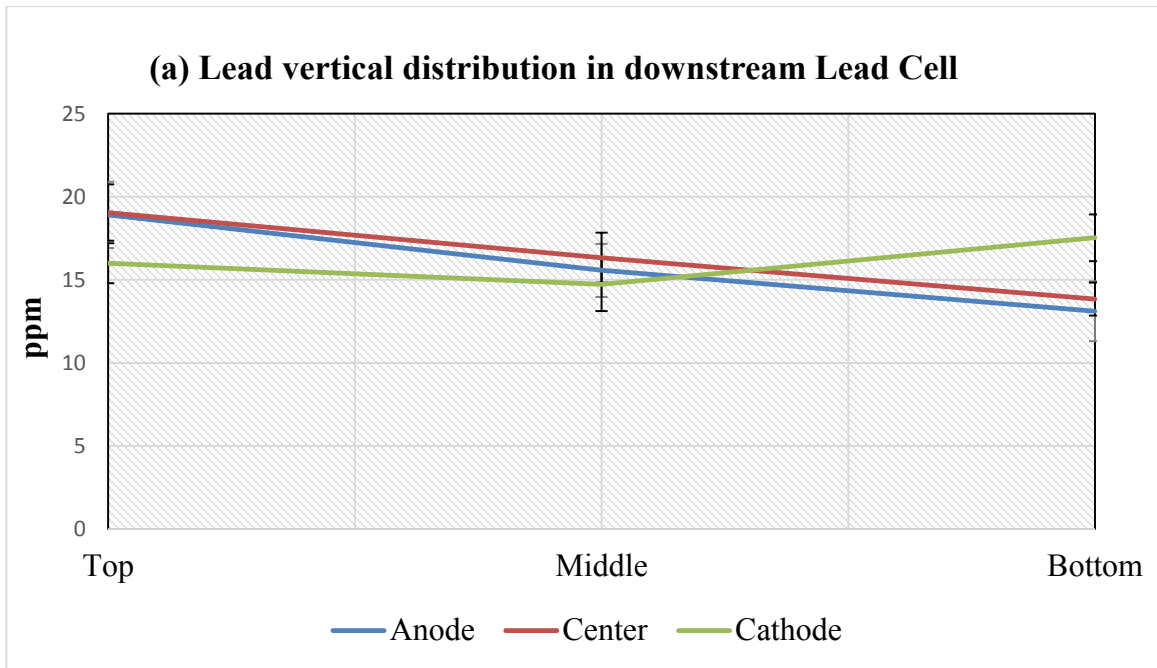


Figure 5.56 Lead distribution in downstream a) Lead and b) Mix metals Cells

5.6 Supercritical fluid extraction (SFE)

As it has been explained in literature review (Ch. 2.6.2), acid digestion might not provide high extraction efficiency for some metals in certain matrices, including oily sludge. Subsequently, another approach was tested with respect to metal extraction efficiency, while CO₂ in its supercritical state was used. Methodological approach in this case was defined in Ch. 4.8.2, where 36 samples were used for the comparative studies. For example, using SFE with EDTA as a chelating agent on a sample collected from the anode area in the upstream Mix Cell, vanadium extraction increased by almost 97%. Furthermore, when metal ions are chelated by suitable organic ligands, their solubility in supercritical CO₂ (SC-CO₂) will significantly increase (Ghoerishi et al., 2012). Figures 5.58 to 5.61 describe the feasibility of applying SFE to enhance in the extraction of target metals in the Mix Cell.

5.6.1 SFE efficiency with Cyanex 301 as chelating agent

Figure 5.57 describes the advantage of applying SFE with the presence of Cyanex 301 (SFE-Cyanex301) as a modifier for metals' extraction. All three metals showed higher extraction efficiency in all areas (anode, center, and cathode). Vanadium was highly extractable in comparison with nickel and lead in all the sections. At the anode area the increase of vanadium concentration in the extract was about 80% more of the concentration resulted from acid digestion alone for the same area. The nickel was extracted by 40% more at the cathode and center areas, and 25 % at the anode area. Lead was extracted by 32% more at the anode area, 25% more at the center, and 17% more at the cathode.

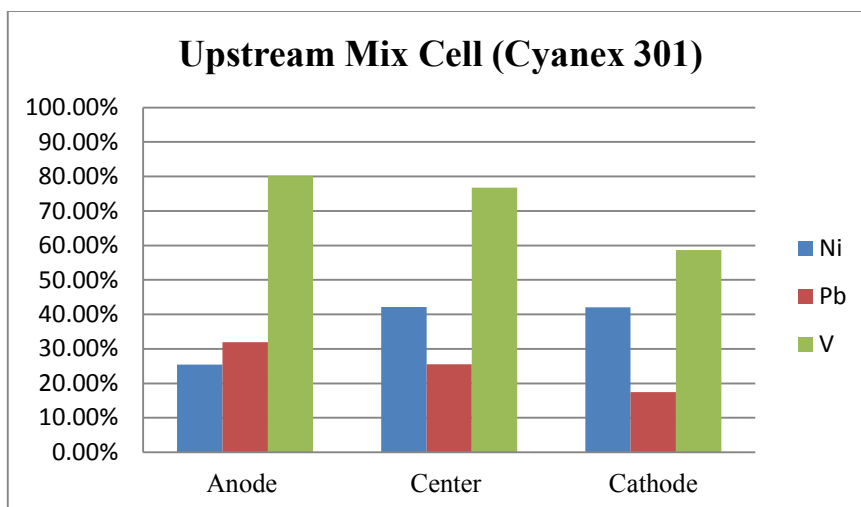


Figure 5.57 Extraction efficiency change in upstream Mix Cell after applying SFE enhanced with Cyanex 301 as a chelating agent.

Figure 5.58 demonstrates the extraction efficiency in the downstream cell, where SFE was applied to the downstream Mix Cell samples. Similar to the upstream cell, vanadium showed better extraction potential with SFE procedure throughout the cell. On the other hand, in the case of lead, SFE didn't increase the amount of extracted lead in the anode area. Furthermore nickel concentration at the anode after SFE, was less than the concentration detected with AAS after acid digestion only. At the center and cathode areas the efficiency increased for the metals, especially the vanadium where it reached over 90% at the center and cathode areas. Lead detected concentration increased by 33%, and 19% at the center and cathode respectively. Ni detected concentration increased by 10%, and 23% at the center and cathode respectively. Obviously the extraction efficiency was affected by the presence of diesel, and the dehydration process in the downstream cell, where lower volumes of water were available in the downstream cells (W/O).

It can be concluded that SFE-Cyanex 301 could be efficiently applied for the extraction vanadium from oily sludge post EK. Biswas and Karmakar, (2013) reported the formation

of extractable (soluble) vanadium species (VO^{+2} , $\text{VO}(\text{OH})^+$, and $\text{VO}(\text{OH})_2$) with the addition of Cyanex 301 to an aqueous medium rich with vanadium.

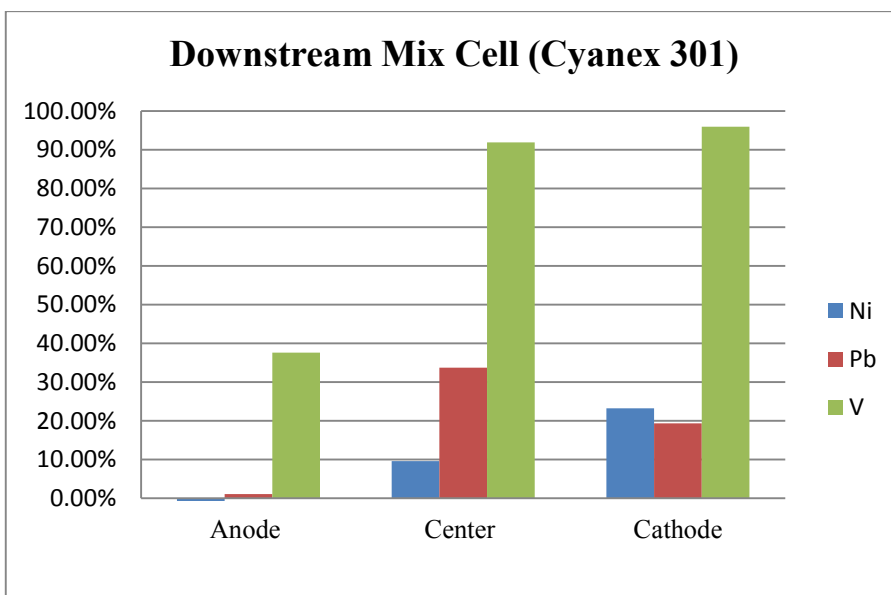


Figure 5.58 Extraction efficiency change in downstream Mix Cell after applying SFE enhanced with Cyanex 301 as a chelating agent

5.6.2 SFE efficiency with EDTA as chelating agent

As it has been explained in the literature review (Ch. 2.6.2) EDTA is usually used to enhance solubility by forming several complexes with metals. Consequently, this would increase the extraction potential of certain metals. In this research EDTA has been used in a very complex matrix (petroleum sludge for the first time). While vanadium showed great increase in its extractability potential in upstream and downstream Mix Cells, lead and nickel concentrations did not increase, except for the anode area in the upstream Mix Cell, where the concentration increased by 7% for nickel and 19% for lead.

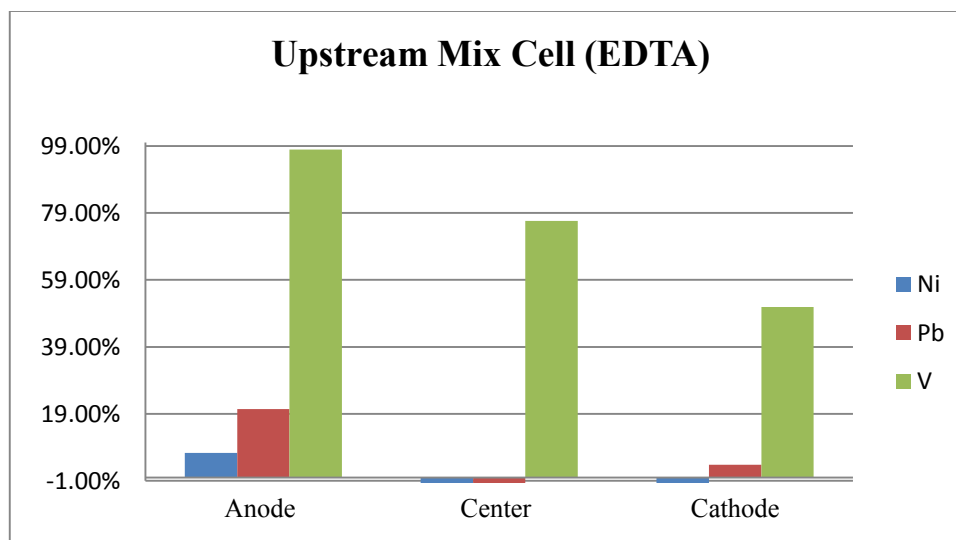


Figure 5.59 Extraction efficiency change in upstream Mix Cell after applying SFE enhanced with EDTA as a chelating agent

Figure 5.59 demonstrates the feasibility of applying SFE enhanced with EDTA (SFE-EDTA) as a chelating agent in the extraction of target metals in the upstream Mix Cell. Then, the vanadium extraction potential increased by: 98% at the anode area, 76% at the center, and 50% at the cathode area. This suggests that EDTA enhanced the extractability potential of vanadium by forming intermediate complexes between vanadium and EDTA that are more soluble and available for extraction. Lead detectable concentration after SFE increased by 20% at the anode and 4% at the cathode. In the center area concentration of lead after acid digestion was higher than its concentration after SFE, which means SFE is not feasible in this section of the cell, possibly because adding EDTA affected the presence of already available soluble lead, by reducing lead into less soluble form. Nickel on the other hand, showed no increase in detectable nickel at the cathode, and center after SFE. Never the less, the anode area showed 7% increase in detectable concentration of nickel after SFE. Which means adding SFE-EDTA techniques would not be feasible in the case of nickel.

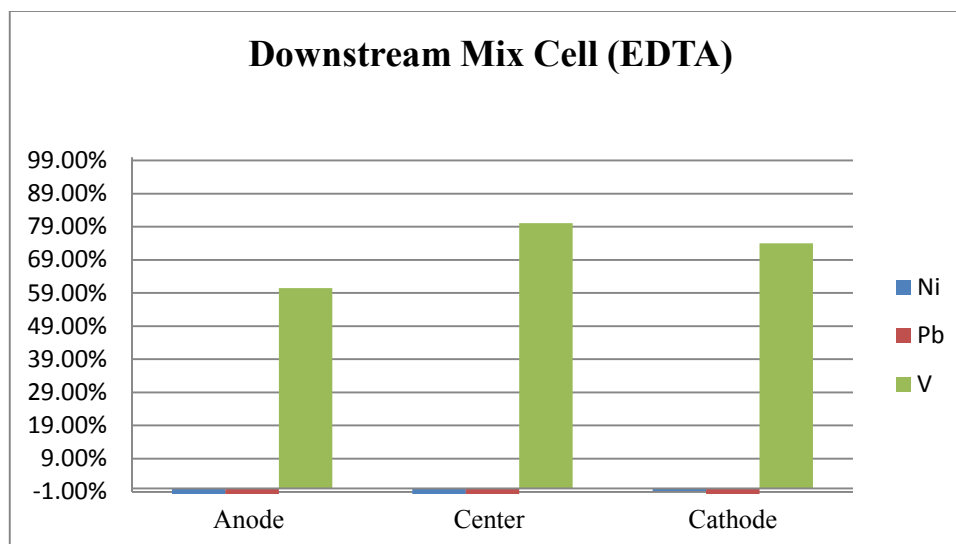
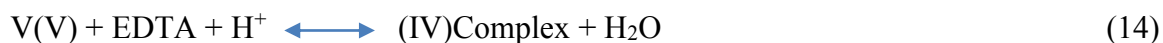


Figure 5.60 Extraction efficiency change in downstream Mix Cell after applying SFE enhanced with EDTA as a chelating agent

Figure 5.60 describes the increase of metals detectable concentration in downstream Mix cell after the application of SFE on samples chelated with EDTA. The Figure shows that only vanadium responded positively to the application of SFE enhanced with EDTA, where the concentration of V increased by 59%, 80%, and 74% at the anode, center and cathode respectively. Adversely, nickel and lead detectable concentrations were lower after SFE than after acid digestion throughout the cell. This point out the fact that SFE enhanced with EDTA is not feasible in the downstream matrix which is primarily made of water, crude oil, diesel, clay and sand.

It can be concluded that SFE-EDTA could be promising in increasing the extraction potential of vanadium species. Adding EDTA to the matrix might have helped reducing Vanadium (V) into more soluble vanadium (IV) by the following equation (Mishra et al., 2009):



5.6.3 Efficiency of SFE techniques in enhancing extraction potential

Table 5.1 compares the AAS detected concentrations of the target metals (V, Ni, and Pb) in the samples that underwent acid digestion only and samples that underwent SFE and acid digestion in the Mix Cells post EK. The purpose of this comparison is to determine the feasibility of SFE techniques versus acid digestion in increasing metals extraction, and to compare the efficiency of EDTA versus Cyanex301 as extracting additives for each metal.

Table 5.1: Concentration of target metals in samples after acid digestion and SFE

Metal	Conc. of metal after acid digestion only (ppm)			Conc. of metal after SFE-Cyanex 301 (ppm)			Conc. of metal after SFE-EDTA (ppm)		
	Anode	Center	Cathode	Anode	Center	Cathode	Anode	Center	Cathode
Nickel	67.45	24.46	12.15	50.7	14.38	7.04	62.50	26.90	19.56
	12.12	10.41	15.79	12.12	9.41	12.12	13.37	13.01	15.79
Lead	8.63	6.01	11.19	5.86	4.51	9.30	6.9	12.47	10.76
	8.59	9.51	14.16	8.5	6.3	11.42	12.88	10.25	24.88
Vanadium	26.66	21.52	15.07	5.33	4.99	6.18	.80	5.16	7.40
	22.97	22.12	20.82	14.33	1.80	.85	9.08	4.39	5.41

Note: ■ Upstream cells, □ downstream cells

Table 5.1 illustrates the feasibility of using supercritical fluid extraction (SFE) techniques for enhancing the potential of extraction of each metal (V, Ni, and Pb). For example the concentration of vanadium in the sample from the anode section that underwent SFE (upstream/Cyanex 301) dropped from initially 26.66 ppm to 5.33 ppm (after SFE), demonstrating an extraction efficiency of 80% (Eq. 10).

In general, vanadium extraction efficiency was high when SFE was used in all upstream and downstream cells regardless which modifier (Cyanix 301 or EDTA) was applied. This

revealed a high solubility of vanadium in supercritical-CO₂ especially in presence of a strong solvent such as Cyanex 301 or a complexation agent as EDTA. These results promoted such procedure to be used for vanadium extraction from an oily sludge matrix (upstream and downstream). However, interesting patterns took place in the extraction efficiency, where in the upstream cells the SFE of vanadium was higher at the anode area, and in the downstream cells the extraction was higher at the cathode area. From Ch. 5.1 it can be seen that the anode area contained higher solid content, thus, applying the solvent created intermediate complexes easily dissolved into the SC-CO₂ flow.

EDTA is known to create complexes with nickel and lead that have relatively high stability constants. However, for vanadium such relationship has been little documented (Elektorowicz and Muslat, 2008).

It can be seen from Table 5.1 that nickel extraction efficiency didn't increase with the presence of EDTA, despite the fact that EDTA has proven to create complexes with nickel that is highly soluble in aqueous phase (Choudhury, 1999). However, the nature of the matrix plays an important role in efficient extraction of metallic compounds. For example, some ligands in clay and organic rich soil compounds may bind strongly to certain metal ions, resulting in delaying their complexation with added chelating agents. Therefore, the lack of variation of parameters applied in this study might have affected the extraction efficiency of nickel under SFE-EDTA process.

Lead showed similar patterns as nickel in the SFE-Cyanex 301 procedure (upstream and downstream), and SFE-EDTA downstream cell. However in the upstream SFE-EDTA procedure, lead showed increase in extraction efficiency at the anode (20%) and cathode (4%), which is higher than nickel extraction in both areas.

It can be concluded that SFE-Cyanex 301 coupled with EK could create an excellent technology to maximize the extraction potential of vanadium, in addition to lead and nickel from an upstream oily sludge matrix. Moreover, SFE-EDTA proved to increase the extraction efficiency of vanadium in upstream and downstream oily sludge matrices, which qualifies it for the same SFE-EK procedure but only for Vanadium Cells. For nickel and lead, SFE parameters such as temperature, pressure, extraction procedure (dynamic and/or static), and extraction times should be re-evaluated.

5.7 FTIR analysis

FTIR analysis of upstream and downstream samples showed different effect of EK on their properties. Such information was crucial in this investigation, since mobility of metals is related to the phase separation process. The electrical field affected the O/W (oil in water emulsion), which represent the upstream sludge in greater extent than the downstream W/O (water in oil emulsion). DC field dissociated lead, nickel and vanadium chlorides, while chloride ions were located mostly in O/W emulsion. Their role was to coordinate the molecules of water according the charge of the cations and anions around the encapsulated droplets of hydrocarbons. The polarizing effect is known to be dependent on metallic species (Vaibhav et al., 1999). Then, because vanadium was the strongest electric conductor among the three target metals, it was expected that vanadium was more responding upon the application of electrical field.

To estimate the influence of vanadium and other target metals on the separation process, an assessment of water (W) and hydrocarbons (HC) distribution in EK cells was required. Therefore, FTIR analyses were performed on all the EK cells (Appendix A).

As it has been explained in the methodology (Ch. 4.5), according to Lambert-Beer law; the absorbance of a FTIR band attributed to substance, is proportional to the concentration of the substance. To compare the values of different spectra in the oily sludge matrix, there is a need of using an internal standard. Figures 5.61 and 5.64 represent the upstream and downstream spectra. From the two Figures, the band in the area 1040 cm^{-1} , which belongs to SiO stretching vibration in bentonite, was used as an ideal inert standard.

Subsequently, the values of two ratios OH/SiO and CH/SiO were calculated and presented in Figures 5.62-5.63 and 5.65-5.66. These ratios were utilized in tracing the movement of hydrocarbons and water in the upstream and downstream cells respectively.

5.7.1 Upstream Cells

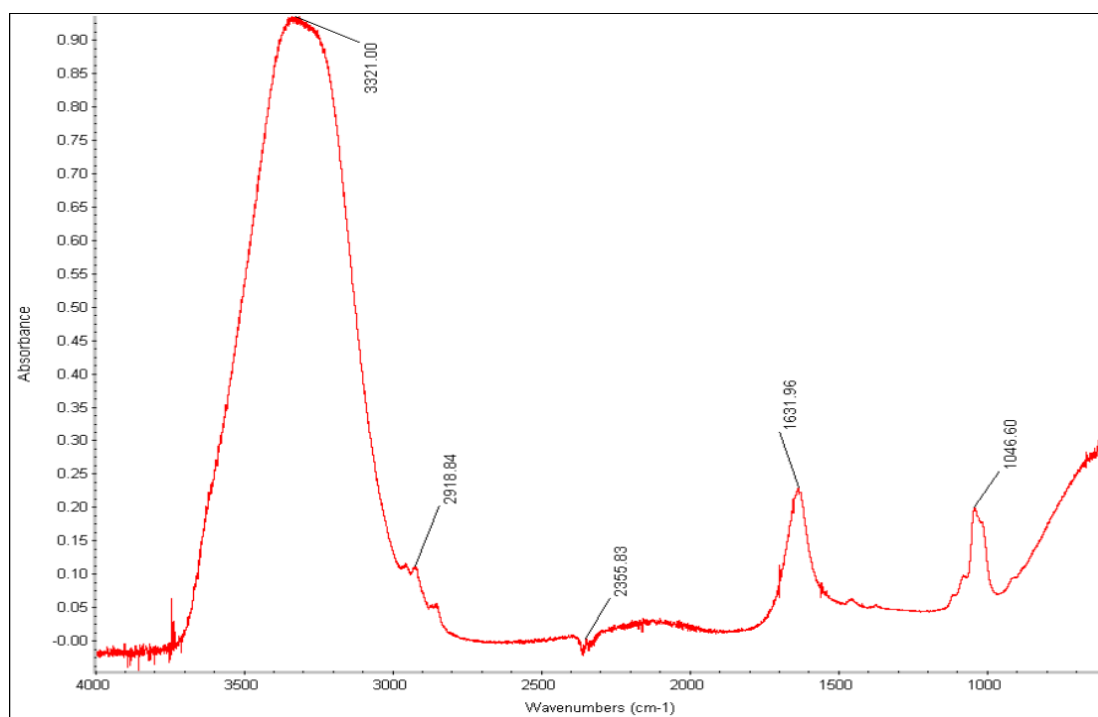


Figure 5.61 FTIR absorbance spectra of the original upstream cell before EK treatment

From Figure 5.61, which represents the FTIR spectra of the initial conditions of upstream sludge before EK treatment, the band 3321 cm^{-1} seemed to be most intensive; however,

bands at 1631 cm^{-1} and 1046 cm^{-1} are relatively weak. The bands at 3321 cm^{-1} and 1631 cm^{-1} have been attributed to stretching and deformation vibrations in bentonite interlayer water. Moreover, the same bands belong to added water with the dissolved chlorides of the target metals (V, Ni, Pb). The absorbance of radiation at 1040 cm^{-1} which belongs to SiO stretching vibrations in bentonite was taken as standard value for the calculation of CH/SiO and OH/SiO ratios.

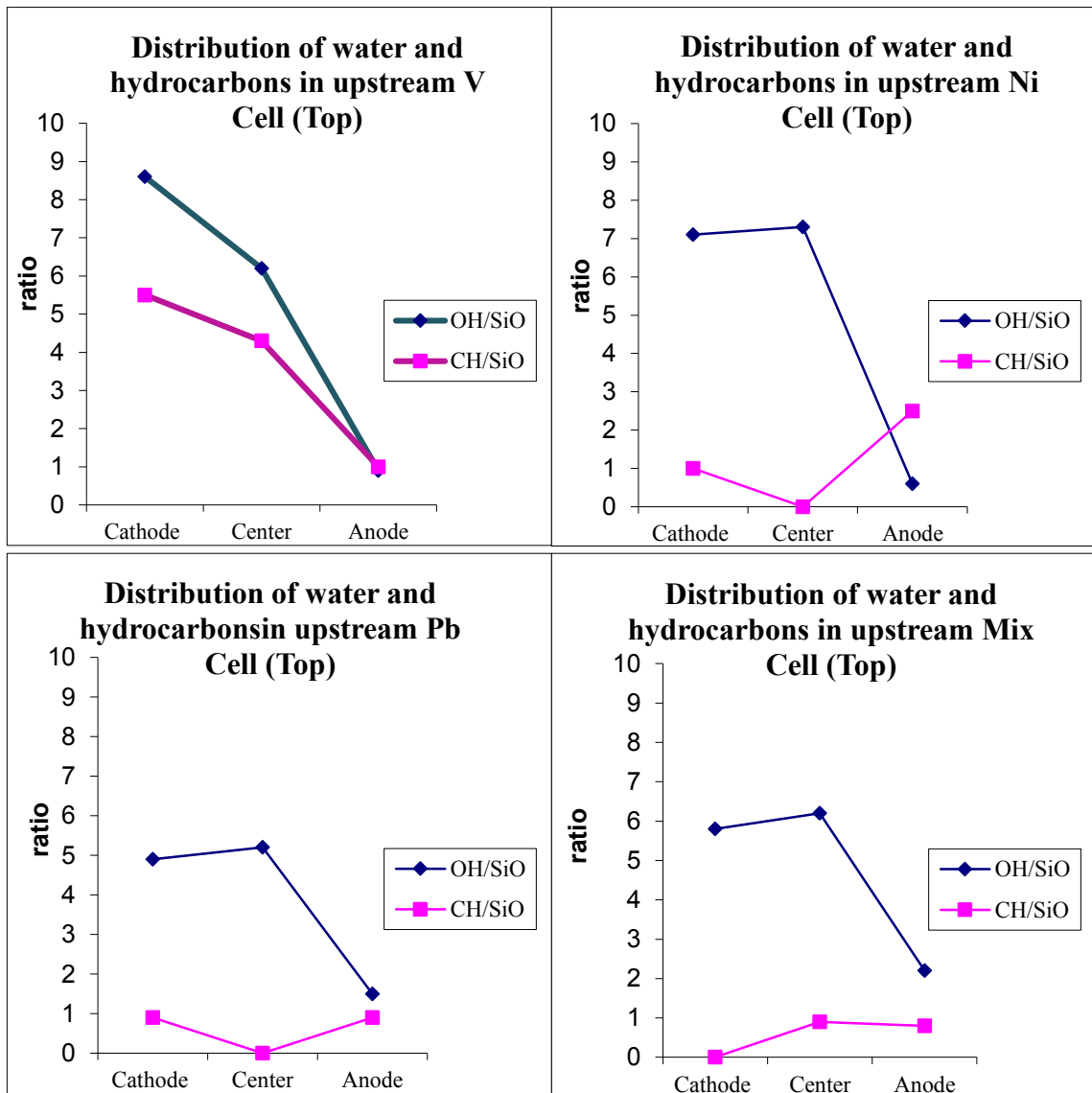


Figure 5.62 Distribution of water and hydrocarbons in upstream cells based on OH/SiO and CH/SiO ratios at the top sections of the cells

Values of OH/SiO (Fig 5.62, Fig 5.63) calculated from all the upstream cells spectra (Appendix. A), were more pronounced at the cathode area than the anode area. This difference was more evident for the Vanadium Cell than for Lead and Nickel Cells. This suggests that the electroosmotic movement of water toward the cathode was more effective in the presence of vanadium.

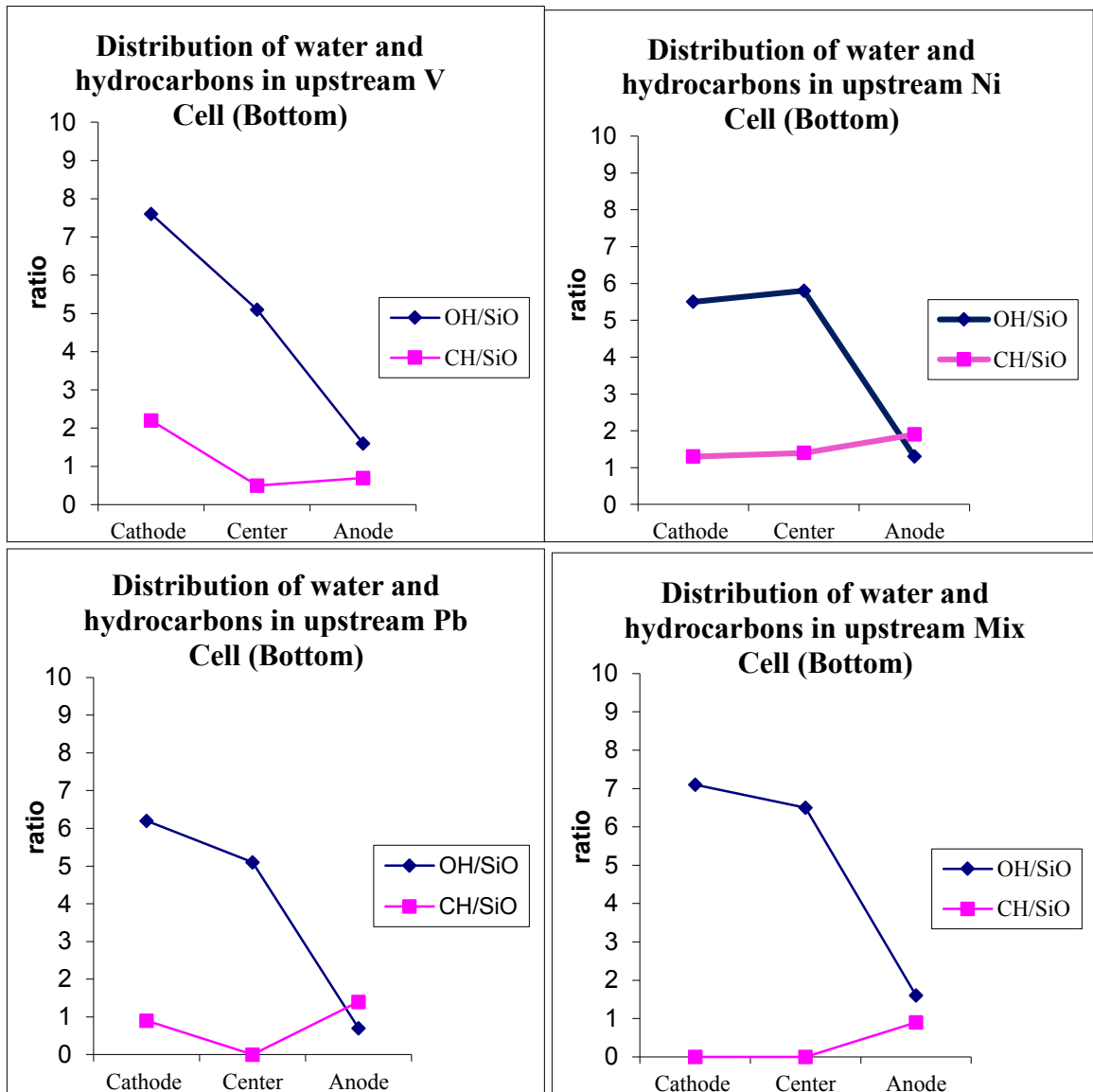


Figure 5.63 Distribution of water and hydrocarbons in upstream cells based on OH/SiO and CH/SiO ratios at the bottom sections of the cells

5.7.2 Downstream cells

From Figure 5.64, it can be seen that the spectra of the downstream sludge (with diesel) before EK treatment is significantly different compared to the upstream oil sludge (Fig. 5.61). The results showed that the bands in 2800-3000 cm^{-1} region (CH-stretching vibrations in aliphatic hydrocarbons of diesel and crude oil) were more intensive, while the band in region 3400 cm^{-1} (interlayer water and bulk water) was less intensive.

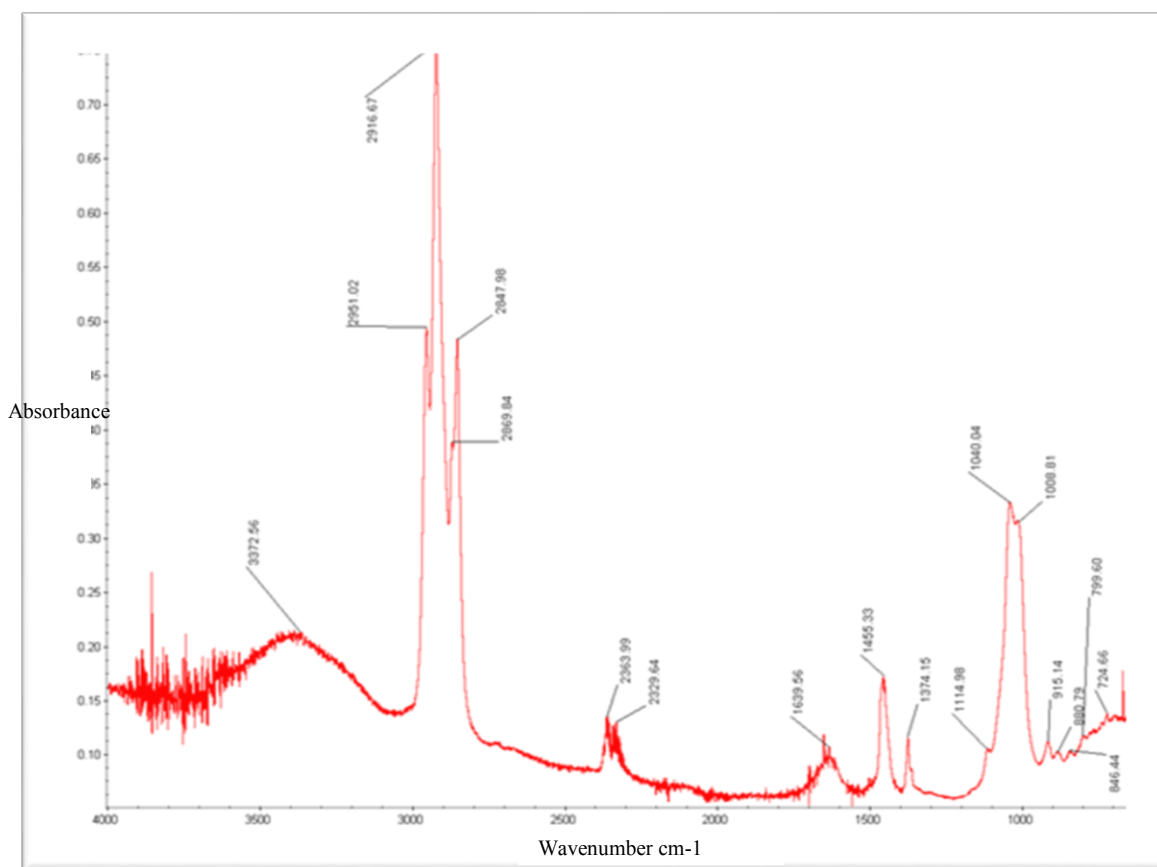


Figure 5.64 FTIR Absorbance spectra of the initial downstream oily sludge before EK treatment

Addition of diesel changed the balance between W/O and O/W emulsions. This resulted in an increase of the hydrophobicity in the system. Moreover, the separation of hydrophilic and hydrophobic phases (which facilitates water movement), might consequently decrease the water content in different sections of the cell.

From the downstream cells spectra (Appendix A), Figures 5.65 and 5.66, demonstrated that the OH/SiO values were very small in all the divisions of the downstream cell (vertical and horizontal). The CH/SiO values were generally higher than the values of OH/SiO throughout the downstream cells.

FTIR, along with previous tests (characterisation of the cells, Ch. 5.1) confirmed that in the presence of diesel; the separation of phases in sludge emulsion was less effective in the Lead Cells. However, a dark spot of solid hydrocarbons largely spreading toward the cathode was observed (Appendix. B, Fig B.4). This visual observation was confirmed by the relatively high CH/SiO ratio (8) in Figure 5.63. The same cell (downstream Lead Cell) demonstrated higher accumulation of water (OH/SiO) at the cathode area than the other three (Nickel, Vanadium and Mix) downstream cells.

In the downstream Nickel Cell, spectrum of the top of cathode region where OH band at 3400 cm^{-1} was small, the narrow band at 3620 cm^{-1} was observed. This band is related to hydroxyls bonded to Si, Al, Mg atoms in bentonite (Si-OH, Al-OH, Mg-OH). These are the structural hydroxyls. The band at 3620 cm^{-1} became more evident when the band at 3400 cm^{-1} did not overlap it. Therefore, it can be concluded, that the process of dehydroxylation did not take place in this experiment. The process of dehydration (dewatering or electroosmosis) is the only process which occurred upon the application of the electrical field into the downstream cells.

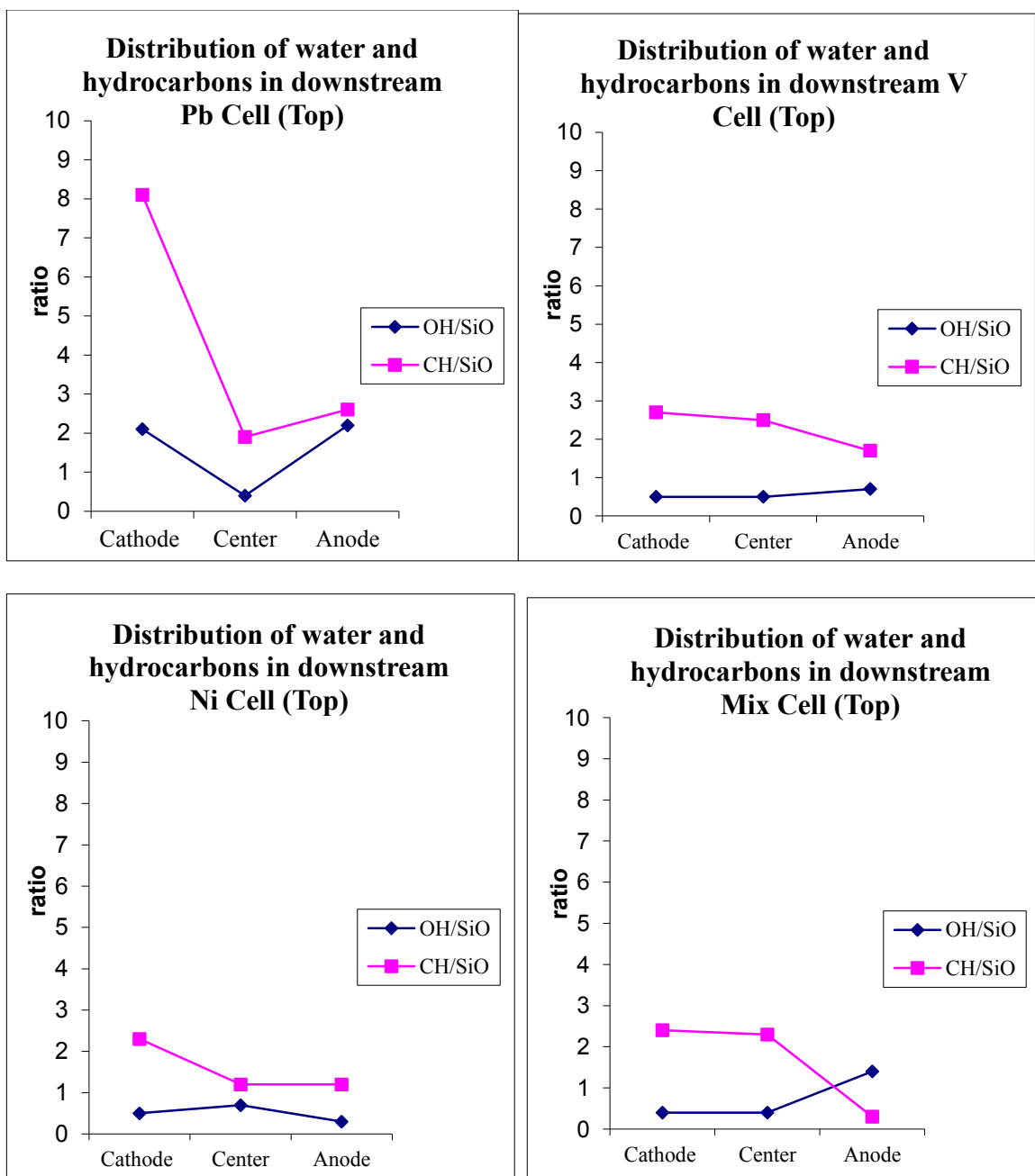


Figure 5.65 Distribution of water and hydrocarbons in downstream cells based on OH/SiO and CH/SiO ratios at the top sections of the cells

Similar patterns of CH/SiO and OH/SiO ratios were observed in the bottom sections of the downstream cells. These values would help in describing the distribution of metals based on the electroosmotic flow (OH/SiO) and adsorption of different metals species to solid particles (Ch. 6).

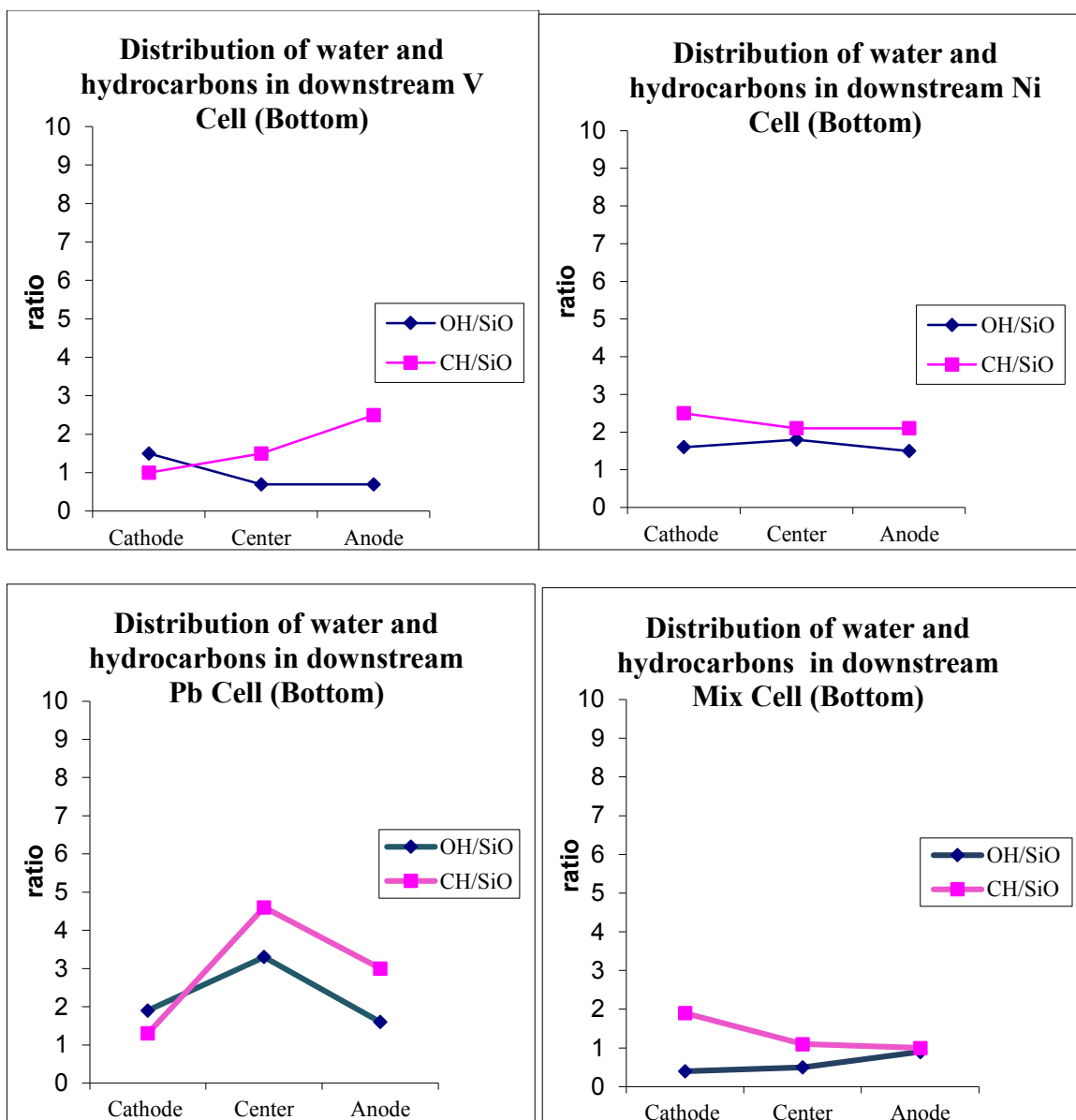


Figure 5.66 Distribution of water and hydrocarbons in downstream cells based on OH/SiO and CH/SiO ratios at the bottom sections of the cells

5.8 X-Ray diffraction (XRD)

This results show an important effect of the presence of diesel fuel fraction in oily sludge.

In the downstream cells the effect of diesel was obvious in preventing the horizontal

separation of fractions. FTIR analysis also showed insignificant dewatering process in the downstream cell.

X-Ray diffraction (XRD) was carried out on the downstream Vanadium Cell, based on physical and visual observations, where downstream cells showed lack of phase separation under EK conditions. However, vanadium compounds (especially vanadium oxides) are a rich and diverse family of compounds with several applications. For example, Vanadium dioxide (VO_2) undergoes a transition from a semiconductor to a metal at 340 °K, accompanied by a structural change (Corr et al., 2008). This structural change would influence the electrical resistivity by approximately 6 orders of magnitude. In addition, vanadium oxides might undergo reversible structural transitions associated with their electrical property changes (Corr et al., 2008). Therefore, detecting the crystalline forms in the downstream Vanadium Cells seemed to be of great importance. Subsequently, XRD was conducted on a solid fraction of the downstream oily sludge matrix using a PHILIPS PW-1050/65 powder diffractometer with a 2θ scan range between 10° and 100° . Powder XRD helped in generating a mineral map in order to evaluate the movement of vanadium in a relatively dry cell (downstream cell after EK), and to identify the crystalline phase(s) present in the sample. Position and intensity matching of the spectrum was performed with reference to the established ICDD (International Centre for Diffraction Data) database. This latter task was carried out with the aid of the accompanied software (X'pert Highscore).

The samples subjected to XRD were taken from the following areas of Vanadium Cell: bottom and top level of the anode zone, the central zone, as well as from bottom and top area of the cathode zone. Such method permitted to identify crystalline and sometimes

pseudo-crystalline forms of species in the sample. The comparative study of samples in various cell locations helped assessing the matrix behaviour and movement of species within electrokinetic cell. Figure 5.67 illustrates the resulted spectra of the XRD of the vanadium downstream cells after electrokinetic treatment. The first (bottom) spectrum represents the downstream cell matrix at its initial conditions, before EK was applied. In the subsequent spectra, their peaks (position and intensity) with respect to the peaks of the initial spectrum gave an indication of the displacement of the crystalline phase present in the cell.

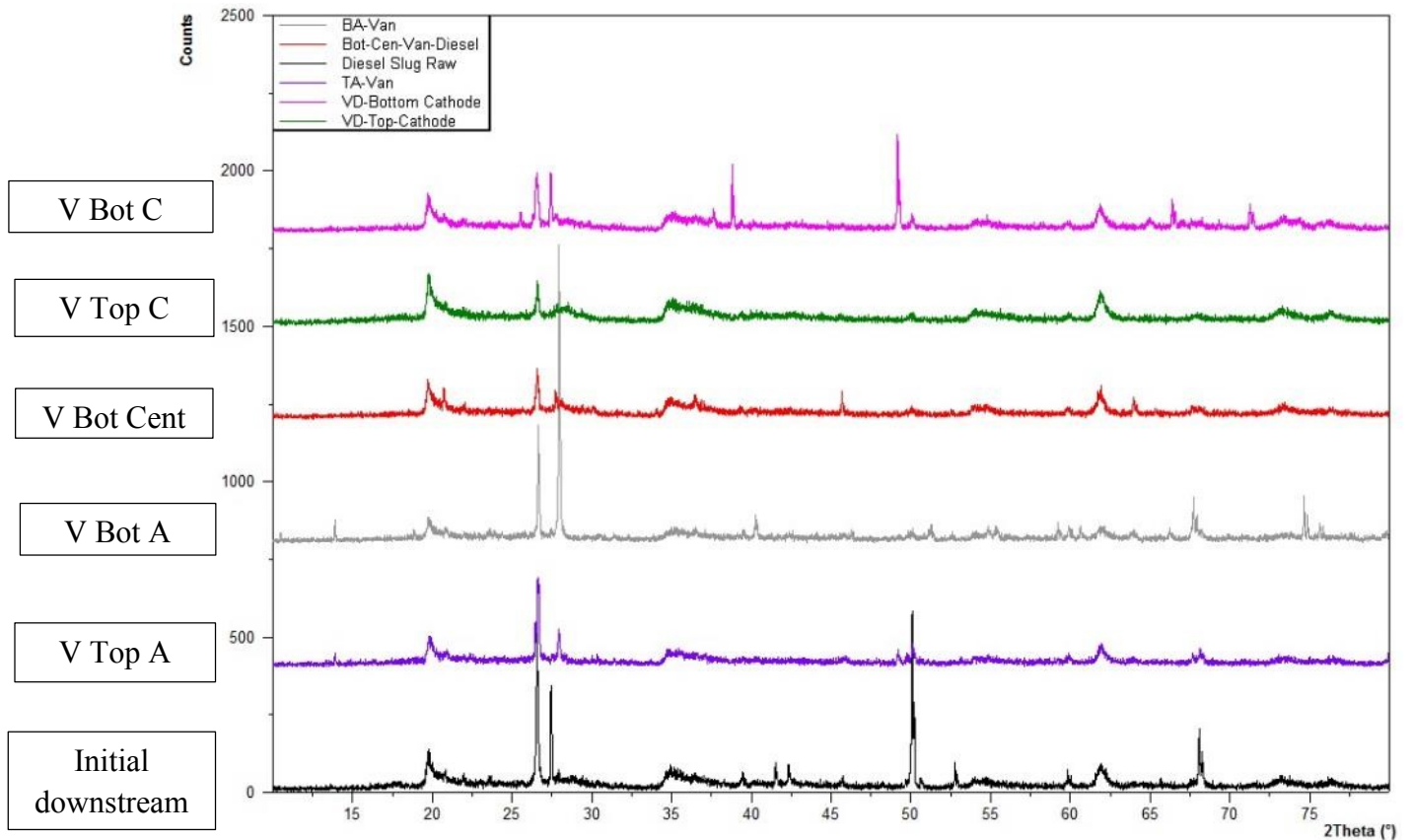


Figure 5.67 XRD spectra of the downstream samples in Vanadium Cell before and after EK treatment

Table 5.2: XRD results, downstream samples in Vanadium Cell after EK treatment

Section	Chemical name	Formula	Score
Top Cathode	Montmorillonite	AlSi ₂ O ₆ (OH) ₂	60
	Quartz	Si O ₂	56
	Benzene	C ₆ H ₆	27
	Vanadium Oxide	V ₄ O ₉	17
Bot Cathode	Quartz, low	Si O ₂	53
	Montmorillonite	AlSi ₂ O ₆ (OH) ₂	48
	Vanadium Oxide	V ₃ O ₄	39
	Aluminum Oxide	Al ₂ O ₃	37
	Desoxybenzoin	C ₁₄ H ₁₂ O	32
	Iron Oxide	Fe ₂ O ₃	13
Central	Quartz, low	Si O ₂	55
	Montmorillonite	AlSi ₂ O ₆ (OH) ₂	48
	Chlorine Oxide	Cl ₂ O ₇	18
	Vanadium Chloride	VCl ₂	27
	Vanadium Oxide	VO ₂	20
Top Anode	Quartz	SiO ₂	65
	Montmorillonite	AlSi ₂ O ₆ (OH) ₂	50
	Calcium Vanadium Oxide	Ca ₂ V ₆ O ₁₇	33
	Cadmium Chloride G	C ₃₆ Cd Cl ₂	49
	poly(p-phenylene vinylene)	(C ₈ H ₆) _n	37
	Vanadium oxide proutadite	C ₁₆ H ₂₈ O ₁₂ ! V ₂ O ₅	13
Bot Anode	PotassiumThallium Chloride	K.92 Tl.08 Cl	48
	Quartz	SiO ₂	47
	Montmorillonite	AlSi ₂ O ₆ (OH) ₂	39
	Vanadium oxide proutodite	C ₁₆ H ₂₈ O ₁₂ ! V ₂ O ₅	21
	Calcium Vanadium Oxide	Ca ₂ V ₆ O ₁₇	21
	Potassium Nickel Oxide	K.14 Ni O ₂	31

Table 5.2 describes the pattern lists for each spectrum presented in Figure 5.67. The fingerprints of these peaks gave the following information: compound's name, chemical

formula, and scores components associated with these peaks for each sample. A higher score is identified with more pronounced presence probability of a particular component in tested location.

XRD confirmed the presence of mineral colloidal particles (e.g. motromorillonite), across the cell, which expresses a high affinity to metals. Nevertheless, inert quartz fraction was mostly prevalent. Furthermore, the cathode zone showed the significant presence of benzene fractions, possibly associated with solid surface of matrix.

In addition, XRD confirmed the presence of vanadium oxide in the entire cell, which is the most popular form of the vanadium in nature. However, other forms of vanadium were observed, particularly in the anode area ($\text{Ca}_2 \text{V}_6 \text{O}_{17}$, $\text{C}_{16} \text{H}_{28} \text{O}_{12} \text{V}_2 \text{O}_5$). It seems that oxidation at the anode permitted to produce ionic forms of vanadium, e.g. $\text{VO}_2(\text{OH})_2^-$, which entered in reaction with available ligands, or made complexes with other metals present in oil (e.g. Ni, Pb, Fe, and Ca).

It was assumed vanadium was very sensitive to redox state changes, which was also confirmed by Pourbaix diagram in simple water-vanadium system (Appendix C, Fig C.1). In such situation, multiple formations of species express different behaviour in sludge and move at different mobility rate. Therefore, despite the lack of visual observations, the mobility of various produced species suggested a possibility of electrophoretic movement of components, especially in the downstream Vanadium and Mix Cells.

Chapter 6

Metals mobility under electrokinetic phenomena in oily sludge matrix

The behaviour of metals in any environment depends on variety of characteristics related to the metal itself and its spatial location. Simplifying, these characteristics can be classified into 1) metal properties and 2) environment around it (matrix type, pH, redox conditions, presence of other metals ...etc.).

Results obtained from experimental procedure described in Chapter 5 are used in this discussion to demonstrate the behaviour of target metals (especially vanadium) inside the oily sludge matrix. Based on physicochemical transformations in the matrix (oily sludge), metals complexation, and changes in the oxidation states, the transformation and thus transportation of vanadium, nickel and lead is discussed in Chapter 6. The relationship between metal final distribution in different parts of the cell, and the associated physicochemical properties of that segment is illustrated. Consequently, appropriate conclusions are made regarding the effect of EK phenomena on the behaviour of metals inside the electrokinetically modified oily sludge matrices.

6.1 Behaviour of vanadium in EK modified oily sludge matrix

Vanadium is considered the major trace metal in petroleum industry (Ch 2.2). In some cases, the concentration of vanadium in petroleum samples might reach up to 1500 ppm (Amorim et al., 2007), which is higher than any other trace metal. In addition to the negative effects vanadium might carry (refining products purity and corrosion in oil-fired power plants), vanadium is considered a valuable metal (Ch 2.2.1). In this study, vanadium

showed additional properties. It was observed that vanadium enriched cells exhibited better separation of oily sludge phases (Ch. 5.1). Which have been based on pH readings, sludge fractioning, visual observations, and FTIR analysis. In addition, the OH/SiO ratios, demonstrated that separation of water and oil fractions was more evident in the upstream Vanadium Cell (Ch. 5.7). It led to a conclusion suggesting that movement of water toward cathode, was more effective in the presence of vanadium.

The following sections describe the behavior and mobility of vanadium in the upstream and downstream sludge matrices.

6.1.1 Upstream oily sludge matrix

The relationship between vanadium distribution and the properties of the EK modified matrix in the upstream Vanadium Cell has been summarized in Table 6.1. The parameters governing the distribution and mobility of vanadium in each section of the cell worked together to create a suitable environment for the accumulation of a certain form of the metal. For example, the area at the bottom of the anode contained the highest content of vanadium (23.4 %). This area is characterized with the lowest pH (4.7) associated with the highest solid content (71.07 %), lowest liquid content (6.77 %), and highest non-volatile organic content (22.17 %).

Table 6.1: Summary of the results: upstream Vanadium Cell after EK

Properties of Vanadium upstream Cell after EK		Anode			Center			Cathode		
		Top	Mid	Bot	Top	Mid	Bot	Top	Mid	Bot
Metal distribution % → 100%		9.78	10.9	23.4	7.6	15.9	14.3	4.12	5.2	7.16
pH		5.36	5.47	4.7	8.22	7.6	7.52	10.7	10.4	9.79
Solid content %		60.03	66.35	71.07	63.67	59.97	58.74	29.17	34.00	45.61
Moisture content %		22.75	19.34	6.77	23.18	39.12	34.43	65.23	55	48.10
Non-VOC % ↓ 100%		17.20	14.37	22.17	13.15	9.91	6.83	5.60	11.00	6.29
Avg-Viscosity as a function of strain (Pa.s)		11000	NA	8500	2520	NA	1130	176	NA	6.15
FTIR	OH/SiO	.9		1.6	6.2		5.1	8.6		7.6
	CH/SiO	1.0		0.7	4.3		0.5	5.5		2.2
XRD (crystalline comp.)		Quartz				Quartz, low				
		Montmorillonite				Montmorillonite				
		Vanadium Oxide V ₂ O ₄				Chlorine Oxide (ClO)				
		Chlorine Oxide (ClO) Vanadium Oxide (V ₂ O ₄)		Vanadium Oxide (VO ₂)		Iron Oxide (Fe ₂ O ₃)		Vanadium Oxide Hydroxyl (VO ₃ OH ₂)		

The variation of pH is initiated by the application of the direct current, where an oxidation and reduction reactions occur at the anode and cathode, respectively. These reactions would result in the formation of OH⁻ ions close to the cathode increasing the pH levels, and H⁺ formation lowering the pH at the anode (Ch. 2.6.1). These phenomena also cause the dissolution and transport of the ions from anode, thereby producing a propagation of an acid front.

These reactions would simultaneously initiate the electro-demulsification, electro-coagulation, electrosomosis and electrophoresis (Ch 2.6.1), which would result in the accumulation of separated solids near the anode area (especially at the bottom), countered by accumulation of the liquids closer to the cathode area. These results were supported by visual observations (Fig 6.1), electrical potential change (Ch. 5.2), and rheological properties measurement (Ch. 5.4).

XRD analysis (Ch 5.8) demonstrated that vanadium in the upstream cell took the following forms (V_2O_4 , VO) and (VO_3OH) at the anode and cathode areas, respectively. Al-Kharafi and Badawy, (1997) demonstrated similar results of vanadium electrochemical behaviour at different pH values. These results were also comparable to the standard Pourbaix diagram of vanadium (Pourbaix 1974; Fig C.1). In the Pourbaix diagram vanadium would take a solid form (V_2O_4) in a pH range of (4.7 - 8) and ionic form (VO^{+2}) in a pH lower than 5. These two cases were clear at the top and bottom of the anode respectively (Table 6.1). Furthermore, the Pourbaix diagram would suggest two forms of vanadium: VO_3OH^{2-} and V_2O_3 in a pH range of 9 to 12. XRD analysis confirmed these assumptions, where vanadium at the cathode area took the form of VO_3OH in a pH zone between 9.79 and 10.7. On the other hand, minerals such as quartz and montmorillonite (clay mineral) were found throughout the cell. However, higher amounts were detected around the anode area, as it was expected, considering the ion exchange phenomena between free cations and negatively charged clay minerals being transported toward the anode, hence, the higher concentration of vanadium around the anode area. Wehrli and Stumm (1989), demonstrated that vanadium generally exists in solutions as the vanadyl ion (V^{4+}) under reducing conditions, and vanadate ion (V^{5+}) under oxidizing conditions, or as an integral part or

adsorbed onto minerals. They reported that in water, vanadyl would form VO^{2+} and $\text{VO}(\text{OH})^+$, and the vanadate would be in the forms: H_2VO_4 and HVO_4^{-2} . Both vanadate and vanadyl species are known to bind strongly to mineral or biogenic surfaces by adsorption or complexing (Wehrli and Stumm 1989). Thus, they assumed that vanadium is present in solution and suspension where it can be transported due to electroosmotic and electrophoretic motions, respectively.

Metals have diffusion tendencies from one phase to another depending on the atomic radius and pH/redox conditions (Elektorowicz, 2009). This study also showed that, metal speciation depends on the separation of the sludge matrix during EK process, where formation of new phases allows vanadium to diffuse into the interior solid phase, especially where cations would neutralize the negative charge of clay particles. Thus, the aggregation of solid particles closer to the anode area, contributes to the accumulation of vanadium at the anode area. Viscosity measurement at the anode area recorded the highest values in the cell (11000 Pa.s, and 8500 Pa.s) at the top and bottom, respectively. Furthermore, lowering the permeability at that section of the matrix affected the solubility of metals in the water trapped within the solids (clay), which inhibited the electro-migration of the vanadium towards the cathode. This could explain the high accumulation of vanadium in the center area. A continuous supply of a flushing liquid and a longer exposure to EK might overcome these unfavorable conditions.

Low pH is favourable to the dissolution and mobilization of metals; on the other hand, the development of high pH near the cathode results in precipitation of heavy metals, forming a “barrier” which lowers the efficiency of electro-migration toward the cathode. Furthermore, vanadium at high pH environment would form a hydroxide precipitate,

thereby ceasing its ability to migrate through the subsurface, which explains the low accumulation of vanadium at the top of the middle and cathode areas.

6.1.2 Downstream oily sludge matrix

Table 6.2: Summary of the results: downstream Vanadium Cell after EK

Properties of vanadium downstream Cell after EK		Anode			Center			Cathode		
		Top	Mid	Bot	Top	Mid	Bot	Top	Mid	Bot
Metal distribution % → 100%		10.09	8.1	9.07	9.75	11.33	12.9	13.3	14.17	11.51
pH		9.42	9.13	9.17	10.17	9.12	9.15	8.99	9.12	9.22
Solid content %		61.84	61.34	56.74	53.86	54.39	58.82	50.15	60.53	56.07
Moisture content %		17.31	23.71	33.37	27	33.41	32.37	30.66	34.47	27.69
Non-VOC % ↓ 100%		20.85	14.99	9.89	19.14	12.20	8.82	19.18	5.00	16.23
Avg-Viscosity as a function of strain (Pa.s)		59.2	NA	1270	316	NA	2170	467	NA	79.4
FTIR	OH/SiO	.7		.7	.5		.7	.5		1.5
	CH/SiO	1.7		2.5	2.5		1.5	2.7		1
XRD (crystalline comp.)		Quartz Montmorillonite Vanadium Oxide Pro Top A Bot A			Quartz, low Montmorillonite Vanadium Oxide VO ₂ Chlorine Oxide Cl ₂ O ₇ Vanadium Chloride VCl ₂			Quartz Montmorillonite Top C Bot C		
		Calcium Vanadium Oxide (Ca ₂ V ₆ O ₁₇) Cadmium Chloride (C ₃₆ CdCl ₂) Poly(p-phenylene vinylene) (C ₈ H ₆) _n	Potassium Thallium (K ₉₂ Tl _{.08}) Chloride Cl	Benzene (C ₆ H ₆) Vanadium Oxide (V ₄ O ₉)	Vanadium Oxide (V ₃ O ₄) Aluminum Oxide (Al ₂ O ₃) Desoxybenzoin (C ₁₄ H ₁₂ O) Iron Oxide Fe ₂ O ₃					

Non-polar compounds of diesel (present in the downstream cells), affected the electrokinetic process (Ch. 5.1). Beside visual observations (Fig. 6.2), Table 6.2 demonstrates the lack of a significant variation in the physical properties of the matrix after EK treatment. For example, pH values didn't change by more than 1.18 between two electrodes (8.99-10.17).

These results affected the distribution of metals, especially that the addition of diesel compounds to a water-in-oil emulsion (downstream) has been found to cause the dispersed water droplets to flocculate and settle out of the oil phase by increasing the hydrophobicity of the particles (Yan et al., 2001). Such behaviour facilitated water movement, however, it affected the EK process in the cell, where the stability of the emulsion was lower than the stability at the upstream cells (before the application of EK), which makes EK application in the downstream sludge (for the purpose of phase separation) more difficult. For example, the presence of undissolved vanadium chloride (XRD analysis; Ch. 5.8) at the center of the cell demonstrated the decrease of solubility and subsequently, the mobility of vanadium species in the downstream Vanadium Cell.

Such conditions allowed different kind of behavior of vanadium in the matrix under DC field. For instance, unlike the upstream cell where the accumulation of vanadium was higher at the anode area, the accumulation in this cell was higher at the cathode area (around 40%), with 14% at the middle section of the cathode alone. This section contained the highest amount of liquids (34.5%) and the lowest amounts of NVOC (5%). Other properties such as pH, OH/SiO and CH/SiO ratios showed similar values throughout the cell.

FTIR analyses showed that the values OH/SiO were very small in all segments of the downstream Vanadium cell (anode, centre, and cathode). The values CH/SiO were higher

(sometimes more than 5 times) than the values OH/SiO, showing low commutation of water in a particular areas. In addition to that, it confirmed that, no significant separation of phases was observed in EK cells containing downstream samples.

The study demonstrated that the mobility of vanadium was related to the capability of phase separation, which was a rather low in this case. Nevertheless, some vertical movement of vanadium was observed even in such harsh conditions. It is speculated that metal movement might be more pronounced when some polar additives are provided (even water) and longer exposure to DC field should be provided.

XRD analysis demonstrated the variability of vanadium complexes and oxidation states in the cell. This indicates the effect of EK on vanadium behavior in such a complicated matrix, despite an insignificant physical separation of phases. For example, vanadium oxides appeared in multiple forms at the anode (VO_2), center of the cell (VO_2 , V_4O_9), and cathode (V_3O_4). These structural changes would cause a change in the electrical resistivity, affecting the electroosmotic and ionic transport, subsequently, the mobility of vanadium species.

It can be concluded that vanadium properties, which promote formation of various compounds, using multiple oxidation states, play an important role in its distribution in oily sludge matrices, especially in the downstream cells where water volume is reduced, thus affecting the electromigration and electroosmotic flow.

Figures 6.1 and 6.2 show the diverse effect of electrokinetic phenomena on both upstream and downstream Vanadium Cells. In the upstream cell, an obvious separation of phases was noticed, where liquids accumulated at the cathode area and solids aggregated around the anode area. These movements affected the distribution of metals as it has been

explained earlier. On the other hand, while lab analysis (Chapters 5.1, 5.2, 5.3, and 5.7) showed little variation of most physicochemical, and electrical properties in the resulted downstream cells, the visual observation showed formation of a thin layer, consisting of light crude oil, extended on the cell surface. This suggests the possibility of a limited cracking process that has been taken place in the cell. These visual observations at the downstream cell were supported by the characterisation of the sludge, where the top layer of the cell at all sections (anode, center, and cathode) contained the highest non-volatile organic content (Table 6.1). Moreover, according to the FTIR analysis, these areas contained higher CH/SiO ratios than OH/SiO, which suggests higher hydrocarbon content.

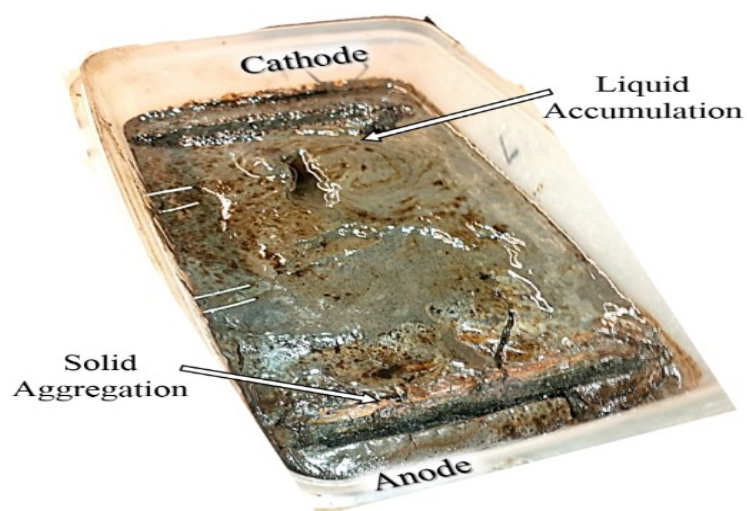


Figure 6.1 Upstream Vanadium Cell post EK

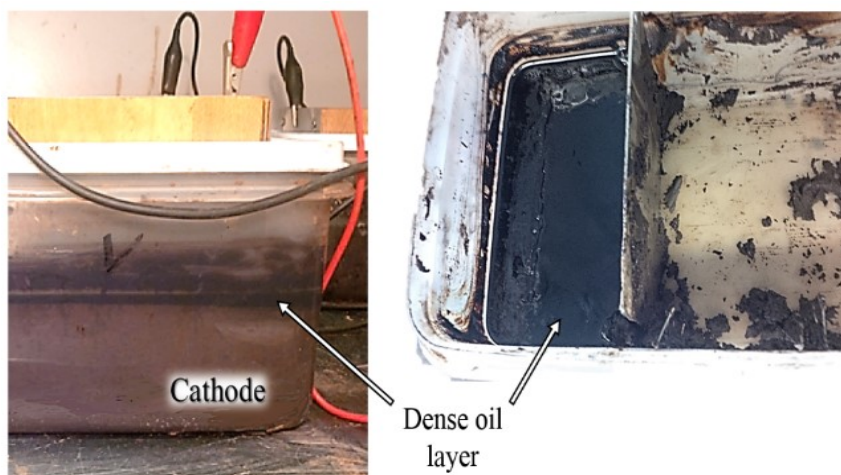


Figure 6.2 Downstream Vanadium Cell post EK (formation of thin layer of dense hydrocarbons on the surface)

6.2 Nickel mobility

Nickel is one of the most common metals that can be found in the crude oil, and consequently in the petroleum sludge. Nickel, generally in its +2 oxidation state is present in a water soluble forms such as nickel chloride, nickel fluoride, nickel nitrate, and others. In this research, nickel has been added as nickel chloride (Ch. 4.1.1). With the complexity of the matrix used in this research, nickel distribution in the cell was affected by components of the oily sludge matrix formed after EK treatment (Table 6.3). The following two sections describe the mobility of nickel inside the upstream and downstream Nickel cells.

6.2.1 Upstream oily sludge matrix

Table 6.3, demonstrates the distribution of nickel inside the upstream sample (Nickel Cell). It points out the characteristics of the cell horizontal sections; namely anode, center of the cell, and cathode, which were divided into vertical sections namely top, middle (Mid) and bottom sections (Bot) (Fig 5.2). Adequately, nickel distribution in all sections is provided.

Table 6.3: Summary of the results: upstream Nickel Cell after EK

Properties of upstream Ni Cell after EK		Anode			Center			Cathode		
		Top	Mid	Bot	Top	Mid	Bot	Top	Mid	Bot
Metal distribution → 100(%)		14.47	15.12	24.99	6.7	9.3	10.90	8.0	7.55	3.4
pH		5.8	5.9	4	10.78	10.69	10.86	11.3	11.5	11.5
Solid content %		78.57	62.0	55.62	34.66	36.22	39.00	45.72	30.91	32.00
Moisture content %		8.25	29.00	34.41	60.44	54.23	55.13	50.21	66.00	64.21
Non-VOC % ↓ 100%		13.17	9.00	9.97	4.90	9.54	5.87	4.07	3.09	3.79
FTIR	OH/SiO	0.6	1.3	7.3	5.8	7.1	5.5			
	CH/SiO	2.5	1.9	0.0 (ND)	1.4	1	1.3			

The results showed different matrix characteristics in all sections of the cell, demonstrating electrokinetic separation of phases. The mobility of nickel followed such changes in matrix characteristics. Nickel accumulation was mostly in the anode area (55%), of which 25% in the bottom of the anode area alone. This area was characterized with high acidic content (where pH = 4 at the bottom of the anode), high solid content (78.57 % at the top of the anode), lowest liquid content (8.25 % at the top of the anode area), and highest NVOC content (13.17 % at the top of the anode area). Comparing this section with others, it was concluded that nickel seems to have affinity to both solid fraction, and probably light fraction of oil (hiding in moisture value). Visual observations ((Appendix B; Fig B.3), and FTIR analysis (Ch. 5.7.1) performed in this research confirmed the physical characteristics of the cell, where the OH/SiO ratios were much lower in the anode area than the center and cathode areas. These ratios are an indication of a low presence of water in this section (Ch. 5.7).

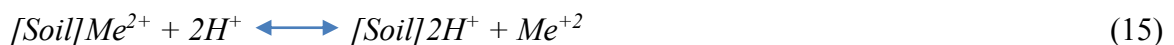
As previously mentioned, the lower part of the anode section contained the highest concentrations of nickel (around 50% of total nickel at the anode). This section contained also higher amounts of moisture than the top anode sections. This indicates that despite a high accumulation of solids around the anode area, the fine particles might have created a stable suspension which never settled at the bottom. Therefore, the bottom section of the anode area might have combined ionic forms of nickel, due to the relatively high water and hydrocarbon content, if compared to the top parts of the anode, since nickel has also affinity to liquid fraction of hydrocarbons. Furthermore, nickel species such as Ni(OH)_2 , might have been adsorbed into the solid content (which is relatively high if compared to the center and cathode sections of the cell). As a result, the bottom section of anode as shown in Table 6.3 contained the most nickel in the cell.

The effect of pH on solubility, which is usually associated with mobility of metals, has been widely documented. For example, a standard Pourbaix diagram for nickel in an aqueous system (Pourbaix 1974 in Thompson and Kaye 2000; Appendix C, Fig C. 2), shows that nickel would take an ionic form (Ni^{+2}) in a pH zone below 8, in strong oxidation conditions, which is the case at the anode zone of this experiment, where pH ranged between 4 and 6. However, in a high alkaline zone, Pourbaix diagram showed the formation of solid NiO and Ni(OH)_2 in a pH zone between 9 and 13. In this study, pH in the upstream Nickel Cell was between 10 and 11.5 at the central and cathode areas (Table 6.3), which suggests the possibility of producing such species as NiO and Ni(OH)_2 .

In an EK cell which does not contain oil products, electromigration and electroosmotic transport of the metallic species are usually initiated toward the cathode, leading to the accumulation of the metals at the cathode area. However, in this research the central and

cathode areas contained low total amounts of nickel (25% and 19%, respectively), with a minimum of 3.4% at the bottom of the cathode area. On the other hand, the anode area accumulated around 56% of the total available nickel. These results suggested that, despite the movement of liquid components toward the cathode area (Ch. 5.1, Ch. 5.7, and visual observations) carrying small amounts of nickel, through electroosmotic flow. Electromigration and electroosmotic transport did not seem to be the main mechanism of transport and distribution of nickel in the cell. It was speculated that nickel in its ionic forms had a high affinity to colloidal phase of the matrix and it was transported by electrophoresis toward the anode.

Generally, the retention of nickel is primarily due precipitation with hydroxide ions, presence of organic matter, and ion exchange with solid colloidal fraction. In this study, electrical resistance (Ch. 5.2) in the anode area was increasing considerably, due to the aggregation of solid particles and the decrease of water content demonstrating electrophoretic transport of particles (including minerals) with nickel. The affinity of metals (adsorption capacity) towards charged matrix, is associated with the physiochemical properties of metals (Eq. 14), and has a great impact on the efficiency of electrokinetic remediation (Kim et al., 2009, Brady, 1990).



If someone would like to reverse nickel transport toward cathode (following other metals behaviour), he should promote electroosmotic transport, then increase the water content in the matrix and extend time of exposure to electrical field. In future considerations, this issue can be dealt with by pumping extra water (electrolyte) into the cell.

The degree to which any metal is hydrolyzed usually dictates the fate of the metal in the subsurface. However, the presence of the complex components of petroleum oily sludge produced an out of normal behavior of nickel that might require extra tests and analysis.

It was concluded that, the type and amount of additional fractions in oil-in-water upstream sludge, (for example, mineral colloidal phase, or light oil) plays an important role in nickel mobility.

6.2.2 Downstream oily sludge matrix

Distribution of nickel in the downstream Nickel Cell is shown in Table 6.4, where the areas with higher liquid content contained higher amounts of metals. For example the bottom layer of the cell (bot anode, center, and cathode combined) accumulated highest amounts (40%) of total nickel. This layer also contained highest liquid content in the three main cell sections: anode, center, and cathode. FTIR showed high hydrocarbon content in the area where nickel was located, demonstrating once more high affinity of nickel to both water and light hydrocarbon fraction. Though, the fact that water was trapped at the bottom can be explained by the possibility that adding non-polar solvent through diesel resulted in increasing the hydrophobicity, which caused further separation of hydrophilic and hydrophobic phases, facilitating water movement and eventually decreasing the water volume in certain parts of the cell, which led to a certain limit of the detention of water at the lower segments of the cell.

Table 6.4: Summary of the results: downstream Nickel Cell after EK

Properties of downstream Ni Cell after EK		Anode			Center			Cathode		
		Top	Mid	Bot	Top	Mid	Bot	Top	Mid	Bot
Metal distribution → 100 (%)		7.9	10.61	15.43	8.83	9.83	10.33	12.88	10.93	13.18
pH		7.9	8.1	8.4	8.2	8.55	8.3	8.15	8.7	8.25
Solid content %		61.68	49.93	43.83	61.65	46.34	39.33	54.19	45.19	41.04
Moisture content %		19.54	37.79	44.11	25.03	44.39	51.46	32.17	50.11	48.40
Non-VOC % ↓ 100%		18.78	12.28	12.07	13.32	9.27	9.21	13.64	4.40	10.55
FTIR	OH/SiO	.3		1.5	.7		1.8	.5		1.6
	CH/SiO	1.2		2.1	1.2		2.1	2.3		2.5

The values of pH (which did not change by more than 1) suggest the possibility that nickel preserved its ionic forms (Ni^{+2}) in cell sections. It is speculated that most nickel species were transported toward cathode by electroosmosis and ionic movement. However, the voltage gradient was not sufficiently high to transport all nickel from anode area toward the cathode, during the experimental exposure time. Probably a longer exposure time, or an increase of voltage, might enhance the transport of nickel toward the cathode in downstream samples. Such investigation might be carried in future work (Ch. 7.4). Similar to the downstream Vanadium Cell, alkalinity was not a factor in the distribution of nickel in the downstream cell.

6.3 Lead mobility

The behavior of heavy metal such as lead in subsurface differs greatly from that of transition metals such as nickel and vanadium (Table 2.4). Lead and vanadium occur naturally in several minerals including vanadinite $Pb_5(VO_4)_3Cl$, where vanadium is widely distributed in small percentages in the oxidized lead and lead-copper ores (Newhouse, 1934). Therefore, the behavior of lead is strongly related to the topic, since important amounts of lead can be found in wasted mining and transformation materials.

The following two sections will focus on the distribution of lead in the upstream and downstream Lead Cells after electrokinetic (EK) treatment. The distribution of lead in the Lead Cells containing upstream and downstream oily sludge was affected by several properties of lead, e.g. high electrical conductivity, low solubility at relatively low pH and high oxidation state levels. These properties were combined with the matrix characteristics to illustrate the distribution patterns of lead in EK cell.

6.3.1 Upstream oily sludge matrix

Similar to the upstream cells that contained nickel and vanadium as sole contaminant, upstream Lead Cell showed excellent separation of phases after applying EK (Appendix B; Fig. B.2)

Table 6.4 shows that 43% of the total lead (highest accumulation of lead) was detected at the cathode, mostly at the middle (17.8%), and bottom (17.86 %) sections. This area contained the highest pH (11), and highest liquid content (58%), confirmed by the highest OH/SiO ratio (6.2 at the bottom of the cathode). These results suggest that lead distribution was mostly related to electromigration and electroosmotic transport, where lead ions Pb^{+2} traveled towards the cathode, which is usually the anticipated behaviour of cations in a

simple EK matrix. High moisture content in cathode area allows the speculation about the important electroosmotic flow of water toward cathode; such flow accelerate transport of lead species, which might not necessary be in a cationic form.

Table 6.5: Summary of the results: upstream Lead Cell after EK

Properties of upstream Pb Cell after EK		Anode			Center			Cathode		
		Top	Mid	Bot	Top	Mid	Bot	Top	Mid	Bot
Metal distribution → 100(%)		5.87	5.05	5.07	18.0	8.35	13.6	7.99	17.8	17.86
pH		8.65	6.8	5.5	10.78	10.9	10.86	11.25	11.23	11.69
Solid content %		71.50	61.45	58.14	42.07	38.23	39.81	43.29	40.33	36.63
Moisture content %		14.81	21.35	31.44	52.69	55.24	53.66	51.50	56.23	58.50
Non-VOC % 100%		13.69	17.21	10.43	5.24	6.53	6.52	5.21	3.44	4.87
FTIR	OH/SiO	1.5	0.7		5.2		5.1	4.9		6.2
	CH/SiO	0.9	1.4		0.0 ND		0.0 ND	0.9		.9

The electrochemical behavior of lead in aqueous matrix is best described through the Pourbaix diagram (Pourbaix, 1974; Appendix C, Fig C.3). According to this diagram, lead is likely to be in the ionic form of Pb^{+2} at the middle (pH=6.8) and bottom (pH=5.5) of the anode area, however, lead hydroxide $Pb(OH)_2$ form would prevail in all the other sections, where pH ranged between (8.65-11.89).

Having a high adsorption capacity to clay, lead is a popular heavy metal in electrokinetic experiments. However, despite the relatively high ionic effective mobility ($10.09 \text{ m}^2/\text{s}\cdot\text{V}$), lead usually shows lower removal efficiency compared to other heavy metals, mainly due its high affinity for adsorption into soil particles (Reddy and Cameselle, 2009).

It can be noticed, that despite the high pH levels at the center section of the cell, large amounts of lead species kept moving towards the cathode, eventually settling at the lower parts of the cathode where the liquid content was the highest. This could be related to the solubility of lead hydroxide produced at pH higher than 6, where it can be seen from the solubility curve (Appendix C, Fig C.4), at pH=9, the solubility is at minimum, and from 9 to 14, the solubility would gradually rise again, accelerating the movement of lead towards the cathode, where pH recorded the highest levels (11.7).

Lead showed better movement towards the cathode comparing to nickel and vanadium in the sole metal cells. In a relatively high organic content (high CH/SiO ratios), lead tends to create organometallic complexes (Hartman, 1983). Therefore, it was interesting that the anode zone contained the least accumulation of lead (15 % of total lead in the cell). In addition, no organo-metallic complexes were detected in the samples used for FTIR analysis (Appendix A, Fig. A25-A.27).

Despite the relatively low solubility of lead, compared to nickel and vanadium (Table 2.4), analysis of the separated phases in the upstream Lead Cell, showed maximum accumulation of lead around the cathode area. Therefore, it can be assumed that electromigration supported by electroosmotic flow were essential in the lead movement.

6.3.2 Downstream oily sludge matrix

Distribution of lead in the Lead Cell containing downstream oil sludge was similar to that of the upstream cell. The cathode zone contained the highest accumulation of lead, where 40% of total available lead was detected in that area. The anode zone contained the least amounts of lead, where only 22 % of total lead was detected.

Table 6.6: Summary of the results: downstream Lead Cell after EK

Properties of downstream Pb Cell after EK		Anode			Center			Cathode		
		Top	Mid	Bot	Top	Mid	Bot	Top	Mid	Bot
Metal distribution →100(%)		8.77	7.18	6.04	14.69	12.61	10.68	13.25	12.20	14.53
pH		7.7	8.3	8.9	8.6	8.6	8.7	8.9	9.4	9.5
Solid content %		41.40	55.38	47.03	38.91	46.55	39.14	45.16	42.62	37.10
Moisture content %		43.31	32.31	38.05	47.47	41.44	47.37	43.61	42.62	51.08
Non-VOC % 100%		15.29	12.31	14.92	13.62	12.01	13.50	11.23	14.70	11.83
FTIR	OH/SiO	2.2	1.6	0.4	3.3	2.1	1.9			
	CH/SiO	2.6	3	1.9	4.6	8.1	1.3			

Despite the less significant separation of phases in the downstream Lead Cell (Ch. 5.1.3), and visual observations, lead accumulation at the center and cathode was almost double of that at the anode zone. This suggests that electromigration largely contributed to the distribution of lead.

The values of pH in this cell (7.7 to 9.5) suggested that lead was available in $Pb(OH)_2$ form (Appendix C, Fig C.3) throughout the cell. The solubility diagram of lead hydroxide (Appendix C, Fig C.4) shows that $Pb(OH)_2$ solubility decreases with the increase of pH. However, at pH around 9, the solubility would start increasing with the increase of pH. Therefore, at the cathode section (pH=9) the solubility of lead was at its lowest value, which could explain the higher accumulation of lead at the bottom of the cathode (14.53%). The presence of diesel in the cell did not seem to affect the mobility of lead. However, it affected the solubility, and eventually the forms of lead in the cell. For example, at pH over

6, lead would take the form of lead hydroxide (which usually precipitates as solid phase), instead of lead ions Pb^{+2} . At a higher pH values (close to 10), lead might take the form PbO^- . In this case, such form might be transported by electromigration toward the anode or by electroosmotic flow toward the cathode, whichever flow is stronger. However, in this study, lead seemed to be mostly subjected to electroosmotic flow.

6.4 Metals distribution in the mixed metals oily sludge matrix

In order to evaluate the efficiency of EK in mobilizing multiple heavy metals in oily sludge, certain matrix, and metal parameters should be recognized. In suspensions such parameters are summarized as (a) the ionic mobility, related to the ionic valance and molecular diffusion coefficient of species, (b) the retardation effect caused by the affinity of metals in solid matrix, and (c) the chemical forms of metals initially existed in the matrix (Kim et al., 2009).

It has been assumed in this study, that the state of heavy metals in the oily sludge matrix belonged mainly to two phases: those adsorbed onto solid particles and those in pore fluid. The latter was expected to be transported by electromigration and/or electroosmosis mechanisms. However in order for adsorbed metals to be transported by electrical field, desorption of metals off the solid particles need to take place as a hydrogen dependent cation exchange reaction. This process is dependent on the hydrolysis of water, where the concentration of hydrogen ions produced at the anode, and pH influence the exchange capacity. Nevertheless, if conditions do not permit such phenomena development, particular forms of metals could be transported thorough electrophoretic movement or strong electroosmotic flow (Elektorowicz, 2009)

Though, with the complexity of oily sludge matrix, there are also several possibilities of adsorption of heavy metals by organic matter. Furthermore, metals compete for adsorption places in the matrix, depending on the type of the matrix, type of the metal and their concentrations. Exchangeable fractions might sometimes be occupied by residual organic contaminants, leading to a decrease in the adsorption capacity of heavy metals. In addition, the mobility of some metals might be affected by the synergistic and antagonistic effects among the metals in the mixed contaminated matrix (Elektorowicz, 2009).

The electrokinetic soil remediation of mixed metals usually shows lower efficiency in removing heavy metals, since the presence of multiple cationic species would affect the zeta potential in the matrix and consequently the electroosmotic flow (Mitchell, 1993).

The following two sections describe the distribution of vanadium, nickel and lead due to their mobility inside the upstream and downstream matrices.

6.4.1 Upstream oily sludge matrix

Table 6.7 describes the accumulation of vanadium, nickel, and lead in each horizontal (anode, center, and cathode) and vertical (top, middle, and bottom) areas in the mixed metals upstream oily sludge matrix. In the cells that contained sole metals in the upstream oily sludge matrices (Ch. 6.1, 6.2, and 6.3), distribution of each metal depended on the properties of the matrix and the metal itself. In this case, vanadium, nickel, and lead were also affected by the properties of other available metals in the matrix.

Mixed Cell showed a very good separation of sludge phases after applying EK (Appendix B, Fig B.4). However, the accumulation of liquids at the cathode (48%) was a little less of that in the sole metal matrices. For example, the maximum accumulation of liquids at the

cathode in the oily sludge matrices that contained vanadium, nickel, and lead as sole contaminant reached 65%, 66%, and 58% respectively.

Table 6.7: Summary of the results: upstream Mix Cell after EK

Properties of upstream Mix Cell after EK		Anode			Center			Cathode		
		Top	Mid	Bot	Top	Mid	Bot	Top	Mid	Bot
Metal distribution 100% →	V	9.4	10.49	9.08	9.10	11.22	14.6	11.92	12.03	12.04
	Ni	26.23	16.56	9.20	5.84	11.5	17.6	4.49	4.08	4.44
	Pb	8.14	5.57	9.27	7.47	13.16	9.35	14.9	15.40	16.73
pH		4.69	4.5	4.3	8.68	8.55	8.2	8.6	9.42	10.4
Solid content %		78.30	76.32	79.68	48.46	49.15	49.7	50.14	51.29	47.82
Moisture content % ↓		11.25	14.35	9.81	46.66	44.11	45	44.99	43.29	48.06
Non-VOC % 100%		10.45	9.33	10.51	4.88	6.73	5.22	4.88	5.41	4.12
FTIR	OH/SiO	2.2	1.6		6.2	6.5		5.8	7.1	
	CH/SiO	0.8	0.9		.9	0.0 (ND)		0.0(ND)	0.0 (ND)	

Other parameters such as pH values, OH/SiO and CH/SiO ratios, showed similar pattern to those in the cells with sole metals (Table. 6.7). For example pH was very low (4.3) at the anode area and high (10.4) at the cathode area. In addition, FTIR analysis confirmed the higher accumulation of water (OH/SiO ratios) at the center and cathode areas.

Since the physical, chemical, and electrical properties of the Mix Cell are similar to those of the sole metal cells, the change in some metals distribution (especially for vanadium) in the upstream Mixed Cell could be related to the synergistic effect, created by the presence of multiple metals in the same matrix.

Figures 6.3, 6.4, and 6.5 demonstrate the changes in each metal distribution, in the presence of the other two metals.

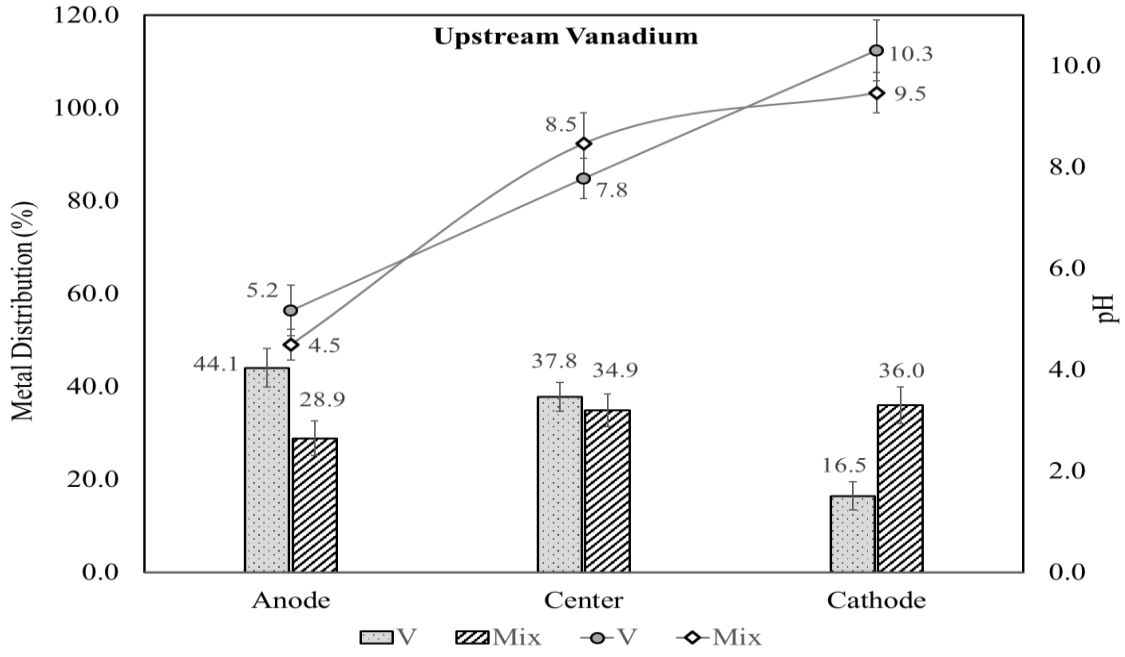


Figure 6.3 Vanadium distribution variation in upstream Vanadium Cell and Mix Cell

Vanadium mobility in the upstream Mixed Cell was affected the most by the presence of other metals (nickel and lead) (Fig. 6.3). It can be noticed in the upstream Mix Cell, that vanadium accumulation at the cathode increased by more than the double (from 16% to 36%) of that in the upstream Vanadium Cell. Such result would suggest that electromigration and electroosmotic flow of vanadium species were more effective in the presence of nickel and lead. Reddy and Chinthamreddy (2004) showed similar results for chromium in an EK cell that contained high amounts of nickel and cadmium, where removal efficiency of chromium was higher, with presence of nickel and cadmium in the mix.

As it has been explained earlier in this chapter, competition of metals for adsorption to solid particles would affect their mobility and distribution in the EK cell. Nickel accumulation (52%), was much higher than vanadium (29%) and lead (23%) at the anode area in the upstream Mix Cell. These numbers suggest that, exchangeable fractions of the sludge at the anode might have been occupied by nickel complexes, leading to a decrease in the adsorption capacity of other heavy metals, rendering vanadium species more available and consequently, transported through electroosmotic flow towards the cathode area.

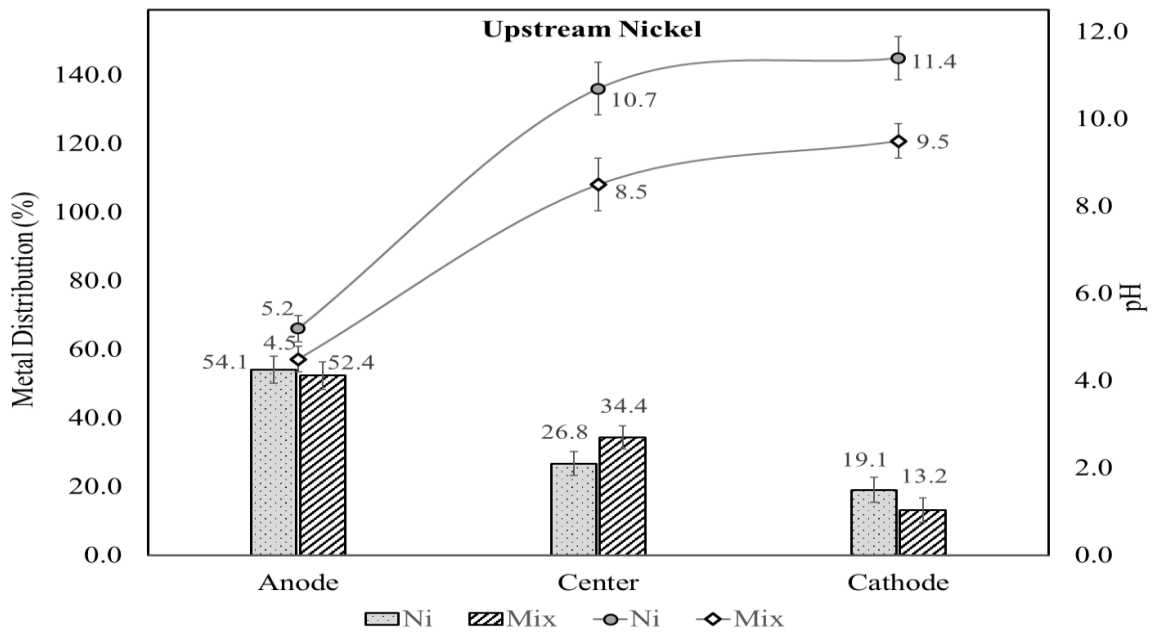


Figure 6.4 Nickel distribution variation in upstream Nickel Cell and Mix Cell

From literature review (Ch. 2.3), nickel has relatively high ability to adsorb hydrogen, produced in the hydrolysis of water at the anode area, forming hydroxide compounds that have high affinity to solid particles. Furthermore, nickel has a smaller hydrated radius than

vanadium and lead, which increases the possibility of being adsorbed into the solid particles (Brady, 1990).

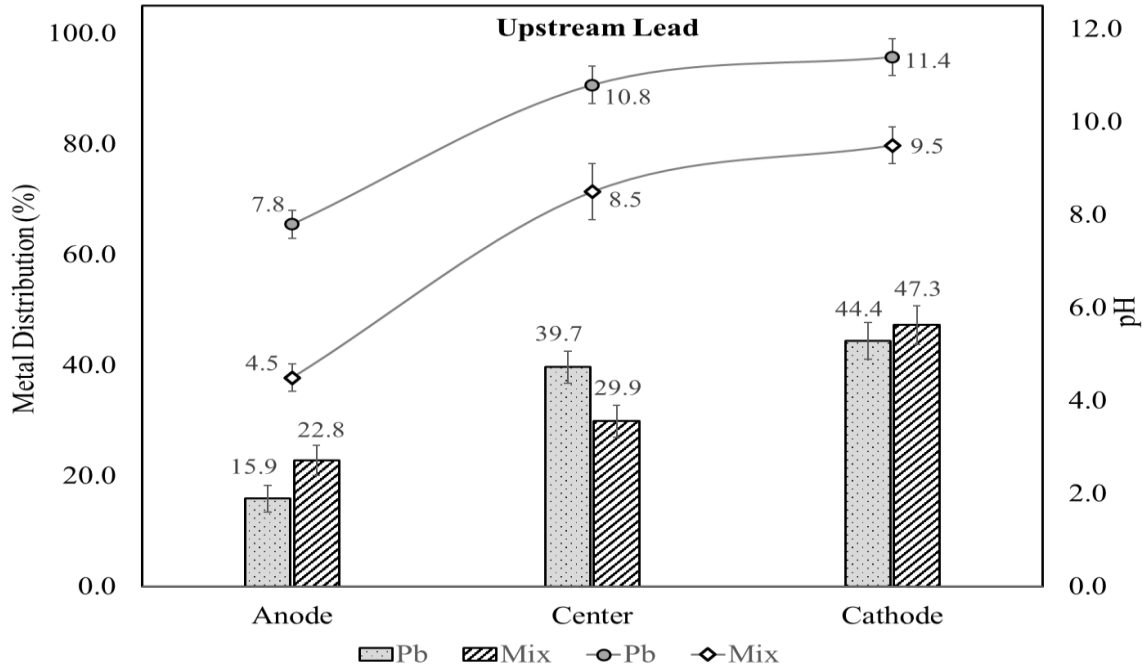


Figure 6.5 lead distribution variation in upstream Lead Cell and Mix Cell

Lead on the other hand, showed similar patterns in the upstream Mix Cell and sole Lead Cell (Fig 6.5), where its accumulations of 47% and 44% respectively, were mostly toward the cathode in both cases.

Vaibhav et al., (1999), demonstrated that the polar fraction of the precipitated asphaltene, would normally contain higher amounts of nickel, vanadium, and iron than any other metal. According to their study, polar fraction of asphaltene would rather precipitate in a low pH region, than alkaline front, which is the case in the anode area in all the upstream cells in this study. This might explain the high accumulation of nickel (Nickel Cell, Mix Cell), and vanadium (Vanadium Cell) at the anode areas compared to lead, where the NVOC (associated with asphaltene) was the highest in the cell.

From Figures 6.3, 6.4, and 6.5 it can be concluded that the presence of multiple metals in the matrix had the greatest effect on vanadium mobility, while nickel and lead were less affected by the presence of the other two metals in the cell. Furthermore, the recuperation of vanadium from oil waste through EK process can be even easier in natural conditions, where a number of metals coexist in upstream sludge.

6.4.2 Downstream oily sludge matrix

Table 6.8: Summary of the results: downstream Mix Cell after EK

Properties of Downstream Mix Cell after EK		Anode			Center			Cathode		
		Top	Mid	Bot	Top	Mid	Bot	Top	Mid	Bot
Metal distribution 100% →	V	7.4	6.8	8.71	14.79	12.84	16.36	12.22	9.44	11.32
	Ni	6.47	8.09	9.42	14.18	12.18	12.6	7.67	10.0	19.31
	Pb	4.8	4.9	8.25	16.88	8.82	16.28	5.85	10.87	22.53
pH		8.67	8.54	8.81	8.45	8.46	8.4	8.21	8.6	8.72
Solid content %		56.35	58.59	57.36	57.79	58.31	56.48	54.75	66.84	68.51
Moisture content %		29.57	28.36	30.43	24.45	28.57	32.08	27.64	17.99	17.46
Non-VOC % 100% ↓		14.09	13.05	12.21	17.76	13.11	11.44	17.61	15.17	14.03
FTIR	OH/SiO	1.4	0.9	0.4	0.5	0.4	0.4	0.4	0.4	0.4
	CH/SiO	0.3	1	2.3	1.1	2.4	1.9			

Downstream cell that contained oily sludge matrix enriched with mixed metals, showed similar characteristics of those in the downstream oily sludge matrices with sole metals. It seemed that the addition of diesel altered the polarity balance of a rather stable emulsion (before EK), subsequently, the efficiency of electrokinetic separation process of oily sludge components was also affected.

Beside visual observations (Ch. 5.1, Appendix B, Fig B.5), Table 6.8 demonstrates the minimal variation in some physical properties of the matrix after EK treatment. For example, pH values didn't change by more than 0.6 between the two electrodes (8.2-8.8). However, FTIR analysis confirmed a significant drop of the water content, through a low OH/SiO ratio in the cell. Accordingly, the metal distribution in the downstream cell did not vary significantly between the Mix Cell and cells that contained vanadium, nickel, and lead alone.

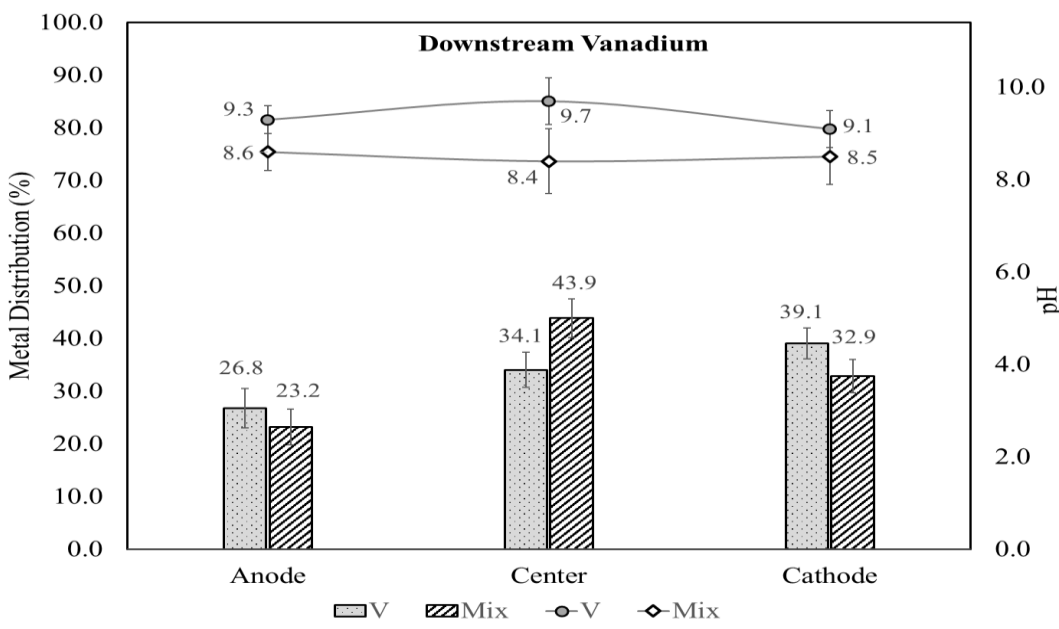


Figure 6.6 Vanadium distribution variation in the downstream Vanadium Cell and Mix Cell

Figures 6.6, 6.7, and 6.8 compare metal distribution in the downstream Mix Cell and Sole metal (Vanadium, Nickel, and Lead) Cells. For all three metals (vanadium, nickel and lead), the accumulation did not vary by much at the cathode area, which suggested that transport by electromigration and electroosmosis was not interrupted by the presence of other metals in the cell.

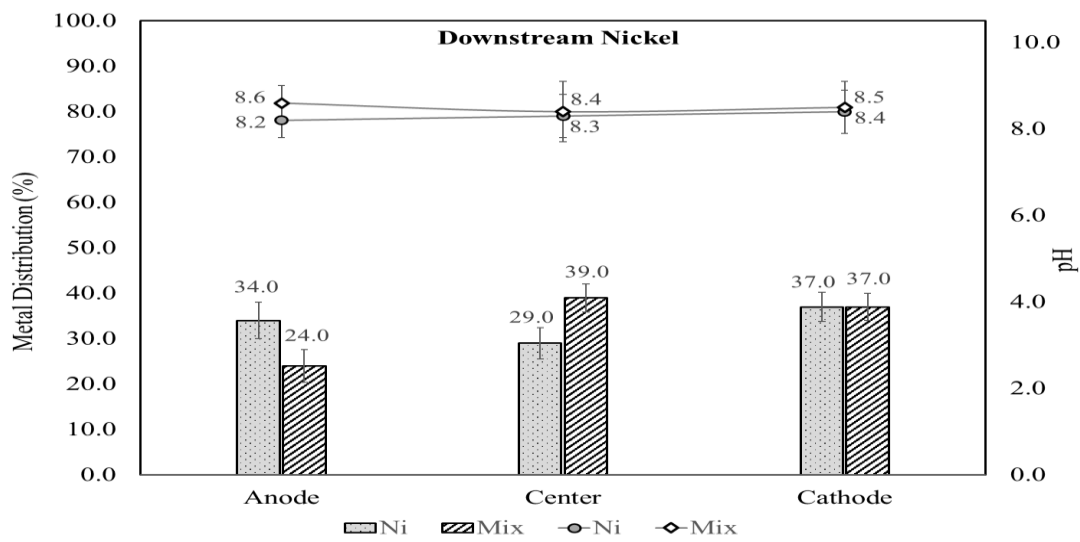


Figure 6.7 Nickel distribution variation in the downstream Nickel Cell and Mix Cell

On the other hand, nickel accumulation at the anode decreased from 34% in the Nickel Cell to 23% in the Mix Cell, which suggested a better movement of nickel towards the center and eventually to the cathode area (Fig. 6.7).

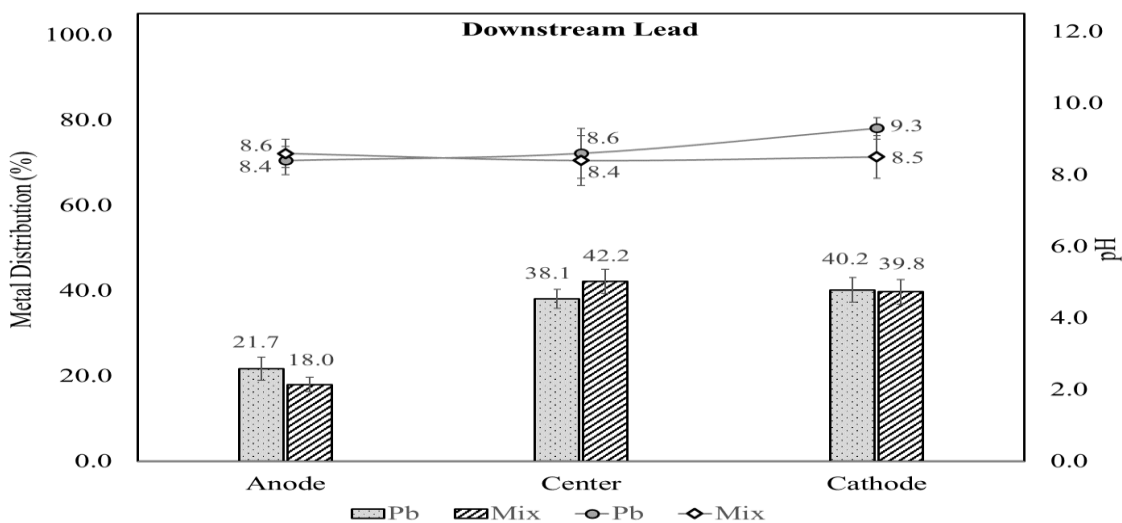


Figure 6.8 Lead distribution variation in the downstream Lead Cell and Mix Cell

Lead distribution variation (Fig 6.8) was similar to that of vanadium (Fig. 6.6) in the downstream oily sludge mix matrix. However accumulation of lead at the anode was

relatively lower of that of vanadium and nickel in both; Mix Cell and Vanadium/Nickel downstream Cells, which suggests a possibly better electroosmotic flow of lead species toward the cathode region.

Results showed that, vanadium EK transport is slow in downstream oily sludge conditions and probably additives have to be considered for vanadium recovery (e.g. Chelating agents or modifiers). The ion exchange process might be accelerated; however, the efficiency of the entire process (Downstream EK remediation) should be re-evaluated.

Chapter 7

Conclusions

7.1 Conclusion

This exploratory study has successfully laid the groundwork for a practical methodology that enables mobilizing and tracing the most dominant heavy metal in the petroleum industry (vanadium), and coupled major metals (nickel and lead) in an oily sludge matrix, making metal recovery more practically viable.

Electrokinetic (EK) phenomena were applied for the first time, for the sole purpose of mobilizing basic target metals in upstream and downstream oily sludge matrices. Furthermore, it demonstrated its efficacy in separating oily sludge into basic liquid and solid phases (especially in upstream cells) (Ch. 5.1).

Stable formulations of upstream and downstream oily sludge were successfully prepared in the lab using components such as water, crude oil, diesel, clay, sand, and heavy metals to mimic real sludge composites. Several scenarios (experimenting with components' ratios, mixing duration/intensity, physicochemical characterisation, and visual observations) were carried out before stable oily sludge emulsions were obtained (Ch. 4.1). In this research, standard composition of upstream (60% liquids, 36 % solids, and 4% non-volatile organic content (NVOC)) and downstream oily sludge (37% liquids, 54% solids, and 9%) were successfully formulated.

The separation of phases influenced the distribution of metals post EK treatment. For example, in the Vanadium Cell, vanadium accumulation (45% of total V) was higher at sections characterized with high solid content (up 71 % at anode), relatively high non-

volatile organic contents (22%), and low moisture content (6.77%) (Ch. 6.1). Nickel showed similar behavior in all cells, showing high affinity to the solid fraction in the Nickel and Mix Cells, consequently collecting up to 55% at the anode area alone (Ch. 6.2). Nickel also showed affinity to light oil fraction. Lead on the other hand, was mobilized towards the cathode areas, in all upstream and downstream cells, accumulating up to 43% of total lead (Ch. 6.3). The latter demonstrated that, lead species would respond to EK even in downstream cells, where separation of components was less significant.

Simultaneously, the presence of target metals influenced the separation process, while under EK phenomena. For example, upstream cells rich with vanadium as a sole metal or mixed with nickel and lead, demonstrated better separation of components. FTIR analysis confirmed these findings, such that; average OH/SiO ratio in the Vanadium Cell was around 8.1, in the cathode area. Compared to 6.5 and 5.5 in the Nickel and Lead Cells respectively. In addition, NVOC (associated with dense solid hydrocarbons) demonstrated higher accumulation (22%) in the anode sections of the Vanadium Cell, compared to a maximum of 13%, and 17% in the Nickel and Lead Cells respectively. Such results are attributed to some valuable properties of vanadium and vanadium species (e.g. high conductivity, behavior as nano-particles).

The presence of mixed metals in the oily sludge influenced the mobilization and distribution of vanadium in the upstream cells. Vanadium accumulation towards the cathode increased by more than two times (16% to 36%) in the presence of nickel and lead in the Mix Cell. Such original findings could be adapted to real life practice, where natural oily sludge contains a mixture of metal species, thus implying better mobilization of vanadium under EK technology.

A comparative study was conducted to optimize the extraction potential of the target metals, where supercritical fluid extraction (SFE) technology was used on samples underwent EK remediation. SFE in upstream Mix Cell demonstrated increase of vanadium extraction efficiency by 97%, comparing conventional method of acid digestion alone. Investigations also showed that SFE efficiency can be enhanced by implementing additives, e.g. Cyanex 301 and EDTA, which demonstrated increase of the extraction potential of vanadium in upstream and downstream oily sludge.

Effects of SFE on nickel and lead extraction potential were less significant (especially in the downstream cells). However, SFE combined with Cyanex 301 (SFE-Cyanex301) in the upstream Mix Cell enhanced the extractability of nickel and lead up to 42% and 32% respectively. These results demonstrated an innovative method for metal removal from complex oily matrices, by combining EK-SFE enhanced by Cyanex 301.

The effect of diesel present in downstream cells was taken into consideration in every step of the experiment. This allowed a comparison between O/W cells (upstream), and W/O cells (downstream). The presence of non-polar components in diesel reduced the effect of EK in achieving high separation of components. For instance, in the downstream Vanadium Cell the maximum deviation of solids quantities of that in the Original Cell, was by 7 % at the anode area. Consequently, the distribution of metals was also affected. However, downstream lead species seemed to travel towards the cathode, regardless of the phase distribution in sole and mixed metals enriched sludge (40%, and 39%, respectively).

This study provided an original procedure for tracing, mobilizing, and analysing vanadium, nickel and lead, in a complex petroleum oily sludge system, through the application of inexpensive, clean, and efficient electrokinetic procedure, supported by extensive

experimental procedures. It also delivered a comparative study for increasing the availability of metals for extraction through EK-SFE-Cyanex 301 and EK-SFE-EDTA techniques.

This research introduced a novel method for managing oily sludge waste, one that not only remediates petroleum wastes but also recycles them, exploiting avenues of possible financial benefit. For example, in this study, EK phenomena provided a potentially inexpensive, yet efficient, procedure for the separation of the main constituents of oily sludge (solid, liquid and hydrocarbons). Furthermore, it helped mobilize target metals (V, Ni, and Pb), and with the aid of analytical techniques (pH readings, electrical measurements, XRD, FTIR analysis, rheological properties, and AAS), helped create a distribution map for vanadium and coupled target metals (nickel and lead). Such mapping would increase the extraction potential of these valuable metals. Vanadium's status as a strategic metal in "green energy" increased its global value and made it highly in demand by utility and manufacturing plants. Vanadium flow battery is an example of high performance green energy innovation. These batteries has virtually unlimited storage capacity, making them of great value to the emerging renewable energy technology sector.

7.2 Contributions

Research work presented in this thesis:

- Proved the possibility of mobilizing metals (V, Ni, and Pb) in non-aqueous systems such as oily sludge using EK phenomena;
- Defined relationships between various oil sludge fractions (solids, moisture, light oil, asphaltenes) and mobility of a heavy metal (lead) and transition metals (vanadium,

nickel) under electrical field. Such information might be crucial for further improvement of metal extraction process.

- Evaluated the synergistic effects in an oily sludge matrix while vanadium is accompanied with other metals (e.g. nickel, lead), under EK conditions;
- Developed EK-SFE-additive (mobilization-extraction) methods for an effective removal of metals from non-aqueous systems;
- Demonstrated the potential high extraction efficiency of vanadium through SFE enhanced with Cyanex 301 or EDTA;
- Illustrated separation of phases of oily sludge containing metals using EK, and mapping target metals distribution in EK cell;
- Described the effect of increasing non-polar compounds (diesel) on EK phenomena separation of phases, and consequently metals distribution;
- Exposed the formation and transformation of vanadium species under EK phenomena at every segment of the upstream and downstream EK cells;
- Improved digestion method for metals extraction from oily sludge matrix, based on combining four strong acids, while continuous heating and shaking were applied.

7.3 Potential applications and benefits

1. Oily sludge revitalization :
 - a. The metal free light liquid hydrocarbon fraction of oily sludge can be efficiently used as high-quality fuel products.
 - b. Since large parts of the non-volatile hydrocarbons concentrated mostly close to the anode contains usually asphaltene, it can be used as a value-added road material.

c. The remaining fractions of the oily sludge can be safely and conventionally biodegraded, since it has an acceptable microorganisms conditions, low metals and volatile organic contents.

2. Metals as value added products:

Fractions of the sludge that contains high concentrations of metals would be subjected to metal extraction processes. These metals present a great economic values that should not be wasted with petroleum sludge. For example, the price of 1 g of vanadium salts in North America ranges between 25\$ to 60 \$. Thus, since the production of sludge can reach more than 230 MT in the USA alone, high concentrations of vanadium (up to 1500 ppm) in the sludge would provide an opportunity to create a considerable profit.

7.4 Future work

This work simultaneously deploys various methods, techniques, and analyses, providing foundation for several lines of research to be pursued. Some of the ideas in this exploratory study that can be inspected and possibly applied would include:

- Conduct tests to verify this study discoveries on a number of oily sludge samples, collected from different oil industry facilities;
- Optimize certain parameters used in EK remediation (e.g. higher/ lower electrical field, temperature effect, electrode materials);
- Optimize supercritical fluid extraction parameters, to improve extractability of nickel and lead. These parameters would include: temperature, pressure, extraction procedure (dynamic and/or static), chelating agents, and extraction periods;

- Introduce new EK cells design that contains oil recovery devices useful for scaling up the process;
- Assess the costs of the processes at pilot scale facilities.

References

- Abd El-Fatah, S., Goto, M., Kodama, A., & Hirose, T. (2004). Supercritical Fluid Extraction of Hazardous Metals from CCA Wood. *Journal of Supercritical Fluids*, 28(2), 21-27.
- Abrishamain, R., Kabrick, R., & Swett, G. (1992). Two Onsite Treatment Methods to Reduce Sludge Waste Quantities. *Oil and Gas Journal*, 90(44), 51-56.
- Acar, Y. B., Gale, R. J., Alshawabkeh, A. N., Marks, R. E., Puppala, S., & Bricka, M. (1995). Electrokinetic Remediation: Basics and Technology Status. *Journal of Hazardous Materials*, 40(2), 117-137.
- Agency for Toxic Substances and Disease Registry. (1992). Toxicological Profile for Vanadium. Atlanta, Georgia. <http://www.atsdr.cdc.gov/toxprofiles/tp58.pdf>
- Agency for Toxic Substances and Disease Registry. (2005). Toxicological Profile for Nickel. Atlanta, Georgia. Retrieved from <http://www.atsdr.cdc.gov/toxprofiles/tp15.pdf>
- Agency for Toxic Substances and Disease Registry. (2007). Toxicological Profile for Lead. Atlanta, Georgia. Retrieved from <http://www.atsdr.cdc.gov/toxprofiles/tp13.pdf>
- Agency for Toxic Substances and Disease Registry. (2012). Toxicological Profile for Vanadium. Atlanta, Georgia. From <http://www.atsdr.cdc.gov/toxprofiles/tp58.pdf>
- Ahmed, N. S., Nassar, A. M., Zaki, N. N., & Gharieb, H. K. (1999). Formation of Fluid Heavy Oil-In-Water Emulsions for Pipeline Transportation. *Fuel*, 78(5) 593-600.
- Al-Futaisi, A., Jamrah, A., Yagi, B., & Taha, R. (2007). Assessment of Alternative Management Techniques of Tank Bottom Petroleum Sludge in Oman. *Journal of Hazardous Materials*, 141(3), 557-564.
- Alloway B. J., & Ayre D. C. (1994). *Chemical Principle of Environmental Pollution* (pp. 37-50), London, UK: Blackie.
- Alonso, E., Cantero, F., García, J., & Cocero, M. (2002). Scale-Up for a Process of Supercritical Extraction with Adsorption of Solute onto Active Carbon. Application to soil Remediation. *Journal of Supercritical Fluids*, 24(2), 123-135.
- Amorim, F. A. C., Welz, B., Costa, A. C. S., Lepri, F. G., Goreti, M., & Ferrei, S. L. C. (2007). Determination of Vanadium in Petroleum and Petroleum Products using Atomic Spectrometric Techniques. *Talanta*, 72(2), 349-359.

- Amrate, S., & Akretche, D.E. (2005). Modeling EDTA Enhanced Electrokinetic Remediation of Lead Contaminated Soils. *Chemosphere*, 60(10), 1376-83.
- Atlas, R. (1984). *Petroleum Microbiology*. New York, NY: Macmillan Publishing Company.
- Ayres, D., Davis, A., & Gietka, P. (1994). Removing Heavy Metals from Wastewater. *Engineering Research Center Report*. University of Maryland.
- Badawieh, A. (2006). Heavy Metal Removal from Petroleum Oily Sludge Using Lemon Scented Geraniums (Master thesis). Concordia University, Montréal, QC.
- Badawieh, A., & Elektorowicz, M. (2006). Heavy Metal Removal from Petroleum Oily sludge Using Lemon-Scented Geraniums. *CSCE Conference*, May 26-28, Calgary, Canada.
- Badawieh A., & Elektorowicz M., (2006), Protection of the runoff quality from refinery disposal sites due to application of a phytoremediation system, *XIX National and VII International Scientific and Technical Conference, Water Supply and Water Quality*”, Zakopane, June,18-21, 2006, Poland
- Banerjee, S., & Law, S. (1998). Electroosmotically Enhanced Drying of Biomass. *IEEE Transactions on Industry Applications*, 34(5), 992-999.
- Baroch, E. F. (2006). Vanadium and Vanadium Alloys. In *Kirk-Othmer Encyclopedia of Chemical Technology* (pp. 1-18). New York, NY: John Wiley and Sons, Inc.
- Bockris, J. O'M. (1977). *Environmental Chemistry* (pp. 461-467). New York, NY: Plenum Press.
- Brady, N.C. (1990). *The nature and Properties of Soils* (10th ed.). New York, NY: Macmillan.
- Biswas, R., & Kramakar, A. (2013). Liquid-Liquid Extraction of V(IV) from Sulphate Medium by Cyanex 301 Dissolved in Kerosene. *International Journal of Nonferrous Metallurgy*, 2 (2013), 21-29
- Burken, J., Ross, C., Harrison, L., Marsh, A., Zetterstrom, L., & Gibbons, J. (2001). Benzene Toxicity and Removal in Laboratory, Phytoremediation Studies. *Practice Periodical of Hazardous, Toxic, and Radioactive Waste Management*, 5(Phytoremediation), 161-171.

- Cabrera-Guzman, D., Swartzbaugh, J. T., & Weisman, A. W. (1990). The Use of Electrokinetics in Hazardous Waste Site Remediation. *Journal of Air Waste Management Association*, 40(12), 1670-1676.
- Camobreco, V. J., Richards, B. K., Steenhuis, T. S., Peverly, J. H., & McBride, M. B. (1996). Movement of Heavy Metals through Undisturbed and Homogenized Soil Columns. *Soil Science* 161, 740-750.
- Canadian Environmental Protection Act. (1999). Published by the Minister of Justice. Retrieved from: <http://laws-lois.justice.gc.ca>.
- Casagrande, L. (1948). Electro-Osmosis in Soils. *Geotechnique*, 1(3), 159-177.
- Chang, C., Nguyen, Q. D., & Rønningsen, H. P. (1999). Isothermal Start-Up of Pipeline Transporting Waxy Crude Oil. *Journal of Non-Newtonian Fluid Mechanics*, 87(2-3), 127-154.
- Chew, C., Zhang, T. (1999). *N-situ* remediation of nitrate-contaminated ground water by electrokinetics/iron wall processes. *Water Science and Technology*, 38(7) 135-142
- Chifrina, R., & Elektorowicz, M. (1998). Electrokinetic Removal of HOC from sludge and sediments. In *Proceedings of the 5th CSCE Environmental Speciality Conference, Halifax, N.S., 10-13 June 1998*. Vol. 2, 183-192.
- Choudhury, A. (1998). Removal of Nickel and Lead from Natural Clay Soil through the Introduction of EDTA and Coupling Ion Exchange Processes with Electrokinetic Methodology (Master Thesis). Concordia University, Montréal, QC.
- Choudhury, A., & Elektorowicz, M. (1997). Enhanced Electrokinetic Methods for Lead and Nickel Removal from Contaminated Soils. 32nd Central Symposium on Water pollution research, February 4, Burlington, ON
- Chu, C. P., Lee, D. J., & Chang, C. Y. (2005). Energy Demand in Sludge Dewatering. *Water Research*, 39(9), 1858-1868.
- Corr, S. A., Grossman, M., Furman, J. D., Melot, B. C., Cheetham, A. K., Heier, K. R., Seshadri, R. (2008). Controlled Reduction of Vanadium Oxide Nanoscrolls: Crystal Structure, Morphology, and Electrical Properties. *Chemistry of Materials*, 20(20), 6396-6404.
- Cunningham, S., Berti, W., Huang, J. (1995). Manipulating Metabolism: Phytoremediation of Contaminated Soils. *Trends. Biotechnology*, 13(9), 393-397.

Dando, D. (2003). A Guide for Reduction and Disposal of Waste from Oil Refineries and Marketing Installations, *Conservation of Natural Clean Air and Water in Europe (Concawe)*, report no. 6/03.

Davis, J. (1967). *Petroleum Microbiology*. Ann Arbor, MI: Elsevier Publishing Company.

Eckenfelder, W.W. & Santhanam, C. J. (1981). *Activated Sludge Treatment of Industrial Wastewater*. New York, NY: Marcel Dekker.

Elektorowicz, M. (2009). Electrokinetic Remediation of Mixed Metals and Organic Contaminants. In Krishna, R. R., Cameselle, C. (2009), *Electrochemical Remediation Technologies for Polluted Soils, Sediments and Groundwater* (pp. 315-331). Hoboken, NJ: John Wiley and Sons, Inc.

Elektorowicz M. & Badawieh A., 2005, Metal removal from oily sludge using Geranium, 40th *Central Canadian Symposium on Water Pollution Research*, Burlington, ON.

Elektorowicz, M., & Boeva V. 1996, Electrokinetic Supply of Nutrients in soil Bioremediation, *Environmental Technology*, 17:1339-1349.

Elektorowicz, M., & Habibi, S. (2005). Sustainable Waste Management: Recovery of Fuels from Petroleum Sludge. *Canadian Journal of Civil Engineering*, 32(1), 164-169.

Elektorowicz, M., & Hakimipour, M. (2002). Electrical Field Applied to the Simultaneous Removal of Organic and Inorganic Contaminants from Clayey Soil. 18th *Eastern Canadian Research Symposium on Water Quality*, October 18, Montreal, Quebec, Canada: CAWQ.

Elektorowicz, M., & Hakimpour, M. (2001). Hybrid Electrokinetic Method Applied to Mix Contamination Clayey Soil, EREM, *3rd Symposium and status report on electrokinetic remediation*, Karlsruhe, Germany.

Elektorowicz, M., & Ju, L. (1997). CSCE/ASCE, *Specialty Environmental Conference*, July 23-25, Edmonton, pp. 531-572.

Elektorowicz, M., El-Sadi, H., & Ayadat, T. (2008). Modeling of Supercritical Fluid Extraction of Phenanthrene from Clayey Soil. *Journal of Separation Science*, 31(8), 1381-1386.

Elektorowicz, M., El-Sadi, H., Lin, J., & Ayadat, T. (2007). Effect of SFE Parameters and Clay Properties on the Efficiency of PAHs Extraction. *Journal of Colloid and Interface Science*, 309(2), 445-452.

- Elektorowicz, M., Emon, M. H., & Ayadat, T. (2008b). Stabilization of Metals and PAHs in Mix Contaminated Soil. Proceedings, CSCE Conference, June 10-13, Québec, QC, Canada.
- Elektorowicz, M., Habibi, S., & Chifrina, R. (2006). Effect of Electrical Potential on the Electro-Demulsification of Oily Sludge. *Journal of Colloid and Interface Science*, 295(2), 535-541.
- Elektorowicz, M., Muslat, Z. (2008). Metal Removal from Petroleum Sludge using Ion Exchange Textile. *Environmental Technology*, 29(4), 393-399.
- El-Sadi, H. (1999). *Efficiency of PAHs Removal from Clayey Soil Using Supercritical Fluid Extraction* (Master thesis). Concordia University, Montréal, QC.
- El-Sadi, H., Elektorowicz, M., & Badawieh, A. (2015). Comparison between extraction and acid digestion techniques to remove heavy metals from soil. *American Journal of Engineering and Technology Research*. 2162-3384.
- Environmental Protection Agency. (1994). *Method 3051A, Microwave Assisted Acid Digestion of Sediments, Sludge, Soils, and Oils*. EPA OSW846 Analytical Methods, U.S.A.
- Environmental Protection Agency. (1997). *Innovative Uses of Compost Bioremediation and Pollution Prevention*. Solid Waste and Emergency Response, U.S.A.
- Environmental Protection Agency. (2000). *Final Standards Promulgated for Petroleum Refining Waste*. Office of solid wastes, EPA 530-F-98-014, U.S.A.
- Environmental Protection Agency. (2000). *Associated Waste Report: Completion and Workover Wastes*. Office of Solid Wastes, U.S.A.
- E-Oil. (2002). Oil Sludge Treatment in Oil Tanks, Tank Farms, & Pipe Lines. Osten Enzyme India (P) LTD. Retrieved from <http://www.e-oil.com/Download/Sludge.pdf>.
- Esmaeily, A. (2002). *Dewatering, Metal Removal, Pathogen Elimination, and Organic Matter Reduction in Biosolids Using Electrokinetic Phenomena* (Master thesis). Concordia University, Montreal, QC.
- Gedah, M. (1987). *Environmental Status Report for the Canadian Petroleum Refining Industry 1983-1984*. Environment Canada: Beauregard Press Limited.

- Ghoreishi, S., Ansaria, K., & Ghaziaskarb, H. (2012). Supercritical Extraction of Toxic Heavy Metals from Aqueous Waste via Cyanex 301 as Chelating Agent. *The Journal of Supercritical Fluids*, 72, 288-297.
- Giannis, A., & Gidakos, E. (2005). Washing Enhanced Electrokinetic Remediation for Removal Cadmium from Real Contaminated Soil. *Journal of Hazardous Materials*, 123(1-3), 165-175.
- Giles, W., Kriel, K., & Stewart, J. (2001). Characterization and Bioremediation of a Weathered Oil Sludge. *Environmental Geosciences*, 8(2), 110-122.
- Gillies, R. G., Sun R., & Shook C. A. (2000). Laboratory Investigation of Inversion of Heavy Oil Emulsions, *Canadian Journal of Chemical Engineering*, 78(4), 757-763.
- Guolin, J., Ming, L., & Shaopeng, Q. (2009). The Use of Non-Ionic and Anionic Surfactant in the Treatment of Oily Sludge. In *ICEET '09. International Conference on International Conference on Energy and Environment Technology* (pp.660-663). Guilin, Guangxi: IEEE.
- Habel, A. (2010). *Electrokinetic Management of Biosolids for the Inactivation of Helminth Ova* (Master thesis). Concordia University, Montréal, QC.
- Habibi, S. (2004). *A New Electrokinetic Technology for Revitalization of Oily Sludge* (Doctoral thesis). Concordia University, Montréal, QC.
- Habibi, S., & Elektorowicz, M. (2004). A New Environmental-Friendly Technology for the Recovery of Fuel from Oily Sludge. *1st Water and Environmental Specialty Conference of the Canadian Society for Civil Engineering*. Saskatoon, SK.
- Hansen, S. H., Larsen, E. H., Pritzl, G., & Cornett, C. (1992). Separation of Seven Arsenic Compounds by High Performance Liquid Chromatography with Online Detection by Hydrogen Argon and Atomic Absorption Spectrometry and Induced Coupled Plasma Mass Spectrometry. *Journal Analytical Atomic Spectrometry*, 7(4), 629-634.
- Harter, D. R. (1983). Effect of Soil pH on Adsorption of Lead, Copper, Zinc and Nickel. *Soil Science Society American Journal*, 47(1), 47-52.
- Hasan, S. (2007). *Rheology of Heavy Crude Oil and Viscosity Reduction for Pipeline Transportation* (Master thesis). Concordia University, Montréal, QC.

- Hatem, G. (1999). *Design of the Surfactant Enhanced Electrokinetic System for Hydrocarbons Removal from Clayey Soils in Pilot Scale Conditions* (Master thesis). Concordia University, Montréal, QC.
- Hejazi, R., Husain, T., & Khan, F. (2003). Landfarming Operation of Oily Sludge in Arid Region—Human Health Risk Assessment. *Journal of Hazardous Materials*, 99(3), 287-302.
- Hertel, R., Maass, T., & Muller, V. (1991). Environmental Health Criteria 108: Nickel. International Program on Chemical Safety. Retrieved from: <http://www.inchem.org/documents/ehc/ehc/ehc108.htm>
- Hwa, T., & Jeyaseelan, S. (1997). Conditioning of Oily Sludge with Municipal Solid Waste Incinerator Fly Ash. *Water Science and Technology*, 35(8), 231-238.
- Ibeid, I., Elektorowicz, M., Oleszkiewicz, J, A. (2015). Electro-conditioning of activated sludge in a membrane electro-bioreactor for improved dewatering and reduced membrane fouling. *Journal of Membrane Science*, 494, 136-142
- International Program on Chemical Safety. (1988). *Environmental Health Criteria 81: Vanadium*. Geneva.
- Interstate Technology and Regulatory Cooperation. (1999). *Phytoremediation Decision Tree*. Washington D.C., U.S.A.
- Iwao, S., Adb El-Fatah, S., Furukawa, K., Seki, T., Sasaki, M., & Goto, M. (2007). Recovery of Palladium from Spent Catalyst with Supercritical CO₂ and Chelating Agent. *The Journal of Supercritical Fluids*, 42(2), 200-204.
- Iwegbue, C. M. A., William, E. S., & Nwajei, G. E. (2008). Characteristic Levels of Total Petroleum Hydrocarbon in Soil Profiles of Automobile Mechanic Waste Dumps. *International Journal of Soil Science*, 3, 48-51.
- Japan External Trade Organization. (2010). *The Study on Oily Sludge Treatment Project for Saudi Aramco in Saudi Arabia*. Toyo Engineering Corporation Mitsui & Co., Ltd.
- Jean, D., & Lee, D. (1999). Expression Deliquoring of Oily Sludge from a Petroleum Refinery Plant. *Waste Management*, 19(5), 349-354.
- Jensen, V. (1997). Effects of Lead on Biodegradation of Hydrocarbons in Soil. *Oikos*, 28(2/3), 220-224.

- Kaoser, S., Barrington, S., Elektorowicz, M., & Wang, L. (2004a). Copper Adsorption with Pb and Cd in Sand-Bentonite Liners under Various pHs. Part I. Effect on Total Adsorption. *Journal of Environmental Science and Health*, 39(09), 2241-2256.
- Kaoser, S., Barrington, S., Elektorowicz, M., & Wang, L. (2004b). Copper Adsorption with Pb and Cd in Sand-Bentonite Liners under Various pHs. Part II. Effect on Adsorption Sites. *Journal of Environmental Science and Health*, 39(09), 2257-2274.
- Karamalidis, A., & Voudrias, A. (2008). Leaching Behavior of Metals Released from Cement-Stabilized/Solidified Refinery Oily Sludge by Means of Sequential Toxicity Characteristic Leaching Procedure. *Journal of environmental engineering*, 134(6), 493-504.
- Karbaschi, M., Orr, B., Bastani, D., Javadi, A., Lotfia, M., & Miller, R. (2014). A novel technique to semi-quantitatively study the stability of emulsions and the kinetics of the coalescence under different dynamic conditions. *Colloids and Surfaces A: Physicochemical and Engineering Aspects*, 460, 327-332.
- Kaschl, A., Romheld, V., & Chen, Y. (2002). The Influence of Soluble Organic Matter from Municipal Solid Waste Compost on Trace Metal Leaching in Calcareous Solids. *Science of The Total Environment*, 29(1-3), 45-57.
- Kim, K. W., Lee, K. Y., & Kim, S.O. (2009). Elektrokinetic Remediation of Mixed Metals Contaminants. In Krishna, R. R., Cameselle, C. (2009), *Electrochemical Remediation Technologies for Polluted Soils, Sediments and Groundwater* (pp. 285-313). Hoboken, NJ: John Wiley and Sons, Inc.
- Korda, A., Santas, P., Tenente, A., & Santas, R. (1997). Petroleum Hydrocarbon Bioremediation: Sampling and Analytical Techniques, In situ Treatments and Commercial Microorganisms Currently Used. *Applied Microbial Biotechnology*, 48, 677-686.
- Kriipsalu, M., Marques, M., Nammari, D. R., & Hogland, W. (2007). Bio-treatment of Oily Sludge: The Contribution of Amendment Material to the Content of Target Contaminants, and the Biodegradation Dynamics. *Journal of Hazardous Materials*, 148(3), 616-622.
- Krukonis, V., Brunner, G., & Perrut, M. (1994). *Proceedings from Third International Symposium on Supercritical Fluids, Strasbourg, France*. Volume 1(1), 1-23.
- Kumar, P., Dushenkov, V., Motto, H., & Raskin, I. (1995). Phytoextraction: The Use of Plants to Remove Heavy Metals from Soils. *Environmental Science and Technology*, 29(5), 1232-1238.

- LaGrega, M. D., Buckingham, P., & Evans, J. C. (2001). *Hazardous Waste Management* (2nd ed.). New York, NY: McGraw-Hill, Inc.
- Lasat, M. (2002). Phytoextraction of Toxic Metals: A Review of Biological Mechanisms. *Journal of Environmental Quality*, 31, 109-120.
- Lewan, M. D., Maynard, J. (1981). Factors controlling enrichment of vanadium and nickel in the bitumen of organic sedimentary rocks. *Geochimica et Cosmochimica Acta* , 46, 2547-2560.
- Li, Z., Yuan, S., Wan, J., Long, H., & Tong, M. (2011). A Combination of Electrokinetics and Pd/Fe PRB for the Remediation of Pentachlorophenol-Contaminated Soil. *Journal of Contaminant Hydrology*, 124 (1-4), 99-107.
- Lide, D. R. (2008). *CRC Handbook of Chemistry and Physics* (88th ed.). Boca Raton, FL: Taylor and Francis Group, LCC.
- Lin, Y., Liu, C., Hong, W., Yak, H. K., & Wai, C. M. (2003). Supercritical Fluid Extraction of Toxic Heavy Metals and Uranium from Acidic Solutions with Sulfur-Containing Organophosphorus Reagents. *Industrial & Engineering Chemistry Research*, 42(7), 1400-1405.
- Mackay, D. (1987). Formation and stability of water in oil emulsions, *Environment Canada Manuscript Report EE-93*, Ottawa, Ontario, 97-99.
- Maini, G., Sharman, A. K., Sunderland, G., Knowls, C. J., & Jackman S. (2000). An Integrated Method of Incorporating Sulfur-Oxidizing Bacteria and Electrokinetics to Enhance Removal of Copper from Contaminated Soil. *Environment Science and Technology*, 34(6), 1081-1087.
- Matso, K. (1995). Mother Nature's Pump and Treat. *Civil Engineering*, 65(10), 46-49.
- Matsui, H., Fukumoto, K., Smith, D. L., Chung, Hee M., Witzenburg, W., Votinov, S. N. (1996). Status of vanadium alloys for fusion reactors. *Journal of Nuclear Materials*. 233–237 (1): 92–99
- Merian, E. (1991). *Metals and Their Compounds in the Environment: Occurrence, Analysis, and Biological Relevance*. Weinheim Publishing Company.
- Mishra A., Khan, R., & Pandey, R. (2009). Kinetic Studies on Effects of EDTA and Surfactants on Reduction of Vanadium (V) to Vanadium (IV) in Sulphuric Acid Medium. *Indian Journal of Chemistry*, 48A (2009) 1228-1234.

- Mishra, S., Jyut, J., Kuhad, R., & Lal, B. (2001). Evaluation of Inoculum Addition to Stimulate In Situ Bioremediation of Oily-Sludge-Contaminated Soil. *Applied and Environmental Microbiology*, 67(4), 1675-1681.
- Mitchell, J. K., (1993). *Fundamentals of Soil Behavior* (2nd ed.). New York, NY: John Wiley and Sons, Inc.
- Morrison, I. D., & Ross, S. (2002). *Colloidal Dispersions: Suspensions, Emulsions, and Foams*. New York, NY: Wiley-Interscience.
- Moskalyk, R. R., Alfantazi, A. M. (2003). Processing of vanadium: a review. *Minerals Engineering* 16 (9), 793.
- Mukhopadhyay, M. (2000). *Natural Extracts Using Supercritical Carbon Dioxide*. New York, NY: CRC Press.
- Muslat, Z. (2005). *Heavy Metals Removal from Oil Sludge using Ion Exchange Textiles* (Master thesis). Concordia University, Montréal, QC.
- Naeeni, M. H., Yamini, Y., Rezaee, M. (2011). Combination of Supercritical Fluid Extraction with Dispersive Liquid-Liquid Microextraction for Extraction of Organophosphorus Pesticides from Soil and Marine Sediment Samples. *Journal of Supercritical Fluids*, 57(3), 219-226.
- Nalwaya, V., Tantayakom, V., Piumsomboon, P., & Fogler, S. (1999). Studies on Asphaltenes through Analysis of Polar Fractions. *Industrial & Engineering Chemistry Research*, 38(3), 964-972.
- Newhouse, W. H. (1934). The Source of Vanadium, Molybdenum, Tungsten, and Chromium in Oxidized Lead Deposits. *American Mineralogist*, 10(5), 209.
- Operations Good Practice Series. (2010). Petroleum Refining Water/Wastewater Use and Management. *The Global Oil and Gas Industry Association for Environmental and Social Issues*. Retrieved from www.ipieca.org.
- Orr, D., & Maxwell, D. (2000). *A Comparison of Gasification and Incineration of Hazardous Wastes*. Texas, U.S.A: Radian International LLC.
- Pamukcu, S., & Wittle, J. K. (1992). Electrokinetic Removal of Selected Heavy Metals from Soil. *Environmental Progress*, 11(3), 241-250.

- Pamukcu, S., Filipova, I., & Wittle J. K. (1995). The Role of Electroosmosis in Transporting PAH Compounds in Contaminated Soils. *Electrochemical Society Proceeding*, 12, 252-263.
- Patterson, C. (2005). Supercritical Fluid Extraction: An Upcoming 'Green' Technology. *Technology Watch*, 2(1).
- Piondexter, M., & Lindemuth, P. (2004). Applied Statistics: Crude Oil Emulsions and Demulsifiers. *Journal of Dispersion Science and Technology*, 25(3), 311-320.
- Pourbaix, M. (1974). Atlas of Electrochemical Equilibria in Aqueous Solutions (2nd ed.). National Association of Corrosion Engineers.
- Prasad, M., & Freitas, H. (2003). Metal Hyperaccumulation in Plants - Biodiversity Prospecting for Phytoremediation Technology. *Electronic Journal of Biotechnology*, 6(30), 285-321.
- Propst, T., Lochmiller, R., Quails, Jr. C., McBee, K. (1999). In Situ (MESOCOSM) Assessment of Immunotoxicity Risks to Small Mammals Inhabiting Petrochemical Waste Sites. *Chemosphere*, 38(5), 1049-1067.
- Quebec Environmental Quality Act EQA, (2010). Regulation Respecting the Burial of Contaminated Soils (R.R.Q., c. Q-2, r.18).
- Ramsey, E. D. (2008). Determination of Oil-In-Water Using Automated Direct Aqueous Supercritical Fluid Extraction Interfaced to Infrared Spectroscopy. *Journal of Supercritical Fluids* 44(2), 201–210.
- Reddy, K. R., & Cameselle, C. (2009). Electrochemical Remediation Technologies for Polluted Soil Sediments and Ground Water (pp. 3-28). Hoboken, NJ: John Wiley and Sons, Inc.
- Reddy, K. R., & Chinthamreddy, S. (2004). Enhanced Electrokinetic Remediation of Heavy Metals in Glacial Till Soils Using Different Electrolyte Solutions. *Journal of Environmental Engineering*, 130(4), 442-454.
- Reddy, K. R., & Saichek, R. E. (2003). Effect of Soil Type on Electrokinetic Removal of Phenanthrene. *Journal of Environmental Engineering*, 129(4), 336-346.
- Reddy, K. R., & Saichek, R. E. (2004). Enhanced Electrokinetic Removal of Phenanthrene from Clay Soil by Periodic Electric Potential Application. *Journal of Environmental Science and Health, Part A—Toxic/Hazardous Substances & Environmental Engineering*, A39, 1189-1212.

- Reddy, K. R., Donahue, M., Saichek, R. E., & Sasaoka, R. (1999). Preliminary Assessment of Electrokinetic Remediation of Soil and Sludge Contaminated with Mixed Waste. *Journal of the Air and Waste Management Association*, 49(7), 823-830.
- Saefong, M. (2015). Saudi Arabia refuses to bow to pressure to cut oil production. Marketwatch. Published: Sept 1, 2015 <http://www.marketwatch.com/story/saudi-arabia-refuses-to-bow-to-pressure-to-cut-oil-production>.
- Said, M., Elektorowicz, M., & Ahmad, D. (2004). Bio-Neutralization of Petroleum Oily Sludge by Fungal-Bacterial Co-Culture. *1st Water and Environment Specialty Conference of the Canadian Society for Civil Engineering*. Saskatchewan, Canada.
- Sanchez, L. E., & Zakin, J.L. (1994). Transport of Viscous Crudes AS Concentrated Oil-in-Water Emulsions. *Industrial and Engineering Chemistry Research*, 33(12), 3256-3261.
- Schnoor, J. (1997). Technology Evaluation Report: Phytoremediation. *Ground-Water Remediation Technologies Analysis Center (GWRTAC) (E) Series*.
- Sengupta, P., Saikia, N., & Borthakur, P. (2002). Bricks from Petroleum Effluent Treatment Plant Sludge: Properties and Environmental Characteristics. *Journal of Environmental Engineering*, 128(11), 1090-1094.
- Serpaud, B., Al-shukry, R., Casteignau, M., & Matejka, G. (1994). Heavy Metals Adsorption (Cu, Zn, Cd and Pb) by Superficial Sediments of Stream, pH, Temperature and Soil Composition, *Revue des Sciences de l'Eau*, 7, 343-365.
- Shah, A. (2004). California Petroleum Refinery Hazardous Waste Source Reduction 1998 Assessment Report, California Environmental Protection Agency, U.S.A.
- Shleck, D. (1990). Treatment Technologies for Refinery Wastes and Waste Waters. *National Petroleum Association (NPRA)*, annual meeting, U.S.A.
- Sihvonen, M., Jarvenpaa, E., Hietaniemi, V., & Huopalahti, R. (1999). Advances in Supercritical Carbon Dioxide Technologies. *Trends in Food Science and Technology*, 10(6-7), 217-222.
- Smart, N. G., Carleson, T. E., Elshani, S., Wang, S., & Wai, C. M. (1997). Extraction of Toxic Heavy Metals Using Supercritical Fluid Carbon Dioxide Containing Organophorous Reagents. *Industrial & Engineering Chemistry Research*, 36(5), 1819-1826.
- Soriano, A., & Pereira, N. (2002). Oily Sludge Biotreatment. The Integrated Petroleum Environmental Consortium (IPEC) Meeting.

- State Water Laboratory of Victoria. (1993). *Victorian water quality monitoring network* (Report No. 110). Victoria, Australia: Hunter, K. M.
- Szente, R., Souza, L., & Pasquini, H. (2003). Treating Petroleum Contaminated Soil and Sludges Using Plasma. *TSL Environmental Corporation, Brazil*.
- Tai, C. Y., You, G. S., & Chen, S. L. (2000). Kinetics Study on Supercritical Fluid Extraction of Zinc (II) Ion from Aqueous Solutions. *Journal of Supercritical Fluids*, 18, 201-212.
- Tessier, A., Campbell, P., & Bisson, M. (1979). Sequential Extraction Procedure for the Speciation of Particulate Trace Metals. *Analytical Chemistry*, 51(7), 844-850.
- Thompson, W. T., Kaye, M. H., Bale, C. W., & Pelton, A. D. (2011). Pourbaix Diagrams for Multielement Systems. In *Uhlig's Corrosion Handbook* (2nd ed.). Hoboken, NJ: John Wiley & Sons, Inc.
- Unido (1993). Incineration Plant for Domestic Wastes, United Nations Industrial Development Organization, File: Z 25.
- US Reporter. (2010). Oil-sludge-processing industry overview. http://russianamericanbusiness.org/web_CURRENT/articles/654/1/Oil-sludge-processing-industry-overview. Published 10/19/2010.
- Vervaeke, P., Luysaert, S., Mertans, J., Meers, E., Tack, F., & Lust, N. (2003). Phytoremediation Prospects of Willow Stands on Contaminated Sediment: a Field Trial. *Environmental Pollution*, 126(2), 276-282.
- Virkutyte, J., Sillanpaa, M., & Latostenmaa, P. (2002). Electrokinetic Soil Remediation-Critical Overview. *Science of the Total Environment*, 289(1-3), 97-121.
- Wang, W., Yin, Z., Wang, Z., Li, X., Guo, H., Wang, D. (2015). Enhanced high voltage electrochemical performance of $\text{LiNi}_{1/3}\text{Co}_{1/3}\text{Mn}_{1/3}\text{O}_2$ cathode material by coating with Li_3VO_4 *Journal of Alloys and Compounds*, 646(2015), 454-460.
- Wang, J. Y., Zhang, D. S., Stabnikova, O., & Tay, J. H. (2005). Evaluation of Electrokinetic Removal of Heavy Metals from Sewage Sludge. *Journal of Hazardous Materials*, 124(1-3), 139-146.
- Wehrli, B., & Stumm, W. (1989). Vanadyl in Natural Waters: Adsorption and Hydrolysis Promote Oxygenation. *Geochemica et Cosmochimica Acta*, 53(1), 69-77.

- Yan, N., Gray, M. R., & Masliyah, J. H. (2001). On Water-In-Oil Emulsions Stabilized by Fine Solids. In *Colloids and Surfaces A: Physicochemical and Engineering Aspects* (Vol. 193, No. 1, pp. 97-107). Amsterdam: Elsevier.
- Yazdi, A., Beckman, E. (1997). Design of Highly CO₂ –Soluble Chelating Agent. Effect of Chelate Structure and Process Parameters on Extraction Efficiency. *Industrial & Engineering Chemistry Research*, 36(6), 2368-2374.
- Yong, R. N., Mohamed, A. M. O., & Warkentin, B. P. (1992). *Principles of Contaminant Transport in Soils*. New York, NY: Elsevier.
- Young, R. C., & Smith, M. E. (1953). Vanadium (II) Chloride, *Inorganic Syntheses*, 4, 126-127.
- Yuan, C., & Weng, C. (2003). Sludge Dewatering by Electrokinetic Technique: Effect of Processing Time and Potential Gradient. *Advances in Environmental Research*, 7, 727-732.
- Zhang, J., Xu Y., Li, W., Zhou J, Zhao, J., Qian, G. (2012). Enhanced remediation of Cr(VI)-contaminated soil by incorporating a calcined-hydrotalcite-based permeable reactive barrier with electrokinetics. *Journal of Hazardous Materials*, 239-240 P 128-134.

Appendices

Appendix A: FTIR spectra for all upstream/downstream cells

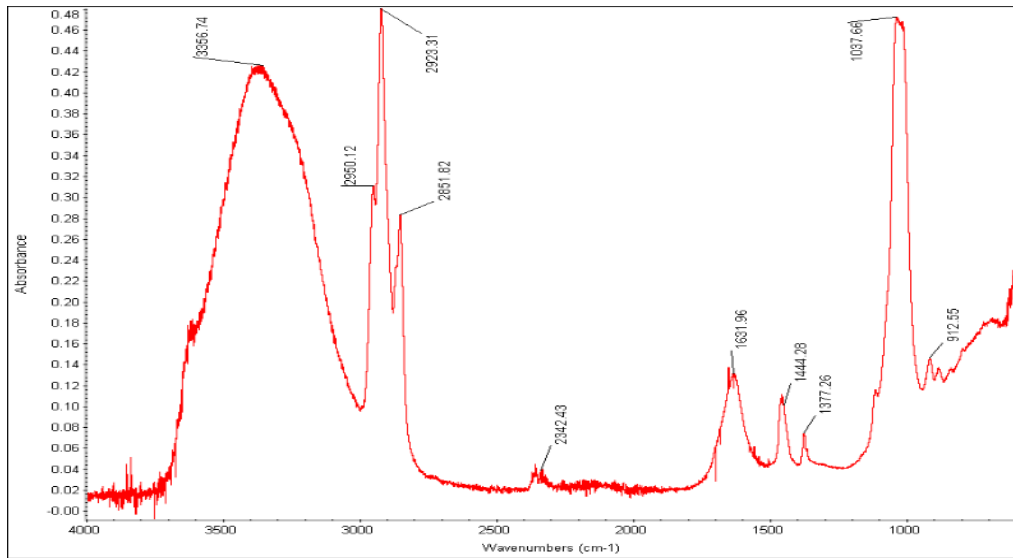


Figure A.1 Top anode upstream Vanadium Cell

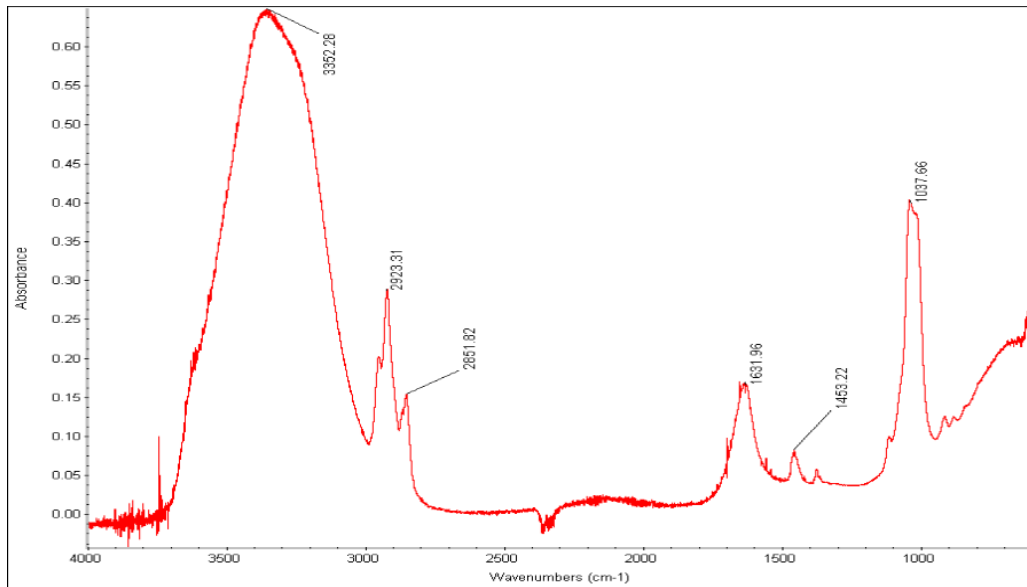


Figure A.2 Bottom anode upstream Vanadium Cell

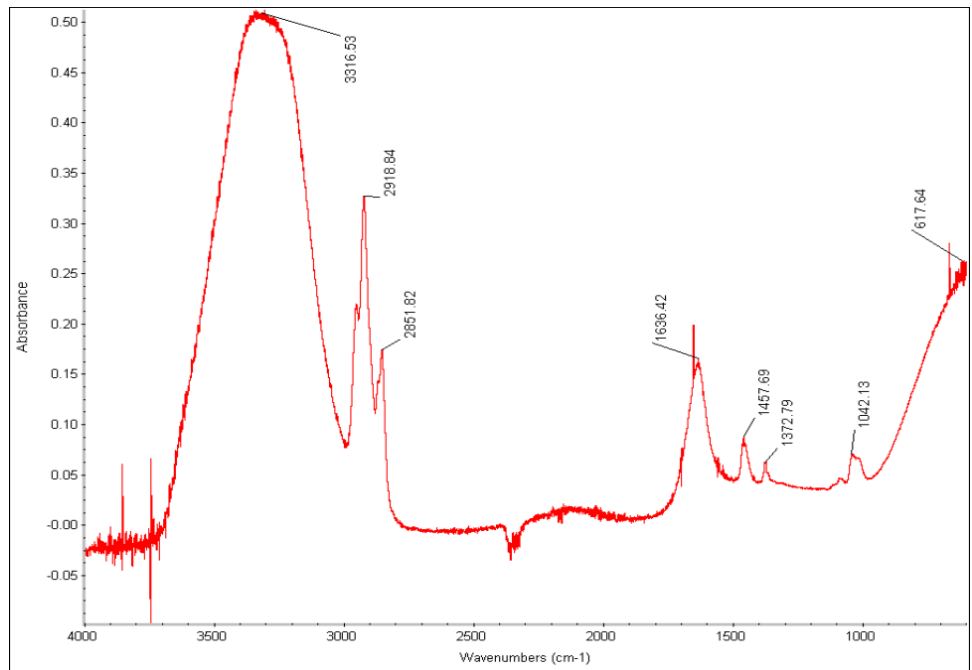


Figure A.3 Top center upstream Vanadium Cell

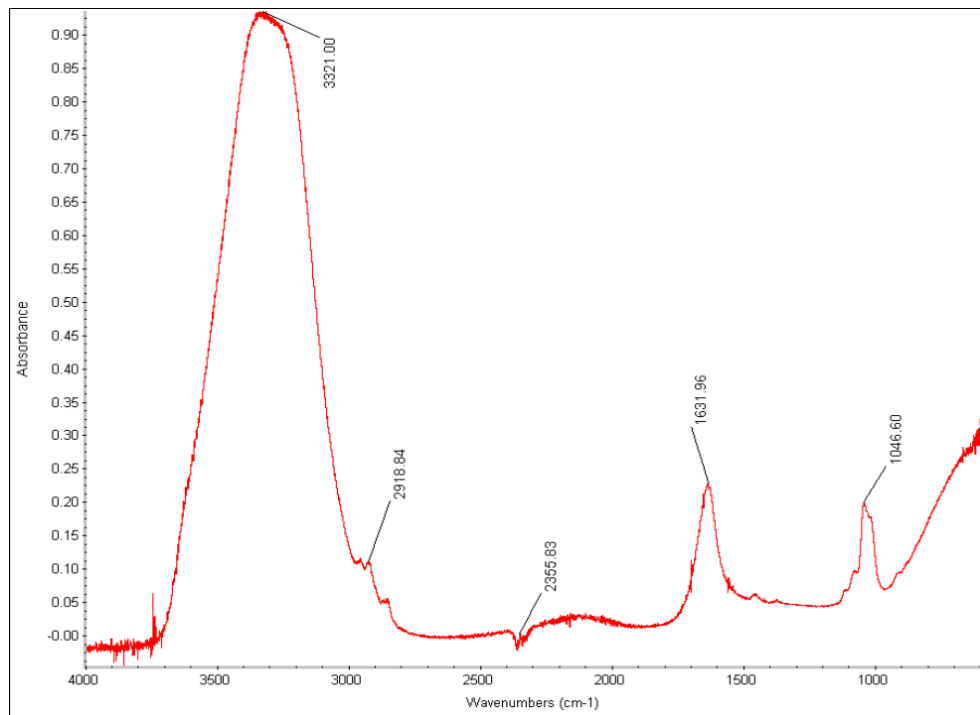


Figure A.4 Bottom center upstream Vanadium Cell

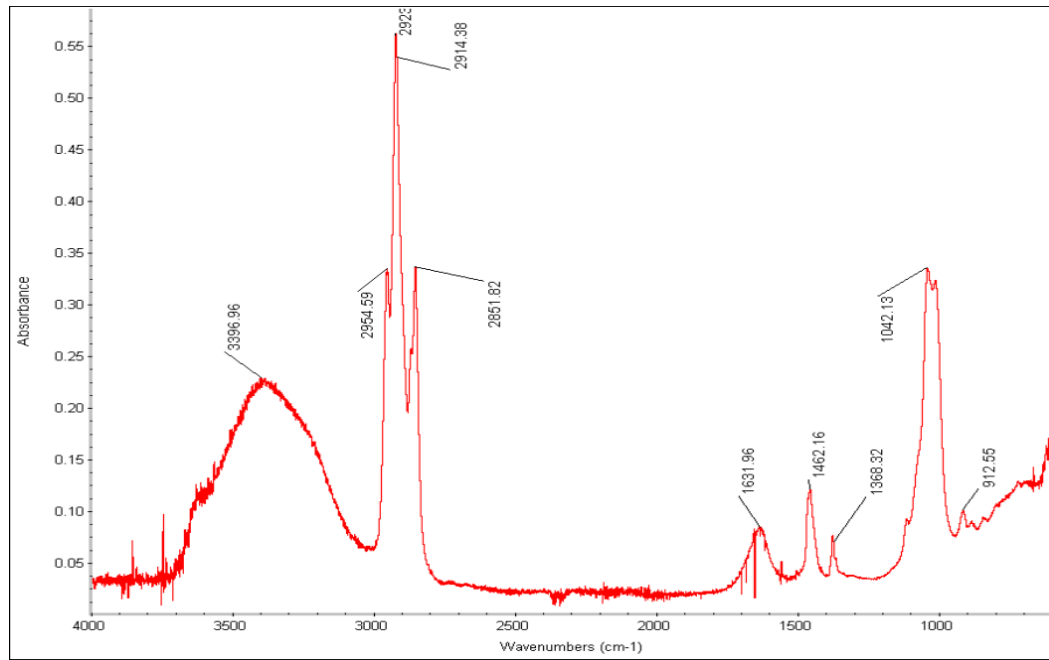


Figure A.5 Top cathode upstream Vanadium Cell

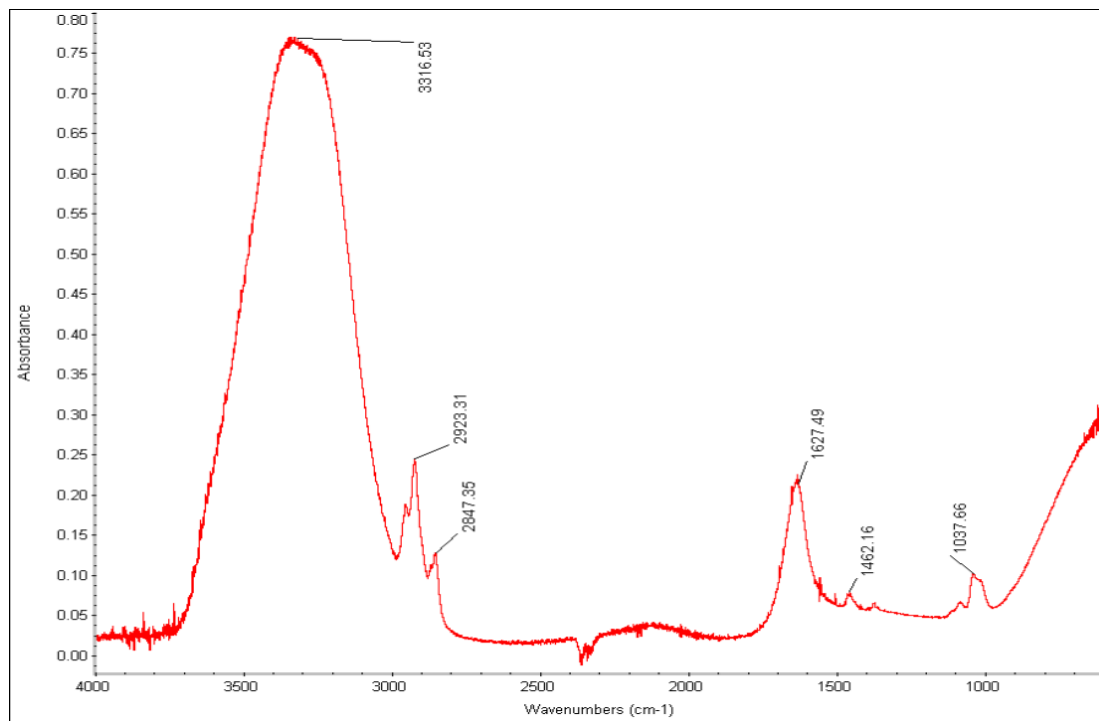


Figure A.6 Bottom cathode upstream Vanadium Cell

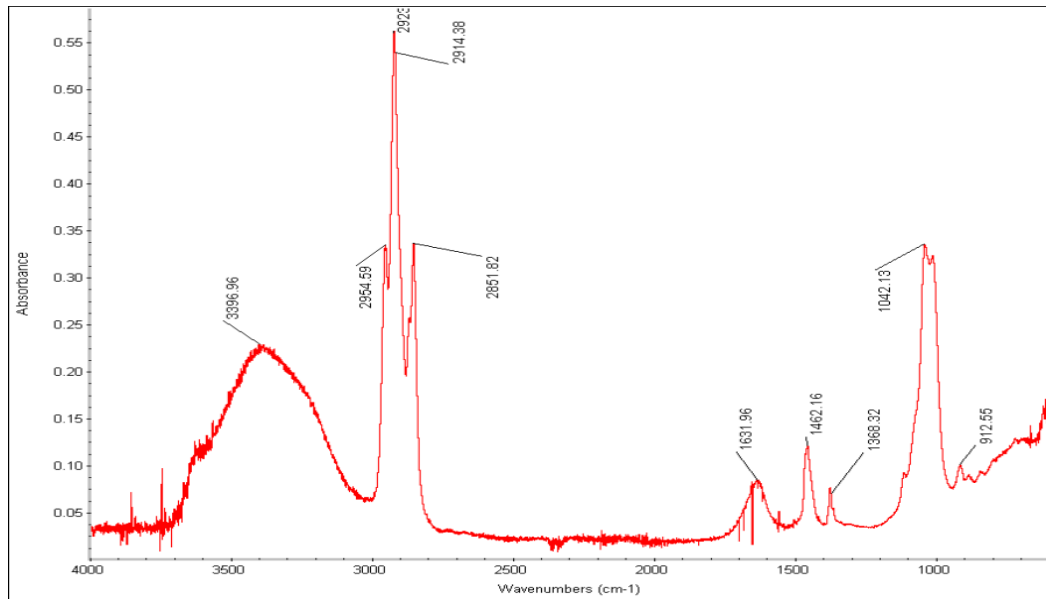


Figure A.7 Top anode downstream Vanadium Cell

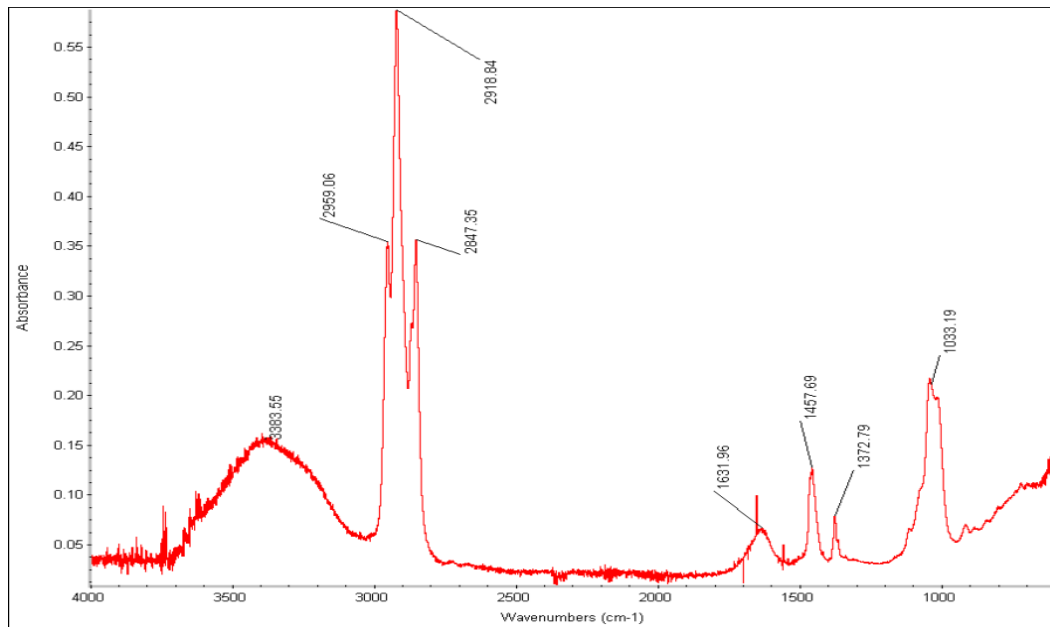


Figure A.8 Bottom anode downstream Vanadium Cell

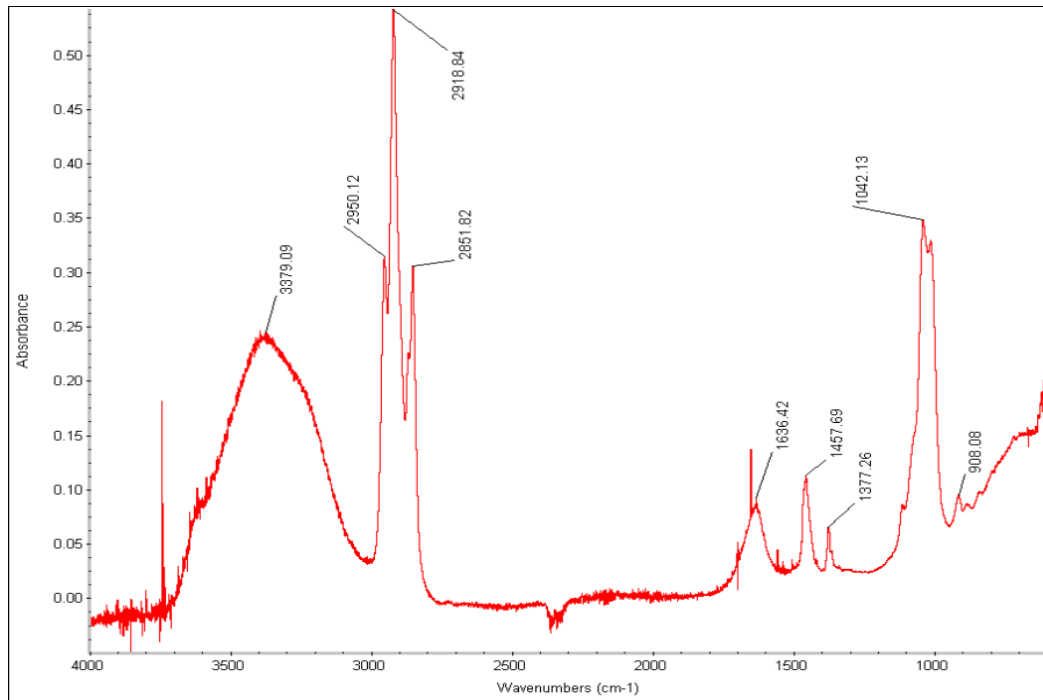


Figure A.9 Top center downstream Vanadium Cell

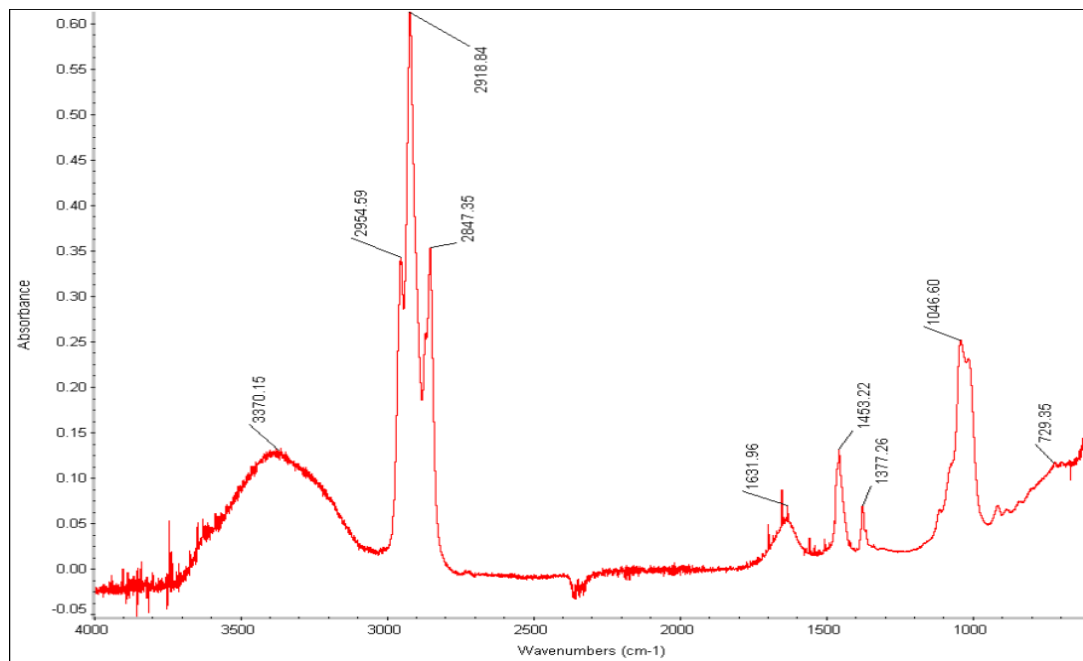


Figure A.10 Bottom center downstream Vanadium Cell

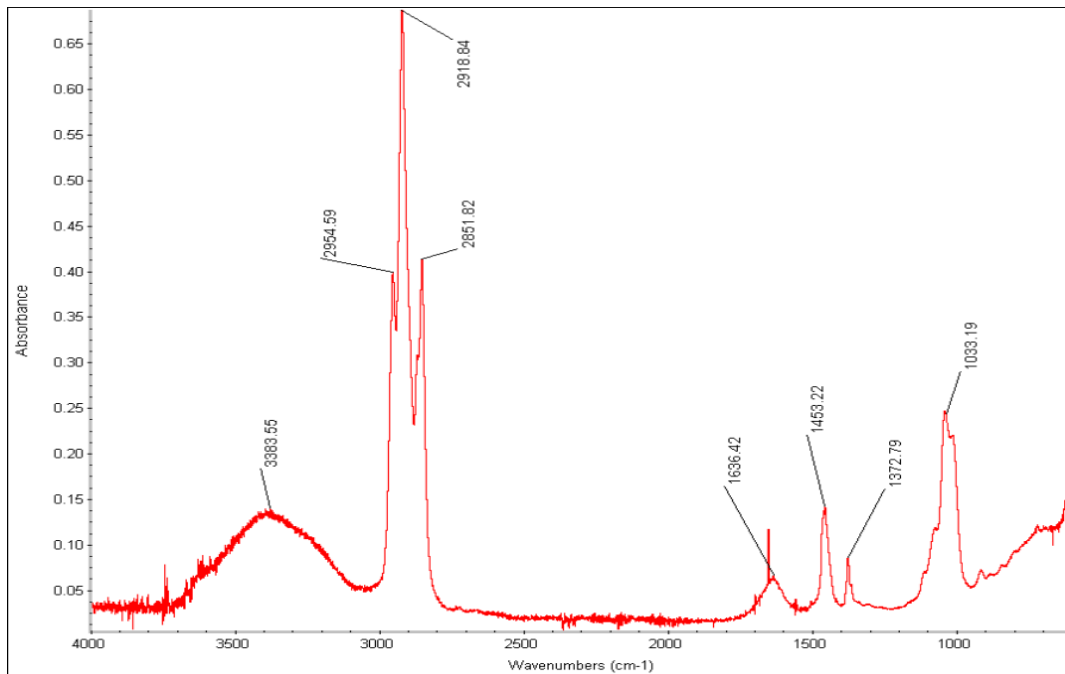


Figure A.11 Top cathode downstream Vanadium Cell

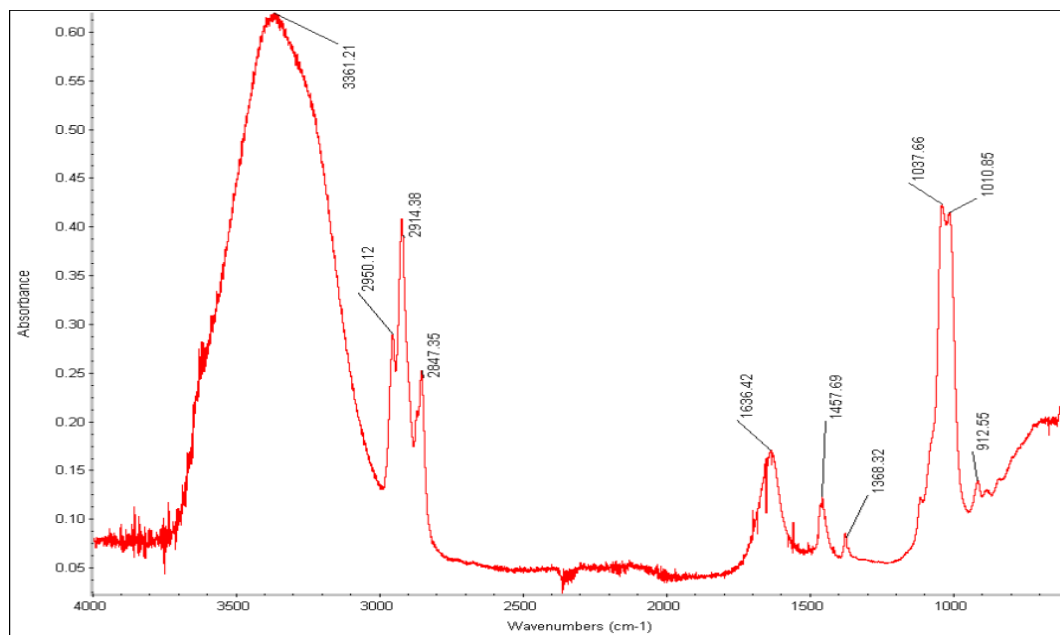


Figure A.12 Bottom cathode downstream Vanadium Cell

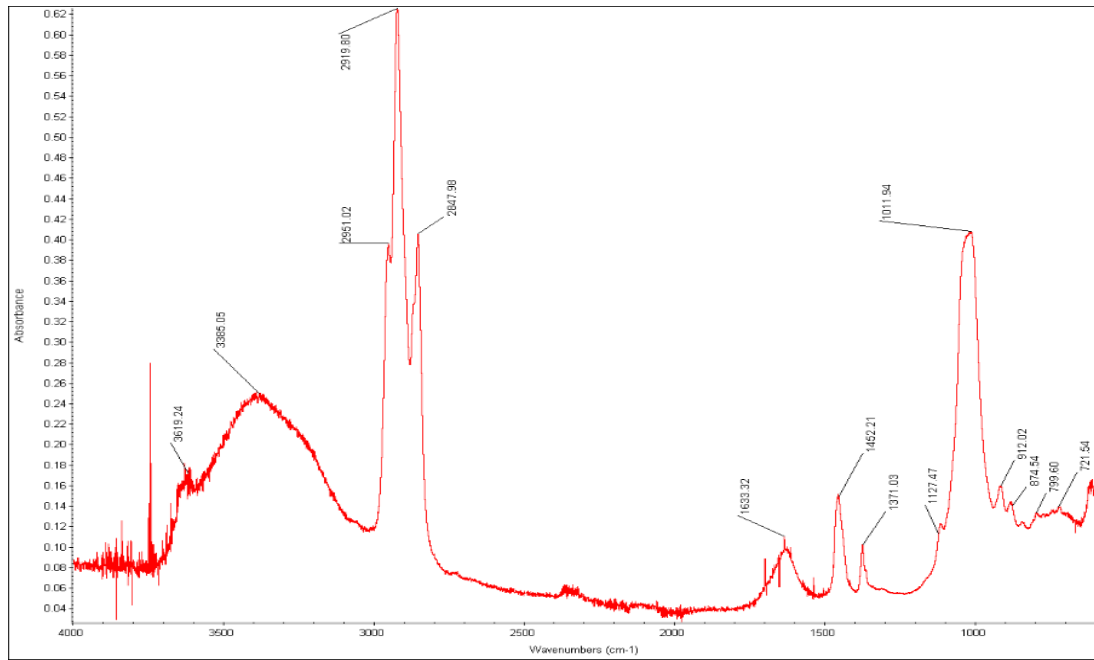


Figure A.13 Top anode upstream Nickel Cell

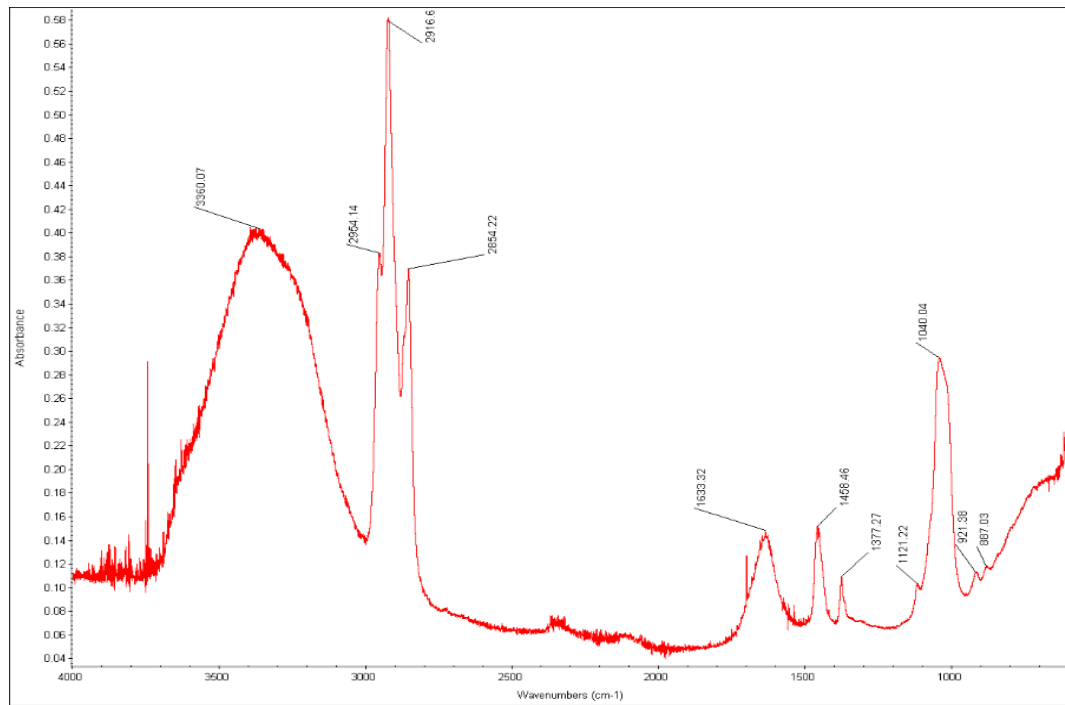


Figure A.14 Bottom anode upstream Nickel Cell

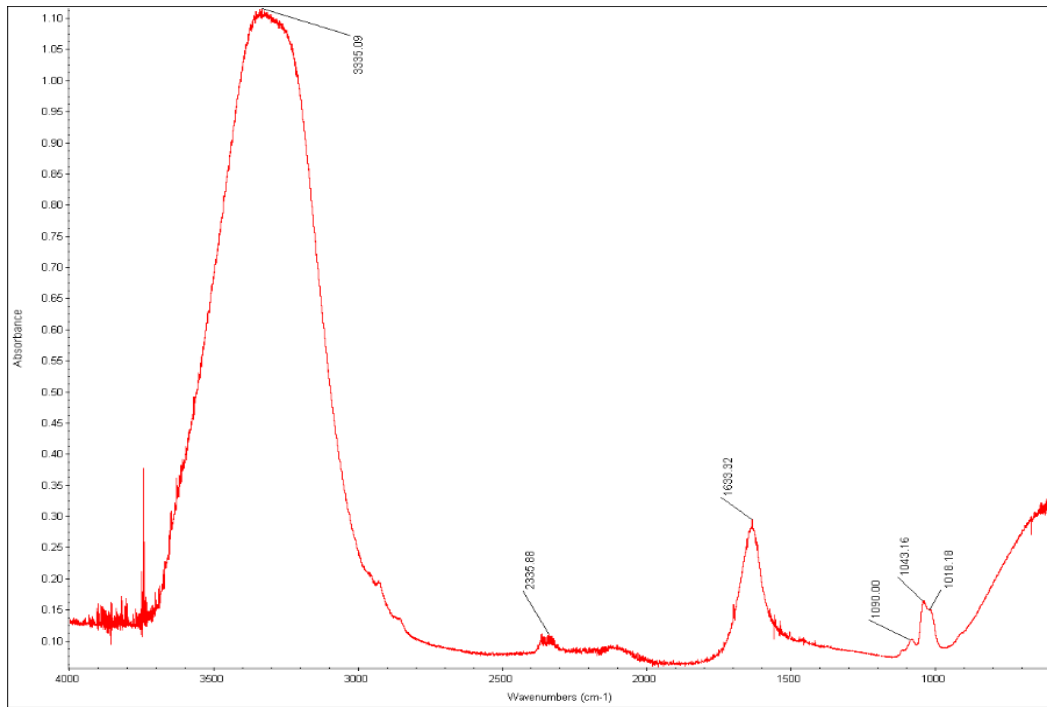


Figure A.15 Top center upstream Nickel Cell

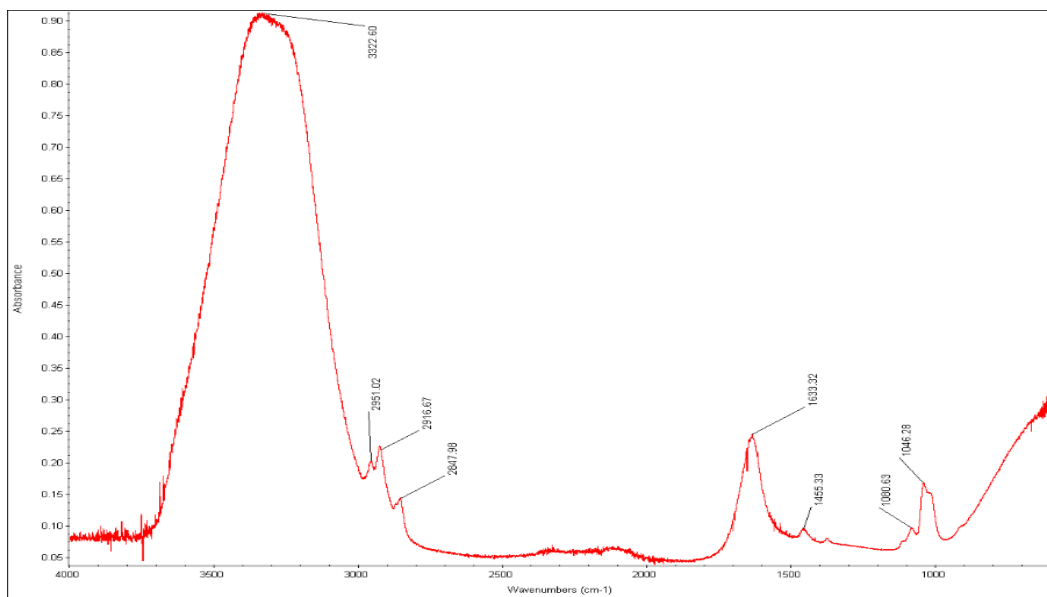


Figure A.16 Bottom center upstream Nickel Cell

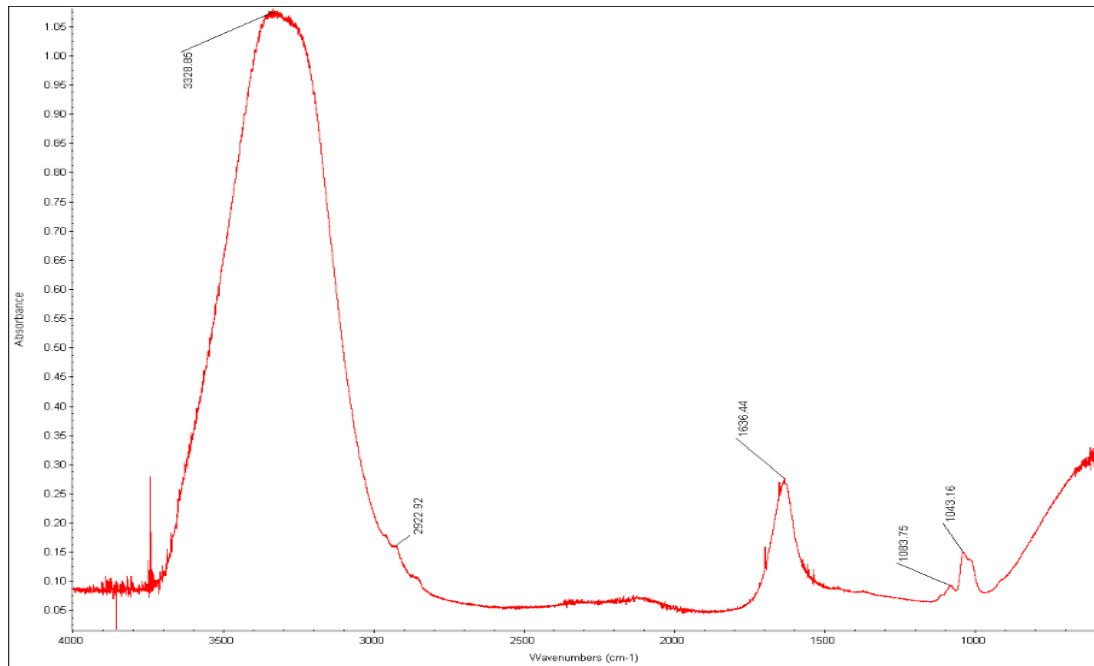


Figure A.17 Top cathode upstream Nickel Cell

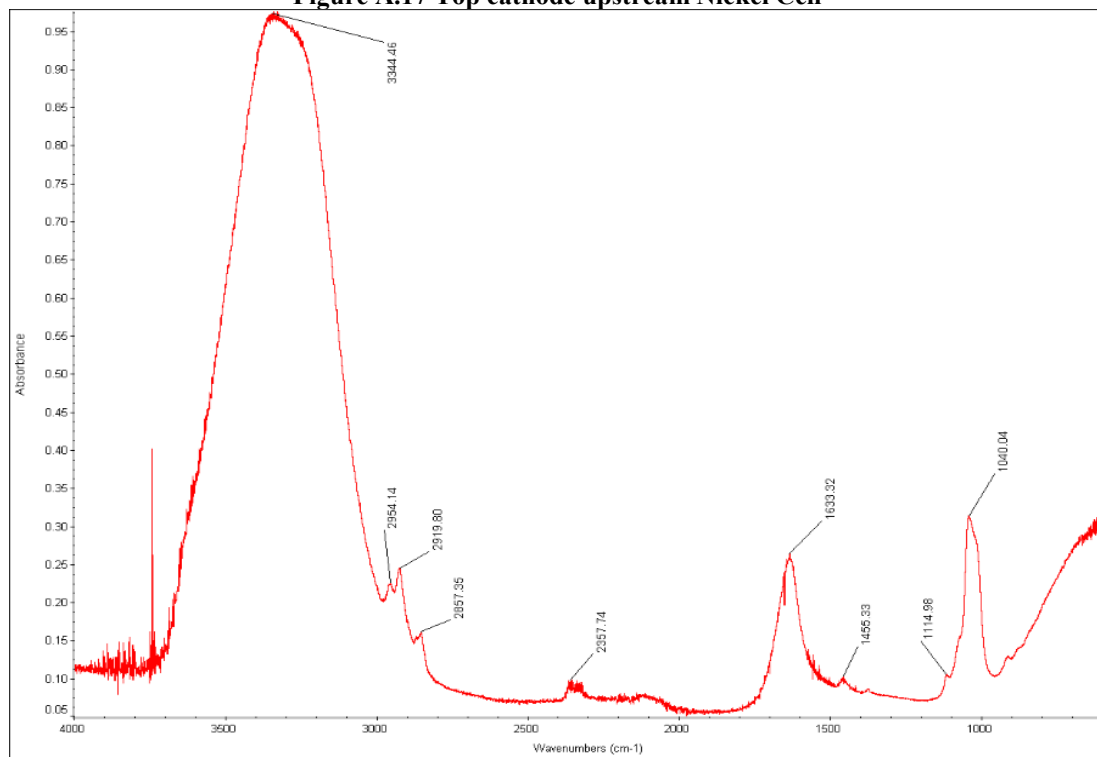


Figure A.18 Bottom cathode upstream Nickel Cell

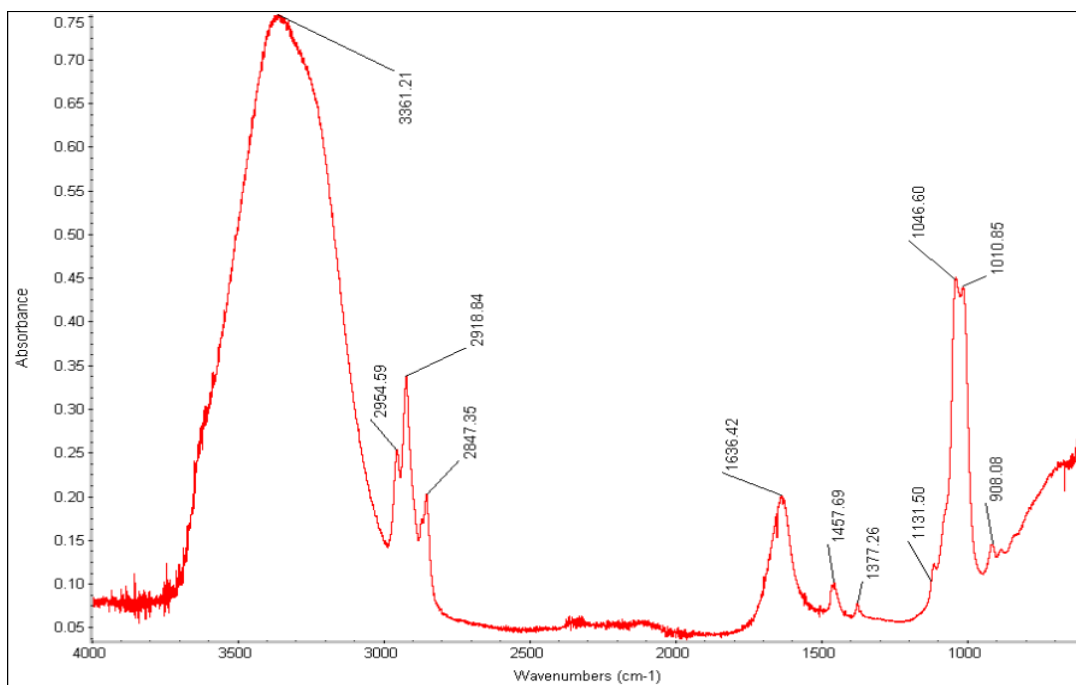


Figure A.19 Top anode downstream Nickel Cell

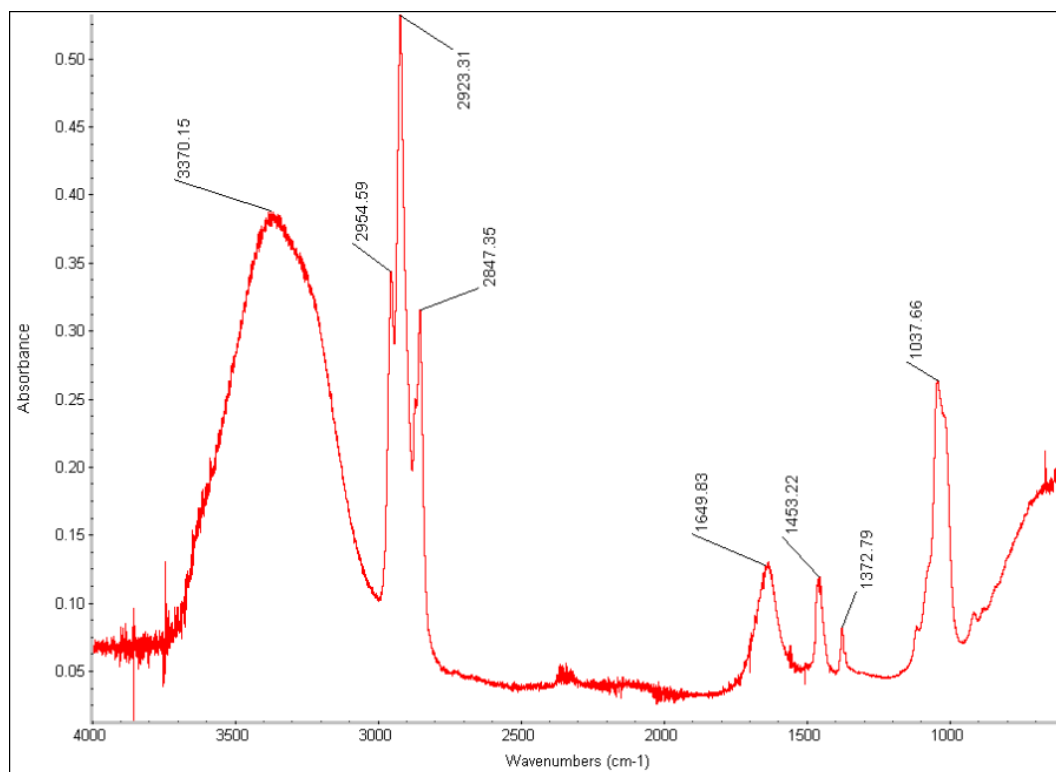


Figure A.20 Bottom anode downstream Nickel Cell

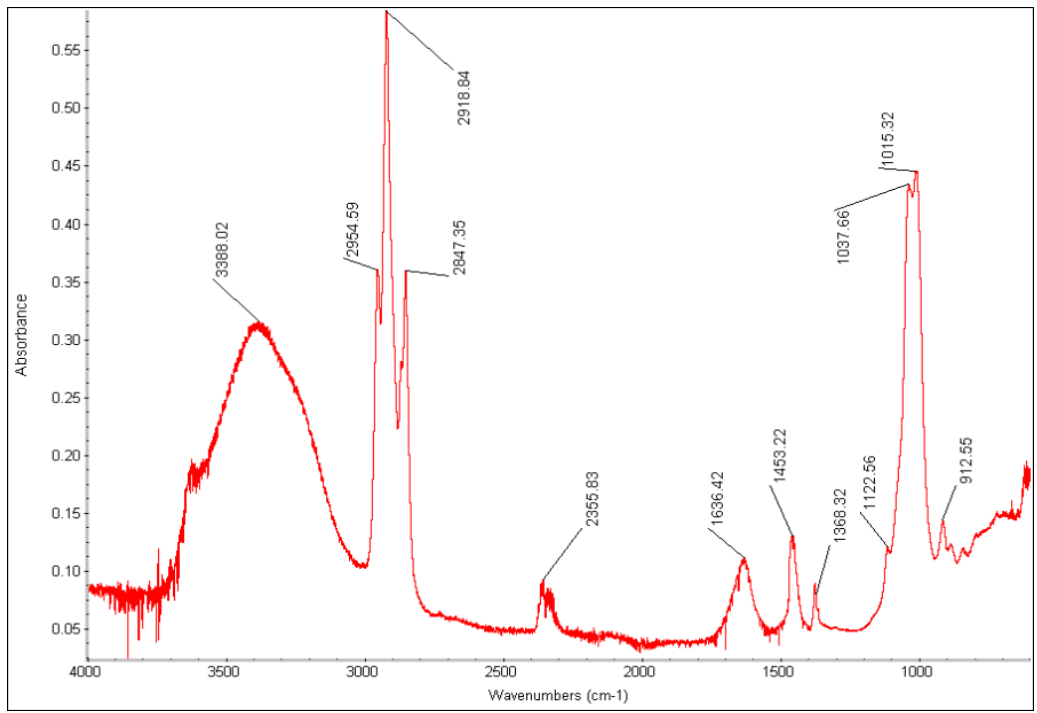


Figure A.21 Top center downstream Nickel Cell

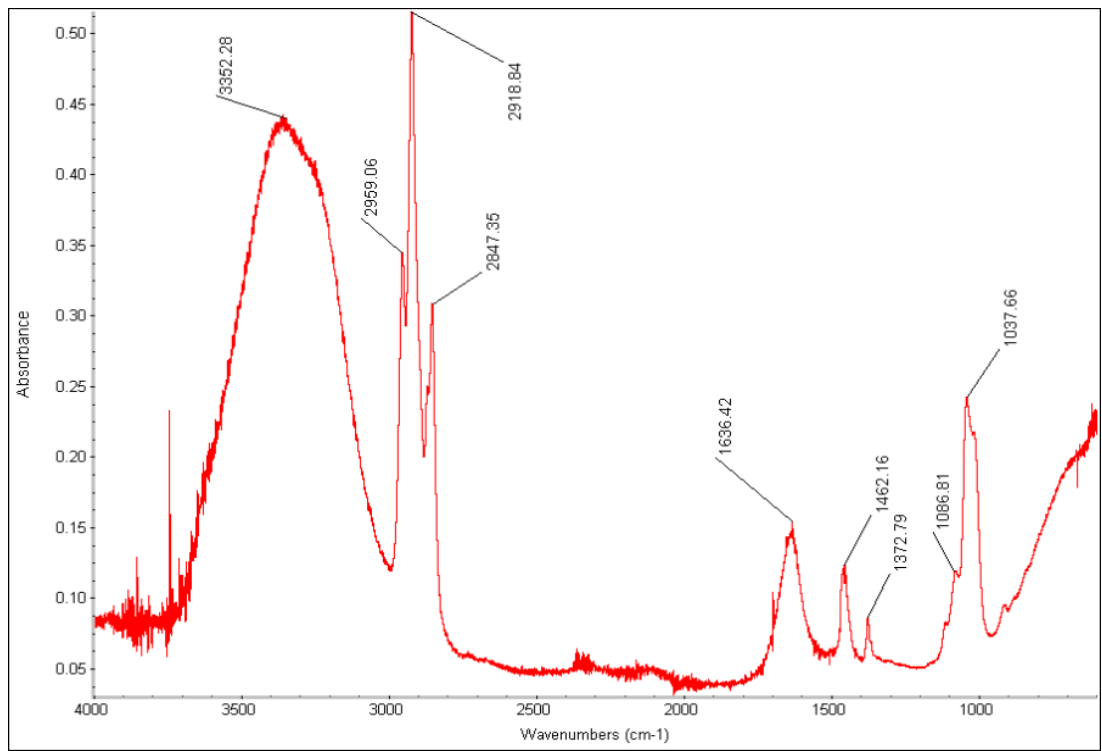


Figure A.22 Bottom center downstream Nickel Cell

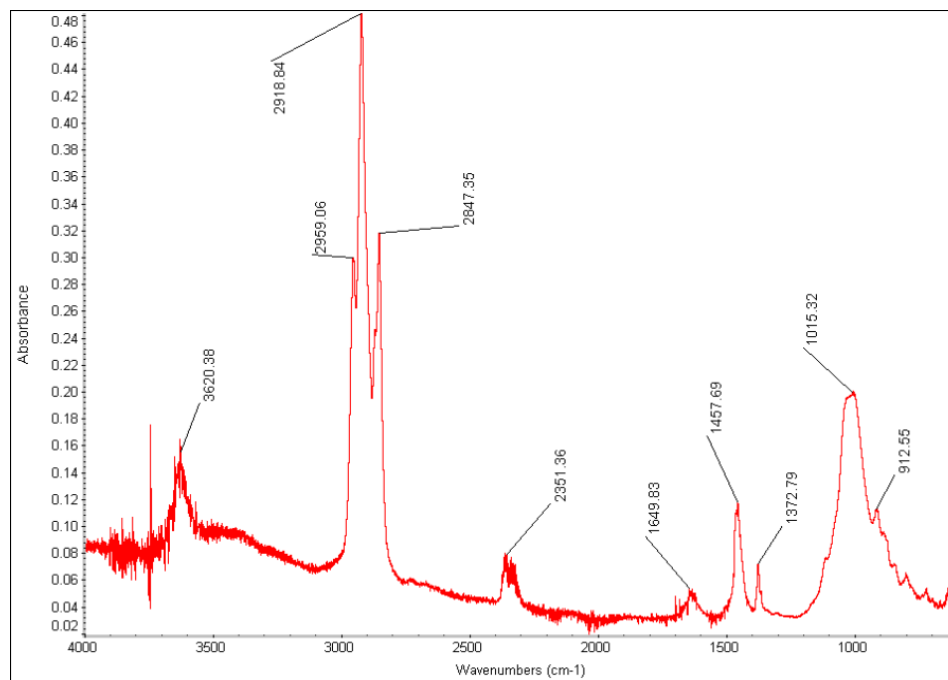


Figure A.23 Top cathode downstream Nickel Cell

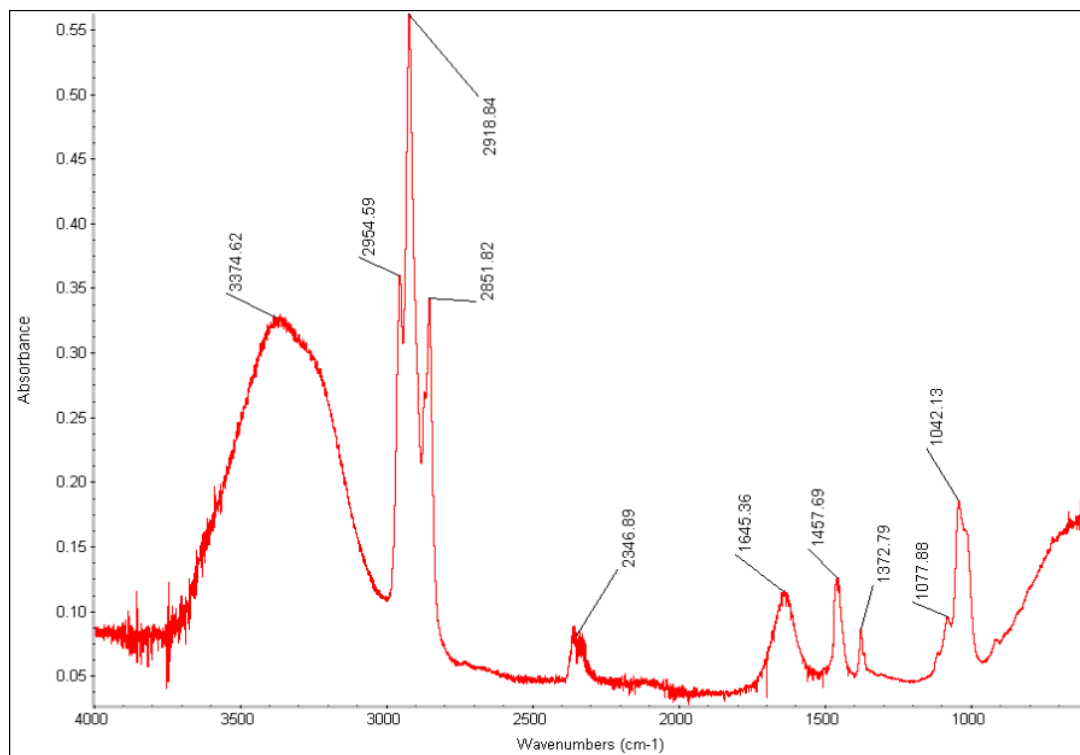


Figure A.24 Bottom cathode downstream Nickel Cell

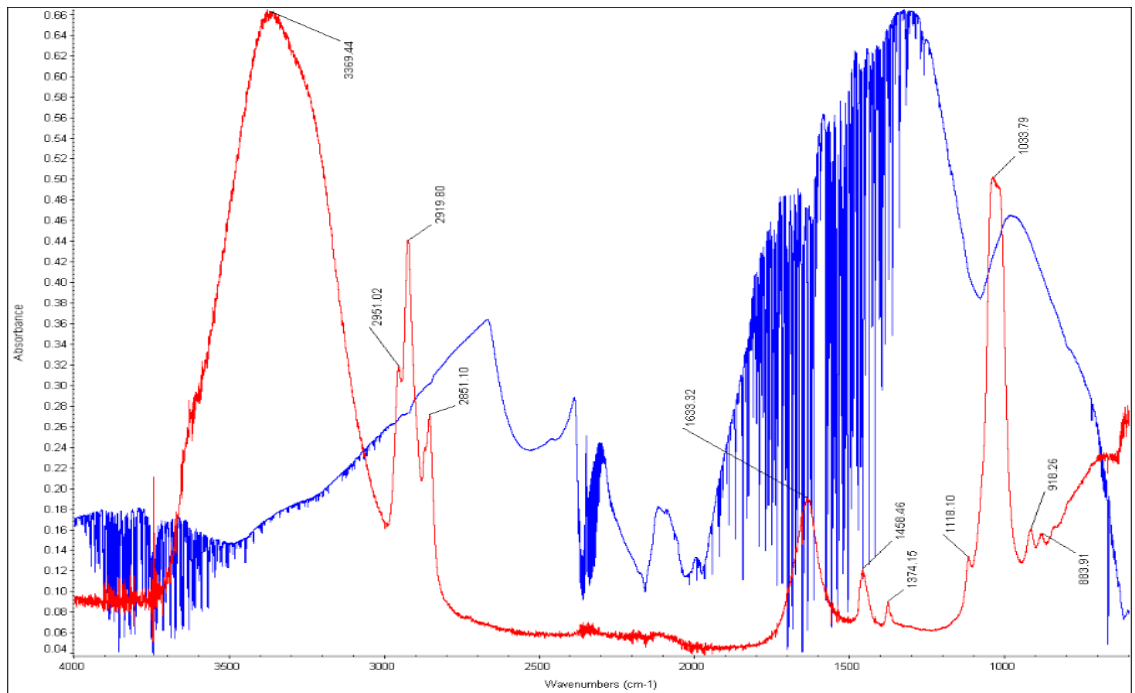


Figure A.25 Top anode upstream Lead Cell (with background noise)

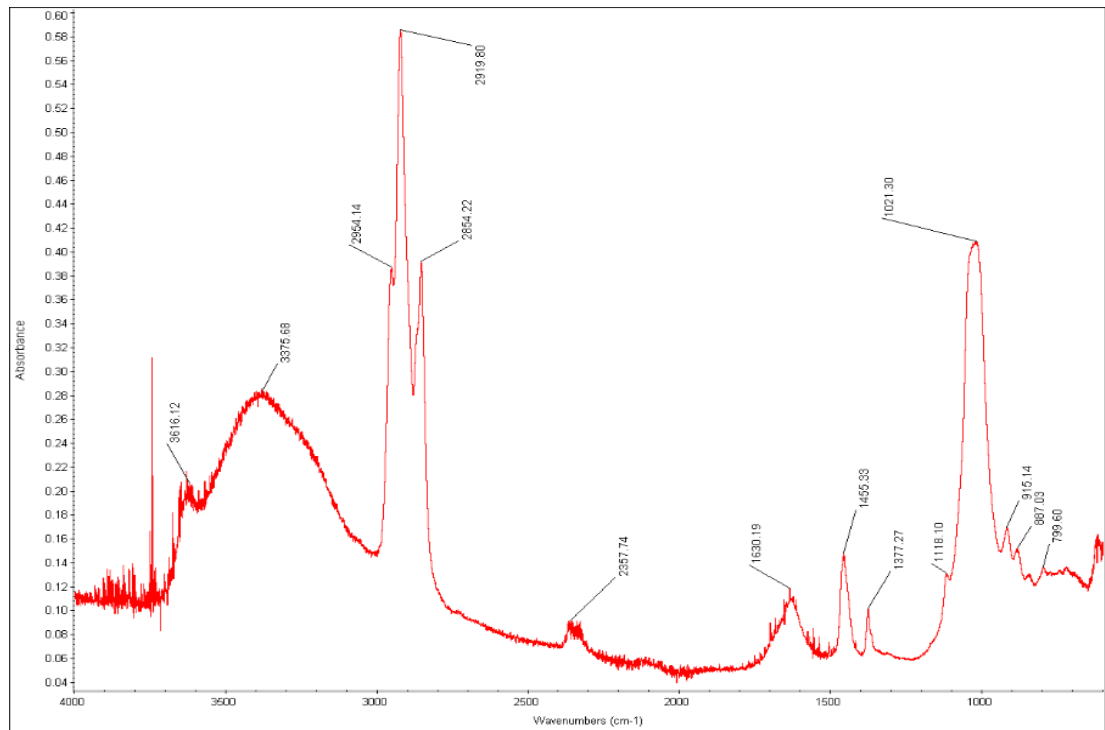


Figure A.26 Bottom anode upstream Lead Cell

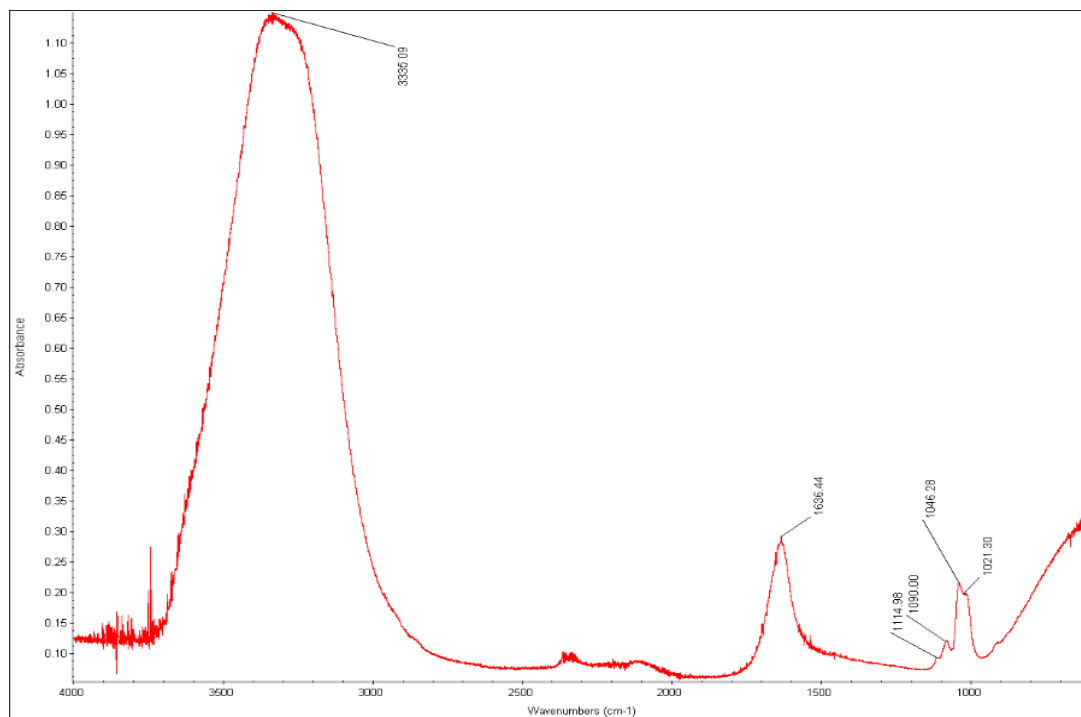


Figure A.27 Top center upstream Lead Cell

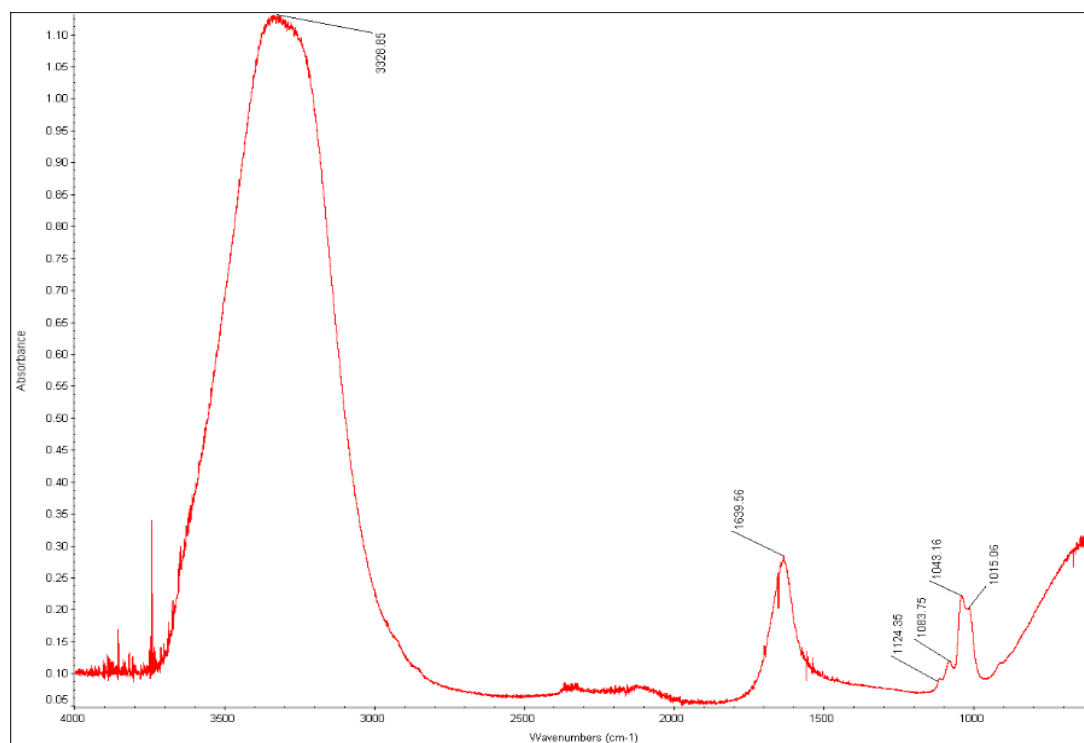


Figure A.28 Bottom center upstream Lead Cell

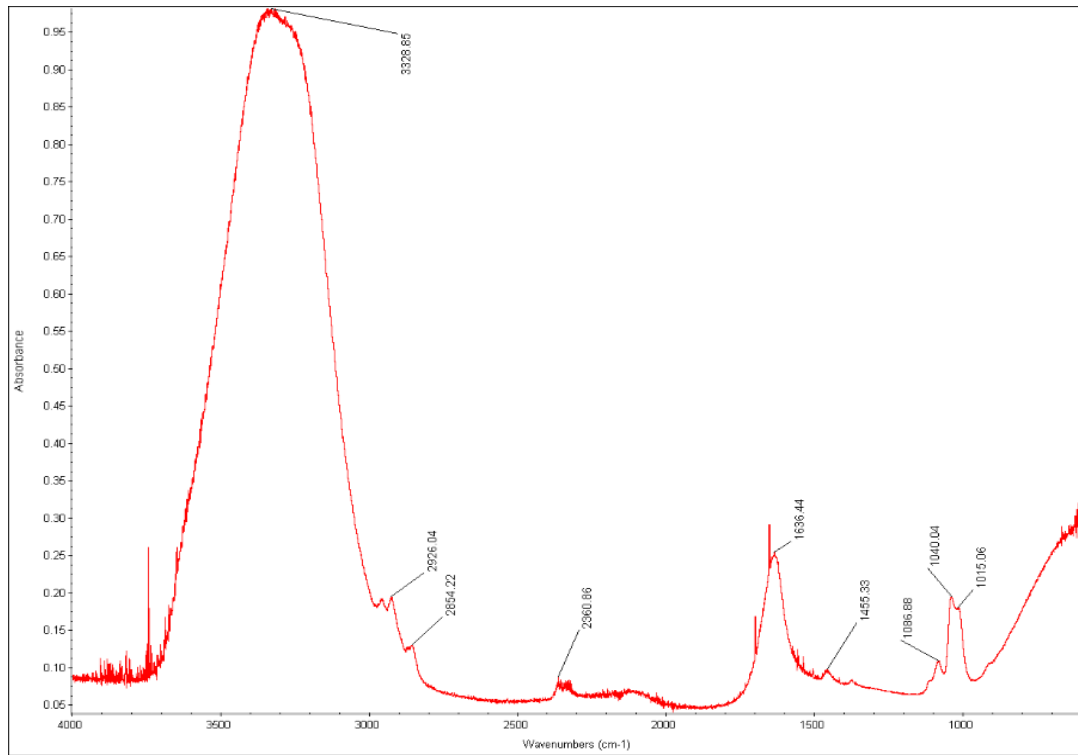


Figure A.29 Top cathode upstream Lead Cell

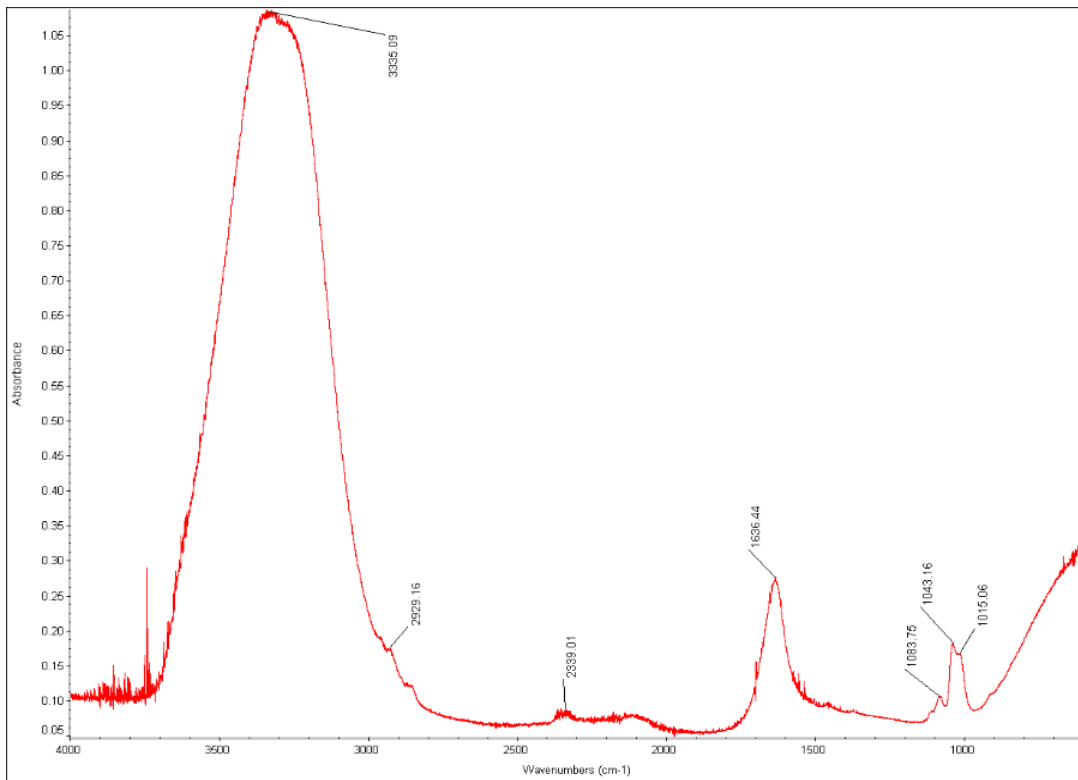


Figure A.30 Bottom cathode upstream Lead Cell

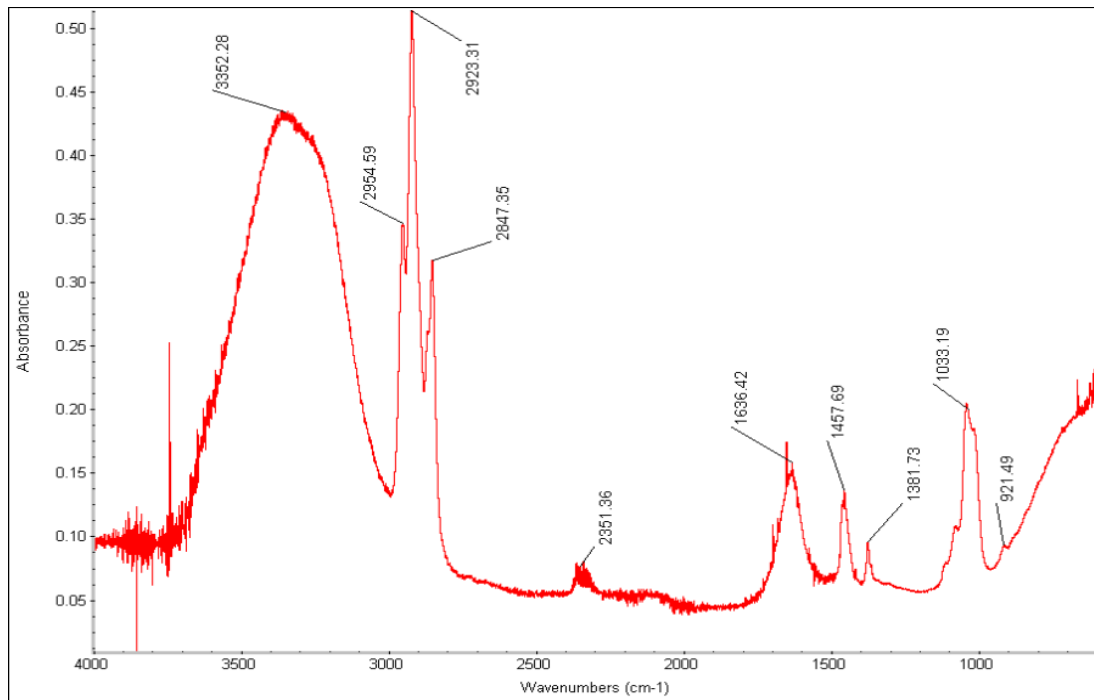


Figure A.31 Top anode downstream Lead Cell

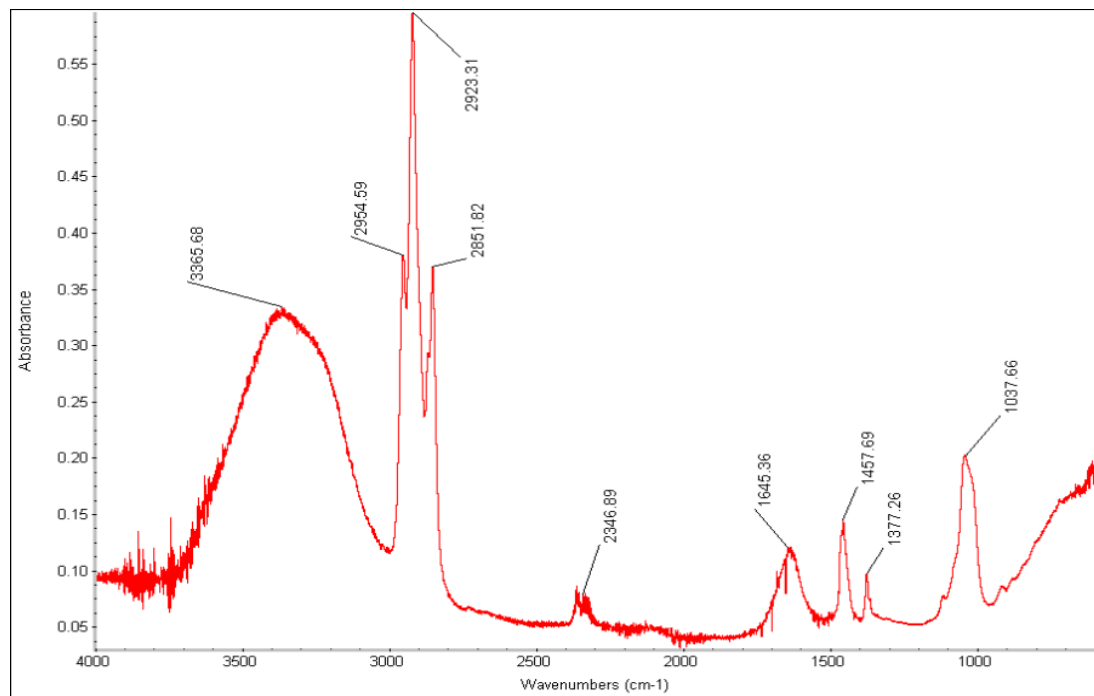


Figure A.32 Bottom anode downstream Lead Cell

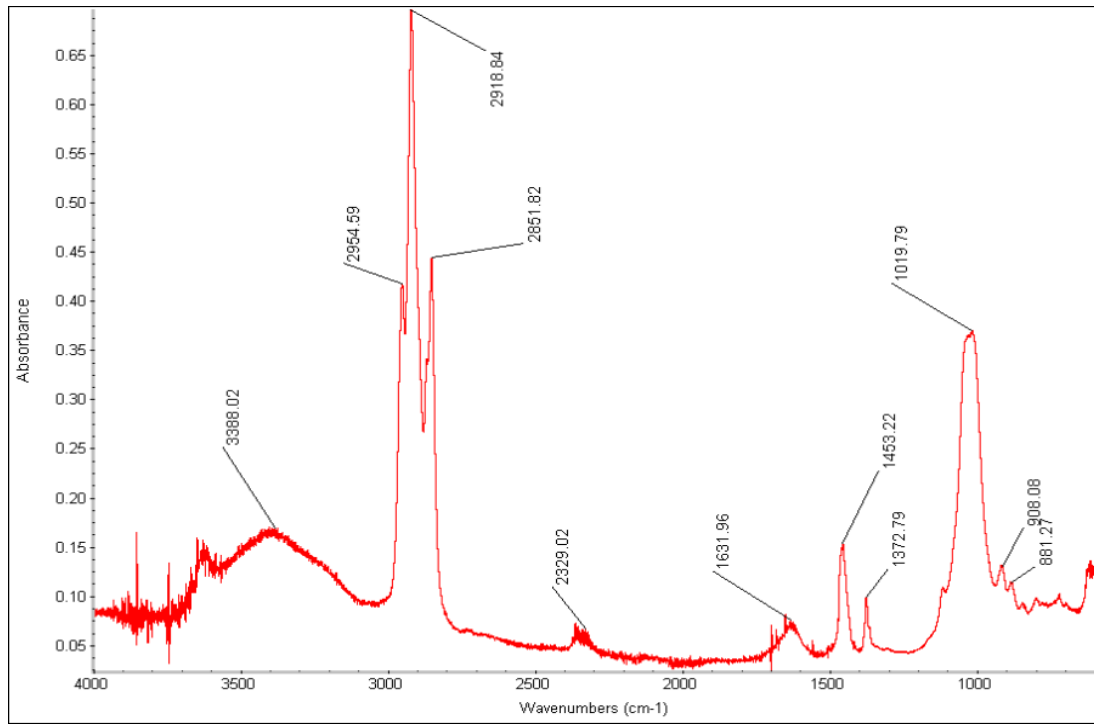


Figure A.33 Top center downstream Lead Cell

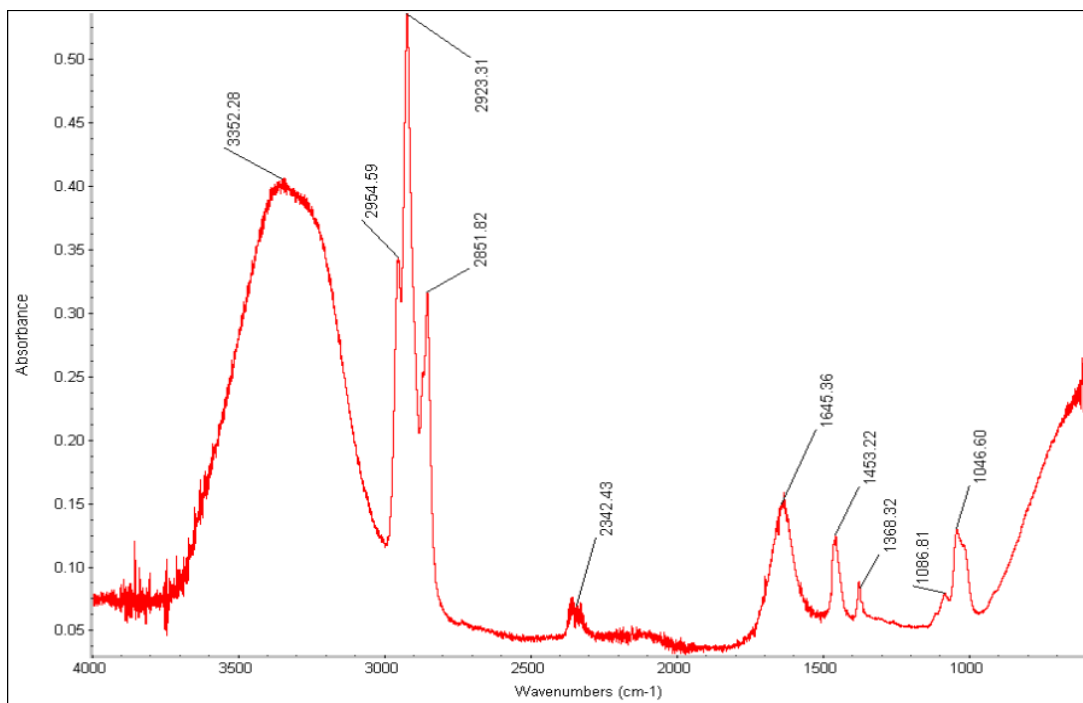


Figure A.34 bottom center downstream Lead Cell

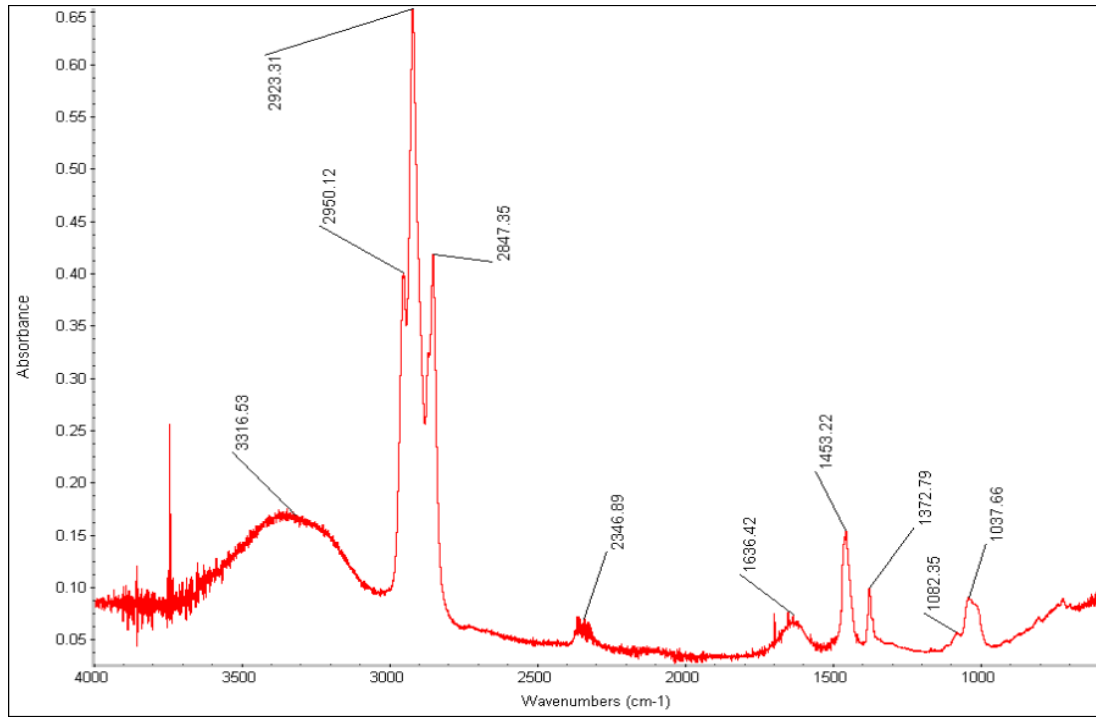


Figure A.35 Top cathode downstream Lead Cell

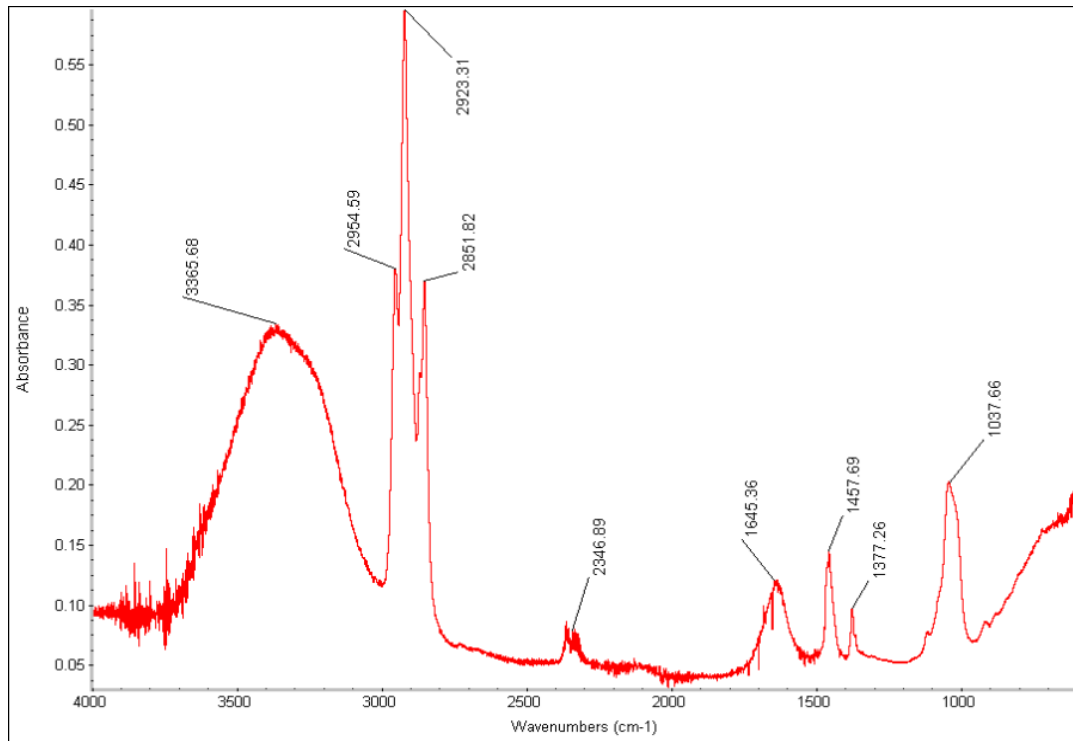


Figure A.36 Bottom cathode downstream Lead Cell

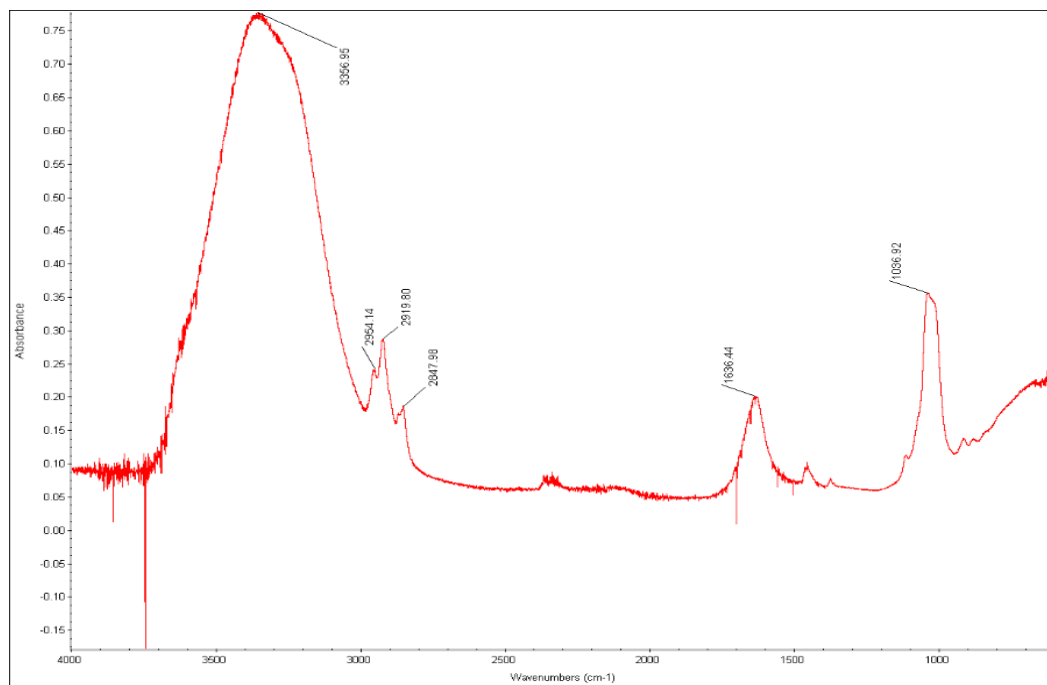


Figure A.37 Top anode upstream Mix Cell

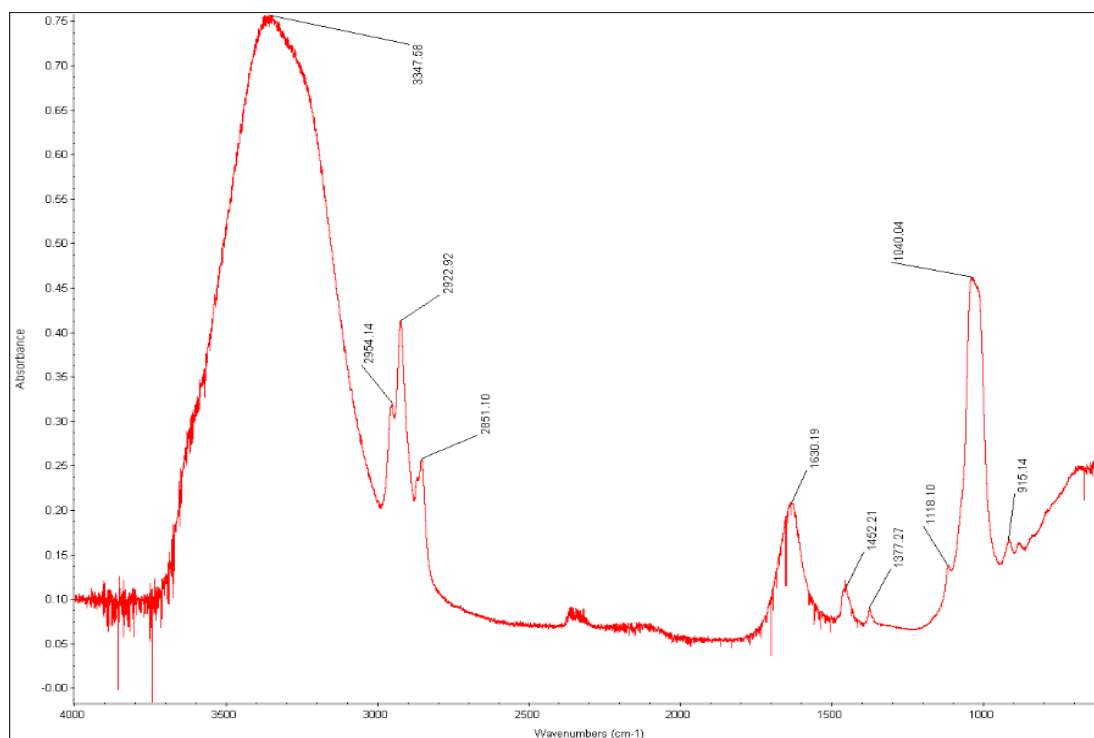


Figure A.38 Bottom anode upstream Mix Cell

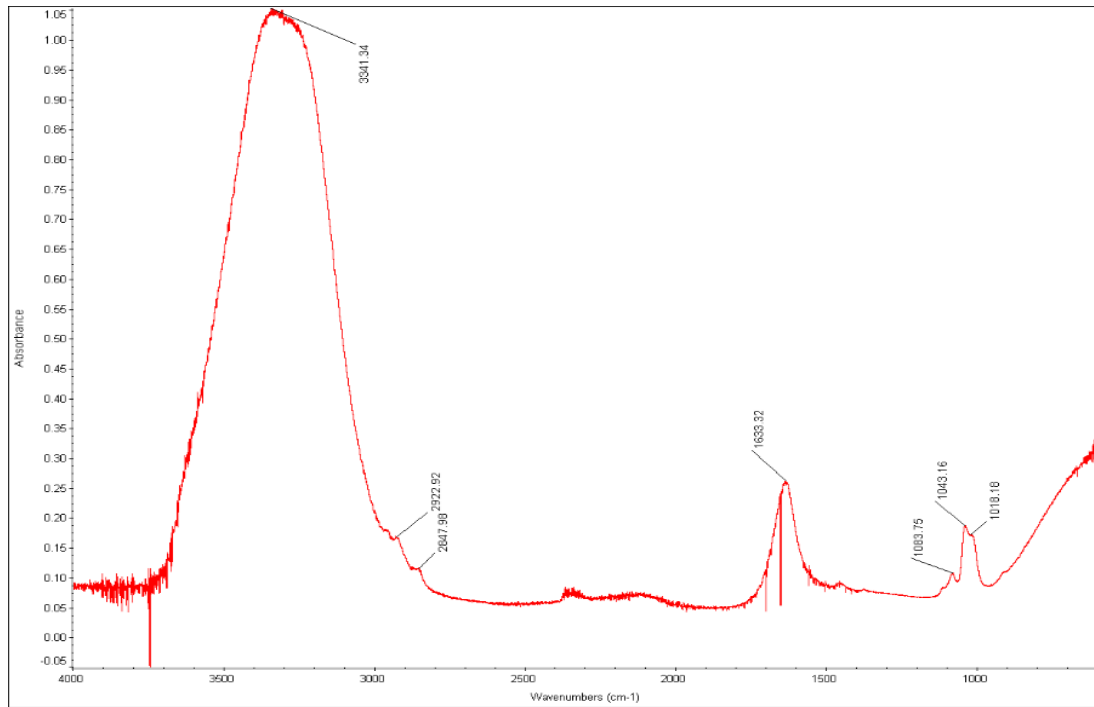


Figure A.39 Top center upstream Mix Cell

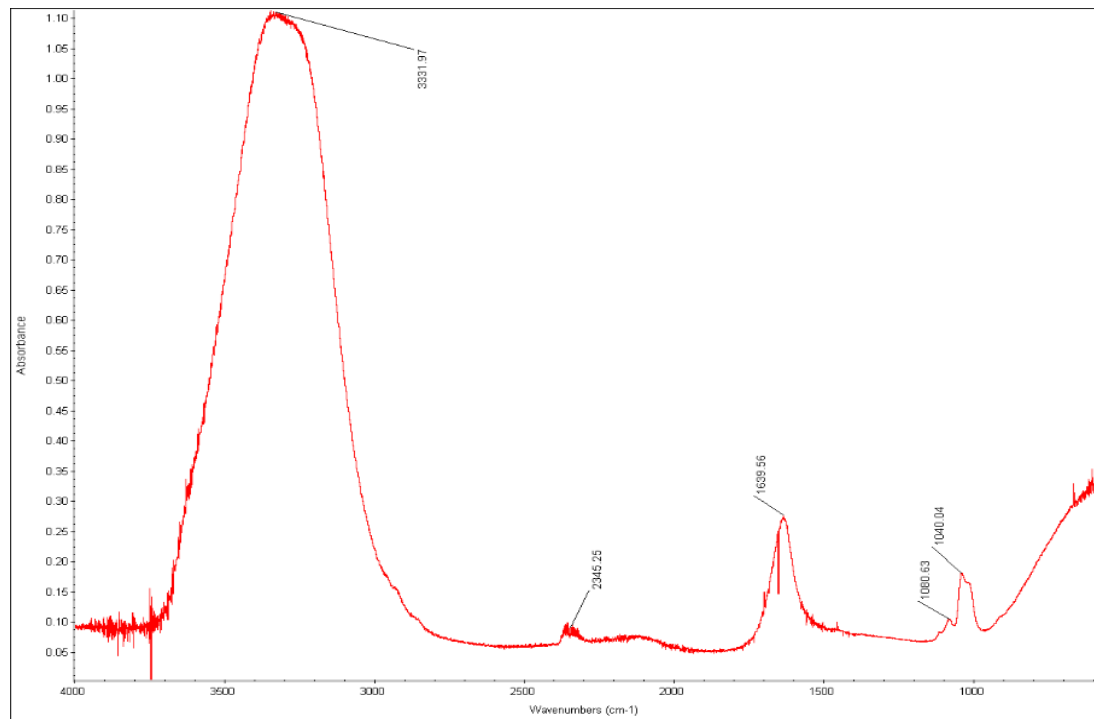


Figure A.40 Bottom center upstream Mix Cell

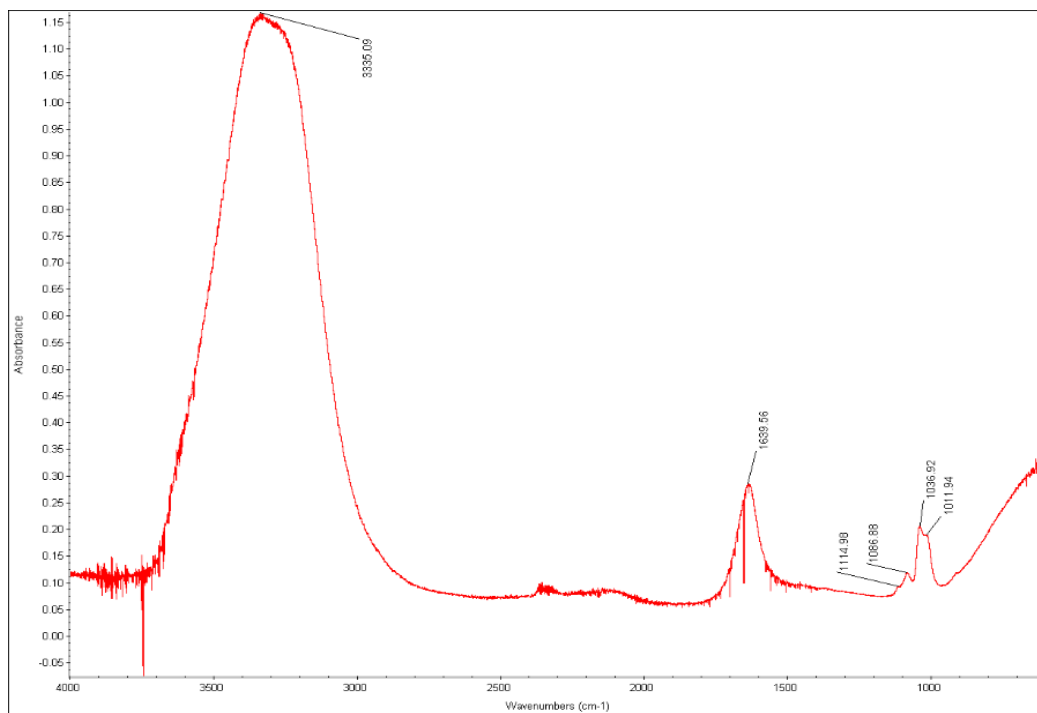


Figure A.41 Top cathode upstream Mix Cell

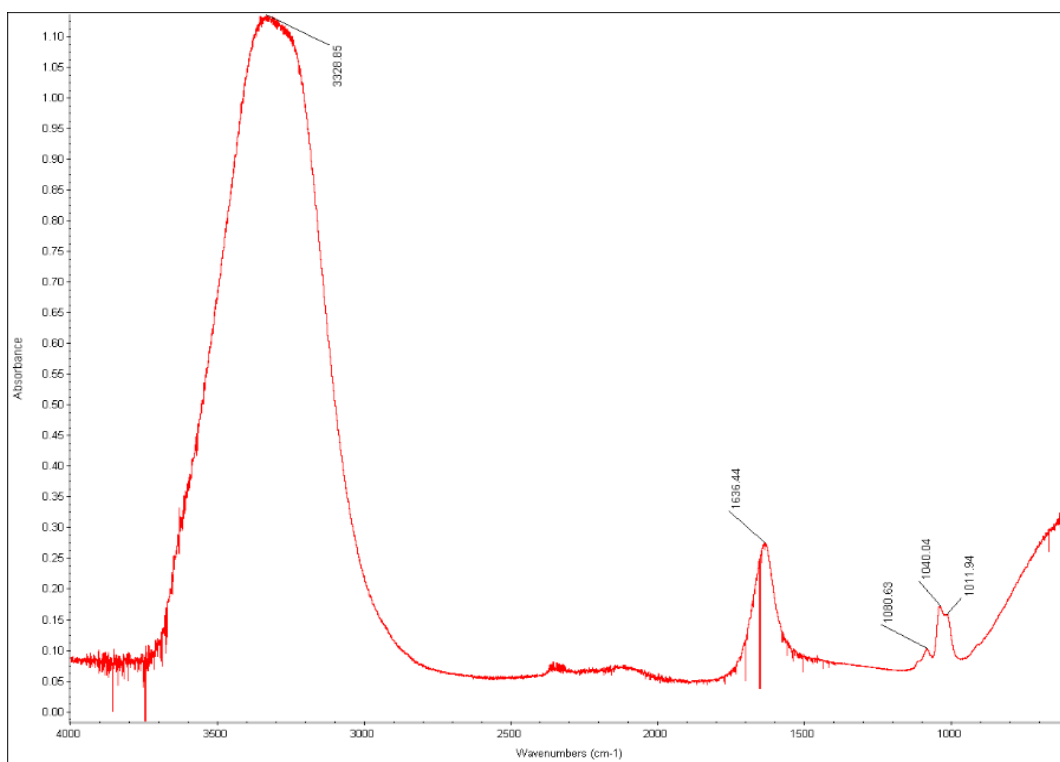


Figure A.42 Bottom cathode upstream Mix Cell

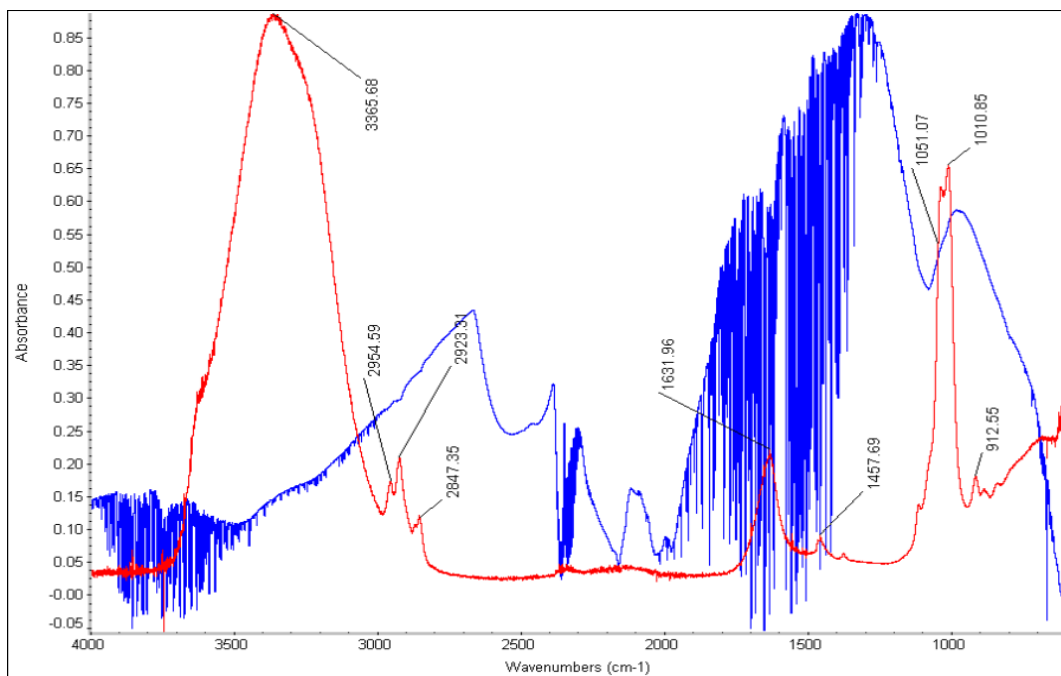


Figure A.43 Top anode downstream Mix Cell (with background noise)

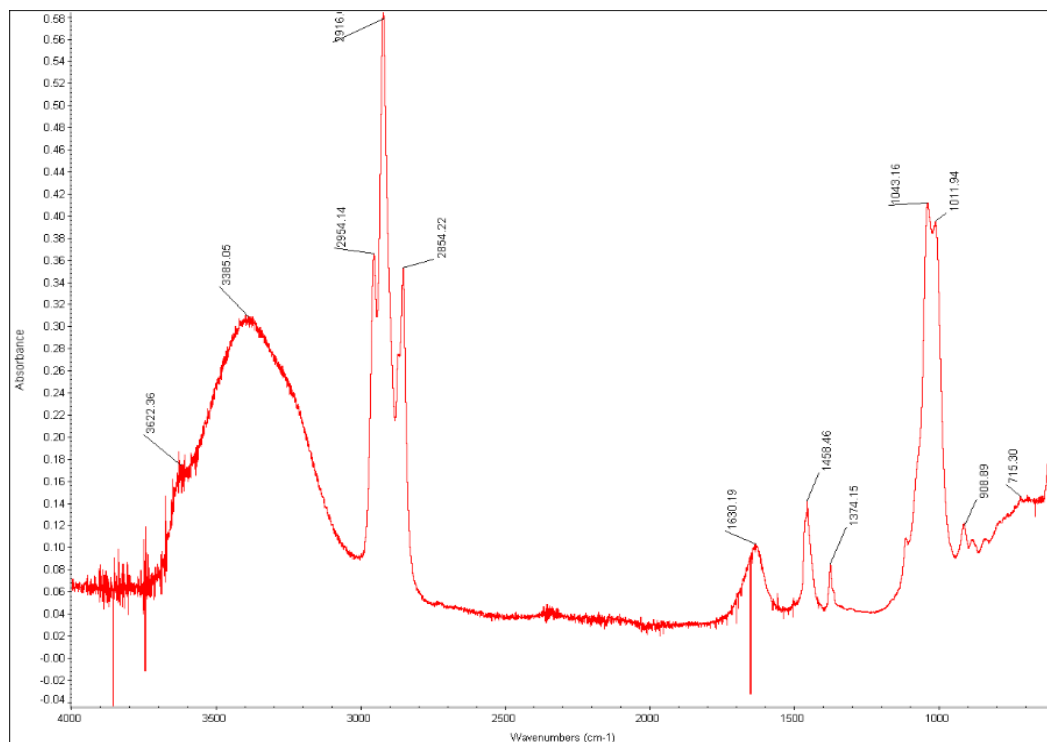


Figure A.44 Bottom anode downstream Mix Cell

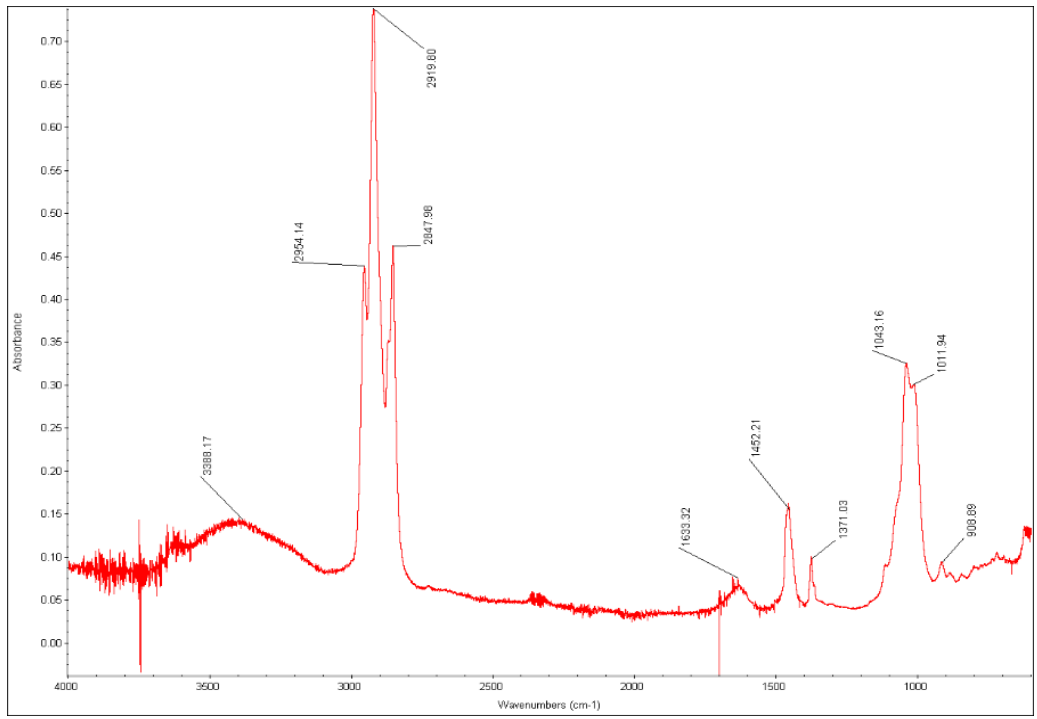


Figure A.45 Top center downstream Mix Cell

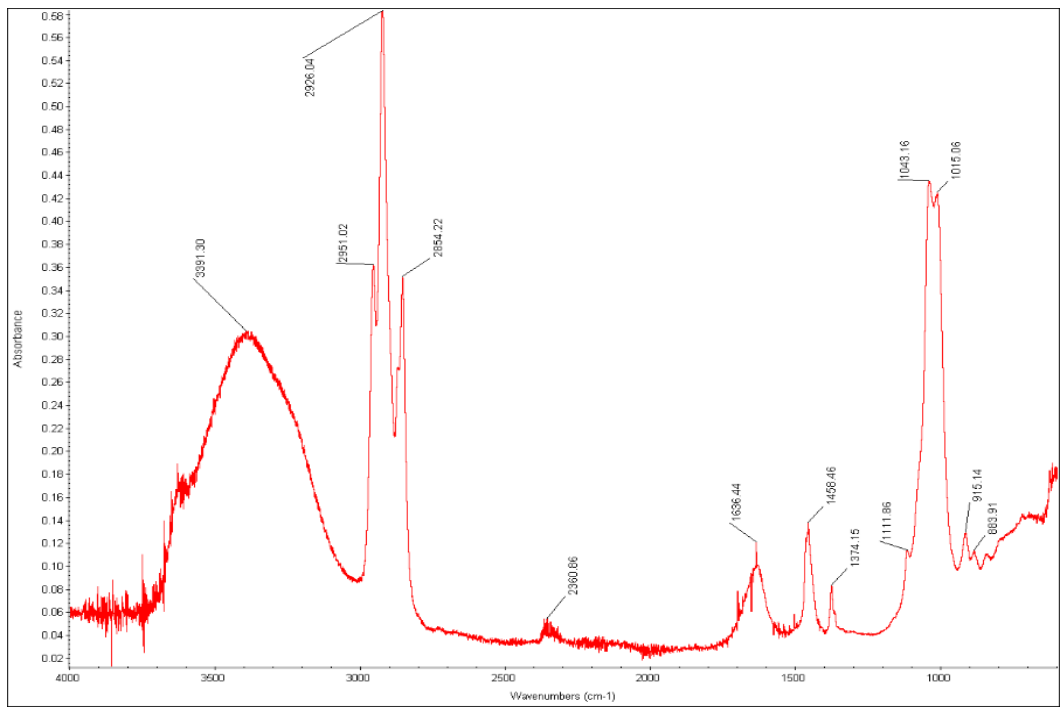


Figure A.46 Bottom center downstream Mix Cell

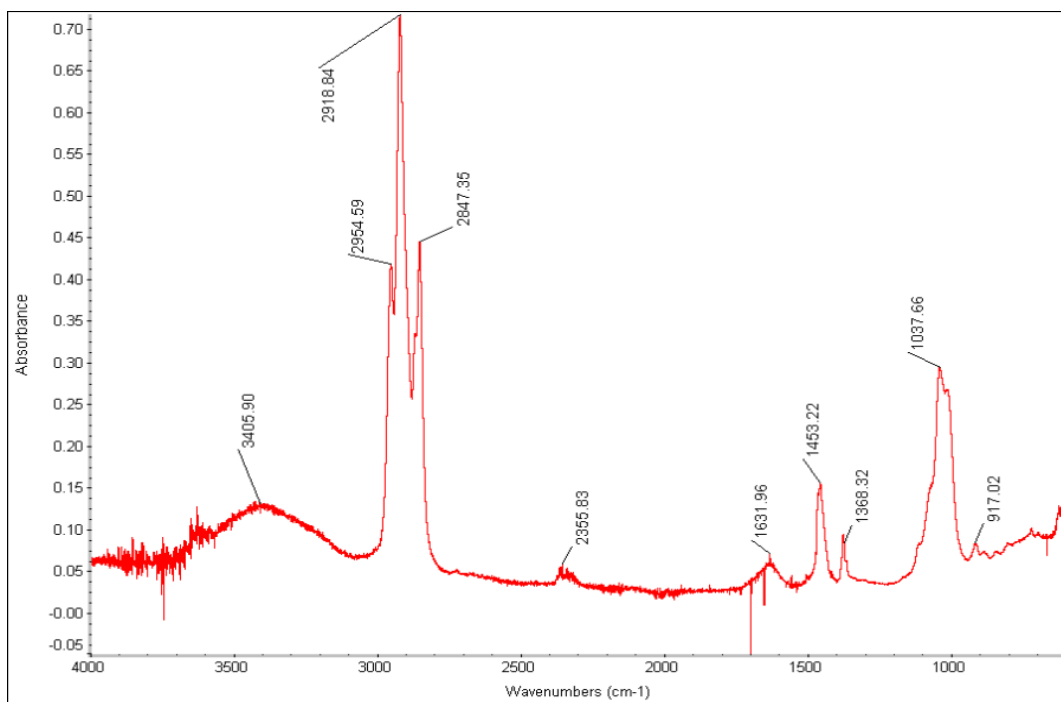


Figure A.47 Top cathode downstream Mix Cell

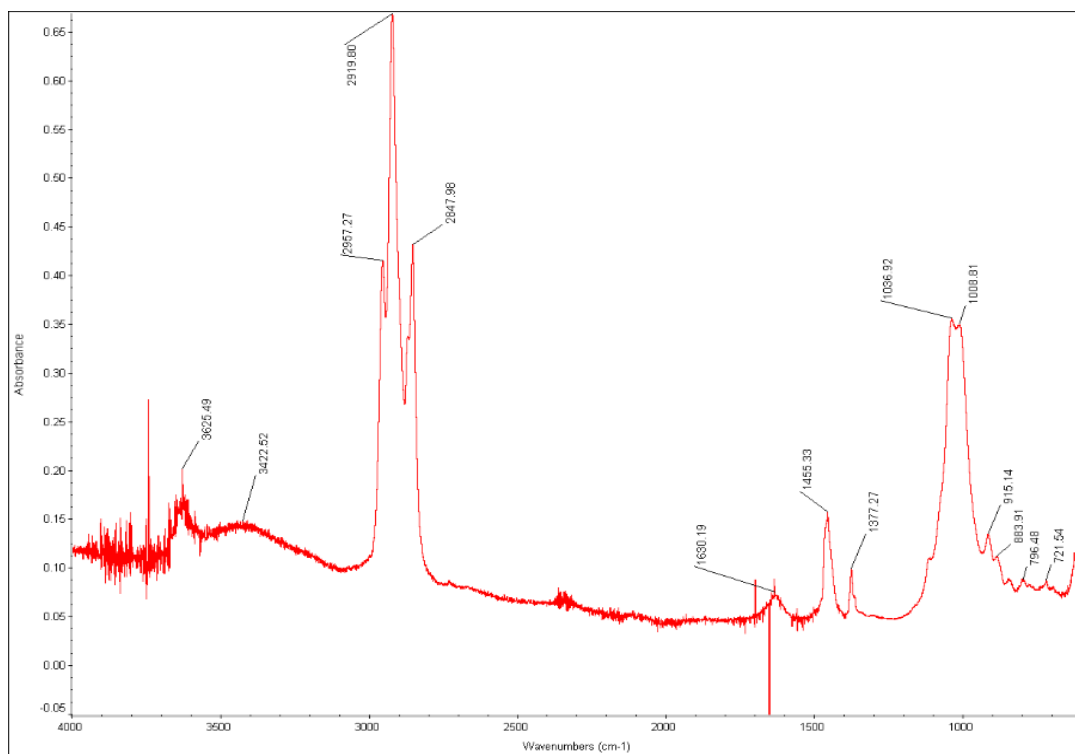


Figure A.48 bottom cathode downstream Mix Cell

Appendix B: Photographs comprising key cells



Figure B.1 Upstream Vanadium cell post EK



Figure B.2 Upstream Lead cell post EK



Figure B.3 Upstream Nickel cell post EK



Figure B.4 Upstream Mix cell post EK



Figure B.5 Downstream Lead cell post EK



Figure B.6 Downstream Mix cell post EK

Appendix C: Solubility diagrams of target metals

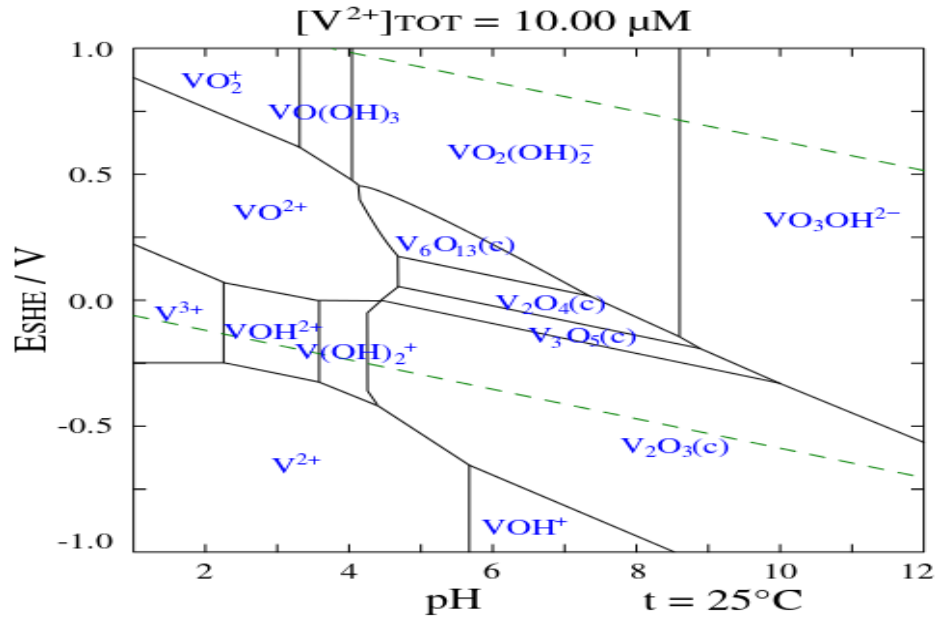


Figure C.1 Pourbaix diagram of vanadium in aqueous medium (Pourbaix, 1974)

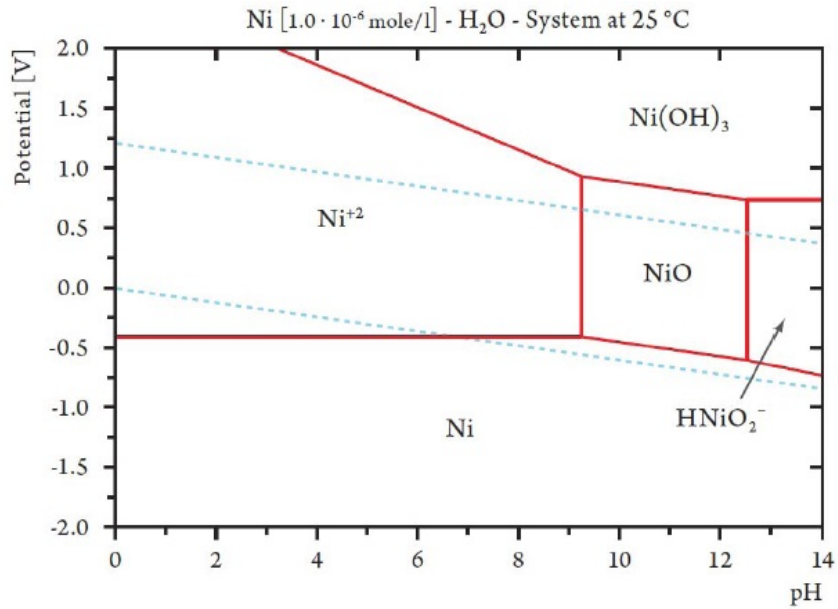


Figure C.2 Pourbaix diagram of nickel in aqueous medium (Pourbaix, 1974)

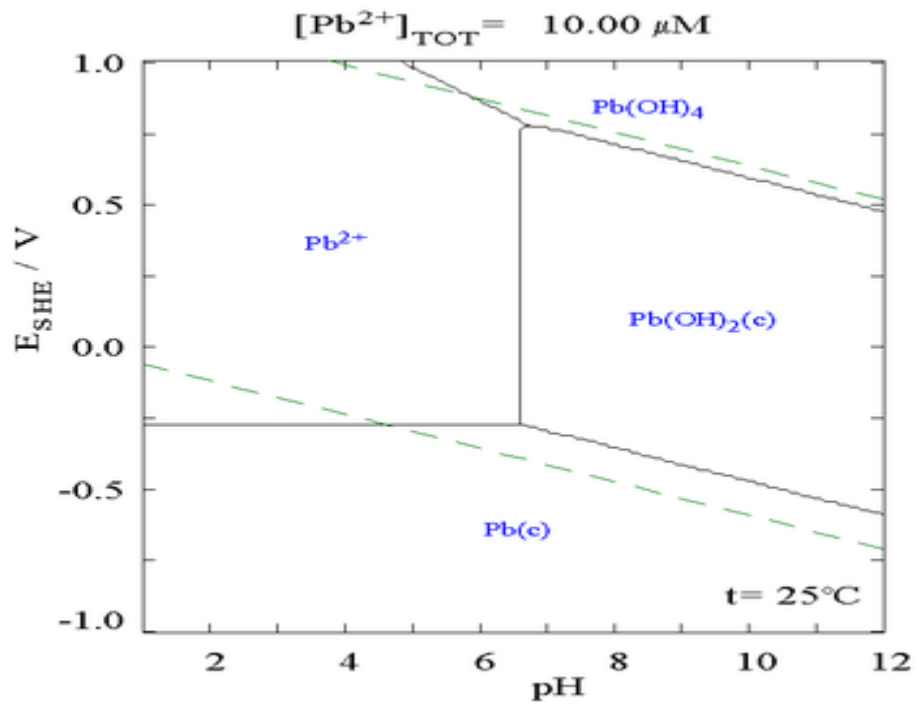


Figure C.3 Pourbaix diagram for lead in an aqueous medium (Pourbaix, 1974)

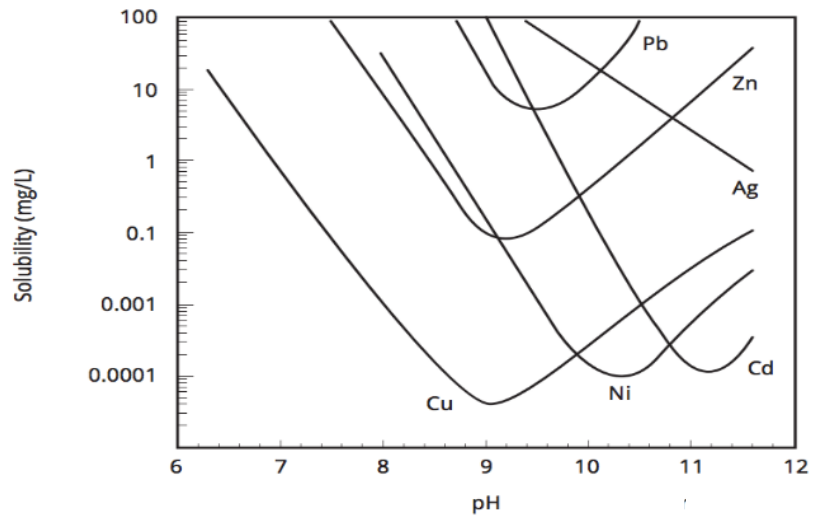


Figure C.4 Theoretical solubility of metals hydroxides vs pH (Ayres et al., 1994)